3612/19-83 OS(1) I-11209

Dr.1771-X

DOE/ET/20279-240

DEVELOPMENT AND EVALUATION OF SOLAR-PHOTOVOLTAIC SYSTEMS: FINAL REPORT

June 1983

Edward C. Kern, Jr.
Marvin D. Pope

DO NOT MICROFILM THIS PAGE

Massachusetts Institute of Technology
Lincoln Laboratory
Lexington, Massachusetts 02173-0073

Prepared for
THE U.S. DEPARTMENT OF ENERGY
UNDER CONTRACT NO. DE-AC02-76ET20279

MASTER

...STER

DISTRIBUTION OF THIS DOCUMENT IS UNLIMITED

DISCLAIMER

This report was prepared as an account of work sponsored by an agency of the United States Government. Neither the United States Government nor any agency thereof, nor any of their employees, makes any warranty, express or implied, or assumes any legal liability or responsibility for the accuracy, completeness, or usefulness of any information, apparatus, product, or process disclosed, or represents that its use would not infringe privately owned rights. Reference herein to any specific commercial product, process, or service by trade name, trademark, manufacturer, or otherwise does not necessarily constitute or imply its endorsement, recommendation, or favoring by the United States Government or any agency thereof. The views and opinions of authors expressed herein do not necessarily state or reflect those of the United States Government or any agency thereof.

DISCLAIMER

Portions of this document may be illegible in electronic image products. Images are produced from the best available original document.

DO NOT MICROFILM
THIS PAGE

This book was prepared as an account of work sponsored by an agency of the United States Government. Neither the United States Government nor any agency thereof, nor any of their employees, makes any warranty, express or implied, or assumes any legal liability or responsibility for the accuracy, completeness, or usefulness of any information, apparatus, product, or process disclosed, or represents that its use would not infringe privately owned rights. Reference herein to any specific commercial product, process, or service by trade name, trademark, manufacturer, or otherwise, does not necessarily constitute or imply its endorsement, recommendation, or favoring by the United States Government or any agency thereof. The views and opinions of authors expressed herein do not necessarily state or reflect those of the United States Government or any agency thereof.

Additional copies available from the National Technical Information Service, U.S. Department of Commerce, Springfield, Virginia 22161.

Price: Paper Copy $28.00
Microfiche $ 4.00

DOE/ET/20279-240

Distribution Category UC 63a-e

DEVELOPMENT AND EVALUATION OF SOLAR PHOTOVOLTAIC SYSTEMS: FINAL REPORT

DOE/ET/20279--240

June 1983 DE83 017776

Edward C. Kern, Jr.*
Marvin D. Pope

Massachusetts Institute of Technology
Lincoln Laboratory
Lexington, Massachusetts 02173-0073

NOTICE
PORTIONS OF THIS REPORT ARE ILLEGIBLE.
It has been reproduced from the best available copy to permit the broadest possible availability.

Prepared for
THE U.S. DEPARTMENT OF ENERGY
UNDER CONTRACT NO. DE-AC02-76ET20279

MASTER

*Now with MIT Energy Laboratory, Northeast Residential Experiment Station, 711 Virginia Road, Concord, MA 01742.

DISTRIBUTION OF THIS DOCUMENT IS UNLIMITED

DISCLAIMER

This report was prepared as an account of work sponsored by an agency of the United States Government. Neither the United States Government nor any agency thereof, nor any of their employees, makes any warranty, express or implied, or assumes any legal liability or responsibility for the accuracy, completeness, or usefulness of any information, apparatus, product, or process disclosed, or represents that its use would not infringe privately owned rights. Reference herein to any specific commercial product, process, or service by trade name, trademark, manufacturer, or otherwise does not necessarily constitute or imply its endorsement, recommendation, or favoring by the United States Government or any agency thereof. The views and opinions of authors expressed herein do not necessarily state or reflect those of the United States Government or any agency thereof.

TABLE OF CONTENTS

Section		Page
	Table of Contents	iii
	List of Figures	xi
	List of Tables	xix
	Acknowledgment	xxi
1.0	INTRODUCTION	1
2.0	THE MEAD, NEBRASKA, 25-KWP PV SYSTEM	4
2.1	Introduction	4
2.2	System Application	4
2.3	Participants	6
2.4	PV System Loads	6
2.4.1	Crop-Irrigation Experiment	6
2.4.2	Grain-Drying Experiment	8
2.4.3	Fertilizer-Generation Experiment	9
2.5	Solar Availability	9
2.6	PV System Description	13
2.6.1	PV Array	14
2.6.2	The Battery	15
2.6.3	Power Conditioning	16
2.6.4	Data Acquisition	18
2.7	System Performance	20
2.7.1	PV Array Performance	20
2.7.2	System Energy Flow	25
2.7.3	PV Energy Usage	26
2.7.3.1	Irrigation Experiment Results	26
2.7.3.2	Grain-Drying Experiment Results	27
2.7.3.3	Fertilizer-Generating-Experiment Performance	27
2.8	Lessons Learned	28
2.8.1	System Complexity	28
2.8.2	Power Overhead	28
2.8.3	Stand-Alone Versus Utility-Interactive Operation	29
2.8.4	Motor Starting	30
2.8.5	Automatic Control	30
3.0	1.6-KWP PV POWER SYSTEM AT CHICAGO MUSEUM OF SCIENCE AND INDUSTRY	33
3.1	Introduction	33
3.2	System Application	33
3.3	Participants	34
3.4	PV System Loads	35

TABLE OF CONTENTS
(continued)

Section		Page
3.5	Solar Availability	35
3.6	PV System Description	35
3.6.1	PV Array	37
3.6.2	Batteries and Charger	41
3.6.3	Data Acquisition	41
3.7	System Performance	41
3.8	Lessons Learned	44
3.8.1	Low Voltage is Beneficial	44
3.8.2	Simple Systems are Reliable	44
3.8.3	Glass-Covered PV Modules are Superior	44
4.0	THE BRYAN, OHIO, 15-KWP PV SYSTEM	46
4.1	Introduction	46
4.2	System Application	46
4.3	Participants	47
4.4	PV System Loads	48
4.5	Solar Availability	48
4.6	PV System Description	52
4.6.1	PV Array	53
4.6.2	The Battery	55
4.6.3	Power Conditioning	56
4.6.4	Data Acquisition	58
4.7	PV System Performance	59
4.7.1	PV Array Performance	61
4.7.2	Battery Performance	62
4.7.3	System Energy Flow	65
4.8	Lessons Learned	66
4.8.1	Lightning Protection	66
4.8.2	Unattended Operation	66
4.8.3	Repair and Maintenance by Nonspecialists	66
4.8.4	Low-Cost PV Array Structures	67
4.8.5	Provide for High Array Output	67
5.0	THE NATURAL BRIDGES NATIONAL MONUMENT 100-KWP PV SYSTEM	69
5.1	Introduction	69
5.2	System Application	70
5.3	Participants	71
5.4	PV System Loads	73
5.5	Solar Availability	74
5.6	PV System Description	74

TABLE OF CONTENTS
(continued)

Section		Page
	5.6.1 Photovoltaic Array	77
	5.6.2 The Battery	78
	5.6.3 Power-Conditioning Equipment	81
	5.6.4 System Control	83
	5.6.5 Data Acquisition	84
5.7	PV System Performance	85
	5.7.1 Comparison of Predicted and Measured Performance	86
	5.7.2 Summary of PV System Performance	88
	5.7.2.1 PV Array Performance	91
	5.7.2.2 Battery Performance	92
	5.7.2.3 Power-Conditioning Performance	95
	5.7.2.4 System Control Performance	96
5.8	Lessons Learned	96
	5.8.1 Unattended Operation	97
	5.8.2 Repair and Maintenance	97
	5.8.3 Simpler Systems	97
	5.8.4 Mercury Relays for Array Shedding	97
	5.8.5 Batteries	97
	5.8.6 Site Energy Audits	98
	5.8.7 PV Modules with Metal Substrates	98
	5.8.8 Design Protection Against High PV Array Output	99
	5.8.9 Inverters	99
	5.8.10 Subarray Structures	99
	5.8.11 Enhanced Output from Modules	99
6.0	MEASUREMENT OF PV MODULE PERFORMANCE AND RELIABILITY	103
6.1	Introduction	103
6.2	25-kWp System at Mead, Nebraska	104
6.3	1.6-kWp System at Chicago Museum	108
6.4	15-kWp System at Bryan, Ohio	108
6.5	100-kWp System at Natural Bridges, Utah	109
6.6	7.5-kWp System at Arlington, Texas	111
6.7	PV System Test Beds at Lexington and Concord, Massachusetts	113
6.8	Arrays in New York City, Cambridge, Massachusetts, and Mount Washington, New Hampshire	115
6.9	Soil Accumulation on PV Modules	117
6.10	Summary	119
6.11	Lessons Learned	120
	6.11.1 General Observations	120
	6.11.2 Specific Observations	121
Appendix to Section 6.0		122

TABLE OF CONTENTS
(continued)

Section		Page
7.0	DEVELOPMENT OF INSTRUMENTS FOR MEASURING PV SYSTEM PERFORMANCE	125
7.1	Introduction	125
7.2	Development of a Sun-Following Pyrheliometer	125
7.2.1	Capabilities of Sun-Following Pyrheliometer	125
7.2.2	System Description	126
7.2.3	Summary	128
7.3	Development of an I-V Curve Tracer	129
7.3.1	Introduction	129
7.3.2	Design Considerations	130
7.3.3	Implementation	131
7.3.4	I-V Curve Tracer Performance	132
7.3.5	Conclusions	134
8.0	BACKGROUND AND OVERVIEW OF RESIDENTIAL PHOTOVOLTAICS ACTIVITY	135
9.0	RESIDENTIAL PV SYSTEM STUDIES	139
9.1	Economic Studies of Residential PV Systems	140
9.1.1	Introduction	140
9.1.2	Worth Analysis of Residential PV Systems	141
9.1.3	Studies of Residential PV/Thermal Systems	142
9.1.4	Cost Goals for Residential PV Systems	144
9.2	Integration of PV Systems with the Utility	146
9.2.1	Introduction	146
9.2.2	The Impact of Residential Photovoltaics on Utility Generation Requirements	147
9.2.3	The Impact of Residential Photovoltaics on Utility Distribution Systems	151
9.2.3.1	Effect of PV on Feeder Capacity	151
9.2.3.2	Effect of PV Feeder Losses and Substation Load Reduction	154
9.2.3.3	Effect of Inverter Harmonics on Feeder Voltage and Current	155
9.2.3.4	Effect of PV on Utility Operation	157
9.3	Analytical Models for PV System Technical Performance	160
9.3.1	Introduction	160
9.3.2	General Framework for Simulation	160
9.3.3	PV Array Thermal Model	163
9.3.4	Electrical Models	163
9.3.5	PV System Model	165
9.3.6	Comparison of Measured and Predicted Performance	166

TABLE OF CONTENTS
(continued)

Section		Page
	9.3.6.1 Array Thermal Model	166
	9.3.6.2 PV Array Current-Voltage Characteristics	172
	9.3.6.3 PV Array Voltage Control	172
	9.3.6.4 Inverter Efficiency	176
	9.3.6.5 Overall Accuracy of System Simulations	178
9.4	The PV Array/Power Conditioner Interface	178
	9.4.1 Introduction	178
	9.4.2 Computer Models and Validation	179
	9.4.3 Array-Operating-Point Control Strategies	181
	9.4.3.1 Fixed-Voltage Operation with Fully Operational Arrays	182
	9.4.3.2 Fixed-Voltage Operation with Degraded Arrays	183
	9.4.4 Conclusions	190
9.5	Development of Codes and Standards	191
	9.5.1 Introduction	191
	9.5.2 Development of Interim Performance Criteria	191
	9.5.3 Development of IEEE Standards for PV Systems	193
	9.5.4 Development of Underwriters Laboratories Standards for Inverters	194
	9.5.5 Revision to 1984 National Electric Code	195
	9.5.6 Development of Safety Inspection Guidelines for PV Residences	195
10.0	RESIDENTIAL PV TECHNOLOGY DEVELOPMENT	199
10.1	Introduction	199
10.2	Development of PV Cells with Self-Contained Bypass Diodes	199
	10.2.1 Background Information	199
	10.2.2 Utilization of a Standard Diode	202
	10.2.3 Utilization of a Backward Diode	205
	10.2.4 Conclusions	209
10.3	Development of Combined PV/Thermal Collectors	209
	10.3.1 Background Information	209
	10.3.2 The Early PV/T Units	210
	10.3.3 Development of Second-Generation PV/T Collectors	213
	10.3.3.1 Production-Ready Collector Designs	214
	10.3.3.2 Experimental PV/T Collector Designs	214
	10.3.3.3 Novel Collector Concept Designs	215
	10.3.3.4 Testing of Second-Generation PV/T Collectors	215
	10.3.4 Conclusion	218

TABLE OF CONTENTS
(continued)

Section		Page
10.4	Development of Solar Cells for PV/Thermal Collectors	219
	10.4.1 Background Information	219
	10.4.2 PV/T Cell Design	223
	10.4.2.1 Cell Back Metallization	225
	10.4.2.2 Reflection Loss Reduction	227
	10.4.3 Conclusions	232
10.5	Methods for Roof-Mounting PV Arrays	232
	10.5.1 Introduction	232
	10.5.2 Requirements of an Array Roof-Mounting Design	233
	10.5.3 Four Generic Roof-Mounting Approaches	234
	10.5.3.1 Integral Array Mounting	234
	10.5.3.2 Direct Mounting	235
	10.5.3.3 Stand-Off Mounting	235
	10.5.3.4 Rack Mounting	236
	10.5.4 Prototype System Installations	236
	10.5.4.1 Carlisle House Stand-Off Mount	238
	10.5.4.2 General Electric Direct Mount	238
	10.5.4.3 TriSolarCorp Integral Mount	239
	10.5.4.4 TEA Rack Mount	240
	10.5.5 Mounting Method Cost Breakdown	240
10.6	Development of Inverters for Residential PV Systems	241
	10.6.1 Introduction	241
	10.6.2 Classification of Inverter Approaches	242
	10.6.3 Development of Waveshaping Inverter	244
	10.6.3.1 Waveshaping Inverter Design	244
	10.6.3.2 Waveshaping Inverter Performance	245
	10.6.3.3 Waveshaping Inverter Manufacturing Costs	247
	10.6.4 Conclusions	248
10.7	Development of Flywheel Energy Storage for Residential PV	249
	10.7.1 Introduction	249
	10.7.2 Flywheel System Design	250
	10.7.3 1/10-Scale Prototype Flywheel System	250
	10.7.4 Measurements on 1/10-Scale Prototype System	255
	10.7.5 Advanced Prototype Flywheel Unit	256
	10.7.6 Conclusions	259

TABLE OF CONTENTS
(continued)

Section		Page
11.0	RESIDENTIAL SYSTEMS TESTS	264
11.1	Background Information	264
11.2	Prototype Systems at the Northeast and Southwest Residential Experiment Stations	265
11.2.1	Northeast Residential Experiment Station (NE RES)	265
11.2.1.1	Evaluation of NE RES Prototypes	268
11.2.2	Southwest Residential Experiment Station (SW RES)	272
11.2.2.1	Evaluation of SW RES Prototypes	273
11.3	Residential Data System	277
11.3.1	Introduction	277
11.3.2	System Description	278
11.4	Experimental PV Residences	280
11.4.1	University of Texas at Arlington Residential PV System	280
11.4.1.1	Introduction	280
11.4.1.2	System Description	280
11.4.2	Experimental PV Residence at Carlisle, Massachusetts	283
11.4.2.1	Introduction	283
11.4.2.2	System Description	283
11.4.3	Experimental PV Residences in Hawaii	287
11.4.3.1	Introduction	287
11.4.3.2	System Description	287
11.4.4	Experimental PV Residence at Cape Canaveral, Florida	293
11.4.4.1	Introduction	293
11.4.4.2	System Description	293
11.4.5	Experimental PV Residence in Phoenix, Arizona	299
11.4.5.1	Introduction	299
11.4.5.2	System Description	301
12.0	SUMMARY OF RESIDENTIAL PV PROJECT	309
12.1	Conclusions and Lessons Learned	309
12.2	Recommendations for Future Work	311
APPENDIX		A1

LIST OF FIGURES

Figure		Page
1-1	MIT Lincoln Laboratory photovoltaic experiments, 1977-1982.	2
2-1	Aerial view of the Mead, Nebraska, site.	5
2-2	Automated gated-pipe irrigation system.	7
2-3	Solar-powered, crop-drying bins.	8
2-4	PV-powered nitrogen-fertilizer generator.	9
2-5	Mead PV system block diagram.	13
2-6	PV array closeup.	14
2-7	Interior view of battery trailer.	16
2-8	Block diagram of inverter control logic.	18
2-9	Data acquisition and reduction system.	19
2-10	Array output versus time.	21
2-11	Total array output versus total tilted insolation.	21
2-12	Factors affecting array output.	23
2-13	In-service performance record for Mead PV modules.	24
2-14	PV energy system flow.	25
3-1	PV power system, Chicago Museum of Science and Industry.	37
3-2	Spectrolab Block I module.	38
3-3	PV array on Museum roof.	39
3-4	Chicago Museum PV array electrical configuration.	40
3-5	Museum PV system, predicted typical day operation.	42
3-6	Battery current flow and voltage versus time of day (sunny).	43
3-7	Battery current flow and voltage versus time of day (cloudy).	43
4-1	Aerial view, WBNO, Bryan, Ohio.	47
4-2	Block diagram, WBNO PV system.	52
4-3	Solarex module.	54
4-4	WBNO array-field closeup.	55
4-5	Battery storage subsystem.	56
4-6	Spare battery cells.	57
4-7	PV power system controller.	58

LIST OF FIGURES
(continued)

Figure		Page
4-8	System performance on sunny day.	60
4-9	System performance on cloudy day.	60
4-10	Bar graph of maximum array power.	63
4-11	System performance on 9 April 1981.	64
4-12	System performance on 9 April 1981.	64
5-1	Sipapu Bridge, Natural Bridges National Monument, Utah.	69
5-2	Natural Bridges National Monument photovoltaic site.	71
5-3	NBNM headquarters area.	73
5-4	NBNM PV power system block diagram.	77
5-5	Spectrolab module.	79
5-6	Motorola module.	79
5-7	Arco Solar module.	79
5-8	Upper row of array.	80
5-9	Battery room.	82
5-10	Multiple plots of I-V scans for all array subfields.	85
5-11	Predicted energy available from array.	86
5-12	Monthly load categories.	88
5-13	Battery plots.	89
5-14	Battery plots.	89
5-15	Block diagram of energy flow.	90
5-16	Bar graph of maximum array power.	93
5-17	Voltage and current versus time.	94
5-18	Voltage and SOC versus time.	95
6-1	Cumulative percentage of failed modules, Mead, Nebraska.	107
6-2	Natural Bridges National Monument aerial view.	110
6-3	University of Texas at Arlington residential system.	112
6-4	MIT Lincoln Laboratory Rooftop Test Facility.	114
6-5	MIT Lincoln Laboratory Residential System Test Facility.	114
6-6	MIT Cambridge, Massachusetts, rooftop module test site.	116
6-7	Mount Washington, New Hampshire, module test site.	116

LIST OF FIGURES
(continued)

Figure		Page
7-1	The sun-following pyrheliometer.	126
7-2	Polar sun-following mount.	127
7-3	Use of a capacitor to measure the I-V curve.	129
7-4	Photograph of 10-kW, I-V curve tracer.	131
7-5	Simplified block diagram of I-V curve tracer.	132
7-6	Output of capacitor-load curve tracer and resistor load.	133
7-7	I-V curve of approximately 7.5-kWp array.	133
8-1	Aerial view, Northeast Residential Experiment Station.	136
8-2	Aerial view, Southwest Residential Experiment Station.	136
9-1	Power output versus time of day for the UTA Solar House utility-interactive PV system on Thursday, July 31, 1980.	152
9-2	Demand at TESCO substation for feeder No. 3511 with and without distributed PV systems for July 31, 1980. Demand for November 11, 1980 is shown for comparison.	153
9-3	Voltage in per unit at the end of TESCO feeder No. 3511 on Thursday, July 31, 1980 at 14:00 hours as a function of PV market saturation and inverter power factor.	154
9-4	Apparent power at TESCO substation and feeder losses for Thursday, July 31, 1980 at 14:00 hours. PV inverter PF = 1.0.	155
9-5	Typical voltage and current waveforms at Pole 17 on CMLP feeder No. 23.	156
9-6	Basic elements of a utility-interactive PV energy system.	161
9-7	Organization of simulation.	162
9-8	Variation of I-V curves as a function of insolation.	164
9-9	Variation of I-V curves with cell temperature.	164
9-10	Efficiency of Gemini inverter (with transformer) as function of dc power and voltage.	164
9-11	Comparison between measured and computed cell temperature for Lincoln array.	167
9-12	Comparison between measured and computed cell temperature for Westinghouse array.	167
9-13	Comparison between measured and computed cell temperature for GE array.	168

LIST OF FIGURES
(continued)

Figure		Page
9-14	Comparison between measured and computed cell temperature for TriSolarCorp array.	168
9-15	Comparison between measured and computed cell temperature for Solarex array.	168
9-16	Measured temperature variation across TriSolarCorp array.	170
9-17	Comparison between measured and computed cell temperature for GE array on winter day.	171
9-18	Effect of snow and ice on cell temperature of Lincoln array.	171
9-19	Effect of inverter failure on cell temperature of TriSolarCorp array.	171
9-20	Comparison of measured and simulated I-V curve.	173
9-21	Comparison of I-V curves for various insolation and cell temperatures of the Lincoln array from measurements and the JPL model.	173
9-22	Current-voltage control characteristics of the Gemini inverter.	173
9-23	Measured and simulated array voltage for Gemini inverter.	174
9-24	Measured and calculated voltages for an Abacus inverter with "searching" maximum-power-point tracker.	174
9-25	Measured and calculated voltages for Abacus inverter with "pilot cell" maximum-power-point tracker.	175
9-26	Comparison of measured and calculated dc power output from TriSolarCorp array.	175
9-27	Comparison of measured and calculated dc power output from Westinghouse array.	176
9-28	Efficiency of Gemini inverter (with transformer) as function of dc power and voltage.	177
9-29	Efficiency of Abacus inverter as function of dc power and voltage.	177
9-30	Comparison of measured and calculated ac power output of TriSolarCorp array with a Gemini inverter.	177
9-31	Comparison of measured and calculated ac power output of Westinghouse array with an Abacus inverter.	177
9-32	Flowchart of PV system simulation program.	180
9-33	Pairs of measured and simulated I-V curves at four combinations of insolation and cell temperature.	181
9-34	A comparison of the energy output as a function of fixed operating voltage and the total available array energy.	183

LIST OF FIGURES
(continued)

Figure		Page
9-35	Three single-glitch I-V curves from degraded PV arrays. Each I-V curve can be uniquely represented by the location of its glitch point.	184
9-36	Total available energy from single-glitch I-V curves plotted at the glitch-point location in the I-V plane. Glitch points with equal available energy are connected by the contours shown.	186
9-37	Total energy collected by operating an array with single-glitch degradation at the BFV of the undegraded array.	187
9-38	Percent of available energy lost (PL) with operation at the undegraded array's BFV relative to unlimited range maximum-power-point tracking.	189
9-39	Percent of available energy lost (PL) with operation at the undegraded array's BFV relative to maximum-power-point tracking over the range indicated.	189
9-40	Percent of available energy of the undegraded array which could be collected with an ideal maximum-power-point tracker operating on degraded arrays.	190
10-1	(a) Series-connected string of PV cells operating at current I_o; (b) intersection of constant current I_o with I-V curve of full (solid) and defective (dash-dot) cells.	200
10-2	Layout of wafer including peripheral-diode region isolated from central PV-cell region.	202
10-3	(a) Edge view and (b) schematic of PV cell with a standard diode in the peripheral location for bypass protection.	203
10-4	Series interconnection of PV cells: (a) without bypass protection (b) with standard diode and (c) with backward diode bypass protection.	204
10-5	I-V curve of PV cell without bypass protection emphasizing (a) reverse breakdown and (b) forward-conduction regions.	204
10-6	I-V curve of PV cell with standard diode-bypass protection at (a) full and (b) expanded scales.	205
10-7	Comparison of I-V curves for conventional (dashed), backward (solid) and tunnel (dash-dot) diodes.	206
10-8	(a) Edge view and (b) schematic of PV cell with a backward diode in the peripheral location for bypass protection.	207

LIST OF FIGURES
(continued)

Figure		Page
10-9	I-V curve of PV cell with backward diode-bypass protection: (a) expanded scale indicating first-quadrant operation with and without the backward diode connected in parallel and (b) normal scale indicating reverse breakdown of the PV cell with and without backward diode.	208
10-10	Spectrolab air PV/T collector.	211
10-11	ARCO liquid PV/T collector.	211
10-12	ARCO air PV/T collector.	212
10-13	ARCO liquid and Spectrolab air maximum power point PV/T electrical performance.	212
10-14	ARCO liquid PV/T collector thermal performance.	212
10-15	Spectrolab air PV/T collector thermal performance.	213
10-16	Internal components of production collector designs.	215
10-17	Thermal performance of production collectors with concurrent PV operation.	217
10-18	Electrical performance of production collectors.	217
10-19	Predicted maximum power point electrical efficiency for experimental air collectors.	218
10-20	Predicted thermal efficiency with concurrent PV operation, for experimental air collectors.	219
10-21	Reflectance and transmittance of a bare silicon wafer in air. Incidence angle $Q_1 = 10^o$.	222
10-22	Contrast of the optical performance of silicon: (a) with full metal back and (b) with a gridded metal back.	224
10-23	Reflectance and transmittance of a silicon wafer with a full metal back.	224
10-24	Measured current versus voltage (I-V) curves for three cell configurations: (a) full metal back, and gridded metal backs without (b) and with (c) a back surface field.	226
10-25	Reflectance from an AR-coated, semi-infinite silicon wafer versus incident angle with wavelength as the parameter.	229
10-26	Reflectance from a textured surface, semi-infinite silicon wafer versus incident angle.	230
10-27	Thermal and electrical efficiencies for the advanced prototype, air PV/T collector.	231

LIST OF FIGURES
(continued)

Figure		Page
10-28	Integral mount.	235
10-29	Direct mount.	235
10-30	Stand-off mount.	236
10-31	Aerial view of the Northeast Residential Experiment Station in Concord, Massachusetts.	237
10-32	Aerial view of the Southwest Residential Experiment Station in Las Cruces, New Mexico.	237
10-33	The Carlisle PV house, stand-off mount.	238
10-34	The General Electric prototype at the NE RES.	239
10-35	TriSolarCorp integral mount modules (backside).	240
10-36	TEA prototype, SW RES, rack mount.	240
10-37	Block diagram of a waveshaping inverter.	244
10-38	Experimental inverter: The $\overline{WR}$ stage is at the far end, the control stage is in the middle, and the I stage is near the front of the photograph (with heat sink).	246
10-39	Oscilloscope measurements of some waveforms of the experimental inverter: (a) voltage (top) and current at the output of the $\overline{WR}$ stage, (b) current (top) and voltage at the I stage.	246
10-40	Plot of measurements of efficiency versus dc power level for the experimental inverter.	247
10-41	Residential photovoltaic flywheel system.	249
10-42	40-kWh residential flywheel energy storage unit.	251
10-43	1/10-scale prototype flywheel system.	252
10-44	Cutaway, 1/10-scale experimental flywheel.	252
10-45	Photograph, six element prototype magnetic bearing.	253
10-46	Diagram of 1/10-scale flywheel unit electrical system.	253
10-47	1 kW utility-interactive inverter.	254
10-48	Utility-interactive inverter output power waveform (less than 2% total harmonic distortion).	254
10-49	Spin-down tare loss.	256
10-50	Advanced prototype flywheel storage unit.	257

LIST OF FIGURES
(continued)

Figure		Page
10-51	Simplified two-element magnetic bearing.	257
10-52	Original six-bearing design (left) compared with new two-bearing design (right).	258
10-53	Composite rotor.	258
10-54	Composite rotor in containment vessel following its failure.	258
11-1	Aerial view of NE RES.	266
11-2	Aerial view of SW RES.	272
11-3	Data system block diagram.	278
11-4	Aerial view of UTA Experiment.	280
11-5	The Carlisle PV house.	283
11-6	Installing the PV modules.	285
11-7	Carlisle house utility and load connections.	285
11-8	Kalihu PV house.	288
11-9	Pearl City PV house.	288
11-10	Molokai PV house.	289
11-11	Florida Solar Energy Center PV house.	294
11-12	Power-conditioning subsystem at FSEC PV house.	295
11-13	John F. Long PV house, Phoenix.	300
11-14	ARCO Solar batten-and-seam PV module.	300
11-15	John F. Long house power-conditioning equipment.	301

LIST OF TABLES

Table		Page
2-1	Insolation and Temperature Data, North Omaha, Nebraska	10
2-2	Mead Insolation Data	11
2-3	Mead Meteorological Data	12
2-4	Mead, Nebraska, PV Power System	22
2-5	Module Failures at Mead Test Site	24
2-6	System Annual Energy Balance	25
3-1	Chicago Insolation and Temperature Data	36
3-2	Spectrolab Block I PV Module Data	38
3-3	Chicago Museum PV Array Characteristics	40
4-1	Average Insolation and Temperature Data - Fort Wayne	49
4-2	Bryan, Ohio, Average Insolation	50
4-3	Bryan, Ohio, Meteorological Data	51
4-4	Solarex Module Characteristics	54
4-5	Ohio PV Power System Energy Flow Summary	65
5-1	Estimated NBNM Site Loads	74
5-2	NBNM Average Daily Insolation	75
5-3	NBNM Meteorological Data	75
5-4	NBNM Meteorological Information	76
5-5	Module Characteristics	78
5-6	Battery Characteristics	81
5-7	System Energy Flow	87
5-8	AC Energy Summary	90
5-9	Measured Average Component and System Energy Efficiencies	91
6-1	Module Physical Degradation at Mead	105
6-2	Cracked-Cell Data at the Mead Test Site	105
6-3	Module Failures at Mead Test Site	106
6-4	MIT Lincoln Laboratory Environmental Test Sites Recent Soil Accumulation Data	118
6-5	Soil Accumulation Study at MIT	119
7-1	Comparison of 10-kW Instruments	134

LIST OF TABLES
(continued)

Table		Page
9-1	Harmonics Measured on CMLP Circuit 23 at Pole 17	156
10-1	Integrated Fraction of Various Solar Spectra	220
10-2	Formulae for Calculation of Reflection from an AR-Coated Surface	228
10-3	Array Installation Costs	241
10-4	Classification Permutations	243
10-5	Variation in Inverter Selling Price as a Function of Efficiency	247
10-6	Measured Efficiency - Utility-Interactive Mode	255
10-7	Measured Efficiency - Stand-Alone Mode	256
11-1	NE RES Prototype Systems: Physical Features	267
11-2	System Performance Extrema	270
11-3	SW RES Prototype Systems: Physical Features	273
11-4	UTA System Performance Summary 9/79 to 8/80	282
11-5	Energy Flow--Carlisle House (Average kWh/day)	286
11-6	Site Equipment Summary	291
11-7	Hawaii PV Systems' Electrical Energy Flows	292
11-8	Monthly Performance of FSEC PV House Array	296
11-9	Monthly Performance of FSEC PV House System	297
11-10	The FSEC Experimental Photovoltaic Residence--Operational Monthly Performance Summary	298

ACKNOWLEDGMENT

In preparing this report, the authors performed mainly a reportorial role, the real work being done by the 50 or more Lincoln Laboratory people involved and many subcontractors. All of their contributions are hereby acknowledged, and further mention of the contributors is made in the various introductory sections of this report. Special thanks are due to Ervin F. Lyon and Ronald W. Matlin, who served with us as Associate Project Leaders during important stages of the program, and to John F. Schaefer and his colleagues at New Mexico State University for their excellent performance in the development and evaluation of residential photovoltaic systems in the Southwest. Special mention also should be made of the administrative services ably provided by C. Ross Peatfield and Jane Sylvester Benoit.

Finally, and with many thanks, we gratefully acknowledge Sharon L. Howland, Project Secretary and Jean H. Hill, Project Editor. Not only were they instrumental in preparing this report, they produced the 240 reports and technical papers listed in the Appendix of this document.

Marvin D. Pope, Project Leader
Edward C. Kern, Jr. Associate Project Leader

1.0 INTRODUCTION

This report covers the six years, from 1976 to 1982, during which MIT Lincoln Laboratory was involved in the National Photovoltaic Program. It is complete in that it summarizes the totality of this activity, providing an overview rather than in-depth coverage. The reader who wishes to explore further any of the subjects discussed here is directed to the more than two hundred Lincoln Laboratory papers and reports referenced herein; they are listed in Appendix A. The format of this report is roughly consistent with the chronological order of the Lincoln Laboratory projects. At the request of the sponsors--first the Energy Research and Development Administration (ERDA), then the U. S. Department of Energy (DOE)--the Laboratory's activities were first focused on nonresidential terrestrial applications of photovoltaics.* Accordingly, the Laboratory managed the design, construction and evaluation of photovoltaic (PV) systems for use in agriculture (at Mead, Nebraska), for a museum display (at the Chicago Museum of Science and Industry), for operating a commercial radio station (at Bryan, Ohio), and for powering a remote site where utility hookup is not available (at Natural Bridges, Utah). These field test systems are discussed in Sections 2 through 5.

The project also evaluated the field performance of PV arrays at the sites mentioned above as well as at over 15 additional locations, where either small PV arrays were located or residential PV systems (which will be discussed later) were installed. The location of all the systems is shown in Fig. 1-1. The results of array evaluations are presented in Section 6.

Next, the work of the project in developing instrumentation for measuring PV system performance is discussed. Two instruments were developed: a pyrheliometer for monitoring insolation at a field site, and a portable

*Although residential PV was recognized early as a very important potential application area, the sponsor requested that the Laboratory defer system testing to a later date. This request was made in order to assure that the National Photovoltaic Program as a whole was ready to deal with the relatively large number of widespread experimental systems involved.

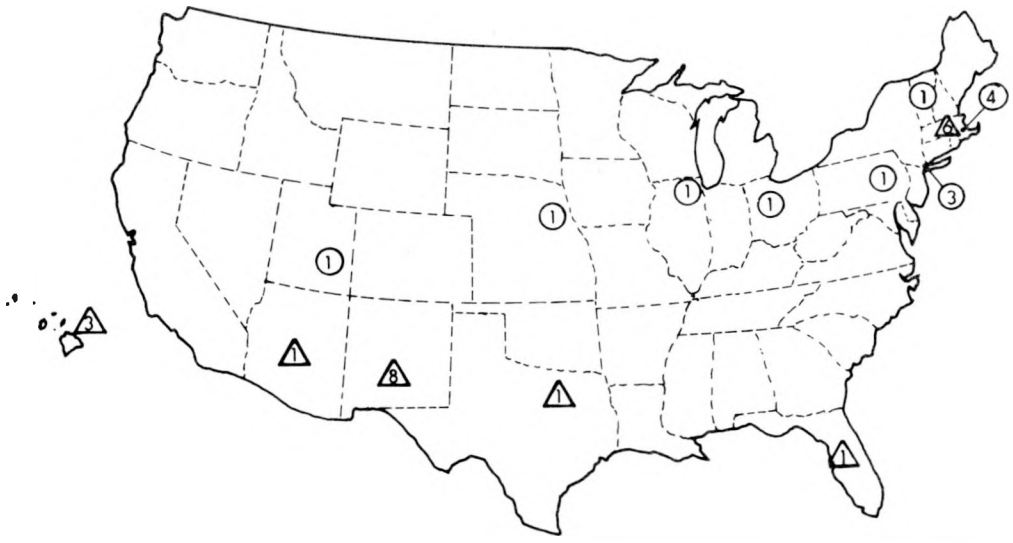

TOTAL kW	283
TOTAL SYSTEMS	33
TOTAL SYSTEM YEARS	35
OPERATING RELIABILITY	96 %

Fig. 1-1. MIT Lincoln Laboratory photovoltaic experiments, 1977-1982. (The numbers inside the symbols indicate the number of PV systems installed.)

unit for determining the current-voltage characteristics of a PV module or array in the field. These activities are summarized in Section 7.

The project's activities regarding development of residential PV systems are then discussed. Whereas the previously mentioned activities are each discussed and summarized in a single section, the much more extensive residential activity is covered in five sections, beginning with an introduction in Section 8 and proceeding through the three major technical efforts--system engineering, technology development and system evaluation--in Section 9 through Section 11, and concluding with a summary in Section 12.

When Lincoln Laboratory withdrew from the DOE Photovoltaic Program in June 1982, DOE assigned overall responsibility for residential PV systems to Sandia National Laboratories, Albuquerque, New Mexico (Dr. Edward L. Burgess). This organization is supported in the Southwest by New Mexico State University

(Dr. John F. Schaefer) and in the Northeast by the MIT Energy Laboratory (Dr. Edward C. Kern, Jr.). These organizations and individuals should be contacted for information about DOE's ongoing program in residential photovoltaic systems.

2.0 THE MEAD, NEBRASKA, 25-KWP PV SYSTEM

2.1 Introduction

In the spring of 1977, Lincoln Laboratory, in cooperation with the University of Nebraska, initiated a project to design and install a 25-kW peak PV power system at the University of Nebraska's Agricultural Research Station in Mead, Nebraska (1). The objectives of the project (2) were to test various energy management strategies for different agricultural loads and to monitor the performance of the entire PV power system, to evaluate PV module performance in an agricultural environment, and to evaluate the match between various agricultural loads (such as irrigation, crop-drying and on-site fertilizer manufacturing) and available solar energy. To achieve these objectives, a comprehensive system of sensors and data-logging equipment was used to collect a wide variety of data on PV system performance at regular 10-minute (daytime) and 20-minute (nighttime) intervals. As anticipated, continuous monitoring of the entire PV system over a three-year period (1978-1980) has produced an extensive library of data on solar insolation, PV-array performance, power-conditioning equipment performance, and weather.

The following sections present additional information on the PV system, its performance, and related agricultural experiments. At the time of its dedication in July 1977, it was the largest PV system in the world.

Contributions to this effort were made by the following individuals: Roy C. Archibald, Alfred E. Benoit, Henry J. Bullwinkel, John D. Cremin, John J. Dunn, John A. Farnsworth, Harvey A. Fenton, Fred Fullam, John H. Helfrich, Raymond F. Hopkinson, John P. Husler, John T. Kelly, Emanuel E. Landsman, Ervin F. Lyon, John C. Mahoney, Ronald W. Matlin, Alan R. Millner, Ernest A. Paquette and William R. Romaine.

2.2 System Application

One of the primary functions of the Mead system was to test the application of a PV power system in a variety of energy-intensive agricultural uses. Since these experiments involved crop irrigation and grain drying, as well as the manufacture of fertilizers, it was expedient that a site be chosen where

each of these on-farm tasks could be conducted. After considerable investigation (3,4), the University of Nebraska's Agricultural Research Station at Mead, Nebraska, located in the heart of the U.S. corn belt, was chosen as the appropriate site.

Figure 2-1 presents an aerial view of the Mead, Nebraska, site. In the foreground lies the 80-acre cornfield which is the object of the PV energy irrigation experiment. In the center are two rows of PV modules which constitute the PV array. The reuse pit, from which excess water from the cornfield is lifted by the solar-powered pump, lies directly behind the array, the rear row of which is sited on the berm of the pit. A cyclone fence surrounds the array for safety purposes.

CP267-1737

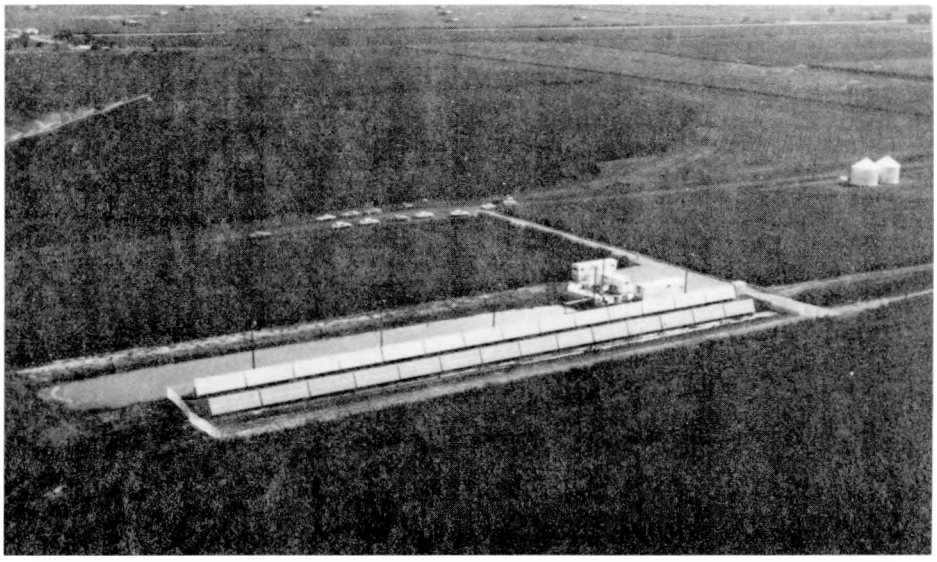

Fig. 2-1. Aerial view of the Mead, Nebraska, site.

In the right center of the photo may be seen three trailers: the large (10 ft. x 36 ft.) trailer closest to the array houses the PV power system switchgear, the control circuitry, the 3-phase inverter, the data acquisition equipment, and other electrical and electronic appurtenances. The center (10 ft. x 22 ft.) trailer houses a 90-kWh-capacity, lead-acid storage battery. The rear trailer houses the 3-kW nitrogen generator used in the fertilizer-manufacturing experiment and also serves as an office and storage area.

In the upper right section of the photo are the two 6000-bushel storage bins which are used in the grain-drying experiment. These bins are used to store and dry the corn harvested from the nearby fields. For drying, each bin is supplied with air by a 5-hp fan which is powered from the PV system.

The five poles located behind the array support air terminals and ground cables, which are strung from pole to pole for lightning protection.

2.3 Participants

The 25-kWp PV system at Mead, Nebraska was designed, built and installed during the first seven months of 1977. The development, implementation and management of the PV system included these principal participants:

U.S. Energy Research and Development Administration (ERDA)
(later to become the U.S. Department of Energy),
Washington, D.C. 20585

MIT Lincoln Laboratory
Lexington, Massachusetts 02173
William Romaine, Project Engineer

University of Nebraska
Agricultural Engineering Department
Lincoln, Nebraska 68503

Charles F. Kettering Research Laboratory
Dayton, Ohio 45429.

The Mead PV power system was formally dedicated on 27 July 1977. The system was then used for the remainder of the irrigation season to power a 10-hp motor used to irrigate the 80-acre cornfield. In the fall of 1977, provisions for supplying ac power to two 5-hp fans for grain drying were implemented and an automatic controller (to allow essentially unattended operation) was installed. In December 1978 the Charles F. Kettering Research Laboratory began development work on a 3-kW nitrogen generator to be powered by the PV collector. This system was installed at Mead and began operation on 25 July 1979.

2.4 PV System Loads

The loads served by the Mead PV system are directly related to each of the following agricultural experiments:

2.4.1 Crop-Irrigation Experiment

The Mead PV system was designed to furnish power to a 10-hp pump plant for 12-hours-per-day irrigation of 80 acres of corn (3,5). This plant pumps water from the two-acre-foot-capacity reuse pit to an automated gated-pipe irrigation system. The pressure in the gated-pipe varies from 4 to 6 pounds

per square inch (gauge) and flow rates vary from 900 to 1100 gallons per minute, depending on the water level in the reservoir and on which section of the site is being irrigated. The automated gated-pipe system (Fig. 2-2) with a reuse pit was selected because of its high water-application efficiency (85 to 92% is directly absorbed by the soil) and its low power requirement.*

CP267-1938

Fig. 2-2. Automated gated-pipe irrigation system.

Irrigations are scheduled through the University of Nebraska-Lincoln's Agricultural Computer Network (AGNET). This scheduling procedure utilizes readings from electrical resistance blocks installed in the fields (which provide a measure of moisture content), a minimum-maximum thermometer to compute projected crop water needs, a water meter, and various other instruments which yield crop and soil data and irrigation system water-application efficiencies. The base data for the crop, the irrigation system, the type of water meter, and the electrical block meter are entered into the field file of the computer. Each week the data are updated with temperature, water meter, and electrical resistance block readings from the various locations

*The energy required to power the gated-pipe system at 900 gpm is only 6 hp compared to 40 hp for a center-pivot sprinkler system.

in the field. A computer program then prints out an update showing crop water use, soil moisture reservoir status, and the date of the next irrigation.

2.4.2 Grain-Drying Experiment

Following its use during the summer irrigation season, electricity generated by the Mead PV unit is used during the fall and winter months to power fans for the in-bin, crop-drying experiment.

Each year, corn harvested from the 80-acre site is stored to dry in two grain bins located near the PV array (Fig. 2-3). Each 27-ft.-diameter bin is capable of holding 6,000 bushels of grain, and is equipped with loading and unloading equipment, full perforated floor, and a 5-hp centrifugal fan, sized to provide one cubic foot of air per minute per bushel of corn (6).

CP267-1734

Fig. 2-3. Solar-powered, crop-drying bins.

The PV system is able to provide electricity to power the two fans for approximately 12 hours per day. Conventional in-bin, grain-drying systems depend on 24-hour-per-day operation. In order to compare performance of an intermittent solar-cell-powered fan operation with that of a conventional, 24-hour-per-day operation, the fan in one of the bins is switched to utility power for continuous operation. The fan in the other drying bin is operated only for the number of hours per day that the solar unit can provide power for the two fans. A direct comparison of the drying results between conventional and solar-cell-powered, in-bin, grain-drying systems could thus be made (3).

2.4.3 Fertilizer-Generation Experiment

In August 1979, a 3-kW nitrogen-fertilizer-generator system, developed by the Charles F. Kettering Research Laboratory and powered by the 25-kWp array, was installed at Mead, Nebraska (7). The purpose of the project was to test the performance of a small nitrogen-fertilizer generator using surplus output from the PV array during those times of the year when irrigation or crop drying are not taking place.

The nitrogen-fertilizer-generator system operates by passing air through a high-voltage electric arc which causes nitrogen and oxygen to combine into nitrogen oxides such as NO, NO_2, and N_2O_4. Next, these nitrogen oxides are trapped in water to produce nitrous acids. Limestone, $Ca(CO_3)$, is introduced to neutralize the nitrous acids into calcium nitrate, $CA(NO_3)$, a desirable form of nitrogen fertilizer. The fertilizer-generator's basic components, a reaction electric cell, power, an air pump, an absorption column containing limestone and water, and a holding tank, are shown in Fig. 2-4.

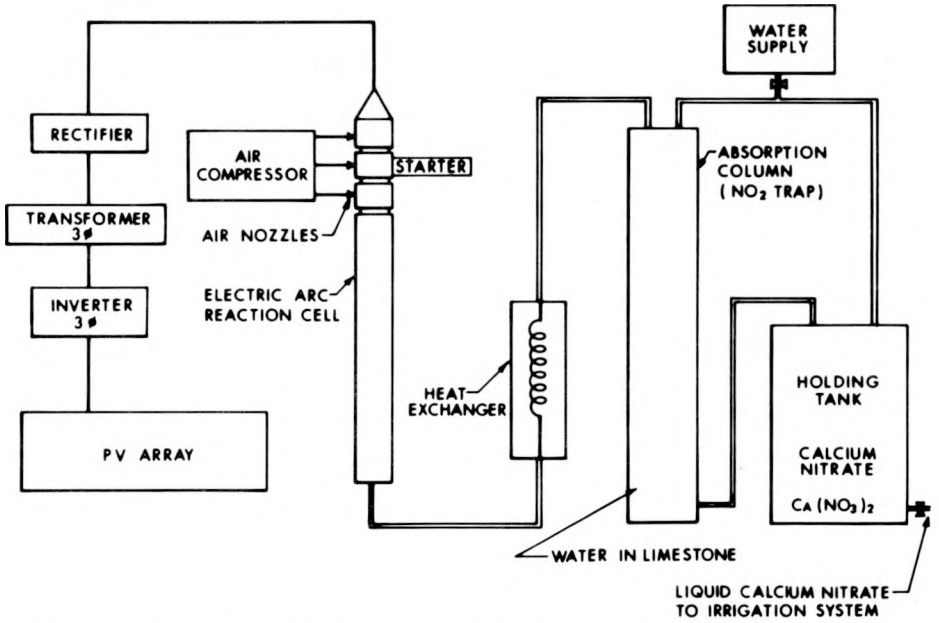

Fig. 2-4. PV-powered nitrogen-fertilizer generator.

2.5 Solar Availability

Mead, Nebraska, located in the heart of the U.S. corn belt, is fairly representative of the central farmland regions of the country. Some of the

significant climatic parameters of the region are presented in Table 2-1. The site latitude and longitude are 41.2°N and 96.5°W, respectively.

TABLE 2-1

INSOLATION AND TEMPERATURE DATA, NORTH OMAHA, NEBRASKA*

	Maximum Daily Temp.°C	Minimum Daily Temp °C	Average Monthly Temp °C	Heating Degree Days Base 18.3°C	Cooling Degree Days Base 18.3°C	Total Global Radiation kW/m^2	Global $\bar{K}_t$ Cloudiness Index
JAN	-1.61	-11.55	-6.55	771	0	61.9	0.494
FEB	1.55	-8.83	-3.61	614	0	78.8	0.509
MAR	6.72	-3.83	1.44	523	0	119.5	0.509
APR	16.11	3.83	10.00	253	3	147.4	0.512
MAY	21.88	10.22	16.05	103	32	183.0	0.534
JUN	26.77	15.66	21.22	18	105	200.8	0.573
JUL	29.66	18.22	23.94	3	177	205.9	0.584
AUG	28.88	17.44	23.16	5	155	181.7	0.574
SEP	24.00	12.00	18.00	55	45	129.9	0.516
OCT	18.83	6.00	12.44	190	7	102.6	0.525
NOV	8.55	-2.05	3.27	451	0	60.9	0.450
DEC	1.27	-8.33	-3.49	676	0	49.9	0.443
ANNUAL	15.22	4.05	9.66	3667	527	1522.3	0.531

*Knapp, C., et al, Insolation Data Manual, SERI/SP-755-789, October 1980, SERI, Golden, Colorado.

Note: These data were collected at SOLMET station #94918, North Omaha, Nebraska, a location in close proximity to Mead. Latitude and longitude of the SOLMET station are 41°22'N and 96°31'W, respectively.

On an annual basis, a horizontal surface at Mead receives an insolation of approximately 1500 kWh/m^2. A summary of the horizontal insolation data measured at the site in 1978, 1979 and 1980 is presented in Table 2-2. Meteorological data measured at the site during this same time period are presented in Table 2-3.

As a test bed for agricultural PV systems, the Mead site provides a location which has experienced temperature extremes of -33°C (-27°F) and 46°C (115°F), and has an average annual rainfall of approximately 28 inches and an average annual snowfall of approximately 30 inches.

TABLE 2-2

MEAD INSOLATION DATA
AVERAGE HORIZONTAL INSOLATION (kW/m^2)

Month	1978 Daily	1978 Monthly	1979 Daily	1979 Monthly	1980 Daily	1980 Monthly
JAN	2.3	71	2.4	74	1.8	56
FEB	3.0	84	3.1	87	2.6	73
MAR	4.0	124	3.2	99	3.9	121
APR	4.6	138	3.7	111	5.0	150
MAY	5.9	183	6.2	192	5.3	164
JUN	7.1	213	6.4	192	6.9	207
JUL	5.7	177	4.9	152	5.8	180
AUG	5.9	183	4.7	146	7.3	226
SEP	4.5	135	4.3	129	4.6	138
OCT	3.4	105	3.0	93	3.6	112
NOV	1.9	57	2.0	60	2.4	72
DEC	1.9	59	1.8	56	1.5	47
ANNUAL		1529		1391		1546

TABLE 2-3

MEAD METEOROLOGICAL DATA

Date	Prec.(in.)	Ambient Temp(°C) Max.	Ambient Temp(°C) Min.	Subfield Temp(°C) Max.	Subfield Temp(°C) Min.	# of Freeze/Thaw Crossovers
1978						
Jan	0.15	-8.7	-17.3	15.9	-19.3	N/A
Feb	0.20	-7.0	-17.5	---	---	N/A
Mar	0.76	---	---	---	---	N/A
Apr	6.05	14.3	5.5	---	---	N/A
May	3.99	21.9	12.0	38.8	---	0
Jun	3.79	32.1	17.4	47.1	---	
Jul	4.25	30.5	19.4	49.9	15.0	
Aug	1.79	28.9	15.5	---	---	
Sep	5.96	27.2	5.3	45.4	12.2	
Oct	0.81	18.3	3.4	37.9	0.8	0
Nov	0.31	7.0	-3.0	20.6	-4.8	8
Dec	0.17	-1.8	-10.8	15.8	-12.5	20
Total	28.23					28
1979						
Jan	0.74	-8.0	-16.9	5.0	-18.6	4
Feb	0.21	-3.4	-16.5	-16.1	-3.4	17
Mar	3.13	9.4	-2.2	25.0	-4.2	28
Apr	1.59	8.0	0.5	22.3	-1.5	12
May	0.09	18.1	6.2	42.0	5.2	0
Jun	2.22	27.4	20.0	45.2	11.7	
Jul	2.36	28.8	17.0	55.2	15.2	
Aug	2.59	28.4	16.6	52.7	14.6	
Sep	0.00	27.2	13.9	52.2	12.8	0
Oct	4.78	18.0	3.7	34.1	-0.1	8
Nov	0.66	6.4	-4.6	24.2	-5.8	30
Dec	0.33	6.6	-6.6	21.6	-7.4	45
Total	18.70					144
1980						
Jan	0.25	-0.8	-9.3	14.6	-9.5	38
Feb	0.32	-1.2	-10.6	14.0	-9.2	42
Mar	0.93	6.9	-3.6	22.7	-3.2	33
Apr	1.67	16.7	4.2	34.0	3.2	0
May	2.47	23.3	10.2	43.6	8.6	
Jun	3.95	31.8	18.1	50.3	16.2	
Jul	0.83	32.0	13.6	56.1	17.7	
Aug	6.56	30.6	14.4	54.0	17.2	
Sep	0.48	25.0	9.1	46.0	9.0	
Oct	0.00	21.6	4.8	34.8	4.8	0
Nov	1.08	13.3	-0.7	29.4	-4.2	6
Dec	0.84	8.5	-7.5	13.6	-7.6	25
Total	19.38					144

2.6 PV System Description

The Mead PV system consists of an array of PV cells which nominally produce a maximum output power of 25 kW at an insolation of 1 kW/m^2. It is a stand-alone system and includes a battery subsystem with a rated storage capacity of 90 kWh, an inverter, a controller, a power dump, and a data collection and management subsystem. Utility power is available in parallel and is used: (1) for carrying the load whenever the battery depth of discharge becomes excessive, (2) for powering a battery charger during periodic equalization of the battery cells, and (3) for taking care of the overhead electrical power needs of all instrumentation, control, heating and cooling units. In addition, the system includes an uninterruptible power supply which is called into play whenever there is a loss of utility power. It also provides power to the instrumentation system, thus ensuring the capture of data if the PV system malfunctions. The block diagram of the system presented in Fig. 2-5 defines the various electrical loads placed on the system and shows the interconnection of all subsystem elements.

C74-385

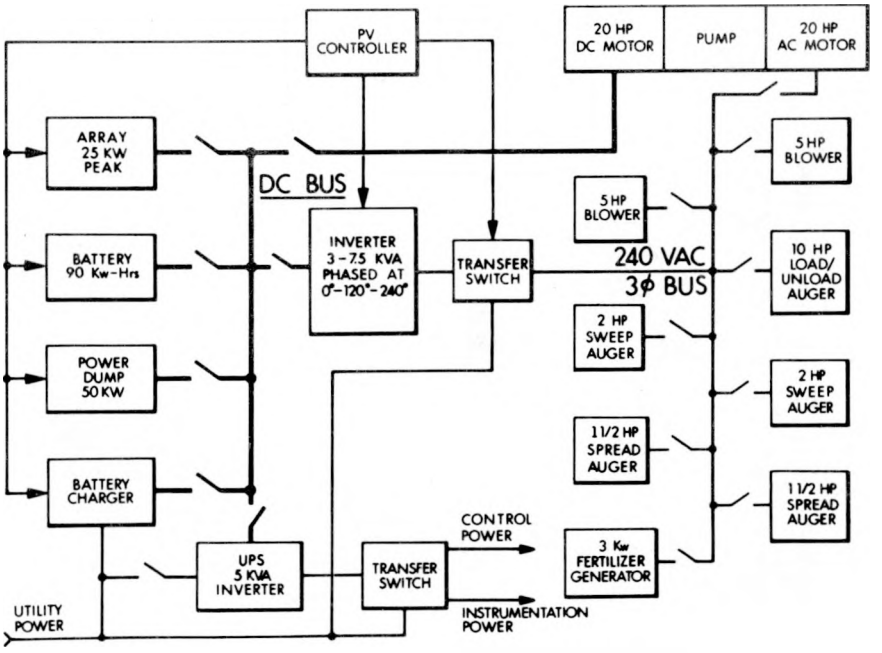

Fig. 2-5. Mead PV system block diagram.

The four major subsystems which comprise the PV power system at the Mead, Nebraska, site are the PV array, the batteries, the power-conditioning equipment, and the data-acquisition unit.

2.6.1 PV Array

The Mead array field consists of 2240 PV modules: 728 Solarex (Block II) and 1512 Sensor Tech (Block II) modules. All of the modules were purchased by Jet Propulsion Laboratory (JPL), Pasadena, California, as part of a 127-kW, multisource "Block II" procurement which they managed for DOE in 1976/1977.

Figure 2-6 shows a closeup of the array, illustrating the two different types of modules which it contains. The front row contains modules manufactured by the Solarex Corporation of Rockville, Maryland. Each module is approximately 2 feet square and generates a specified power output of 16 W minimum at 60°C at an insolation of 100 mW/cm^2. Each module contains 42 series-connected, 3-in.-diameter cells; the module terminal voltage under maximum power operation is 15.8 V minimum.

CP267-1670

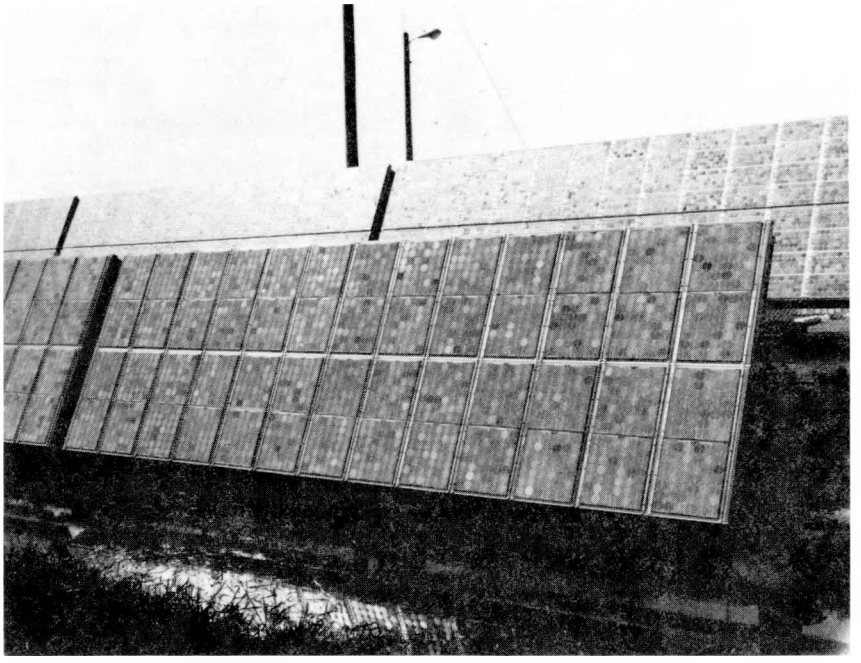

Fig. 2-6. PV array closeup.

The rear row is filled with modules manufactured by Photowatt (then Sensor Technology) Corporation, Chatsworth, California. These modules are

approximately 1 ft. x 2 ft., and each contains 44 series-connected cells 2-1/8 in. in diameter. Specified power is 8.17 W minimum at 60°C for insolation which is 100 mW/cm^2. Output voltage is 16.5 V under specified conditions.

Altogether the Mead array contains approximately 100,000 silicon solar cells arranged in 2240 silicon-encapsulated PV modules. The modules are grouped into 28 flat panels, each 2.5 m high by 7.6 m long. The panels are arranged in two southfacing rows of 14 each, and are mounted on trunnions to permit individual control of the panel elevation from 0 to 65° above horizontal. Although these limits of tilt were imposed by constraints of the hydraulic elevation-control mechanism, computer simulations (8,9) indicate little or no advantage in tilt angles greater than 65° for the Mead latitude. The array, which occupies 1/3 acre, was constructed on the berm of the Mead reservoir to avoid using valuable farmland. It was designed to withstand 100-mph winds.

2.6.2 The Battery

The Mead battery subsystem consists of two parallel banks of 6-V, lead-acid batteries manufactured by C&D Corporation (Type 3CBSB-11), rated 375 ampere-hours (Ah) each at an eight-hour discharge rate. These batteries were designed for railroad caboose service and have an expected life of five years when deeply discharged once a day. To enhance life in deep-discharge service, the batteries employ a hybrid lead-antimony-calcium construction with PbSb anodes and PbCa cathodes.

There are 20 batteries in each bank with a nominal (2 V per cell, 3 cells per battery) terminal voltage of 120 V and a total capacity of 90 kWh (72 kWh to the recommended 80% depth of discharge). At installation the nominal battery voltage was 120 V. Later, one module was dropped from each of the two strings in order to make better use of the 750-Ah rated capacity. This reduced the nominal voltage to 114 V and the energy capacity from 90 to 86 kWh. The useable capacity is 80% of the rated capacity.

Figure 2-7 is a view looking into the battery trailer. The positive and negative outputs of each battery bank are brought separately to the equipment trailer for switching onto the main dc bus. In addition, each bank can be

divided at its midpoint by a fused disconnect in order to render the entire battery safer during periods of maintenance or for the replacement of individual units. Although not visible in the figure, a hydrogen gas sensor is mounted high on the trailer's west wall. The electronics for this sensor, including an audible alarm, are located in the equipment trailer.

CP267-1751

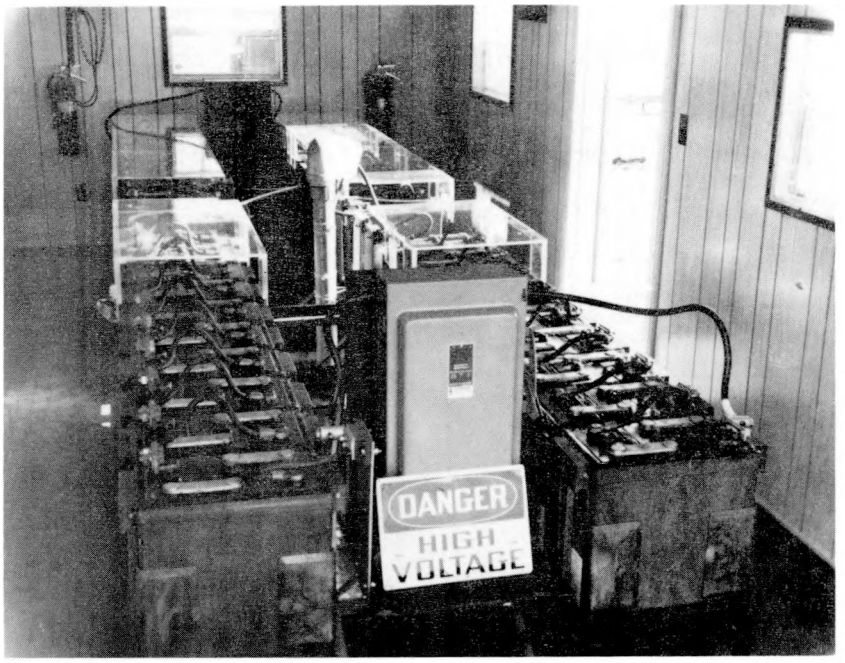

Fig. 2-7. Interior view of battery trailer.

Minimal maintenance is required on the Nebraska battery. Equalizations are made on an average of every six months, the frequency depending upon the types of tests being run throughout the year. If the batteries are lightly cycled and fully charged by the array on most days, then frequent equalizations are not necessary. The more time the battery is kept from full charge, the more often equalizing charges are needed. The battery must be watered at least every three months, and this requirement will increase with battery age because of electrochemical reactions caused by the antimony in the plates (10).

2.6.3 Power Conditioning

The two principal power-conditioning elements are the three-phase inverters, used for coverting the array-battery output from dc to

three-phase ac, and a solid-state solar controller, used for automatically regulating system loads and various other inverter and battery-charging functions.

- Inverters

The dc power from the array is converted to three-phase ac power by three separate single-phase, 7.5-kVA units, built by NOVA Electric Company in Nutley, New Jersey, and modified extensively by Lincoln Laboratory. The three inverters are controlled by a single master circuit which is capable of producing any frequency-voltage output desired between 30 and 60 Hz and 120 and 240 V, respectively. This variable-frequency feature of the inverters permits variable-speed operation of the pump motor, used during the irrigation experiments (11).

A simplified block diagram of the inverter control is shown in Fig. 2-8. The main elements, following the phase-lock loop which synchronizes the 60-Hz output to an external reference (the utility line), are the ramp generator and subsequent voltage-to-frequency converter. With this control scheme the inverter delivers ramped voltage- and frequency-time functions, which enhance motor startup. Typical values for the Mead system (e.g., to start either the 15-hp induction motor or the crop-drying fan motors) were a 60-second ramp starting at 120 Vac/30 Hz and proceeding to full voltage and frequency, namely, 240 Vac/60 Hz.

- Solid-State Solar Controller

The solid-state solar controller performs the following automatic functions: (1) battery voltage is constrained to remain within preset limits which are presently 147 and 110 V (incremented steps of the power dumps are used to keep the voltage below the upper limit), (2) the system load is switched to utility and the inverter is turned off whenever the voltage drops below 110 V, and (3) the inverter is turned on whenever the bus voltage exceeds the preset limit and uses the power dump to keep the array from overcharging the battery (2).

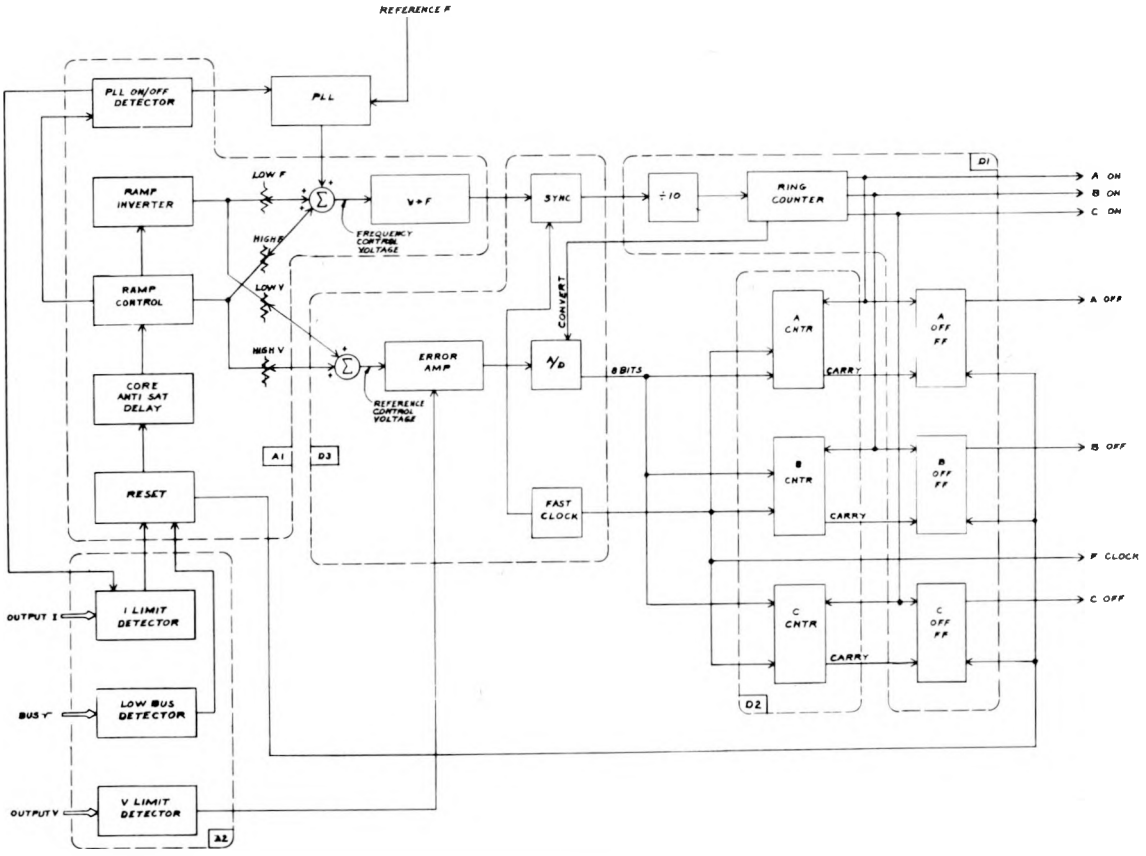

Fig. 2-8. Block diagram of inverter control logic.

2.6.4 Data Acquisition

The Mead, Nebraska, data-acquisition system uses a comprehensive collection of sensors and data-logging equipment to monitor and collect a wide variety of data at regular 10-minute (daytime) and 20-minute (nighttime) intervals (12). As anticipated, continuous monitoring of the entire PV system over the past several years has produced an extensive library of data on solar insolation, weather and PV system performance.

Figure 2-9 presents a block diagram of the data-acquisition system as it existed during the early (1978-1979) stages of operation. As the figure illustrates, the initial data-acquisition system consisted of a Fluke 2240-A, 60-channel data logger with a Tektronix 4923 cartridge recorder and 4051 terminal connected to a 202 data set on a dial-up telephone system. Data were

transmitted from the site at regular intervals to a Tektronix 4051 terminal at Lincoln Laboratory, then to the Laboratory's time-sharing system (an IBM 370/168) for processing and archiving. Once the data were transferred to the IBM 370/168, three principal forms of reduced output became available: a SOLMET-formatted tape which provided weather and insolation data, a tape containing the measured system parameters, and graphic and tabular summaries of the measured data.

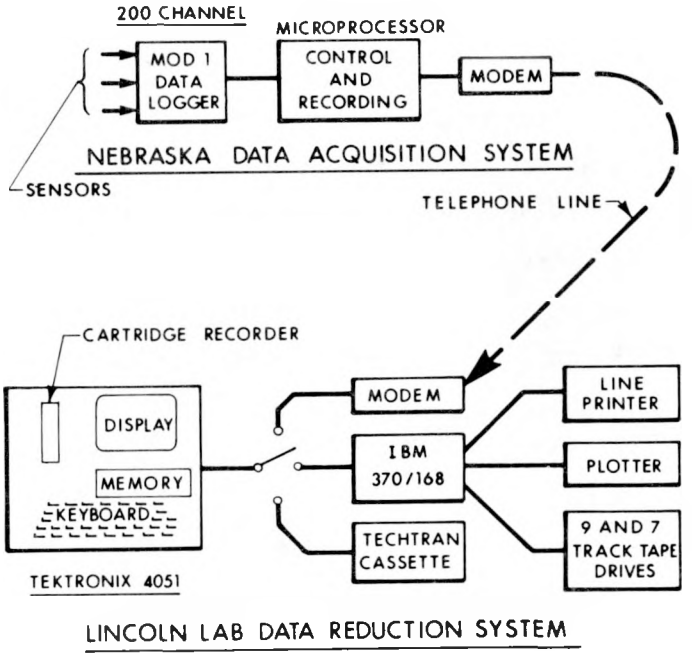

Fig. 2-9. Data acquisition and reduction system.

The present data system, installed in mid-1979, no longer makes use of the Fluke 60-channel data logger and the dial-up telephone data-transmission system shown in Fig. 2-9. Instead, the system uses a Consolidated Control 200-channel data logger under program control of the 4051. Data are recorded on a Columbia 300-D cartridge manufactured by Columbia Data Products, Columbia, Maryland. Data collected by the data system are recorded on 450-ft.-length 3M-tape data cartridges and mailed to Lincoln Laboratory at regular 7-day intervals for processing and archiving on the Laboratory's Amdahl 470 time-sharing system.

Experience has shown that the high storage capacity of the Columbia recorder (2-3 weeks), as well as its unique power fail-restart capability, make it ideal for that remote and frequently unattended site. In addition, this method of storing and retrieving data has proven to be far superior to the more costly and frequently disruptive telephone dial-up service previously used.

2.7 System Performance

During the three-year period (1978-1980) when measurements were made on the Mead system on a continuous basis, the 25-kWp PV system provided approximately 107 MW hours of energy. Electrical energy produced by the PV system provided 100% of the power needed throughout the growing season to meet the irrigation requirements of the 80-acre cornfield, as well as significant portions of the power required for the other PV-related grain-drying and fertilizer-manufacturing experiments. Array peak output power, measured during the 1978, 1979 and 1980 winter and summer months, averaged 18 kW and 22 kW, respectively. During January, the average electric energy produced by the array per day was 81 kWh; during August it averaged 148 kWh over the same three-year interval. Data analyses indicate that the Mead system has performed up to expectations, if due allowance is made for degradation of various components and seasonal soil/snow accumulation on the array.

2.7.1 PV Array Performance

Figure 2-10 presents a composite plot of the three-year array output versus time. These data indicate a signature of gradually decreasing array output with periodic repeatability. During the first year of operation (1978), for example, the array output totaled 37.7 MWh, whereas the 1979 and 1980 total array outputs were 36.4 MWh and 32.9 MWh, respectively. A tabulated monthly summary of array output, as well as total tilted insolation values measured over the same period by a pyranometer set at the same inclination as the array, are presented in Table 2-4. A computerized "scatter" plot of total array energy output versus total tilted insolation, measured during each day of 1979, is presented in Fig. 2-11.

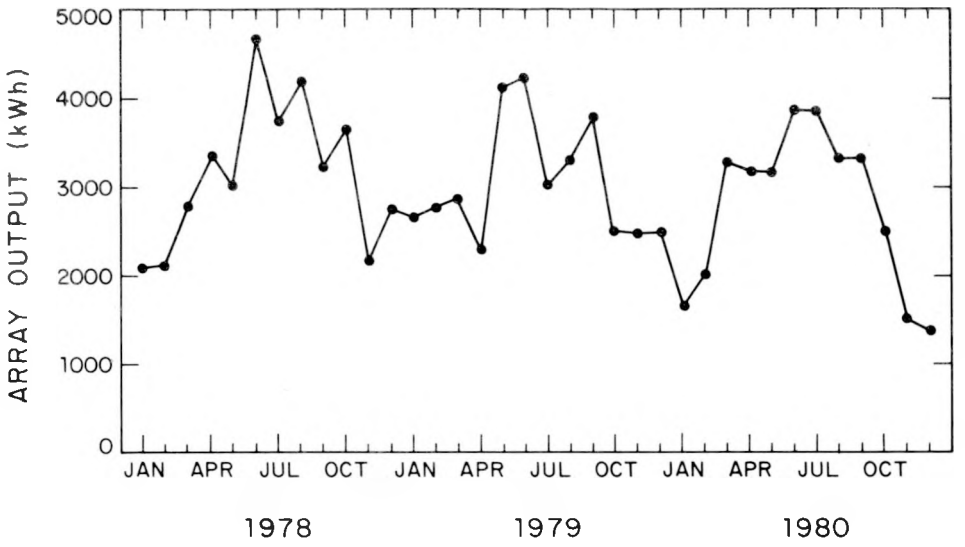

Fig. 2-10. Array output versus time.

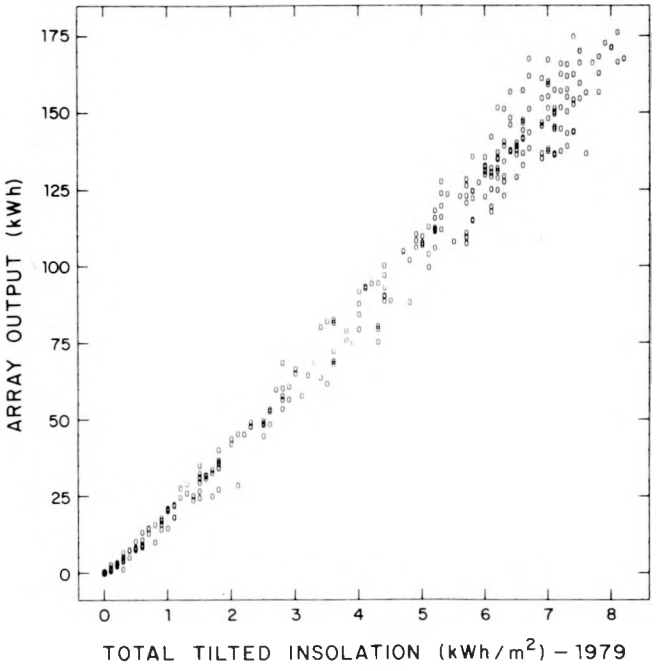

Fig. 2-11. Total array output versus total tilted insolation.

TABLE 2-4

MEAD, NEBRASKA, PV POWER SYSTEM

	TOTAL ARRAY OUTPUT (kWh)			TOTAL TILTED INSOLATION (kWh/m^2)		
	1978	1979	1980	1978	1979	1980
JANUARY	2,075	2,671	1,648	104	130	95
FEBRUARY	2,086	2,755	2,002	120	125	96
MARCH	2,787	2,845	3,285	128	149	156
APRIL	3,352	2,284	3,185	111	108	170
MAY	3,015	4,157	3,171	161	192	163
JUNE	4,668	4,248	3,877	220	203	214
JULY	3,727	2,996	3,835	190	152	194
AUGUST	4,197	3,300	3,333	201	167	187
SEPTEMBER	3,228	3,769	3,307	162	181	169
OCTOBER	3,623	3,494	2,520	178	139	138
NOVEMBER	2,154	2,462	1,505*	97	120	119
DECEMBER	2,751	2,482	1,287*	118	119	80
TOTALS	37,663	36,463	32,954	1,790	1,785	1,781

*Low array output values measured during November and December, 1980, are attributed to interruptions in the continuous recording of data during this time interval.

Array output averages of 21.4 kWh for every 1.0 kWh/m^2 of insolation during 1978, of 20.4 kWh in 1979, and of 19.0 kWh in 1980 indicate a 10% decrease in array output over the three-year period (13). This decrease is attributed to degradation of various components, as well as insufficient array cleansing. During 1980, for instance, the array was not washed; it had been manually cleansed twice a year during the two previous years of operation. After many months of field operation, a 10-15% loss is not unrealistic for the silicone-encapsulated modules used in the Mead system.

Figure 2-12 presents a detailed plot of the daily performance of the Nebraska array versus individual days for 1978 and 1979, with full monitoring beginning on 24 March 1978 (14). These data clearly reflect the effects on the array of various field and environmental activities such as array washing, crop planting and harvesting, pollination, and snow cover. Dramatic increases of 8%, 6% and 13% in array output on 27 March 1978, 24 September 1978 and

17 October 1979, respectively, are the direct results of array washings, whereas noticeable decreases in array performance coincide with soil settling upon the arrays during corn planting (April) and harvesting (October).

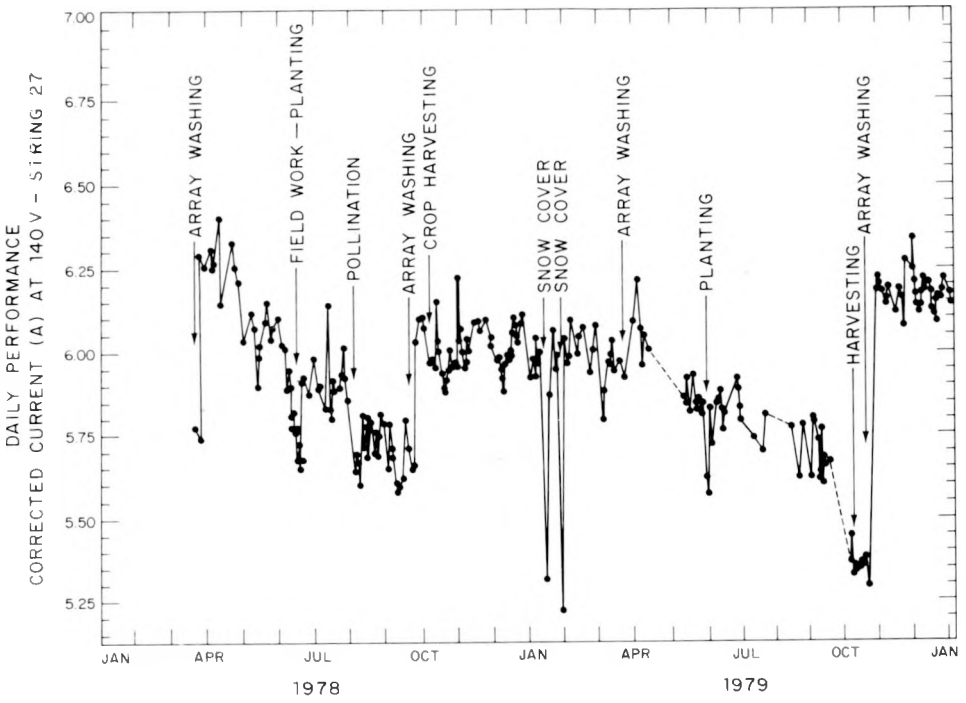

Fig. 2-12. Factors affecting array output.

After 39 months of field operation, the number of PV module failures at Mead totaled 96, or 4.28% of the 2240 modules installed there (15,16). (A failed module is one which produces less than 75% of its nominal short-circuit current under the measurement conditions.) Table 2-5 summarizes the number of failures found during each module investigation.

The cumulative number of failures (expressed as a percentage) is plotted as a function of time in Fig. 2-13. As both the table and figure indicate, this curve has been rising at an increasing rate over the past years.

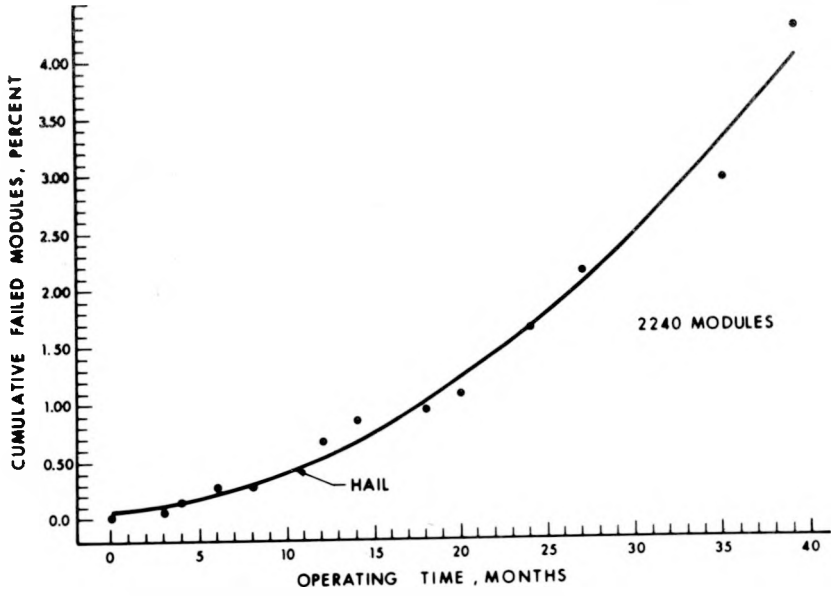

Fig. 2-13. In-service performance record for Mead PV modules.

TABLE 2-5

Module Failures at Mead Test Site

Front Row = 728 Modules
Back Row = 1512 Modules
Starting Date = July 1977

Date of Search	Number of Failures Found	
	Front Row	Back Row
Oct. 1977	0	1
Nov. 1977	1	1
Feb. 1978	0	3
Mar. 1978	0	0
Jul. 1978	6	3
Sep. 1978	3	1
Feb. 1979	2	0
Mar. 1979	1	2
Jul. 1979	6	7
Oct. 1979	1	10
Jul. 1980	11	7
Oct. 1980	4	26
TOTALS	35	61

2.7.2 System Energy Flow

Table 2-6 shows the array, battery, power dump and inverter energy-balance histories for 1978, 1979 and 1980. The energy balance is calculated from the sum of the array and battery discharge energy less the battery charge, inverter, power dump, UPS and dc motor energies. As these data illustrate, the entire system-energy balance is within 1% of the total energy supplied by the array.

TABLE 2-6

SYSTEM ANNUAL ENERGY BALANCE

	Array Output (kWh)	+	Bat. Out (kWh)	=	Bat. In (kWh)	+	Inv. In (kWh)	+	UPS (kWh)	+	Power Dump (kWh)	+	DC Motor (kWh)
1978	37.7×10^3		7.3×10^3		9.9×10^3		21.0×10^3		0.8×10^3		12.7×10^3		
1979	36.4×10^3		6.5×10^3		8.8×10^3		19.5×10^3		6.3×10^3		7.8×10^3		
1980	32.9×10^3		6.0×10^3		7.4×10^3		10.0×10^3		7.0×10^3		10.8×10^3		3.9×10^3
TOTALS	107.0×10^3		19.8×10^3		26.2×10^3		50.5×10^3		14.1×10^3		31.3×10^3		3.9×10^3
ENERGY BALANCE			126.8×10^3	=	126.0×10^3 kWh (within 1% agreement)								

A block diagram, showing the Mead system energy flow during the three-year measurement period, is presented in Fig. 2-14. Estimates of various subsystem efficiencies also are given in this figure.

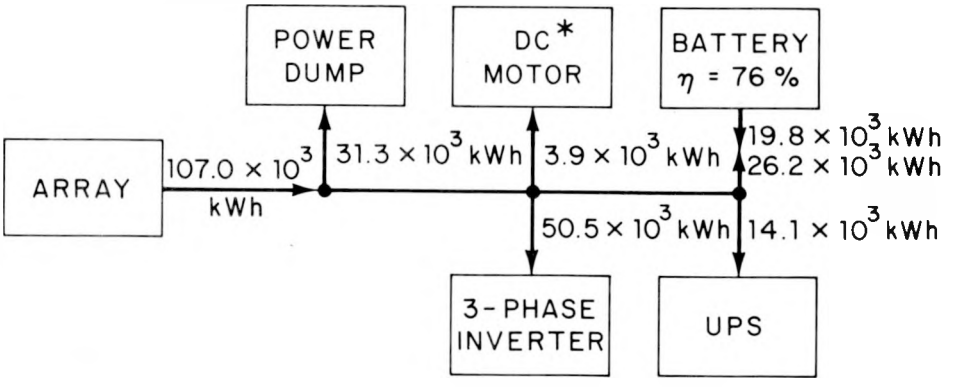

*DC MOTOR INSTALLED 3 JULY 1980

Fig. 2-14. PV energy system flow.

Data analyzed on the Nebraska battery subsystem show a range of battery out/in efficiencies from 66 to 84%, depending upon the load profile. The 78% efficiency, based on three years of operation with no system breakdowns, agrees very favorably with battery energy efficiencies of 80% and 77%, measured during two identical tests in October 1978 and April 1980, respectively. During this same measurement period, the main inverter operated for more than 6,000 hours before experiencing a breakdown, and it exhibited an efficiency of 80% at full load.

2.7.3 PV Energy Usage

Data results show that the Mead, Nebraska, PV system has produced approximately 35,000 kWh of dc electricity annually over the past three years. Of this total, the irrigation and grain-drying systems each consumed an average of 7,500 kWh per year, leaving approximately 20,000 kWh of energy, produced primarily during the winter and spring months, for alternative uses. This excess energy was typically used to operate the nitrogen-fertilizer generator which produced approximately one pound of fixed nitrogen per day (7).

2.7.3.1 Irrigation Experiment Results

During three years of field operation, the PV-powered irrigation system provided all the power necessary to pump from the storage reservoir and meet the crop water-use requirements for the 80-acre cornfield. Data collected during 1978, for example, indicate that during the heart of the irrigation season from 1 August to 10 September, 81% of the 5,220 kWh of energy produced by the array was used to pump 114,000 m^3 of water (17). The electric motor used for running the irrigation pump consumed power from the array at a peak rate of 12.5 kW. This includes the 10% inverter-loss factor.

Installation in 1980 of a 20-hp dc motor to operate the irrigation pump increased irrigation efficiency by 10%. By better matching the load to the available PV power, the new motor provided the advantages of reducing the amount of energy transferred to and from the battery-storage system and permitting a reduction in the battery-storage capacity to 20 kWh (7).

2.7.3.2 Grain-Drying Experiment Results

In 1978 and 1979, harvesting took place during the first and last weeks of October, respectively, and the grain was immediately placed in grain-drying bins. Throughout the drying operation, the PV system provided electricity to power the two 5-hp fans for approximately 12 hours a day. Since conventional in-bin, grain-drying systems depend on 24-hours-per-day operation, utility backup power was used during intervals when solar energy was not available. Thus, the PV system was able to serve approximately 50% of this particular demand. Approximately 7,500 kWh of PV-array-produced energy were used to operate the crop-drying fans during each grain-drying season.

2.7.3.3 Fertilizer-Generating-Experiment Performance

Since July 1979, the PV array has been supplying power to the nitrogen generator at Mead, Nebraska (18). Data analysis shows that the 3-kW generator produces approximately 16 grams N/kWh, or 480 grams per 10-hour day. Based on this performance, the system, if run continuously, could produce between two and three tons of calcium nitrate fertilizer per year in water solution (17% nitrogen by weight).

At the system's present efficiency, about 50,000 kWh of electric power from the PV system are required to produce one ton of 100% nitrogen fertilizer. It is reasonable to examine the economics of using excess PV energy for this function as opposed to the other logical alternative, namely, selling it to the local utility. At commercial rates for electricity in Lincoln, Nebraska (about 5¢ per kWh), assuming a 100% sell-back rate and based on the present efficiency of this system, the cost of calcium nitrate fertilizer (the Mead product is 17% pure nitrogen) is about $375 per ton. The current market price of calcium nitrate (with a pure nitrogen content of 15.5%) is $150 per ton delivered. Thus, in order to be competitive with commercially produced calcium nitrate, the nitrogen generator at Mead must be able to produce on-site calcium nitrate at a cost of roughly half its present value. Research is being conducted by Kettering to increase the present system efficiency. Also, a large proportion of the energy input into the system appears as heat, which can be used for crop drying or space heating and thus further improve the overall economics of the system.

2.8 Lessons Learned

Lessons learned while operating, maintaining and evaluating the PV solar system during the past several years are summarized below.

2.8.1 System Complexity

The complexity of the present Mead system is a result of several factors: (1) the "flexible test bed" nature of this experimental system, (2) the desire to imbed a significant number of data-collection sensors within the system, (3) the stand-alone feature of the system design, as opposed to a utility-interactive design with no on-site storage, and (4) the first-time nature of the field test. Although the resultant system complexity, both in terms of mechanical and electrical elements, is understandable, it is obvious that a major challenge facing designers of future operations will be to simplify all portions of such systems.

Greater simplification in design is required for all major mechanical and electrical components such as array foundations, panel support and tilt mechanisms (if any), wiring, control and switchgear. In contrast, the electronic functions associated with automatic control can beneficially accept a high degree of internal, but not external, complexity.

Taken as a whole, streamlining follow-on PV systems for agricultural applications will serve to reduce cost as well as to simplify on-farm maintenance. These factors are essential for the viability of similar PV systems.

2.8.2 Power Overhead

The Mead system, as implemented, operates as a stand-alone system with utility backup. This was done because the local utility (a rural electric cooperative) was not willing to have a utility-interactive PV system connected to it. This stand-alone feature incurs significant power overhead associated with operation of an uninterruptible power supply and with environmental control for battery. In addition, utility power is used for various overhead demands such as lights, heat, summer air conditioning (when required for personnel purposes) and the data and control subsystem. Shortly

after turn-on in 1977, it became obvious that overhead consumption, particularly for winter heat and summer air conditioning, would put a significant dent in the annual net energy production. Although much of this overhead is chargeable to the experimental character of the system, and thus could be reduced for future systems, the overhead associated with UPS and battery system operation is likely to be part of future systems. On the basis of three years of operation at Mead, it can amount to almost 20% of the total annual energy production of the PV system.

2.8.3 Stand-Alone Versus Utility-Interactive Operation

As a result of the decision to incorporate energy storage, the solar-derived electricity can be used for farm purposes at times when sunshine is either absent or intermittent. A consequence of this design was the complicated start-up sequence required of the inverter and control subsystems because of the lack of connection to the extremely stiff utility. (The alternative was to oversize the inverter drastically in order to accommodate the high starting currents, which would have resulted in significant decreases in inverter operating efficiency.)

Despite the minor advantage of being able to operate through a utility outage and at any time of the day or night, it now seems obvious that the disadvantages of stand-alone operation outweigh the advantages. As a consequence, one can expect that future systems will operate in parallel with the utility when one serves the site (i.e., utility interactive), with excess solar energy being sold back to the utility for later repurchase during periods of solar shortage.

This shift to parallel operation has the major advantage of significantly reducing cost, complexity and overhead by eliminating the battery-storage subsystem and many of the attendant system-control functions. It also allows the utility to absorb the motor-starting transients thereby obviating the need for a variable voltage/frequency motor-starting sequence. This in turn would eliminate any problems associated with the use of PV power for simultaneous applications such as pumping (with motor-startup sequence) and nitrogen-fertilizer generation or lighting, etc.

2.8.4 Motor Starting

As was discussed above, the demands on a stand-alone system associated with starting large motors are a significant driver in the overall design. Although utility interaction is the preferred solution, this is not possible in many rural applications, particularly in developing nations. For this reason, the motor-starting problem still requires a solution. However, for many such applications, this problem could be handled differently than was done at Mead. In particular, if an all-dc system is possible, the battery-storage unit can easily handle the large transient current demands. In the event that batteries are not present, the designer faces a problem comparable to the ac startup sequence used at Mead.

2.8.5 Automatic Control

Early in the course of the Mead project, it became obvious that two automatic-control subsystems were essential to the efficient and cost-effective use of PV power. One system is needed to control the PV system operation (e.g., battery charging, system protection, etc.) and another would be required to control the system applications (e.g., irrigation, crop drying, fertilizer production, etc.). Both should be designed for minimal operator intervention and should permit extended intervals (weeks) of unattended operation.

REFERENCES

1. Matlin, R. W., et al., "The 25-Kilowatt Photovoltaic Powered Agricultural Experiment in Mead, Nebraska," MIT Lincoln Laboratory Technical Report, 21 April 1978, COO-4094-4.

2. Bucciarelli, L. L., et al., "The Mead 25 kW Photovoltaic System," 1978 IEEE PV Specialists' Conference, Washington, DC, 5-8 June 1978, COO-4094-19.

3. Matlin, R. W., "PV Powered Irrigation Experiments in the U.S.," Atelier Pompage Solaire, Perpignan, France, 3-8 July 1978, COO-4094-28.

4. Romaine, W., "Description of the Mead PV Power System," MIT Lincoln Laboratory Technical Report, 5 January 1979, COO-4094-28.

5. Matlin, R. W. and Katzman, M. T., "The Economics of Solar Photovoltaic Energy Systems for Crop Irrigation in the United States," Atelier Pompage Solaire, Perpignan, France, 3-8 July 1978, American Journal of Agriculture Economics, Volume 60, November 1978, COO-4094-29.

6. Matlin, R. W., "25-kW PV Powered Irrigation and Grain Drying Experiment," International Solar Energy Congress, New Delhi, India, January 1978, COO-4094-13.

7. Hopkinson, R. F., "Performance of a PV-Powered 20-hp DC-AC Irrigation System and a 3-kW Nitrogen Generator," 14th IEEE PV Specialists' Conference, San Diego, CA, 7-10 January 1980, COO-4094-68.

8. Bucciarelli, L. L. and Hopkinson, R. F., "Performance of the Mead, Nebraska, 25-kWp Photovoltaic Solar Energy System Comparison with Simulation," 14th Intersociety Energy Conversion Engineering Conference, Boston, MA, 5-10 August 1979, COO-4094-43.

9. Bucciarelli, L. L. and Grossman, B. L., "A Comparison of Two Techniques for the Simulation of PV Systems," Second Annual Systems Simulation and Economics Analysis Conference, San Diego, CA, 23-25 January 1980, COO-4094-79.

10. Brench, B. L., "Operational Experiences in Lead-Acid Batteries for Photovoltaic Systems," presented at the 15th IEEE PV Specialists' Conference, Orlando, FL, 11-15 May 1981, COO-4094-118.

11. Landsman, E. E., "Motor Starting with PV Systems," 1978 IEEE PV Specialists' Conference, Washington, DC, 5-8 June 1978, COO-4094-16.

12. Cremin, J. D., "Design, Development and Implementation of Data Acquisition Systems for PV Tests and Applications Project," MIT Lincoln Laboratory Technical Report, 28 September 1978, COO-4094-24.

13. Bullwinkel, H. J. and Hopkinson, R. F., "Three-Year Performance Study of the Mead, Nebraska, 25-kWp Photovoltaic Power System," presented at the American Section of International Solar Energy Society Annual Meeting, Philadelphia, PA, 27-30 May 1981, COO-4094-122.

References (con't)

14. Holmes, J. M., "Estimating Degradation of Photovoltaic Array Performance from Array Output," submitted as thesis to Massachusetts Institute of Technology, June 1980.

15. Forman, S. E. and Themelis, M. P., "Performance Reliability of Photovoltaic Modules at Various MIT Lincoln Laboratory Test Sites," 14th IEEE PV Specialists' Conference, San Diego, CA, 7-10 January 1980, COO-4094-69.

16. Forman, S. E., "Detection of Electrically Failed Photovoltaic Modules at MIT Lincoln Laboratory Test Sites," MIT Lincoln Laboratory Technical Report, February 1981, COO-4094-112.

17. Sullivan, N. W., et al., "Management of Solar Cell Power for Irrigation," ASAE Paper No. 78-4529 (ASAE Vol. 23, No. 4), St. Joseph, MI, 1980.

18. Rein, B. K., et al., "Nitrogen Fertilizer from Solar Energy," ASAE Paper No. 80-3545, St. Joseph, MI, 1980.

3.0 1.6-KWP PV POWER SYSTEM AT CHICAGO MUSEUM OF SCIENCE AND INDUSTRY

3.1 Introduction

In 1977, MIT Lincoln Laboratory was contacted by the then U. S. Energy Research and Development Administration (ERDA) to assist in the design and construction of a PV system for use in a new ERDA-sponsored energy exhibit at the Chicago Museum of Science and Industry. The Museum is among the city's most popular attractions, and is the nation's largest science-oriented museum. It is situated on the shores of Lake Michigan, just south of the downtown area, and is visited annually by more than five million people from all over the world.

The 1.6-kWp PV system operating at the Museum has several unique features; the load is exclusively low voltage dc and the solar array is used only during the business hours of the Museum. The PV array is sized to meet this constant daytime-only load and to charge batteries with any excess power. The batteries supplement the array when output is low during early morning, late afternoon and cloudy weather; the net daily result is a discharging of the batteries. Battery charging with utility power is normally done only during off-peak hours, thereby aiding in utility load-leveling. For this reason, systems of this design are desirable from a utility's standpoint.

Contributions to this effort were made by Edward C. Kern and Miles C. Russell.

3.2 System Application

The "Energy Lab," as the museum exhibit is called, includes dozens of displays which provide information on energy concepts, our nation's energy supply problems, and possible solutions to these problems. Energy conservation and various forms of energy supply--including solar, fossil, nuclear and other alternatives--are presented in dynamic displays and demonstrations within the Energy Lab.

The PV power system is both an integral part of the exhibit and a source of energy for powering the lights and displays in the Energy Lab exhibits.

3.3 Participants

Participating in this project were the following organizations and individuals:

U.S. Energy Research and Development Administration
Office of Public Affairs
Washington, DC
Mr. Chester F. Gray (Chief, Exhibits Operation Section)

U.S. Energy Research and Development Administration
Chicago Operations Office
Argonne, Illinois
Mr. Robert Bauer (Manager)

Chicago Museum of Science and Industry
Chicago, Illinois
Mr. Dan MacMaster (President)
Mr. Olaf Harringer (Director of Exhibits)
Mr. Robert Diehl (Engineering Department)
Mr. Tom Scheffel (Exhibit Maintenance)

MIT Lincoln Laboratory
Lexington, Massachusetts
Mr. Marvin D. Pope (Principal Investigator)
Mr. Steven Sacco (Project Engineer)
Dr. Edward C. Kern, Jr. (Project Engineer)

Exhibits, Inc.
Franklin Park, Illinois
Mr. Albert L. Eischen (Manager of Engineering)

ERDA provided funding and sponsorship for the entire Energy Lab exhibit, including the PV display. The Chicago Operations Office of ERDA assisted in coordinating the opening ceremonies and disseminating information to the press and public.

MIT Lincoln Laboratory designed and engineered the PV array, the electrical wiring, and the control system. Specific areas of MIT Lincoln Laboratory support during the conceptual design stage included determination of insolation availability, optimization of array tilt and azimuth to match the load, array siting based on shadowing studies, and performance prediction using both physical scale models and computer simulation. During the detailed design stage, specific system-wiring layouts, system-control strategy, battery operational characteristics, and array-support-frame structural analysis were

recommended. During construction and system checkout, MIT Lincoln Laboratory assisted by providing PV array modules and test equipment, and by sending personnel to check out the system and resolve any problems encountered in the final days of construction.

Following the opening of the Energy Lab exhibit, MIT Lincoln Laboratory provided instrumentation to monitor system performance for several years.

3.4 PV System Loads

The loads served by the PV system are all low voltage dc and consist of incandescent lighting for one display, overhead chaser lights in the Energy Lab room, and a small dc motor which drives a revolving "solar fountain" display. The lighting load is predominantly resistive, and is approximately 1600 W. The lights themselves are 12 V, but are series/paralleled to achieve a 24-V, 66.7-A system. The motor uses 500 W making the total dc load of 2100 W. These lights are turned on daily for approximately 8 hours, from 9:00 a.m. to 5:00 p.m., the Museum open hours. The net daily energy consumption is approximately 17 kWh.

3.5 Solar Availability

Chicago, Illinois, is fairly representative of the central cold-climate regions of the country. Some of the significant climatic parameters are given in Table 3-1. This site latitude and longtitude are $41^{o}47'$ N and $87^{o}45'$W, respectively.

As a proving ground for solar PV systems, the Museum provides a location which has experienced temperature extremes of -21^{o}F and 105^{o}F, has an annual rainfall of approximately 34 in. and an annual snowfall of approximately 48 in.

3.6 PV System Description

The PV system at the Museum consists of a 1.6-kWp PV array, made up of early-technology Block I modules, a 27-kWh bank of batteries, a battery charger and the 2.1-kW lighting and motor load. The system was designed such that even on the "best" solar day the PV system will not overcharge the batteries,

TABLE 3-1

INSOLATION AND TEMPERATURE DATA
Chicago, Illinois*

	Maximum Daily Temp. °C	Minimum Daily Temp. °C	Average Monthly Temp. °C	Heating Degree Days Base 18.3 °C	Cooling Degree Days Base 18.3 °C	Total Global Radiation kJ/m^2	Global $\overline{K_t}$ Cloudiness Index
Jan	-0.27	-8.33	-4.27	701	0	5754.0	0.402
Feb	1.44	-6.55	-2.55	585	0	8620.0	0.439
Mar	7.00	-1.66	2.66	485	0	12562.0	0.464
Apr	15.16	4.66	9.94	251	0	16558.0	0.481
May	21.27	9.83	15.55	115	29	20302.0	0.511
June	27.00	15.72	21.38	14	106	22777.0	0.542
July	29.11	18.33	23.72	0	167	22060.0	0.539
Aug	28.50	17.83	23.16	4	153	19513.0	0.533
Sept	24.33	13.33	18.83	31	46	15365.0	0.511
Oct	18.33	7.55	13.00	175	10	10996.0	0.489
Nov	8.94	0.33	4.66	410	0	6419.0	0.402
Dec	1.83	-5.77	-1.94	628	0	4557.0	0.355
Ann	15.22	5.44	10.33	3403	513	13790.0	0.492

*Reference 1

thus eliminating the need for any battery-overcharge controller. During the night the charger brings the batteries up to full charge, so that over the course of the ensuring day the load can be met even if there is no solar contribution.

A block diagram of the PV system is shown in Fig. 3-1. The PV array is mounted on the southeast corner of the museum roof. A PV-system/manual-disconnect switch is located at the west end of the array. Wiring is brought down four stories to a small, locked back room in the exhibit area. A second disconnect switch is located in this room, along with the battery charger, the main dc bus and control wiring, and the distribution fuse box.

Both the batteries and the loads are located in the exhibit area. The batteries are kept in a locked glass case which also contains a photograph of the PV array on the roof (the PV array is not accessible to visitors) and a closed-circuit television monitor which displays the PV array as a roof-mounted camera pans back and forth across it. System ON/OFF is controlled from the display room for the convenience of those opening and closing the museum daily.

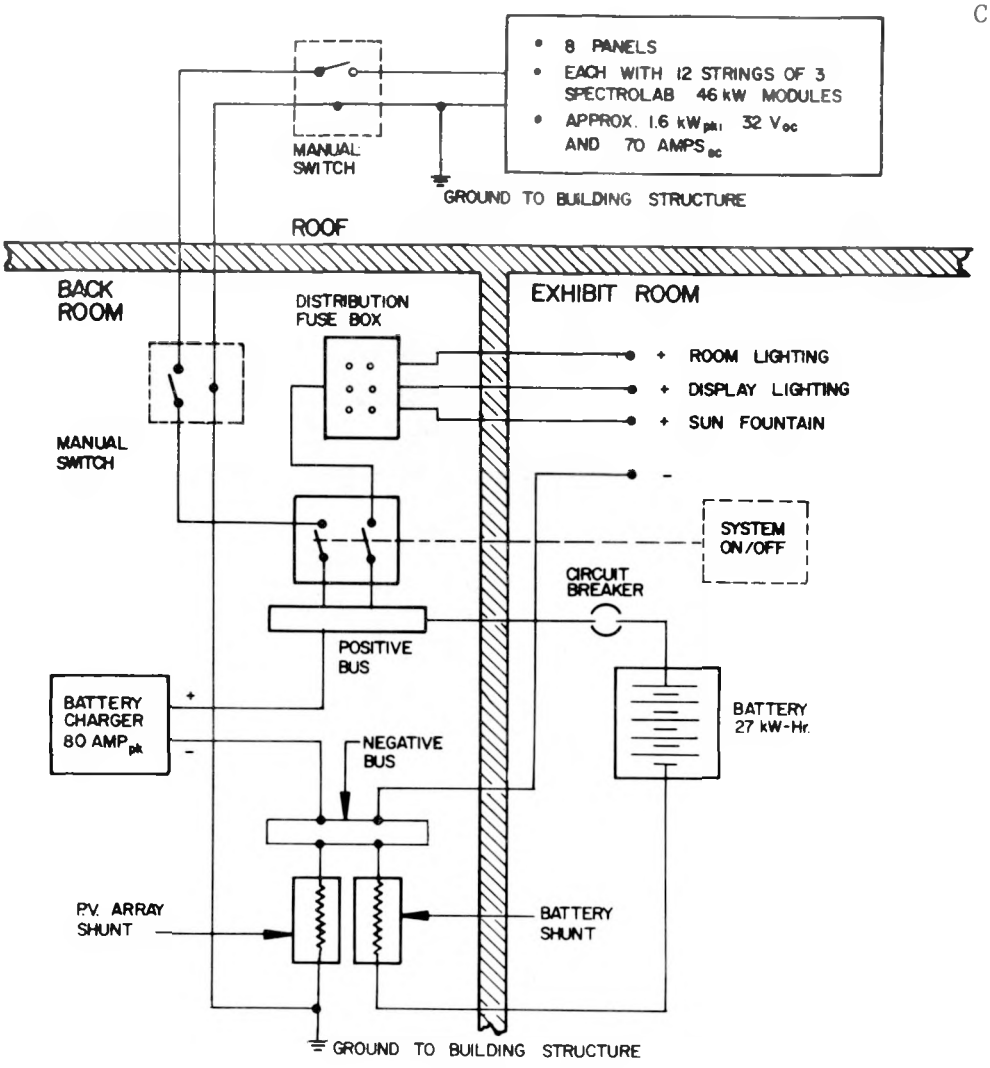

Fig. 3-1. PV power system, Chicago Museum of Science and Industry.

The four subsystems discussed below are the PV array, the batteries and charger, the system control, and data-acquisition equipment.

3.6.1 PV Array

The modules used for this project were manufactured by Spectrolab and were purchased by JPL as part of a multisource procurement in 1976/77, commonly known as the Block I module procurement. The Spectrolab module is shown in Fig. 3-2 and specific characteristics of the module are give in Table 3-2. The module substrate is an aluminum "I-beam." Twenty round silicon PV cells, encapsulated in silicone, are mounted on the substrate and glass is used as a superstrate covering.

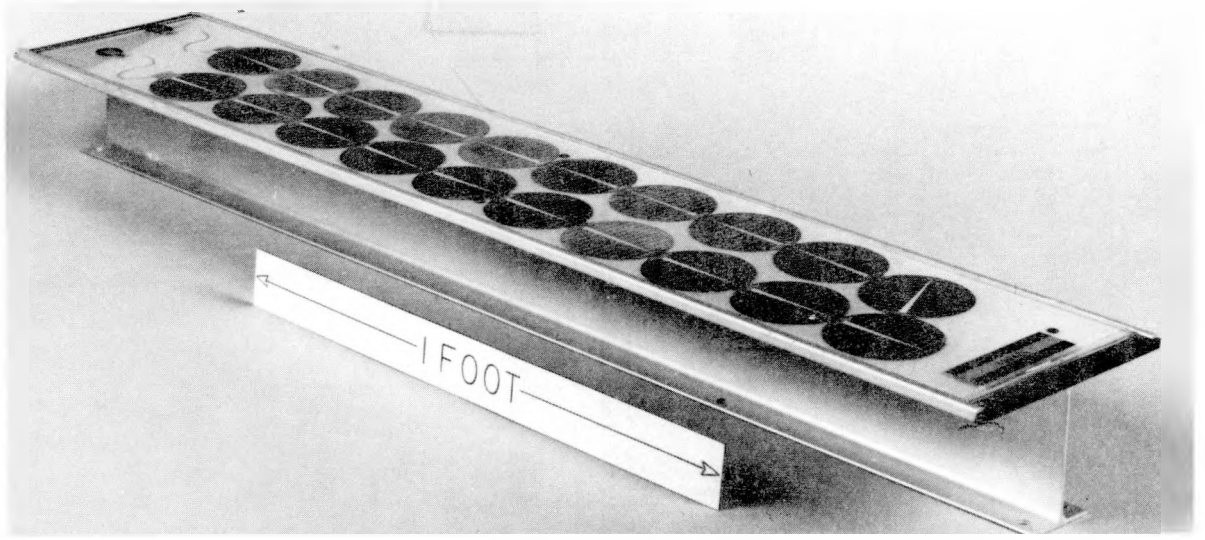

Fig. 3-2. Spectrolab Block I module.

TABLE 3-2

SPECTROLAB BLOCK I PV MODULE DATA

Manufacturer:	Spectrolab, Inc. Sylmar, California
Description:	Block I JPL Procurement 1976/77 I-beam aluminum substrate, glass superstrate
Dimensions:	633 mm long 124 mm wide 69 mm high
PV Cells	20 per module Circular, 50-mm diameter
Electrical Configuration:	20 cells in series no diodes
Electrical Performance:	Voc = 11.6 volts Isc = 0.66 amps Pmax = 5.45 watts Efficiency (%) = 6.6 } at 1000 W/m^2 insolation, 28°C cell temperature

The PV array consists of 288 Spectrolab modules mounted on steel frames placed on the southeast section of the Museum's roof (see Fig. 3-3).

P267-1543

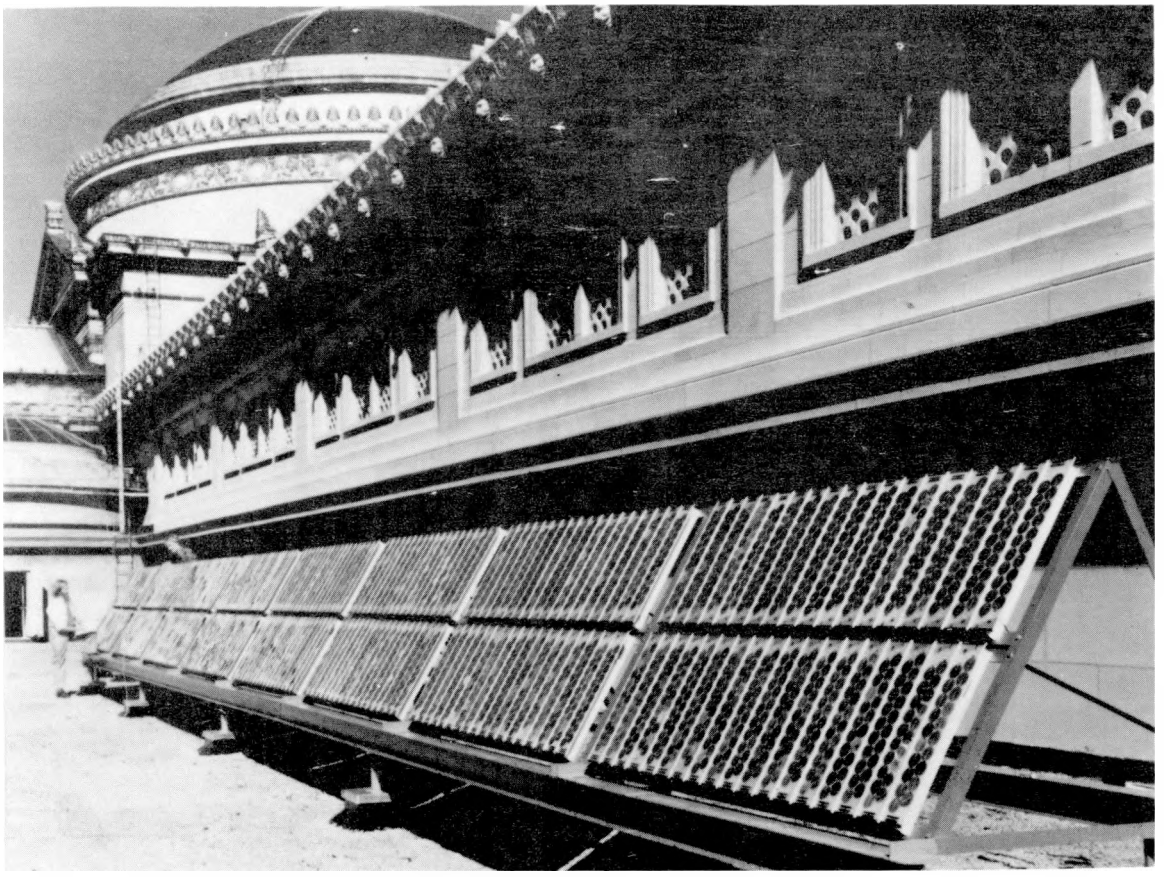

Fig. 3-3. PV array on Museum roof.

The frames, made of 2-in. x 2-in. steel angle, support the modules at a 60^{o} angle from the horizontal. When the frames are viewed from the east or west, they appear as an equilateral triangle. Diagonal crossbraces are used to stiffen the frames, which are welded to two large east-west I-beams, each supported by five through-the-roof posts. The PV array is divided into eight subframes, each holding 36 modules. The array is oriented true south. Overall dimensions of the array are: slant height--55 in., subframe east-west length--90 in., array east-west length--60 ft.

The electrical configuration of the array is shown in Fig. 3-4. In each subarray there are 12 parallel strings, each containing 3 modules in series. Blocking diodes protect the individual series strings. In the overall array

there is a total of 96 parallel strings of 3 series modules each. Number 14 wire is used within a subarray, and number 00 wire is used for connecting subarrays. The negative side of the electrical circuit is grounded, along with all metal framing members. A manual disconnect switch is mounted at the west end of the PV array, immediately "upstream" of the wiring roof penetration.

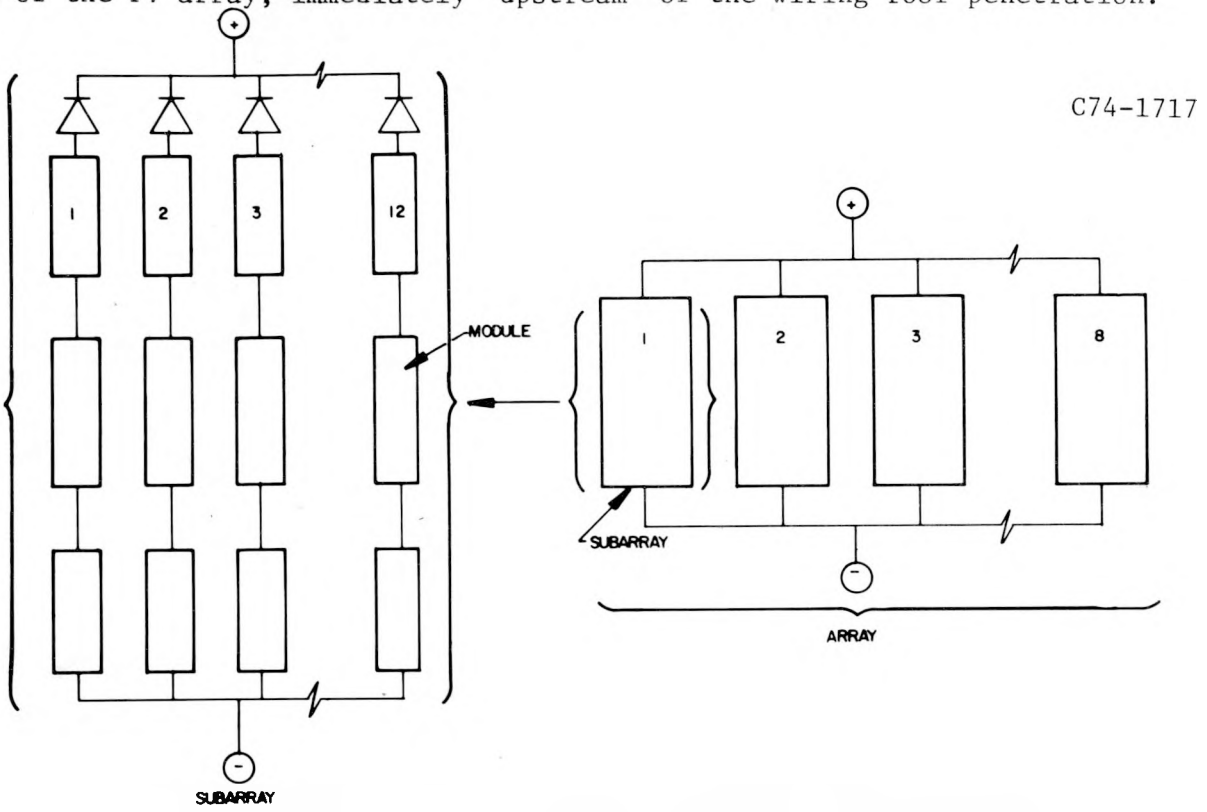

Fig. 3-4. Chicago Museum PV array electrical configuration.

Table 3-3 summarizes the characteristics of the PV array.

TABLE 3-3

CHICAGO MUSEUM PV ARRAY CHARACTERISTICS

Number of Modules	288	
Tilt Angle	60°	
Azimuth	0° (due south)	
Electrical Configuration	3 series x 96 parallel	
Diodes	Blocking, each series string	
Voc (V)	345	1000 W/m^2 insolation
Isc (a)	64	
Pmax (W)	1570	28°C cell temperature

3.6.2 Batteries and Charger

A total (usable) capacity of 27 kWh exists in the PV system's battery bank. This corresponds to 1125 Ah (at an 8-hour discharge rate) at a nominal 24 V. The batteries were manufactured by Globe Union, Inc., of Milwaukee, Wisconsin, and are of a lead-acid hybrid type, containing lead-antimony positive plates and lead-strontium negative plates (as opposed to the more common lead-calcium negative plates). According to the manufacturer, the lead-strontium plates have identical electrochemical properties to lead-calcium, but offer better casting (manufacturability) properties.

The battery charger used in the Museum PV system is model A-11 manufactured by LaMarche Manufacturing Co. of Des Plaines, Illinois. The unit is a completely automatic, solid-state, constant-voltage charger which employs transistor-controlled magnetic amplifier circuits to provide continuous "taper" charging. There are two manually adjusted settings on the charge voltage, to allow both operating-voltage charging and equalization-voltage charging. The nominal maximum current rating of the charger is 60 A at 24 V, or 1440 W.

3.6.3 Data Acquisition

For the first two years of PV system operation, a two-channel, strip-chart recorder was used to record battery (system) voltage and battery charge/discharge current. After that period the equipment was removed.

A switchable, resistive load box with shunts to display PV array current and voltage is kept in the display back room. This equipment was used periodically to generate a current-voltage curve on the whole array to assess its operational status.

Most recently, visits to this system have been made at eight- to twelve-month intervals to assess the physical and electrical condition of the PV array. This is now the only data-acquisition activity for the Museum PV system.

3.7 System Performance

Figure 3-5 shows a projected typical day of system operation. The top half of the figure shows a simplified system block diagram, and the lower half shows the battery state of charge over the course of the day as the charger,

load, and solar output are enabled. As can be seen from the figure, the system is designed such that the PV output and the batteries are required to meet the daily load energy demand. By the end of the working day, the batteries are at an approximate 50% state of charge. During utility off-peak hours, the charger brings the batteries back up to full charge, ready for the next day's load. The approximate hours of operation of the load, solar and charger are shown in the figure.

C74-12A

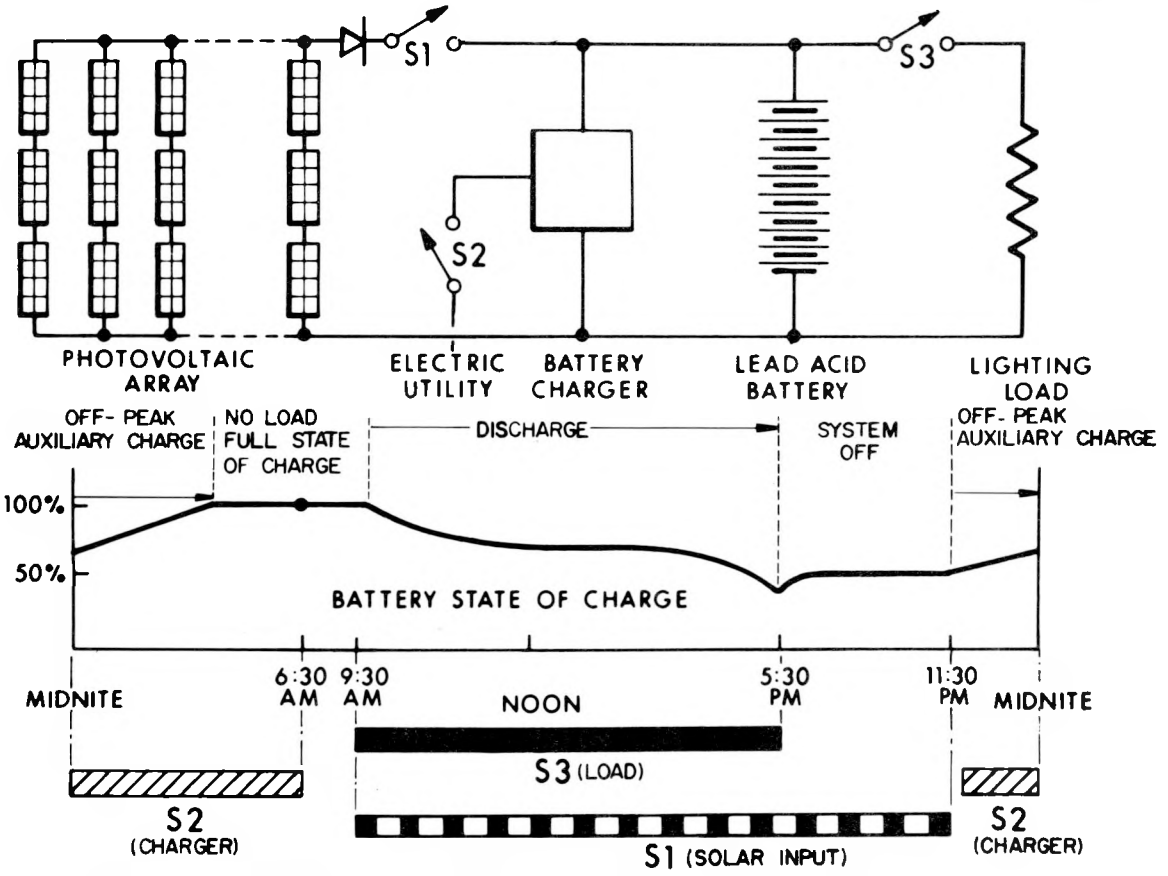

Fig. 3-5. Museum PV system, predicted typical day operation.

The predicted performance can be compared with data for an actual clear-sky day of system operation, as shown in Fig. 3-6. As can be seen, the actual battery-voltage curve agrees with the predicted behavior for battery state of charge in the previous figure. On this day battery voltage climbed when PV array output exceeded the load, and declined steadily as the PV output diminished. The charger came on in the evening and brought the batteries back up to full charge.

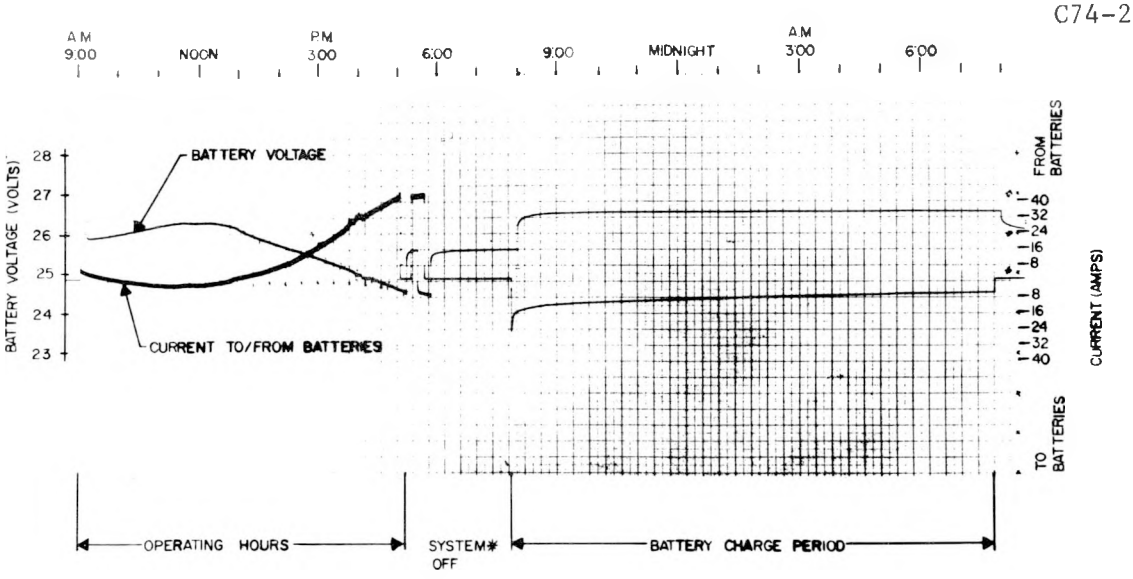

*BRIEF TURN-ON IS DUE TO AFTER HOURS CLEANING CREW. THIS OCCURS SEVERAL TIMES PER WEEK.

Fig. 3-6. Battery current flow and voltage versus time of day (sunny day).

Performance data for a second operating day, during which the solar output was very low all day, are shown in Fig. 3-7. As can be seen, the batteries supplied virtually all the power to the load, and the battery voltage dropped to below 2 V/cell.

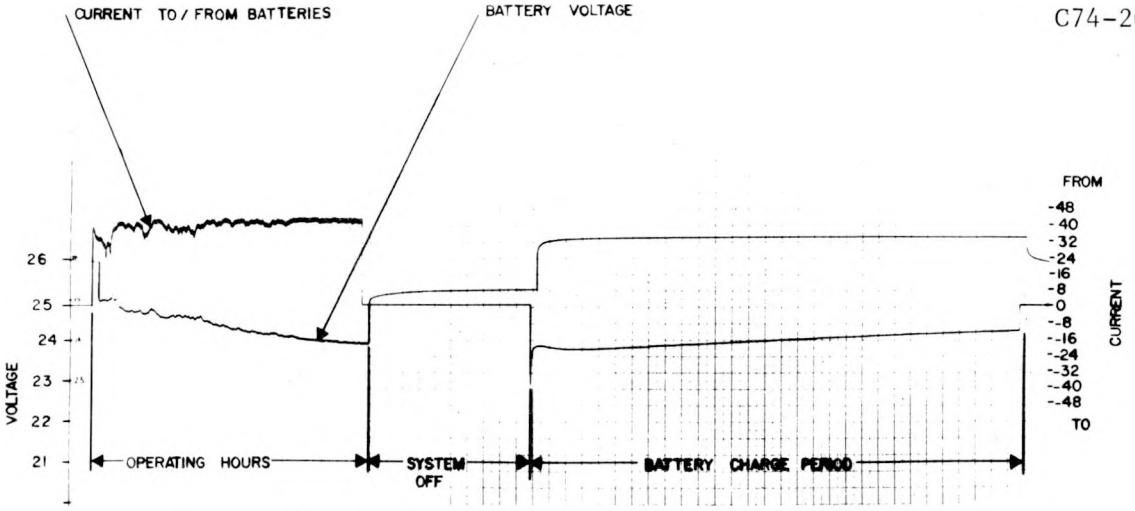

Fig. 3-7. Battery current flow and voltage versus time of day (cloudy day).

The system operates without problems in both sets of extreme conditions.

Since system turn-on in August 1977 to date, there have been no module failures at the Museum. With regard to the rest of the system, a modification was made to the battery charger after the first few months of operation to correct erratic charging behavior. This was the only abnormal occurrence over the entire operating period from August 1977 to September 1982. Though operation at relatively low voltage probably contributes to its high reliability, this PV system, one of the oldest in the U.S. Department of Energy PV program, has nevertheless set a reliability standard unmatched by any other system to date.

3.8 Lessons Learned

The outstanding reliability of this system apparently derives from several happy circumstances, all of which deserve replicating whenever possible in other PV applications. They are listed below.

3.8.1 Low Voltage is Beneficial

Low dc voltages result in lessened electrical stressing of the PV cells, connections and insulation. They also totally eliminate any electrical shock hazards and greatly simplify working on the array and array wiring. It is worth noting that the PV modules selected for this project were supposedly rejects, because at higher voltages they exhibited excessive leakage currents to ground. Yet in this low-voltage application there has not been a single failure.

3.8.2 Simple Systems are Reliable

Two attributes of this system--being dc-only, and not needing any kind of array-shedding control to avoid battery overcharging--have resulted in its being extremely simple and foolproof. Wherever possible, this type of design should be utilized.

3.8.3 Glass-Covered PV Modules are Superior

It is perhaps ironic that this, one of the earliest PV modules developed in the DOE PV program, should prove to be one of the most reliable designs.

This derives in no small measure from the use of glass as the superstrate/ weatherseal for the modules. Current trends in advanced PV module designs are back to utilizing glass again, after several unsuccessful attempts with silicones and other plastic weatherseals.

REFERENCES

1. Knapp, C. L., Stoffel, T. L., Whitaker, S. D., "Insolation Data Manual, Long-term Monthly Averages of Solar Radiation, Temperature, Degree-days and Global $\bar{K}_t$ for 248 National Weather Service Stations," October 1980, SERI/SP-755-789.
2. Forman, S. E., "Endurance and Soil Accumulation Testing of Photovoltaic Modules at Various MIT Lincoln Laboratory Test Sites," MIT Lincoln Laboratory Technical Report, 28 September 1978, C00-4094-23.
3. Forman, S. E. and Themelis, M. P., "Quarterly Report, Solar Photovoltaic Project Materials, Processes and Testing Activities for the Period 1 April 1979 to 30 July 1979," MIT Lincoln Laboratory Technical Report, October 1979, C00-4094-60.

4.0 THE BRYAN, OHIO, 15-KWP PV SYSTEM

4.1 Introduction

In November 1978, Lincoln Laboratory initiated a project with Radio Station WBNO, Bryan, Ohio, to install a 15-kWp PV system at their station. The system was turned on nine months later. Developed by Lincoln Laboratory, the system was designed to be economically attractive and to supply power primarily to dc loads requiring minimal energy storage. In line with these objectives, the WBNO radio station PV system is of simple construction and uses relatively low-cost, prefabricated, transportable sub-array units designed for quick and easy installation with minimum site preparation.

Although the 15-kW peak PV system is used primarily to power the AM transmitter, it also provides power for other loads such as lighting in the broadcast studio. The system uses a lead-acid battery storage subsystem, which is sized to provide about one day of storage in cloudy weather. Automatic control for the entire PV system is implemented with a microprocessor-based system controller. Control of battery-charging current and voltage is accomplished by automatic shedding and/or addition of individual sections of the PV array.

Contributions to this effort were made by the following individuals: Roy C. Archibald, Anthony A. Augustine, Henry J. Bullwinkel, John P. Husler, Martin J. Janiak, Leonard J. Lopez, Carl H. Much, Burt E. Nichols and Paul J. Rothenheber.

4.2 System Application

The primary objective of the Bryan, Ohio, application was to test the technical feasibility of using PV systems to power an AM radio station. Earlier studies (1) indicated that an AM daytime radio station would be an ideal application for photovoltaics. The AM transmitter provides a good match for a PV power system because it has a constant, predictable dc load; most of the electrical loads in radio broadcasting stations are dc, of which the largest is the transmitter final power amplifier. In addition, the operation of an AM daytime radio station obviously presents a good match to the solar resource.

On the basis of a competitive procurement, radio station WBNO in Bryan, Ohio, was selected as the site for the PV system. An aerial photograph of the site is presented in Fig. 4-1.

CP267-5017

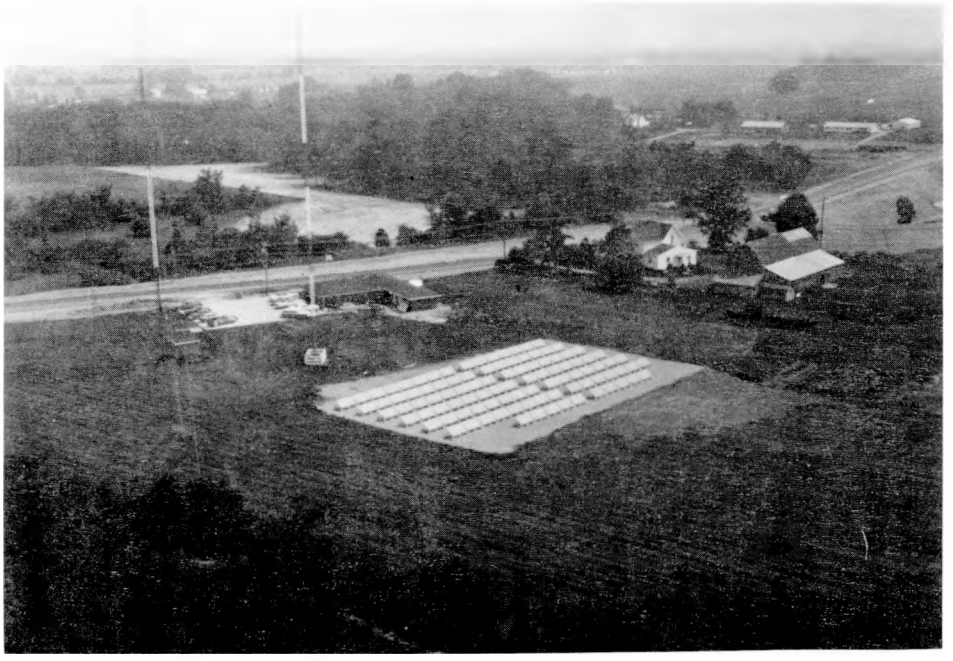

Fig. 4-1. Aerial view, WBNO, Bryan, Ohio.

4.3 Participants

The 15-kW peak PV system at Bryan, Ohio, was designed, built and installed during the spring and early summer months of 1979. The principal organizations which participated in the development, implementation and management of the PV solar system include:

U. S. Department of Energy
Photovoltaic Energy Systems Division
Washington, DC

MIT Lincoln Laboratory
Lexington, MA
Burt E. Nichols (Project Engineer)

Williams County Broadcasting System, Inc.
Radio Station WBNO
Bryan, OH

As a joint undertaking of MIT Lincoln Laboratory and radio station WBNO beginning in November 1978, the PV system installation and testing were essentially completed in August 1979. During the installation phase, Lincoln Laboratory furnished the solar PV modules, the system controller and data logger, and, by subcontract, provided the PV module mounting racks, cables and battery, and complete system installation at the site. Radio station WBNO, which operates and monitors the system, furnished the site, the building, the transmitter load, and the interface equipment.

4.4 PV System Loads

The loads served by the PV array consist of an AM transmitter, two commercial radio station studios, a production office, a newsroom and much of the building lighting and office equipment electricity requirements. The transmitter is operated from sunrise to sunset at full power except for the first two hours after sunrise and the last two hours before sunset; during these periods the FCC requires that transmitter power be halved.

During the first eleven months of field operation, the load to the PV power system consisted only of the AM transmitter, two broadcasting studios, and much of the radio station lighting. In mid-July 1980, dc-dc inverter-interface equipment was added to the system, and additional station loads were added to this inverter. Since July 1981, the PV site has been using a "load-switching" system which further utilizes any surplus energy that is available from the array. This system automatically connects additional studio, news-room and/or production room loads to the system during those periods when the battery is at full charge and there still is an abundance of solar energy. In the event that excess power is still available, the control system then disconnects portions of the PV array output. The total amount of surplus energy which is expected to be generated over a period of one year is in the range of 5 to 30% of the total annual transmitter load (2).

4.5 Solar Availability

Bryan, Ohio, located in the uppermost northwest corner of the state, is fairly representative of the central cold-climate regions of the country. Some of the significant climatic parameters of the region are presented in Table 4-1. The site latitude and longitude are 41.5^{o}N and 84.6^{o}W, respectively.

TABLE 4-1

AVERAGE INSOLATION AND TEMPERATURE DATA
Fort Wayne, Indiana*

	Maximum Daily Temp.°C	Minimum Daily Temp.°C	Average Monthly Temp.°C	Heating Degree Days Base 18.3°C	Cooling Degree Days Base 18.3°C	Total Global Radiation kW/m^2	Global $\bar{K}_t$ Cloudiness Index
JAN	0.33	-7.83	-3.72	683	0	44.5	0.349
FEB	1.94	-6.83	-2.44	581	0	61.6	0.394
MAR	7.27	-2.27	2.50	491	0	95.9	0.407
APR	15.27	3.88	9.61	261	0	128.7	0.445
MAY	21.22	9.38	15.33	120	26	163.4	0.476
JUN	26.72	14.88	20.83	12	87	174.2	0.497
JUL	28.66	16.88	22.77	0	139	174.7	0.495
AUG	27.88	15.77	21.83	6	115	155.8	0.492
SEP	24.38	11.66	18.05	50	41	120.5	0.476
OCT	18.11	5.83	12.00	201	5	90.3	0.458
NOV	9.05	0.00	4.55	413	0	48.8	0.356
DEC	2.05	-5.88	-1.88	626	0	36.1	0.315
ANN	15.22	4.61	9.94	3449	415	1292.0	0.450

*Knapp, C., et al, Insolation Data Manual, SERI/SP-755-789, October 1980, SERI, Golden, Colorado.

Note: These data were collected at SOLMET station #14827, Fort Wayne, Indiana, a location in close proximity to Bryan, Ohio. Latitude and longitude of the SOLMET station are 41°0'N and 85°12'W, respectively.

The monthly and annual average daily insolation and temperature values have been computed from a base of 25 years of data (1952-1977).

On an annual basis, a horizontal surface at Bryan receives an insolation of approximately 1300 kWh/m^2. Insolation data measured at the site during 1980 and 1981 are presented in Table 4-2. Additional meteorological data collected at Bryan during this same period are presented in Table 4-3. Included in this table are monthly recordings of both ambient temperature and PV array panel temperature extremes, the number of freeze/thaw temperature crossovers experienced by the array panels during the colder months, and precipitation measurements.

As a test bed for radio broadcasting PV systems, the Bryan site provides a location which has experienced temperature extremes of $-31^{o}C$ ($-23^{o}F$) and $41^{o}C$ ($106^{o}F$), and has an average annual rainfall of approximately 34 in. and an average snowfall of approximately 36 in.

TABLE 4-2

BRYAN, OHIO, AVERAGE INSOLATION (kWh/m^2)

Date	Horizontal Daily	Horizontal Monthly	Tilted(40°) Daily	Tilted(40°) Monthly	Ultra-Violet Daily	Ultra-Violet Monthly	# Days Complete Data	Peak Total Tilted	Peak Total Array Power (kW)
1980									
JAN			2.4	75	0.07	2.3	30/31		
FEB			3.8	109	0.14	4.0	28/29		
MAR			4.0	124	0.14	4.3	29/31		
APR			3.6	107	0.18	5.3	24/30		
MAY			5.4	167	0.23	7.0	27/31		
JUN			5.2	156	0.23	7.0	23/30		
JUL			5.2	162	0.24	7.4	26/31		
AUG			5.1	158	0.22	6.8	23/31		
SEP			4.9	148	0.19	5.7	27/30		
OCT			4.0	125	0.12	3.8	29/31		
NOV			2.9	89	0.07	2.2	25/31	1.16	15.89
DEC			1.9	58	0.05	1.6	27/31	1.00	12.09
TOTAL				1478		57.4			
1981									
JAN	2.0	62	3.3	102	0.10	3.1	31/31	1.30	11.10
FEB	2.1	58	3.0	85	0.10	2.8	28/28	1.31	15.76
MAR	3.5	108	4.5	140	0.14	4.4	31/31	1.39	13.79
APR	4.3	129	4.8	144	0.17	5.0	24/30	1.23	13.96
MAY	4.7	146	4.7	146	0.17	5.2	29/31	1.18	13.00
JUN	5.6	168	5.3	159	0.21	6.3	29/30	1.18	10.58
JUL	5.3	163	5.1	159	0.20	6.3	28/31	1.15	11.08
AUG	4.6	143	5.0	154	0.18	5.7	30/31	1.14	10.14
SEP	3.4	101	4.2	125	0.14	4.3	29/30	1.30	12.00
OCT	2.7	84	4.0	123	0.12	3.8	31/31	1.32	13.64
NOV	1.6	49	2.7	81	0.07	2.2	30/30	1.01	8.62
DEC									
TOTAL									

*Horizontal pyranometer was installed in late December, 1980.

TABLE 4-3

BRYAN, OHIO, METEOROLOGICAL DATA

Date	Prec.(in.)	Ambient Temp(°C) Max.	Ambient Temp(°C) Min.	Subfield Temp(°C) Max.	Subfield Temp(°C) Min.	# of Freeze Thaw Crossovers
1980						
JAN	0.55	12.8	-15.4	37.9	-21.3	38
FEB	0.72	5.5	-17.5	33.5	-21.6	48
MAR	5.00	12.7	-17.9	36.2	-22.6	48
APR	1.24	23.3	0.6	44.6	-5.9	4
MAY	3.61	30.8	0.2	58.2	0.2	0
JUN	4.66	30.9	9.4	58.9	5.2	0
JUL	8.74	36.4	12.7	60.5	9.2	0
AUG	3.63	40.6	14.3	61.5	11.3	0
SEP	3.04	31.9	2.7	56.0	0.9	0
OCT	1.45	30.6	-3.2	50.8	-8.4	8
NOV	0.86	24.6	-6.7	32.9	-10.6	60
DEC	1.69	22.1	-19.6	31.3	-23.3	54
TOTAL	35.19					260
1981						
JAN	0.47	6.6	-27.1	34.0	-33.5	68
FEB	2.92	10.3	-21.5	41.4	-24.4	39
MAR	0.24	25.6	-10.1	46.3	-13.1	68
APR	3.16	23.3	-2.1	45.9	-5.3	21
MAY	2.48	26.4	0.9	52.7	-2.3	7
JUN	8.72	31.2	5.6	58.2	3.3	0
JUL	2.20	32.5	10.6	66.7	8.9	0
AUG	1.71	28.7	8.3	59.4	5.1	0
SEP	6.10	28.0	2.2	60.7	0.4	0
OCT	2.46	20.4	-6.3	54.2	-9.7	28
NOV	0.98	20.3	-9.3	43.9	-12.6	44
DEC	1.43					
TOTAL	32.87					275

4.6 PV System Description

The PV system at the Bryan, Ohio, radio station consists of an array of PV cells which nominally produce a maximum output power of 15 kW at an insolation of 1 kW/m^2, a large battery subsystem with 40 kWh of usable energy storage, two inverters, a microprocessor-based system controller, an alarm system, and a comprehensive data collection and management subsystem. Utility power, converted to dc, is available in parallel and is used only when there are extended periods of cloudy weather and the state of charge of the battery subsystem is low.

A block diagram of the entire solar PV power system is presented in Fig. 4-2. As indicated in the figure, dc power is provided by the PV array to the array patch panel and then to the power panel, where the power is monitored and circuit protection is provided. The dc power from the power panel is then made available to the three types of loads (transmitter, fixed, and auxiliary loads) through the dc-to-dc converter or through two dc-ac inverters, as determined automatically by the system controller or by manual means. Surplus power from the PV array is directed into the battery storage subsystem to keep the battery state of charge at a high level (3).

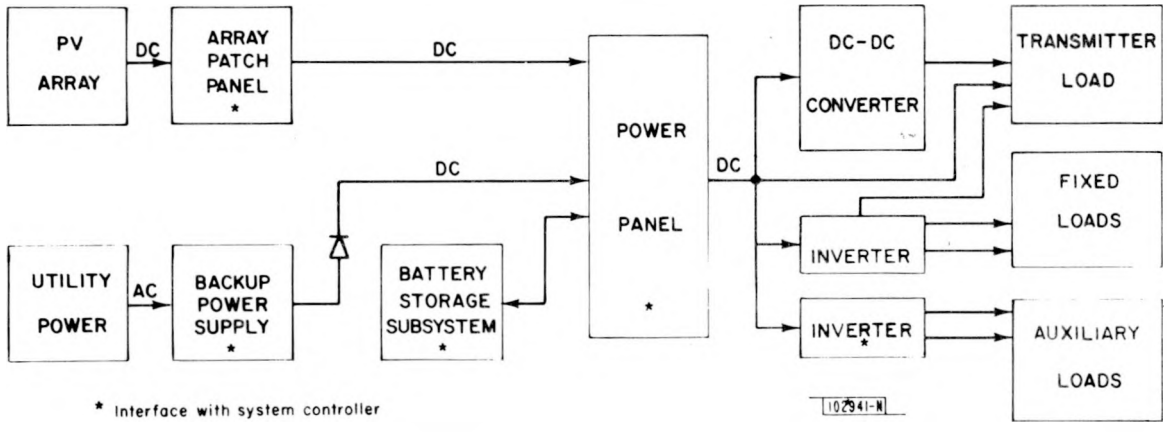

Fig. 4-2. Block diagram, WBNO PV system.

When the sun is shining and solar output is large, the Bryan, Ohio, 15-kW array supplies all the current to the load, and any excess current is used to charge the battery. When the bus voltage reaches its upper limit (typically, 150 V), the battery approaches full state of charge, and additional loads are switched in to use the available energy. If all loads are connected and there is still excess energy, part of the array is shed to keep the bus voltage from going too high. As energy from the array decreases, the portion of the array that was shed is reconnected and the extra loads are disconnected. Should any rapid changes occur in bus voltage, as happens when the sun emerges from behind a cloud, sufficient array strings are shed to prevent overvoltage, thereby preventing overcharging the battery.

When solar output drops to less than the load requires, the battery supplements the array output. Whenever the battery approaches a low state of charge, the utility-powered backup power supply is turned on to take over the load from the battery and apply a small trickle charge to the battery. Once solar power returns, the array automatically takes over the load from the power supply and recharges the battery.

The four major subsystems which make up the PV power system at the Bryan, Ohio, site are the PV array, the batteries, the PV-power-system controller and the data-acquisition unit.

4.6.1 PV Array

The array field contains 800 PV modules manufactured by Solarex Corporation of Rockville, Maryland. All of the modules were allocated by the DOE from the Low-Cost Solar Array Project (Block III procurement) at the Jet Propulsion Laboratory, Pasadena, California.

Each module is approximately two feet square and generates a minimum of 16 W at $60^{\circ}C$ for insolation of 100 mW/cm^2. Each module contains 42 series-connected, 3-in.-diameter silicon cells. The module terminal voltage under specified conditions (maximum power) is 15.8 V minimum. Additional characteristics of the Solarex modules are given in Table 4-4 (4). A photograph of the Solarex module is presented in Fig. 4-3.

TABLE 4-4

SOLAREX MODULE CHARACTERISTICS

Physical Dimensions		Electrical Properties	
Length (in.)	22.9	Power rated (watts)	18.5
Width (in.)	22.9	Voltage rated (volts)	15.8
Height (in.)	1.8	Current (amps)	1.17
Weight (lbs.)	9.8	Voltage open circuit	21.3
No. of cells per module	42	Current short circuit	1.42
Cell diameter (in.)	3.0	Module efficiency (%)	5.6

CP267-1808

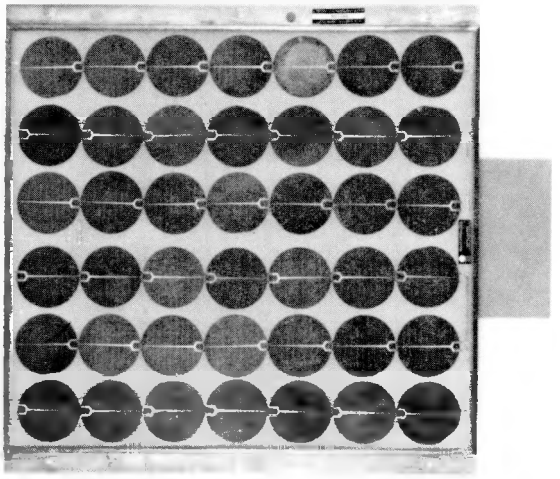

Fig. 4-3. Solarex module.

The PV array contains a total of 33,600 silicon solar cells arranged in 800 silicon-covered PV modules. The modules are grouped, eight to a unit, into 100 flat-panel racks, each of which produces 150 W peak power under ideal conditions on a clear day at noon. These racks, each measuring 4 ft. wide by 8 ft. long, are divided into seven parallel rows (Fig. 4-4) which face south and are positioned at a tilt angle of 40° from the horizontal. To reduce shadowing effects caused by the shade of one row falling on another, each row is separated from an adjacent row by 12 ft. The total land area occupied by the array field measures 100 by 150 ft., or about one-third of an acre.

CP267-5029

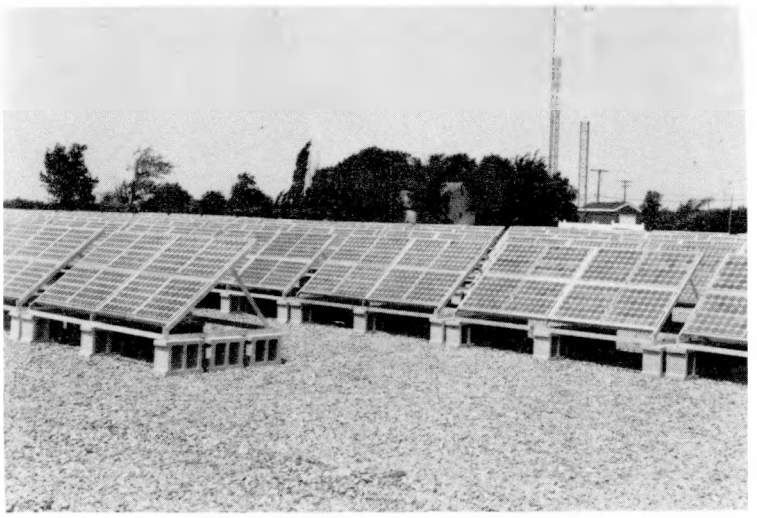

Fig. 4-4. WBNO array-field closeup.

It should be noted that in order to develop a multipurpose system with low total PV system cost, considerable effort was directed towards designing a module structure which minimized site preparation and foundation expense. To achieve this objective, a simple, bolted, galvanized steel rack was used to hold each group of eight PV modules (Fig. 4-4). Since each rack is bolted to nine 8 x 12 x 16-in. concrete blocks, no poured concrete foundation was required, only grading and provisions for drainage. In addition to the concrete blocks, further hold-down force is provided by small steel auger-type anchors screwed into the earth and fastened to the rack assembly. Tests conducted prior to field installation indicated that these rack assemblies are capable of withstanding wind speeds in excess of 100 miles per hour (2).

4.6.2 The Battery

The battery-storage subsystem at the Ohio site (shown in Fig. 4-5) comprises 60 lead-acid battery cells grouped into four Exide Ironclad UD-466 batteries. These low-cost batteries, manufactured by ESB Technology Corporation in Yardley, Pennsylvania, are designed for diesel-starting duty and have a long cycle life.

P267-809

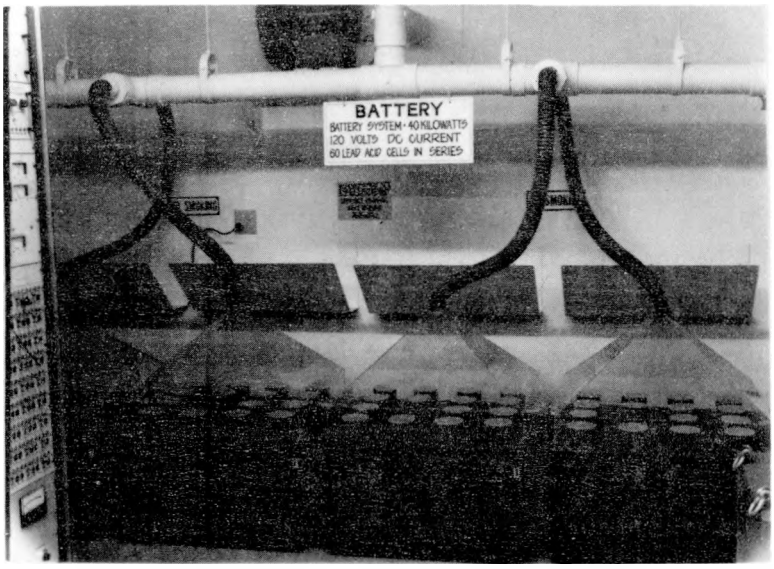

Fig. 4-5. Battery storage subsystem.

Each cell has a rated capacity of 466 Ah at the 8-hour rate to 1.70 V per cell. Because the load at the radio station is never as high as the 8-hour rate (58 A), the allowable depth of discharge (DOD) is greater than the typical 50% seen by these batteries in their conventional usage as diesel starters. Thus the usable energy capacity is approximately 40 kWh and has been warranteed to last 5 years at an average daily DOD of 55% with a maximum of 60 to 70%. Battery equalizations are necessary with the relatively deep discharges and are performed at regular intervals (5).

The complete battery-storage subsystem weighs about two tons and requires 36 square feet of floor space. Also included as part of the battery-storage subsystem is a monitor panel, a venting system, a gas detector and interconnecting cabling. As shown in Fig. 4-6, four spare cells are also included, in case one or more of the normally used cells fails.

4.6.3 Power Conditioning

The two principal power-conditioning elements are the inverters, used to convert the array-battery output from dc to ac, and a controller, used to switch system loads automatically, to add or shed electrical sections of the array, and to control operation of the back-up power supply.

P267-801

Fig. 4-6. Spare battery cells.

- Inverters

Solar energy is supplied to the radio station as ac power by two separate single-phase 5-kW inverters, built by the NOVA Electric Company in Nutley, New Jersey. Each unit is synchronized with 60-cycle utility power to ensure waveform compatibility.

One inverter converts dc power to ac for use in the transmitter and for the AM studio, while the second inverter converts dc power to ac for auxiliary loads.

- System Controller

Although control of the radio station PV power system may be exercised manually by front-panel controls, routine operation of the system is automatically handled by a microprocessor-based controller, which was designed and fabricated by Lincoln Laboratory. In addition to allowing for unattended operation of the system, the controller (shown in Fig. 4-7) also performs three unique tasks: (1) it monitors the array output, (2) it governs the charge and discharge of the battery, and (3) it provides backup power supply switching.

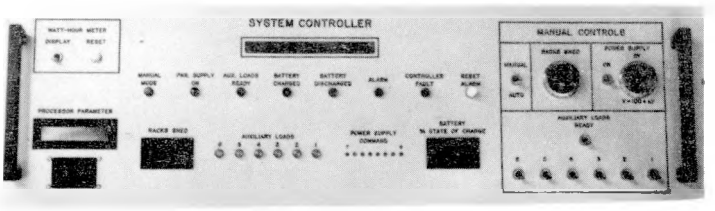

Fig. 4-7. PV power system controller.

When the battery is fully charged and the array output is more than the load requires, either additional loads are added to the bus or a portion of the array is shed (disconnected) in order to reduce the battery charge current. The controller monitors the state of charge of the battery by measuring voltage and current and, when full charge is reached, the controller automatically switches on additional load and switches off sections of the array as needed.

When the battery reaches a low state of charge, the controller switches on the backup power supply to replace the battery discharge current. When the array can furnish power for the load and begin to recharge the battery, the controller will switch off the power supply. Additional information about the system controller can be found in Reference 6.

4.6.4 Data Acquisition

The Bryan, Ohio, data-acquisition unit uses a comprehensive system of sensors and data-logging equipment to monitor and collect a wide variety of data at regular five-minute intervals. As anticipated, continuous monitoring of the entire PV system since August 1979 has produced an extensive library of data on solar insolation, PV array performance, power-conditioning equipment performance, and weather.

Principal components of the data-acquisition system include one Fluke 2240-A, 60-channel data logger manufactured by the John Fluke Mfg. Co., Seattle, Washington, and one Columbia 300-D data cartridge recorder manufactured by Columbia Data Products, Columbia, Maryland. Data collected by the system are recorded on 450-ft.-length 3M-type data cartridges and mailed to Lincoln Laboratory, at regular seven-day intervals, for processing and archiving on the Laboratory's Amdahl 470 time-sharing system.

Once the data have been transferred to the Amdahl 470, three principal forms of reduced output become available: a SOLMET formatted tape which provides weather and insolation data, a tape containing the measured system parameters, and graphic and tabular summaries of the measured data.

4.7 PV System Performance

Since 29 August 1979, the Bryan, Ohio, PV system has been operating continuously, except for a few short periods when site maintenance and/or system modification and repair required utility back-up. During the 734 days from September 1979 to September 1981, the PV power system was on-line and operating 695 days, or 94.7% of the time. During the two-year period (1979-1981) when data measurements of the entire PV system performance were made on a continuous basis, the 15-kWp PV system provided approximately 19 MW hours of energy. Electrical energy produced by the PV system during this period supplied 88% of the total energy required to operate the WBNO AM transmitter and other auxiliary radio station loads. These data indicate that the Ohio PV system, designed to supply 70 to 90% of the total energy required by the transmitter on an annual basis, has performed up to expectations.

Figure 4-8 presents a sample plot of typical system performance on a clear, sunny day (9 October 1980). As the figure illustrates, the radio station began broadcasting at 6:30 a.m. Since there was no solar output at that time, the battery supplied the load. By 8:00 a.m. the array output exceeded the load, and battery recharging began. At 9:15 a.m. the controller began shedding array racks/strings to reduce battery charging. By 10:30 a.m. the battery was fully charged, and for the next several hours only enough array was left connected to supply the load and trickle-charge the battery. At 5:05 p.m., array output had decreased enough to reactivate the battery, and the battery was used to supply the load until 6:45 p.m. when the station went off the air.

Typical system performance on a sunny day with occasional clouds passing over (17 July 1980) is shown in Fig. 4-9. As shown in this figure, the clouds caused the load to be alternately supplied by the array and the battery.

C74-2022

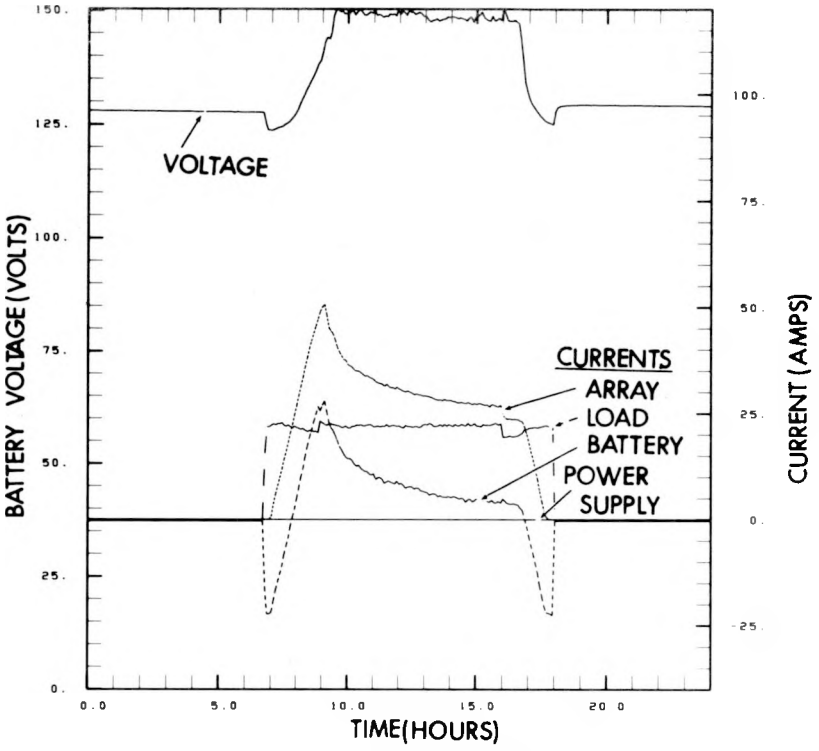

Fig. 4-8. System performance on sunny day (9 October 1980).

C74-2021

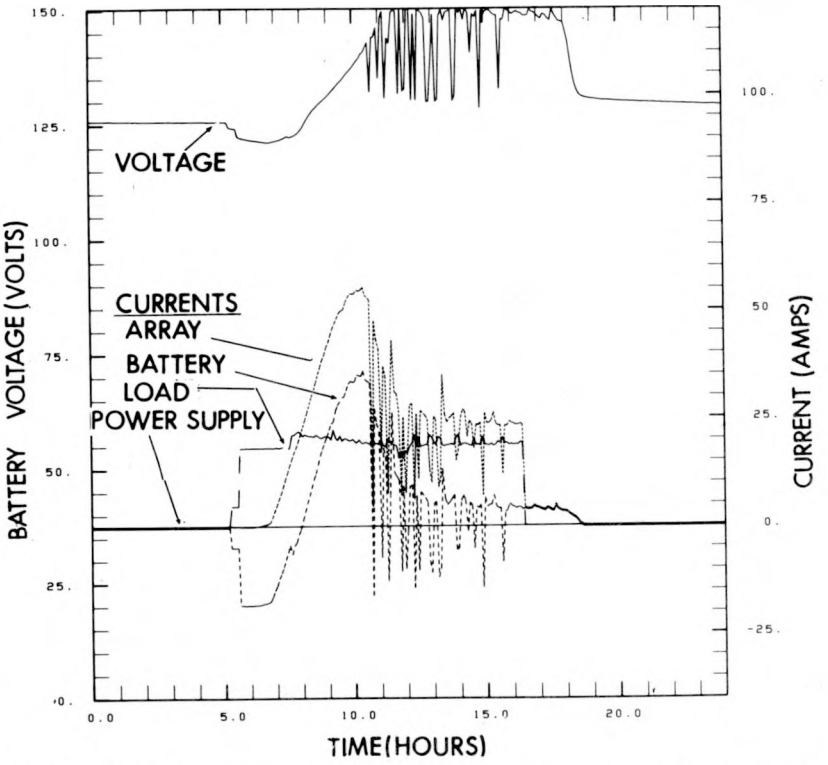

Fig. 4-9. System performance on cloudy day (17 July 1980).

This resulted in large variations in the bus voltage as the battery was switched between charging and discharging. However, the load was satisfied as the bus voltage remained in the required 100-to-150-V range. On both of these sample days, the load was supplied entirely by solar energy and the utility-powered backup power supply was not turned on.

It should be noted that since the Ohio PV power system began operation in August 1979, plots similar to those shown in Figs. 4-8 and 4-9 have been generated on a daily basis. As a further aid in evaluating the performance of the system, tabulated data on these and various other system parameters have been recorded at regular 5-minute intervals, day and night.

During the initial testing of the WBNO PV system, the FM antenna tower at the station suffered a direct lightning strike. The PV system is located under the guywires of the antenna towers, and while these seem to have prevented a direct hit on the PV equipment, the system was damaged by induced voltages in the system cabling. Damage occurred to integrated circuits in the system controller, one of fifty Darlington transistors used for array shedding, an isolation diode for the backup power supply, and a fuse. The system was returned to operation within two hours by the installation crew that was at the site. A number of metal oxide varistors were added to clamp induced voltages from the cabling. These seem to have been effective since the system has not been damaged by subsequent strikes, including one that damaged the FM transmitter (7).

4.7.1 PV Array Performance

After 26 months of field operation (August 1979 through September 1981), 120 of the 800 modules (15%) have failed due to failure of one or more pairs of cell-to-cell interconnects. Many of the failed modules were replaced with spare modules during scheduled site-maintenance sessions. In September 1981, a purchase order was placed with the Solarex Corporation, manufacturer of the modules, for a three-year warranty on the array. Solarex contracted to repair or replace with a new module any defective module found during the warranty period. So far 72 modules have been replaced. A detailed discussion of the Ohio module performance and failures is presented in Reference 8.

Except for the cell-to-cell interconnect failures discussed above, the performance of the Ohio PV array continues to be satisfactory. On several occasions, large array outputs, the result of insolation and temperature extremes, have been recorded on the 15-kW peak system. On 12 April 1980, for example, a peak insolation of 1.39 kW/m^2* produced a peak array power of 16.75 kW on the 15-kW peak PV system. Since battery state of charge was low (54%), all array feeders were on-line. Additional data obtained during the time of peak radiation include the following:

Battery Voltage:	141.2 V
Battery Current:	118.6 A
Ambient Temp.:	20°C
Array Temp.:	8°C

Figure 4-10 presents a bar graph history of maximum array power output during a typical month. As the graph illustrates, a maximum power of 11.1 kW was registered on Day 201 (20 July 1981), a sunny day with a peak insolation of 1.05 kW/m^2. On the previous day (Day 200), which was very cloudy and overcast with peak insolation of 0.19 kW/m^2, a maximum power of only 2.3 kW was recorded.

4.7.2 Battery Performance

The performance of the lead-acid battery system at Ohio has been closely monitored during the past two years of field operation. Two types of measurements have been conducted to monitor the battery performance: physical measurements on the cells themselves and electrical measurements via the data logger.

The physical measurements are of individual cell voltages, electrolyte levels and specific gravity. These measurements are taken manually at regular 90-day intervals, and are made at the end of an equalizing charge when the battery is in a fully charged state. Specific gravity readings, as well as readings of 60 cell voltages (done with a voltmeter), can be taken and recorded by one person in less than an hour. The watering operation required to adjust battery electrolyte levels takes about one man-hour and, since it is done with the battery on charge, must be done with extra care.

*The phenomenon of unusually high insolation is usually the result of natural concentration of sunlight through apertures in fast-moving scattered clouds. On other occasions, reflections from snowfields surrounding the array have also produced larger-than-normal array output.

C74-2025

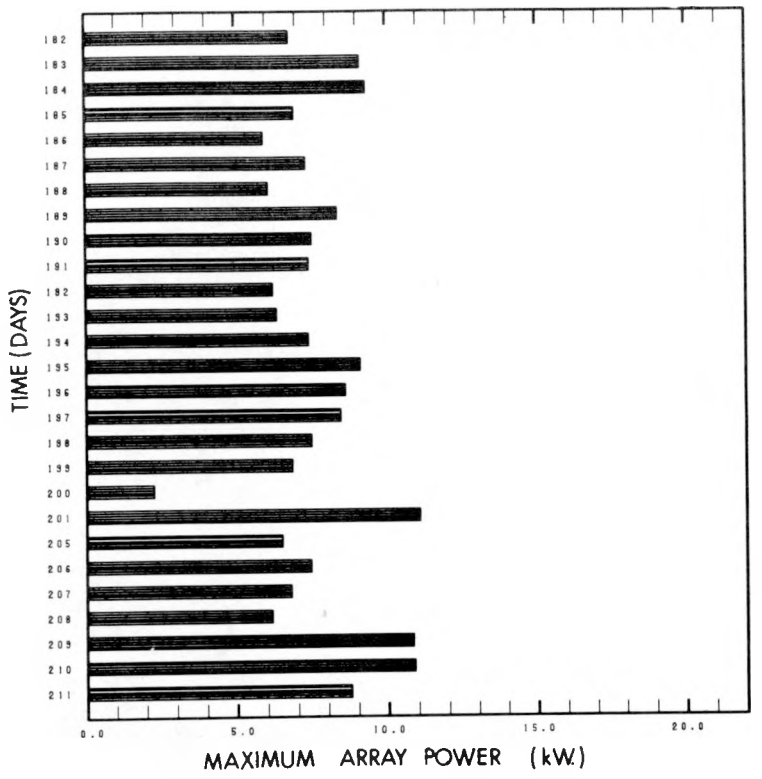

Fig. 4-10. Bar graph of maximum array power (7/81).

Electrical measurements, which include battery voltage, current and state of charge are recorded on the data logger at regular 5-minute intervals. Figure 4-11 shows a typical daily plot of battery voltage and current versus time for a sunny day, 9 April 1981. Note that the battery voltage rises to 150 volts by about noon and the battery-charging current drops to a fairly low value of less than 5 A very shortly thereafter. As Fig. 4-12 illustrates, the battery state of charge reaches 99% (highest value displayed) at approximately the same time, and arrays begin shedding to prevent overcharging of the battery.

The battery subsystem at Ohio continues to perform satisfactorily, and after more than two years of continuous field operation has an overall average efficiency of 84%. The only problem observed during the past year, and this is regarded as a minor one, was low specific-gravity readings measured on 2 cells which continually fail to attain the higher levels recorded by the other 58 cells. Additional information on battery performance, maintenance and efficiency is given in References 2 and 5, and below.

C74-2023

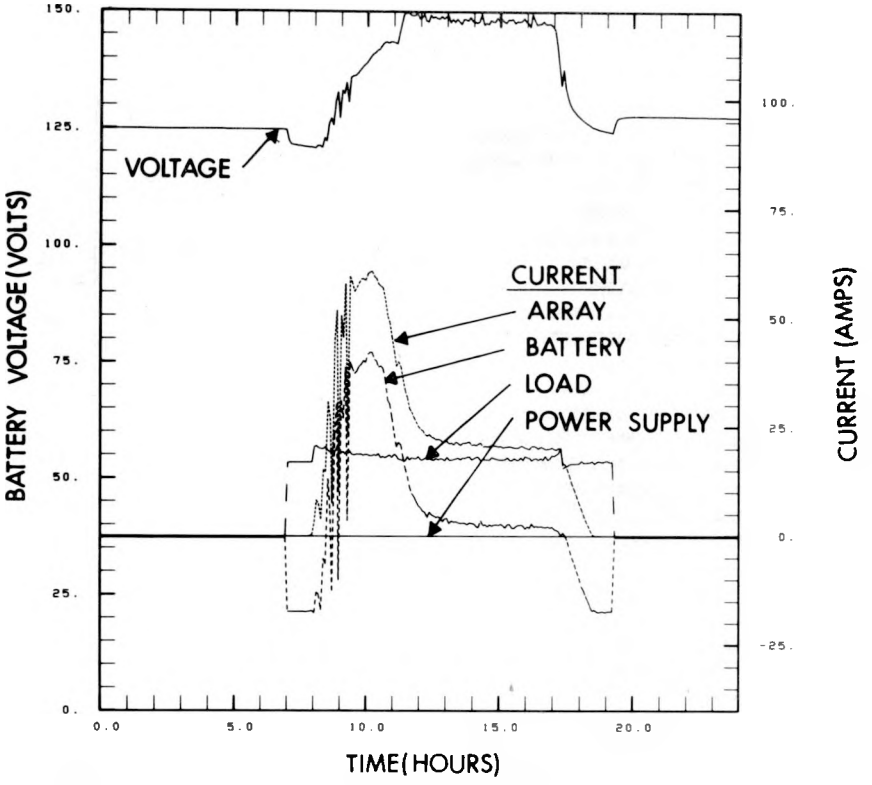

Fig. 4-11. System performance on 9 April 1981.

C74-2024

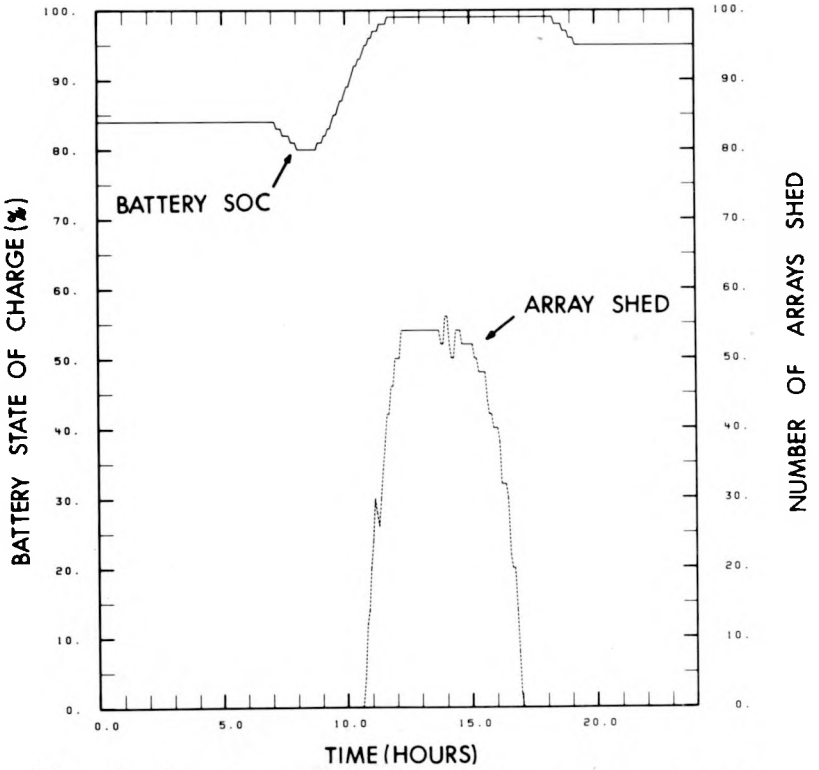

Fig. 4-12. System performance on 9 April 1981.

4.7.3 System Energy Flow

Table 4-5 presents a tabulated summary of the Ohio PV power system energy flow for the first two years of operation. During this period, 88% of the site load was provided by solar energy. This percentage provides not only an indication of how well the system worked, but also how favorable the weather was. As Table 4-5 illustrates, a cyclical pattern of solar/utility relationship is evident in the data. Between the generally cloudy and shorter daylight months of October through January, only 73% of the energy required by the site derived from the sun. Between the sunnier months of February through September, however, most of the site energy requirements were met by the PV system, with little or no utility backup assistance. Average loads imposed upon the PV power system during the first two years of field operation were 30 kWh per day.

TABLE 4-5

OHIO PV POWER SYSTEM ENERGY FLOW SUMMARY

Date	System On-Line (Days/Mo.)	System Off-Line (Days)	Load (kWh)	Array to Load(kWh)	% of Load Supplied by Solar	Utility to Load (kWh)	% of Load Supplied by Utility	Average Load (kWh/Day)	Battery (kWh) In/Out	Battery (kWh) % Effic.
1979										
SEP	33*	3	1089	1067	98	22	2	36	363/279	77
OCT	28/31	3	863	651	75	212	25	31	277/253	91
NOV	30/30	0	807	641	79	166	21	27	407/321	79
DEC	29/31	2	736	563	76	173	24	25	446/375	84
1980										
JAN	31/31	0	763	571	75	192	25	25	238/215	90
FEB	28/29	1	707	617	87	90	13	25	191/181	95
MAR	29/31	2	848	806	95	42	5	29	312/289	93
APR	29/30	1	937	807	86	130	14	32	284/236	80
MAY	31/31	0	1050	1041	99	9	1	34	408/279	68
JUN	29/30	1	1148	1148	100	0	0	38	302/259	86
JUL	28/31	3	1065	1044	98	21	2	34	396/339	86
AUG	15/31	16**	514	513	100	1	0	34	170/130	77
SEP	29/30	1	1061	1032	97	29	3	37	370/348	94
OCT	31/31	0	793	678	86	115	14	28	329/285	87
NOV	26/30	4	837	628	75	209	25	23	320/303	95
DEC	31/31	0	582	363	62	219	38***	19	240/181	75
1981										
JAN	31/31	0	731	399	55	332	45***	24	194/146	75
FEB	28/28	0	702	589	84	113	16	25	239/223	93
MAR	31/31	0	767	733	96	34	4	25	351/260	74
APR****										
MAY	31/31	0	1194	999	84	195	16	38	429/344	80
JUN	28/30	2	949	811	85	138	15	34	370/268	72
JUL	31/31	0	1198	1176	98	22	2	39	387/367	95
AUG	30/31	1	1139	1060	93	79	7	38	420/387	92
SEP	30/30	0	877	761	87	116	13	29	328/245	75
TOTAL	695/734	39	21,357	18,698	88	2659	12	30		84

* Includes 3 days in August.
** Inverter failure.
*** Heavy snow and ice on array required extra utility back-up power.
**** Complete data not available (system controller problem).

Data analyzed on the Ohio battery subsystem show a range of battery in-out efficiencies from 68 to 95%, depending upon the load profile. The average battery efficiency was 84%, based on two years of operation with no system breakdowns; this agrees favorably with predicted performance.

During this same measurement period, the inverters at the Ohio site operated satisfactorily except for a two-week shutdown in August 1980, when there was a delay in receiving parts from the manufacturer. Experience has shown that it would have been advantageous to locate the inverters in a cool area, away from the broadcasting studios. This would help to eliminate premature failure from overheating (in the summer months) and to prevent sound intrusion into nearby studio areas.

4.8 Lessons Learned

Lessons learned during the design, construction and operation of the WBNO system are summarized below.

4.8.1 Lightning Protection

Any PV system which contains long electrical cables (hundreds of feet) is susceptible to problems from lightning-induced voltages. In the WBNO system, it was found necessary to utilize copious quantities of varistors in order to protect the solid-state electronics components in the control unit and the data-acquisition equipment. On the other hand, no lightning problems were experienced in the PV array.

4.8.2 Unattended Operation

As a result of the use of the microprocessor-based control unit, the system repeatedly demonstrated its ability to run unattended for literally months on end, and all that was required was for someone to make daily checks on the system status.

4.8.3 Repair and Maintenance by Nonspecialists

It was found that the site engineer responsible for maintaining the radio station electrical and electronic equipment was also able to maintain the PV system. However, there are two essential prerequisites:

1. On-site spares must be provided; and
2. Up-to-date and identical sets of documentation are needed both at the site and at the system designer's facility (in this case, Lincoln Laboratory) in order to provide real-time assistance to the site in troubleshooting faults and failures.

4.8.4 Low-Cost PV Array Structures

The low-cost designs for the PV array structures and foundations gave excellent performance in the WBNO environment. No problems have been experienced from wind or snow loading, and the lack of large, deep foundations has not resulted in any problems relating to settlement or frost heaves.

Perhaps the best indicator of the success of the low-cost array structure is that the manufacturer of this hardware for WBNO was the successful bidder for similar hardware on another large PV system subsequently built for DOE at the Beverly High School, Beverly, Massachusetts.

4.8.5 Provide for High Array Output

Although the previously noted high insolation level of 1.39 kW/m^2 did not cause any problems with the WBNO PV system, such circumstances could do so for similar designs, particularly if the inverter input voltage window is narrow, or, for a system with storage, if the batteries are fully charged. In light of the experiences with this system and the Natural Bridges PV system (see Section 5), a PV system apparently should be able to withstand safely, say, 1.5 kW/m^2 insolation for exposure times of less than one hour.

REFERENCES

1. Nichols, B. E., and Katzman, M. T., "Solar Photovoltaic Power for Broadcasting Stations: An Engineering and Economic Analysis," MIT Lincoln Laboratory Technical Report, August 1982, DOE/ET/20279-223.

2. Nichols, B. E., "A Solar Photovoltaic Power System for a Radio Station," MIT Lincoln Laboratory Technical Report, December 1980, COO-4094-85.

3. Klein, D. N., "Photovoltaic Operations Manual Radio Station WBNO," MIT Lincoln Laboratory Technical Report, March 1981, DOE/ET/20279-110.

4. Smokler, M. I., "User Handbook for Block III Silicon Solar Cell Modules," February 1979, DOE/JPL-1012-79/6.

5. Brench, B. L., "Operational Experiences in Lead-Acid Batteries for Photovoltaic Systems," 15th IEEE PV Specialists' Conference, Orlando, FL, 11-15 May 1981, COO-20279-118.

6. Much, C. H., and Rothenheber, P. J., "Microprocessor-based Control of the Photovoltaic Solar Power System for an AM Radio Station," presented at IECI Spring Conference on Applications of Mini- and Microcomputers, Philadelphia, PA, 17-19 March 1980.

7. Nichols, B. E., "A Lightning Strike at Bryan, Ohio," MIT Lincoln Laboratory Technical Report, February 1980, COO-4094-81.

8. Forman, S. E., and Themelis, M. P., "Technical Progress Report, Materials, Processes and Testing Laboratory for July-October 1981," MIT Lincoln Laboratory Technical Report, February 1982, DOE/ET/20279-173.

5.0 THE NATURAL BRIDGES NATIONAL MONUMENT 100-KWP PV SYSTEM

5.1 Introduction

The Natural Bridges National Monument (NBNM), located in the high desert country of southeastern Utah, is one of the nation's most beautiful national monuments. In 1883, a prospector named Cass Hite became the first non-Indian to view the three magnificent sandstone bridges in what is now known as Natural Bridges National Monument. Carved throughout the centuries by the occasionally violent scouring action of desert streams, the bridges first received national publicity in 1904 through the National Geographic Magazine. In 1908, President Theodore Roosevelt proclaimed the area to be a national monument. Today, approximately 80,000 visitors arrive annually to view the bridges and enjoy the natural beauty of the surrounding region (1). Sipapu, one of the Natural Bridges, is portrayed in Fig. 5-1.

CP267-5300

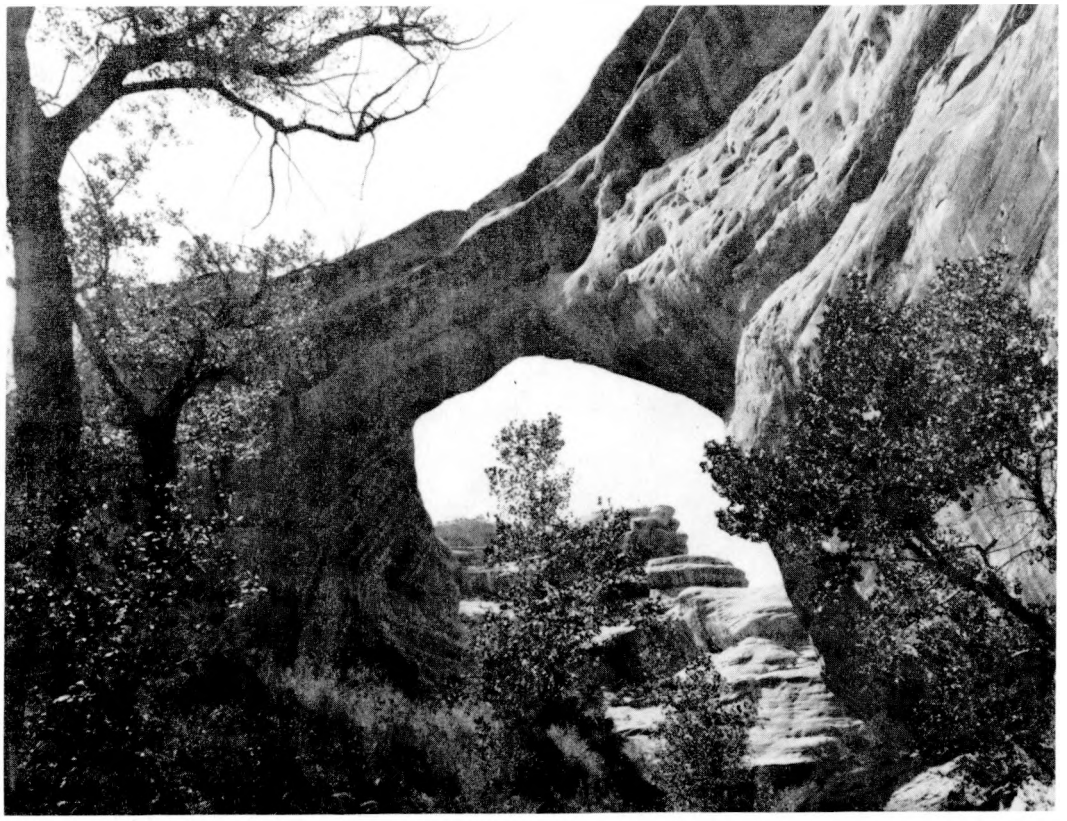

Fig. 5-1. Sipapu Bridge, Natural Bridges National Monument, Utah.

In late 1978, MIT Lincoln Laboratory was contracted by the then Energy Research and Development Administration (ERDA) to develop and evaluate a large stand-alone PV system typical of what might be required in a remote site (2). It soon became apparent that an ideal site for such a system would be one of the major national parks or monuments. After an exhaustive evaluation of 63 potential sites (3,4), NBNM was chosen. The combination of a remote location, a lack of public utility power, a reasonable range of electrical demand and energy consumption, and abundant year-round insolation made NBNM an ideal choice.

The 100-kWp PV system at NBNM is designed to provide ac power for all site loads on a continuous, 24-hours-per-day basis. For electrical storage, the system uses a lead-acid storage battery subsystem, sized to provide about two days of storage in cloudy weather. Automatic control for the entire PV system is implemented with a microprocessor which is primarily used to monitor and manage the battery state of charge. AC power is delivered from a dc-to-ac inverter. Control of battery-charging current and voltage is accomplished by automatic shedding and/or addition of individual subfield arrays. The site's existing diesel-electric generators which formerly operated 24 hours per day as the prime power source, serve as backup for use during extended periods of cloudy weather. At the time of dedication (June 1980), the NBNM system was the largest PV system in the world.

Contributions to this effort were made by the following individuals: Anthony A. Augustine, Alfred E. Benoit, Bronwyn L. Brench, Henry J. Bullwinkel, Sandra B. Clarke, Joseph D. Doucet, John J. Dunn, Harvey A. Fenton, John H. Helfrich, Philip O. Jarvinen, John T. Kelly, Jr., Emanuel E. Landsman, Antonio R. Leyenaar, Ervin F. Lyon, Carl H. Much, C. Ross Peatfield, Edward Ralowicz, F. John Solman, III, Cornelius M. Sullivan and Michael C. Wong.

5.2 System Application

Natural Bridges National Monument is located in a remote region in the southeast corner of Utah, almost 40 miles west of Blanding, Utah (the location of the nearest public utility), and approximately 55 miles east of Lake Powell. To protect and maintain the area, a small group of National Park Service personnel, along with other seasonal and transient additions, are the principal residents of the remote community at NBNM.

Before installation of the PV power system, all electricity for NBNM was produced as 240/120V, 60-Hz single-phase power by a 50-kVA/40-kW diesel generator which operated continuously. Since completion of the PV power system, the diesel-powered generator has been relegated to use as a backup-power source and the PV system has supplied the electrical power required by the regular NBNM community and the tens of thousands of annual visitors. An aerial photograph of the site is presented in Fig. 5-2.

CP267-5520

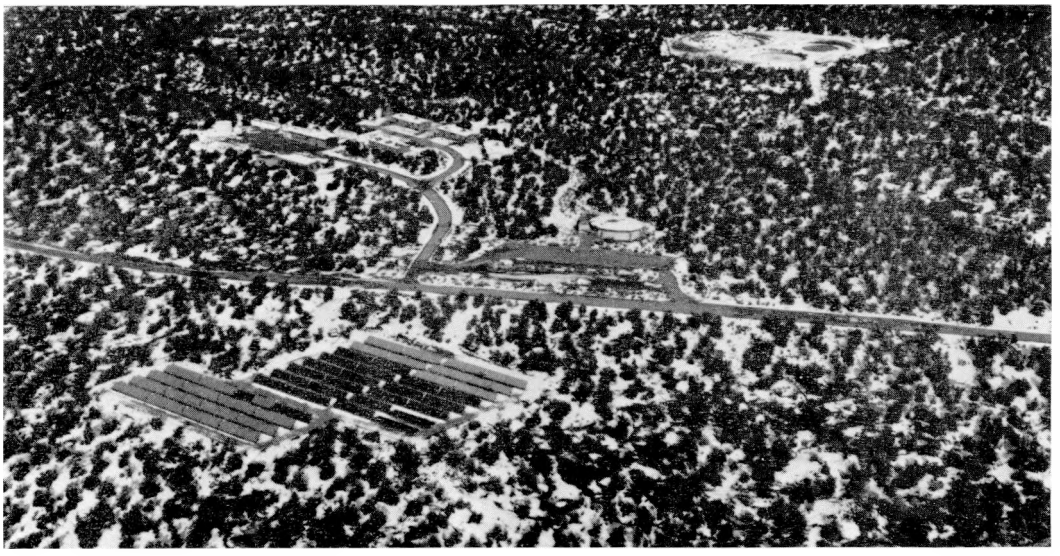

Fig. 5-2. Natural Bridges National Monument photovoltaic site.

5.3 Participants

The principal individuals and organizations which participated in the development and implementation of the NBNM photovoltaic power system include:

U.S. Energy Research and Development Administration (ERDA)
Office of Public Affairs
Washington, DC
Morton B. Prince (Project Director)

MIT Lincoln Laboratory
Lexington, MA
Ervin F. Lyon (Project Leader)
F. John Solman (Project Engineer)

U.S. Department of Energy (DOE)
Washington, DC
Paul Maycock (Director, PV Program)

U.S. Department of the Interior (DOI)
Washington, DC

Ford, Bacon and Davis
Salt Lake City, UT
Lynn P. Walker (Manager)

F. J. Burton
Salt Lake City, UT

Wasatch Electric Co.
Salt Lake City, UT
Mr. Richard K. Bertach

The U.S. Energy Research and Development Administration (later to become the U.S. Department of Energy) contracted MIT Lincoln Laboratory to design and install the 100-kWp PV system. As a joint undertaking of the Department of Energy (DOE) and the Department of the Interior, the national park installation was essentially completed in February 1980. F. J. Burton of Salt Lake City was selected by the National Park Service (NPS) as the contractor for site preparation and construction of the PV building, while Ford, Bacon and Davis, also of Salt Lake City, Utah, was contracted by MIT Lincoln Laboratory to design, fabricate and install the overall PV power system.

The Department of the Interior, through the NPS, provided all site development. This included preparation of the array field area, construction of a PV building to house the battery subsystem and the power system's electronic components, development of a lightning protection subsystem, and installation of underground power and signal cables. In addition, NPS also was responsible for the construction of access roads and trails as well as an interpretive overlook of the PV array (5).

The Department of Energy, through MIT Lincoln Laboratory, provided the PV arrays, the battery subsystem, the control and power-conditioning systems, the alarm subsystems and a complete weather and data subsystem.

Specific areas of MIT Lincoln Laboratory support during the early design stage included determination of insolation availability, optimization of array tilt and azimuth to match the load, array siting based on shadowing studies (6), and system performance predictions using both physical scale models and computer simulation (7,8,9). During the detailed design stage, specific

system-wiring layouts, system-control strategy, battery operational characteristics, and array-support-frame structural analyses were recommended and researched (10, 11). During construction and system checkout, MIT Lincoln Laboratory assisted by providing inspected modules for the array, building special test equipment, and sending personnel to check out the system and resolve any problems encountered at the site. After the system became operational, the Laboratory monitored its performance for approximately two years.

5.4 PV System Loads

Electricity produced by the NBNM PV power system is consumed by a variety of lighting, appliance and machinery loads. These loads consist of a visitor center, three detached, single-family residences, three small apartment complexes, three house trailers for temporary staff, a water-pumping station and a maintenance building. Minor site loads include a generator building, a fee station and the PV building which houses the PV system batteries, power-conditioning, control, and data units. Figure 5-3 shows the layout of the NBNM headquarters area.

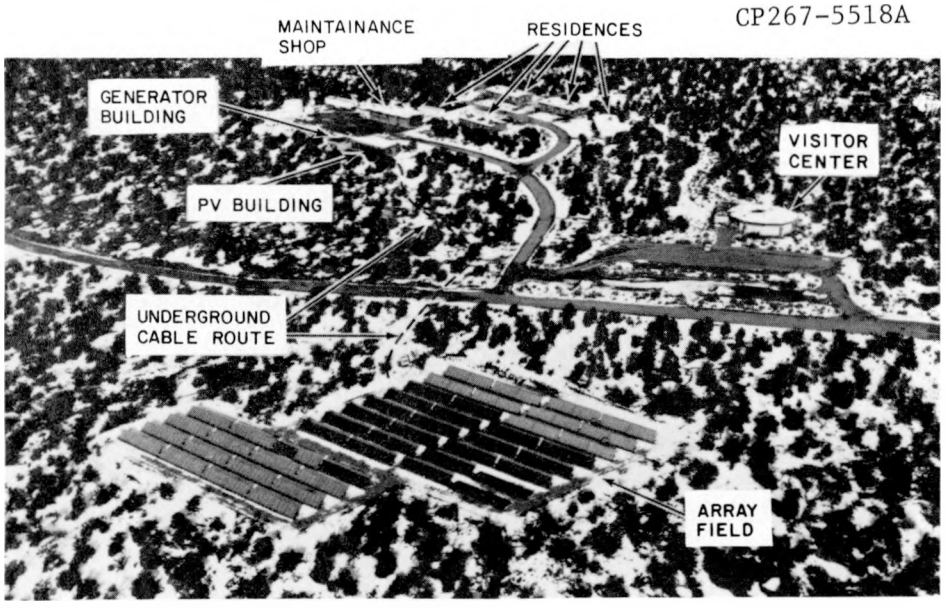

Fig. 5-3. NBNM headquarters area.

The most recent site load measurements and estimates show that the average daily load, after invoking conservation measures, is less than 10 kW, see Table 5-1. As shown in the table, the average consumption before the PV installation was 12 kW in the summer and 17 kW in the winter. (The high winter load was due to heavy use of electric heaters which has since been curtailed.) Before the PV installation, the peak power demand ran as high as 27 kW.

TABLE 5-1

ESTIMATED NBNM SITE LOADS*

Load Sites	Summer Loads (kW/24 hrs) Before PV	After PV	Winter Loads (kW/24 hrs) Before PV	After PV
Visitor Center	7.0	4.0	7.5	3.0
Residences	2.5	2.0	3.5	2.0
Maintenance Building	2.0	1.5	5.5	2.5
Generator Building	0.5	0	0.5	0.5
PV Building	0	0.5	0	1.0
TOTAL	12.0	8.0	17.0	9.0

*Loads inferred from spot measurements.

5.5 Solar Availability

Natural Bridges is situated 6500 feet above sea level in an area where prevailing clear skies (300 days annually), abundant solar insolation, dry air and usually moderate temperatures combine to produce an excellent climate for solar applications. The site latitude and longitude are 37^{o} 36'N and 110^{o} 04'W, respectively. On an annual basis, a horizontal surface at NBNM receives an insolation of approximately 2500 kW/hrs/m^2. A summary of the average daily insolation values recorded at NBNM during recent months is presented in Table 5-2. Meteorological data measured at NBNM during this same time period are presented in Table 5-3, and meteorological data averages over a 14-year period are presented in Table 5-4.

5.6 PV System Description

The stand-alone PV system at Natural Bridges National Monument includes a nominal 100-kilowatt peak PV array, containing 48 subfield arrays of about 2 kW (peak) output each, a large battery subsystem with 600 kWh of usable

TABLE 5-2

NBNM AVERAGE DAILY INSOLATION (kWh/m^2)

Date	Horiz.	Tilt(40°)	Dir. Norm	UV(Horiz.)	# Days Complete Data
1980					
JUL	8.62	8.43	NA	0.365	17/31
AUG	8.93	9.77	NA	0.415	20/31
SEP	5.66	7.60	NA	0.300	26/30
OCT	4.20	6.86	NA	0.239	28/31
NOV	2.96	5.61	NA	0.205	19/31
DEC	2.39	4.84	5.44	0.148	31/31
1981					
JAN	3.01	5.77	6.41	0.173	28/31
FEB	3.85	6.37	6.54	0.225	28/28
MAR	4.42	5.83	5.34	0.228	28/31
APR	6.44	7.33	8.21	0.297	30/30
MAY	6.30	6.35	6.41	0.265	31/31
JUN	7.89	7.35	9.92	0.304	27/30
JUL	6.90	6.73	7.56	0.277	31/31
AUG	7.81	8.54	8.52	0.344	18/31
SEP	4.97	6.37	6.28	0.247	30/30
OCT	3.89	6.13	6.37	0.215	26/31
NOV					
DEC					

TABLE 5-3

NBNM METEOROLOGICAL DATA

Date	Prec.(in.)	Ambient Temp(°C) Max.	Ambient Temp(°C) Min.	Subfield Temp(°C) Max.	Subfield Temp(°C) Min.	Max. Wind Speed(mph)	# of Freeze/Thaw Crossovers
1980							
JUL	0.20	33.2	13.2	65.4	10.9	23.6	0
AUG	0.24	32.4	11.1	63.8	8.1	30.5	0
SEP	1.42	28.1	6.2	60.1	-0.3	29.8	2
OCT	0.77	26.6	-2.7	55.3	-7.8	28.1	22
NOV	0.33	17.6	-8.5	45.2	-12.5	29.7	37
DEC	0.30	13.6	-6.5	43.4	-12.2	22.9	97
1981							
JAN	0.25	12.6	-7.7	41.7	-13.8	27.4	65
FEB	0.38	13.8	-10.8	45.7	-13.2	31.1	53
MAR	2.32	15.9	-5.4	46.6	-10.2	29.4	58
APR	0.83	27.5	-4.2	53.1	-8.7	34.9	14
MAY	1.82	26.5	0.6	57.8	-5.1	40.2	6
JUN	1.18	33.9	5.4	61.6	0.5	31.1	0
JUL	0.76	33.2	13.2	60.8	10.9	32.7	0
AUG	2.13	31.9	11.1	60.7	8.8	35.5	0
SEP	2.17	32.2	9.4	56.1	5.4	25.0	0
OCT	3.73	21.7	-2.7	50.3	-6.7	31.8	14
NOV							
DEC							

TABLE 5-4

NBNM METEOROLOGICAL INFORMATION*

Month	Precipitation: Average Precip. In Inches	Precipitation: Average Snowfall In Inches	Temperature (°C): Highest Recorded (Year)	Temperature (°C): Average Maximum	Temperature (°C): Average Minimum	Temperature (°C): Lowest Recorded (Year)
JAN	0.95	9.47	16(1971)	4.1	-8.6	-24(1971)
FEB	0.97	9.05	18(1972)	7.6	-5.6	-18(1972)
MAR	0.93	6.43	23(1971)	11.2	-2.9	-15(1975)
APR	0.81	3.36	26(1969)	15.8	0.6	-14(1975)
MAY	0.61	0.28	29(1978,79)	23.0	4.5	-8(1967)
JUN	0.55	----	38(1970)	26.7	9.6	2(1969,79)
JUL	1.60	----	39(1971)	32.6	15.1	9(1969)
AUG	1.44	----	37(1969)	30.3	13.6	4(1965)
SEP	0.76	----	34(1976,79)	25.5	9.5	-2(1978)
OCT	1.41	0.93	28(1969,79)	18.2	3.8	-14(1971)
NOV	1.04	5.20	26(1973)	10.0	-2.4	-17(1975)
DEC	1.43	15.12	15(1977)	4.5	-7.5	-22(1975,78)
Accum. Total	12.50	49.84	Accum. Total	17.4	2.5	

*These data are based on weather measurements made at Natural Bridges National Monument over a 14-year period, from June 1965 through December 1979. Relative humidity at NBNM generally varies between 10 to 20% in summer and 30 to 40% in winter.

energy storage, two inverters, a battery charger, an automatic control subsystem, and an extensive data-acquisition unit. Since electric utility service is not available at Natural Bridges, a 40-kW diesel-powered generator is maintained as a backup for the PV system during periods of reduced solar availability.

A block diagram of the NBNM PV power system is shown in Fig. 5-4. Power from the array field is fed through a 1000-ft. underground cable to power-conditioning and control equipment housed in the PV building. For safety purposes, lightning-protection devices are provided at each cable end. Array power is then fed through the array field control-switching circuit to charge the 600-kWh battery bank. The control-switching circuit has the capability of shedding part or all of the 48 array subfields whenever the battery approaches a full state of charge. Finally, the array power flows through the dc bus to the battery bank, the main inverter, or the uninterruptible power supply (UPS) inverter.

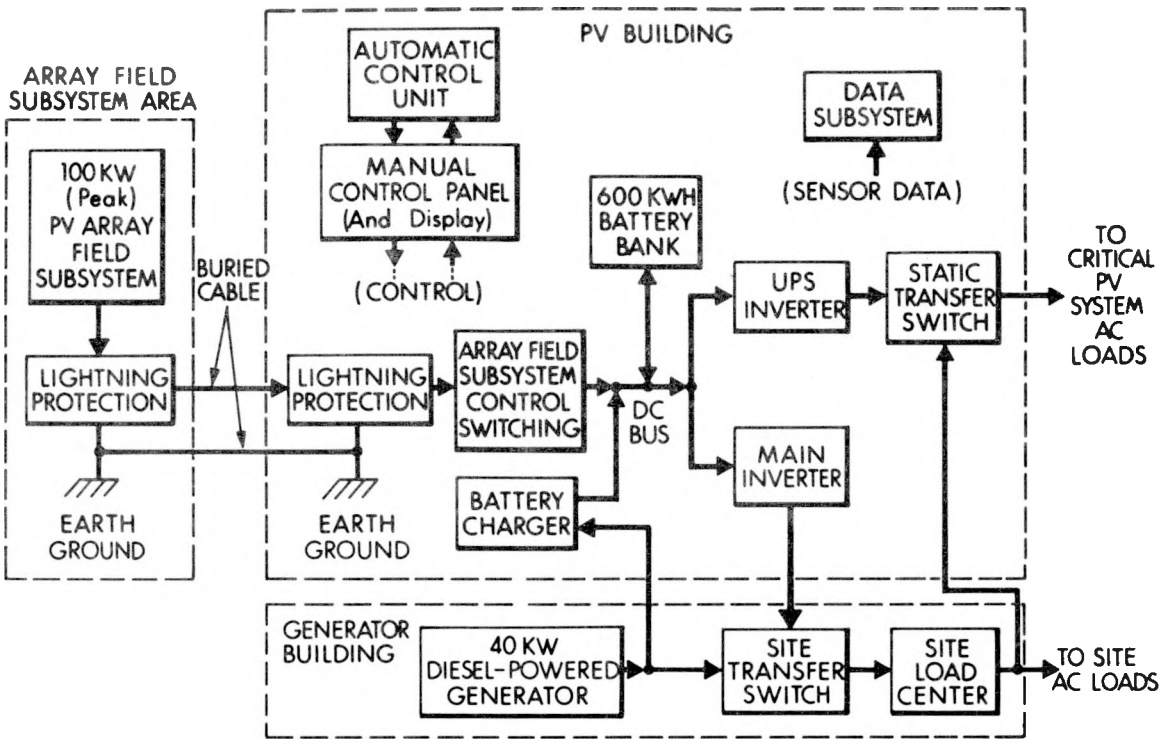

Fig. 5-4. NBNM PV power system block diagram.

Under normal operation, site ac power is supplied by a 50-kVA main inverter which draws dc power from the battery bank. During periods of adverse weather, the diesel generator backup unit charges the batteries through a battery charger. Management of the entire PV power system is automatically performed by a microprocessor-based automatic control unit.

The five major NBNM PV power subsystems discussed below are the PV array, the batteries, the inverters, the system control, and the data-acquisition unit.

5.6.1 Photovoltaic Array

The PV modules at Natural Bridges were manufactured by Spectrolab, Motorola and Arco Solar Corporations. The Spectrolab modules were purchased by Jet Propulsion Laboratory, Pasadena, California (JPL) as part of a 127-kW, multisource, "Block II" procurement in 1976/1977, whereas the Motorola and Arco Solar modules were purchased by JPL as part of a 259-kW, multisource,

"Block III" procurement in 1978/1979. Figures 5-5, 5-6 and 5-7 are photographs of the Spectrolab, Motorola and Arco Solar modules, respectively. Specific characteristics of each manufacturer's modules are given in Table 5-5.

TABLE 5-5

MODULE CHARACTERISTICS

	Arco Solar	Motorola	Spectrolab
Physical Dimensions			
Length(in.)	46.0	23.0	46.0
Width(in.)	9.1	23.0	15.3
Height(in.)	1.4	2.0	1.4
Weight(lbs.)	8.1	14.5	13.5
No. of Cells per module	41	48	120
Cell diameter(in.)	3	3	2
Electrical Properties			
Power rated (watts)	18.5	23.2	25.6
Voltage rated(volts)	15.8	5.0	15.8
Current(amps)	1.17	4.64	1.62
Voltage open circuit	20.9	6.4	21.9
Current short circuit	1.40	4.91	1.88
Module efficiency(%)	7.2	6.8	6.3
Thermal Characteristics			
Temperature range(°C)	-40 to +90	-40 to +90	-40 to +90

The PV array at NBNM contains a total of 266,028 silicon solar cells arranged in 4716 glass-covered PV modules. The modules are grouped into 48 array subfields, each of which produces just over 2 kW at a bus voltage of 220 Vdc on a clear day. These 48 flat panels, each 2.5 m high by 7.6 m long, are positioned at a tilt angle of 40^{o} from the horizontal and are arranged in 12 rows which take advantage of a 6^{o} southward slope in the natural terrain.

Figure 5-8 shows a view of one of the upper rows (4 modules) of the array. Also shown in this photograph are the lightning rods associated with the array. As can be seen, considerable effort was spent on lightning-protection measures.

Total land area occupied by the PV array is 1700 m^2. Since there are 990 m^2 of actual silicon cells, the land utilization factor is 58%.

5.6.2 The Battery

Energy storage at NBNM is provided by a large battery system, designed and built by C&D Batteries of Plymouth Meeting, Pennsylvania. The complete

P267-386

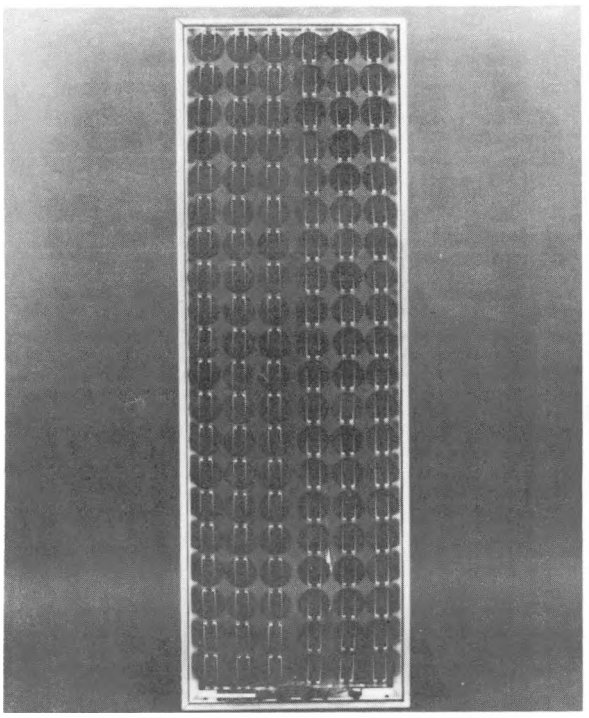

Fig. 5-5. Spectrolab module (front).

P267-382

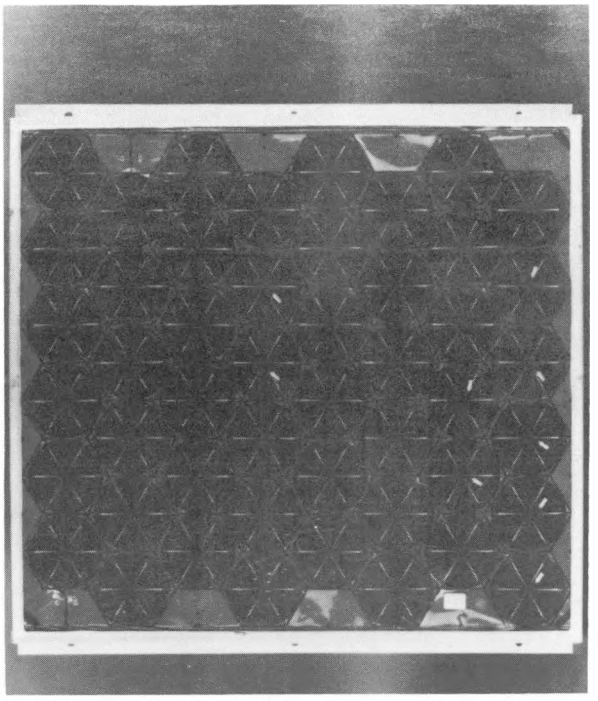

Fig. 5-6. Motorola module (front).

P267-384

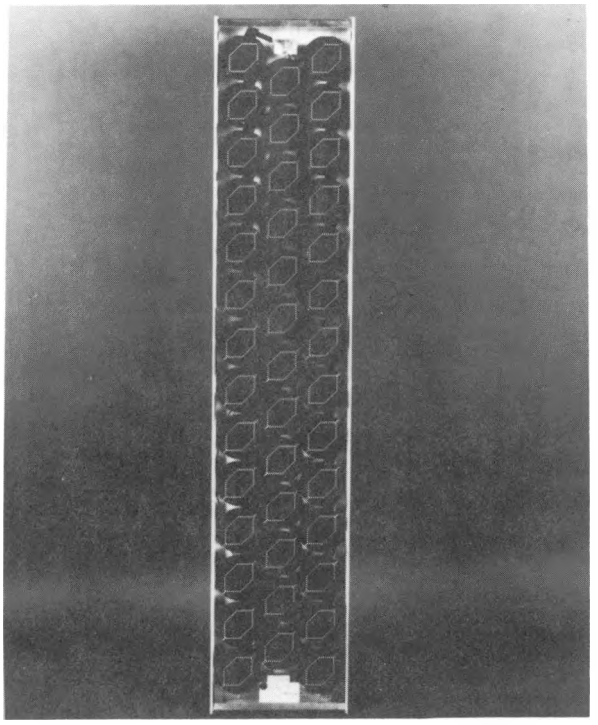

Fig. 5-7. Arco Solar module (front).

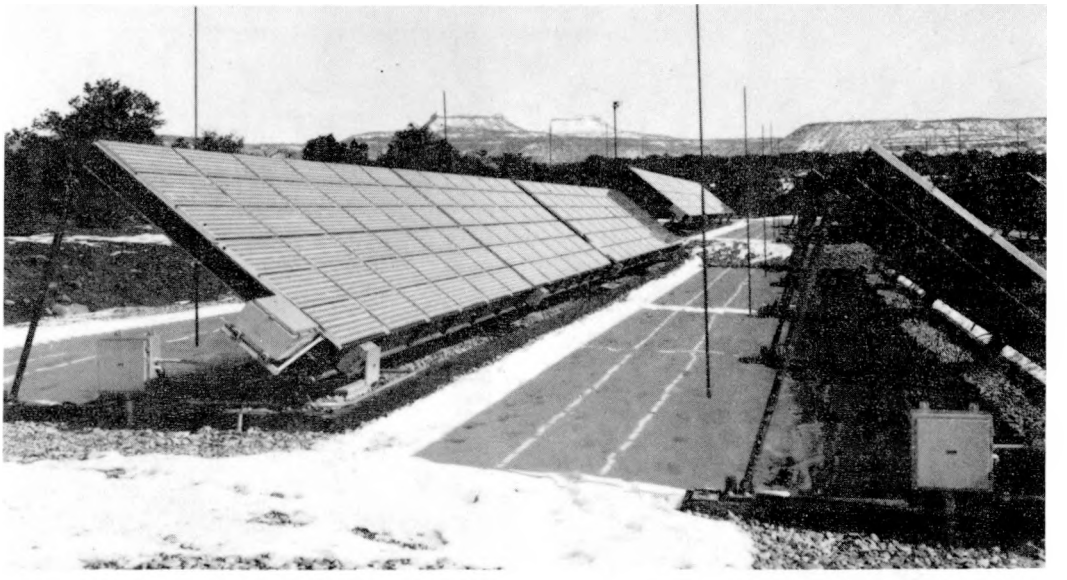

Fig. 5-8. Upper row of array.

battery system includes 224 lead-acid cells, hydrogen recombiners, air-lift pump system and electrolyte level indicators. Each cell includes a total of 23 plates--11 positive and 12 negative. Each cell has a capacity of 1760 Ah, at a 6-hour discharge rate, to a final discharge voltage of 1.70 V per cell. The 600 kWh total capacity of the entire battery bank is sufficient to operate the site from 24 to 48 hours, depending on the load. Maximum depth of discharge is 80% (600 kWh) of the rated capacity (750 kWh). Battery characteristics are summarized in Table 5-6.

Although these batteries are designed to operate over a wide voltage range, the main inverter design of the NBNM PV system dictated the relatively narrow range of 210-280 Vdc. The upper end of this range corresponds to a battery voltage of 2.5 V/cell, which is somewhat less than the maximum reached by stationary batteries. (A higher cell voltage would increase the gassing at end of charge and thus provide a beneficial mixing of the electrolyte.) To enhance mixing, an air-lift system was employed which permits stirring of the electrolyte at the end of daily charge, and thus prevents stratification within the cells.

TABLE 5-6

BATTERY CHARACTERISTICS

Type	Lead Acid
Plates	Lead-Calcium Alloy
Initial Capacity	750 kWh
Usable Capacity (at end of 5 years)	600 kWh
Average Daily Discharge	450 kWh
Ampere Hour Rating	3520 Ah
Voltage Range	210-280 V
Configuration	2 parallel strings
Cells per string	112
Packaging	8 cells per module
Weight of Module	2400 lbs.
Number of Modules	28
Spare Modules	1

The hydrogen recombiners in the NBNM batteries return gaseous hydrogen and oxygen liberated during recharging to the battery cells as water. This safety feature reduces the danger of explosion. It also minimizes the amount of water that must be added to the cells. As an additional safety measure, the NBNM battery subsystem is housed in a separate room which is sealed off from the remainder of the PV building in order to prevent the transfer of potentially explosive hydrogen gas evolved from the batteries during overcharge (12,13). A solid concrete interior wall divides the battery room from the other areas of the building. A view of the interior of the battery room, with 14 battery modules lined up next to each wall, is shown in Fig. 5-9. Additional information on the NBNM battery characteristics and performance is presented in References 3, 14, 15 and 16.

5.6.3 Power-Conditioning Equipment

The three principal power-conditioning units at the NBNM site are the main inverter, used to convert the array-battery output from dc to single-phase 120/240 Vac; a battery charger, having the unique feature of drawing essentially constant input ac power during battery charging; and a small uninterruptible power source (UPS) inverter, used to power special system loads such as the data-acquisition system and the PV system controller.

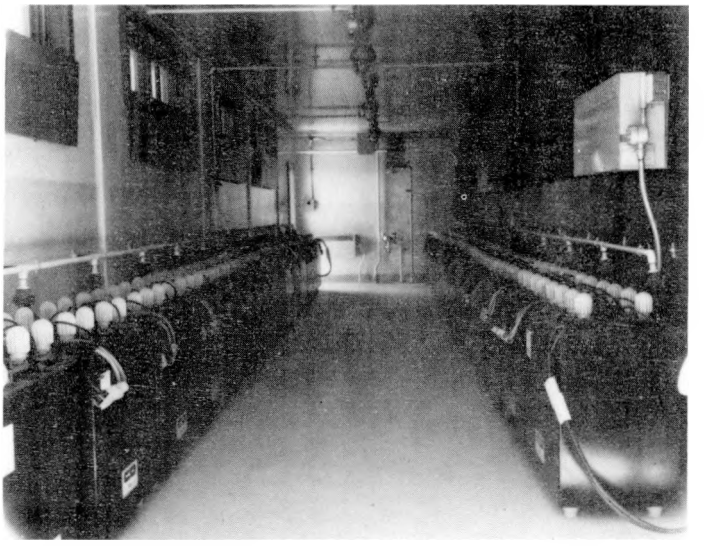

CP267-5860

Fig. 5-9. Battery room.

- Main Inverter

Solar energy is supplied to the site and overhead loads as ac power through a 50-kVA, single-phase, 60-Hz inverter, built by Cyberex Inc., Mentor, Ohio. The rather high rating of this inverter relative to the expected range of base loads results from the need to supply the peak current demand during the starting transient of any of the 3-hp induction motors at the site. This type of transient load, with initial peaks typically six to eight times the rated full-load current, represents the most difficult and stressful load for an inverter.

- Battery Charger

The battery charger is a 40-kW unit manufactured by Ratelco Corp., Seattle, Washington. The design utilizes the "controlled ferroresonance" technique, and thus has a relatively clean (harmonic free) ac input current waveform. (By contrast, more conventional designs utilizing phase-controlled SCRs have significant harmonic content in their input current waveforms. When interconnected with a diesel-powered generator, an adverse interaction between the charger and generator control loops frequently results. Controlled ferroresonant chargers offer a solution to this problem.)

Another important feature of the charger is the inclusion of a constant input current control loop, which allows the charger to draw essentially constant input ac power during battery charging, thereby maintaining a constant load on the diesel-powered generator. Thus, the variation of dc bus voltage with battery state of charge will not affect the diesel loading.

- UPS Inverter

A small (5-kVA) inverter, configured as a UPS, provides ac power to critical system loads such as the control, data and alarm subsystems. The inverter, manufactured by NOVA Electric Mfg. of Nutley, New Jersey, provides regulated 120-Vac, 60-Hz, single-phase output from a variable dc input voltage over the range of 200 to 300 V. Efficiency is rated at 89% at full load with distortion less than 5%. To enhance system reliability further, a static transfer switch is incorporated to switch these critical loads to site power in the event of failure of the UPS inverter.

5.6.4 System Control

Control of the PV power system is accomplished by a manual control panel (MCP) and a microprocessor-based automatic control unit (ACU). Although system control may be exercised manually through the MCP, which includes all display functions, routine operation of the system is handled by the ACU. In addition to permitting unattended operation of the system, the ACU also performs the following tasks:

1. Battery-charge control by shedding of one or more (up to 48) of the array subfields when the battery state of charge (SOC) reaches 100% and the available solar PV power exceeds the demand of the two inverters.
2. Automatic start-up of the diesel-powered generator when the battery SOC drops to 20% (600 kWh drawdown).
3. Automatic shutdown of the main inverter, thus dropping power to the site, in the event that the diesel fails to start.
4. Automatic shutdown of the UPS inverter, thus eliminating <u>all</u> battery drain, if the battery SOC reaches 15%.
5. Automatic scheduling and operation of a biweekly equalizing cycle utilizing the diesel-powered generator and battery charger.

5.6.5 Data Acquisition

The NBNM data-acquisition system contains a comprehensive system of sensors and data-logging equipment to monitor and collect, at 10-minute intervals, a wide variety of electrical and environmental variables which characterize the entire PV system performance (16). As anticipated, continuous monitoring of the entire PV system since June 1980 has produced an extensive library of data on solar insolation, PV-array performance, power-conditioning equipment performance, and weather.

In addition to gathering system-performance data, the data-acquisition system also collects, on a daily basis, current-versus-voltage (I-V) measurements on each of the 48 subfield arrays. The I-V measurements are automatically taken with a Lincoln Laboratory-constructed data logger and an INTEL 80/20 minicomputer manufactured by Intel Corp., Santa Clara, California. Each day at noon, the ACU switches in different resistors (in the I-V load box) and the I-V data logger takes 33 voltage and current readings on each of the 48 array subfields. Figure 5-10 presents a representative sample of I-V curve data taken at Natural Bridges on 24 February 1981. "Stair-step" I-V curves of subfield #136 and #139, which are the signatures of subfields containing shorted modules, are clearly visible.

Principal components of the data-acquisition system include one Fluke 2240-A, 60-channel data logger manufactured by the John Fluke Mfg. Co., Seattle, Washington, and two Columbia 300-D data cartridge recorders manufactured by Columbia Data Products, Columbia, Maryland. The Fluke data logger and Columbia recorder combination is used to gather 10-minute interval system data while the I-V data logger and the other Columbia recorder are dedicated to collecting I-V data on a regular daily basis. Data collected by both data systems are recorded on 450-ft.-length 3M-type data cartridges and mailed to Lincoln Laboratory at regular 7-day intervals for processing and archiving on the Laboratory's Amdahl 470 time-sharing system.

Experience at NBNM has shown that the high storage capacity of the Columbia recorder (2-3 weeks), as well as its unique power fail-restart capability, make it ideal for that remote and frequently unattended site.

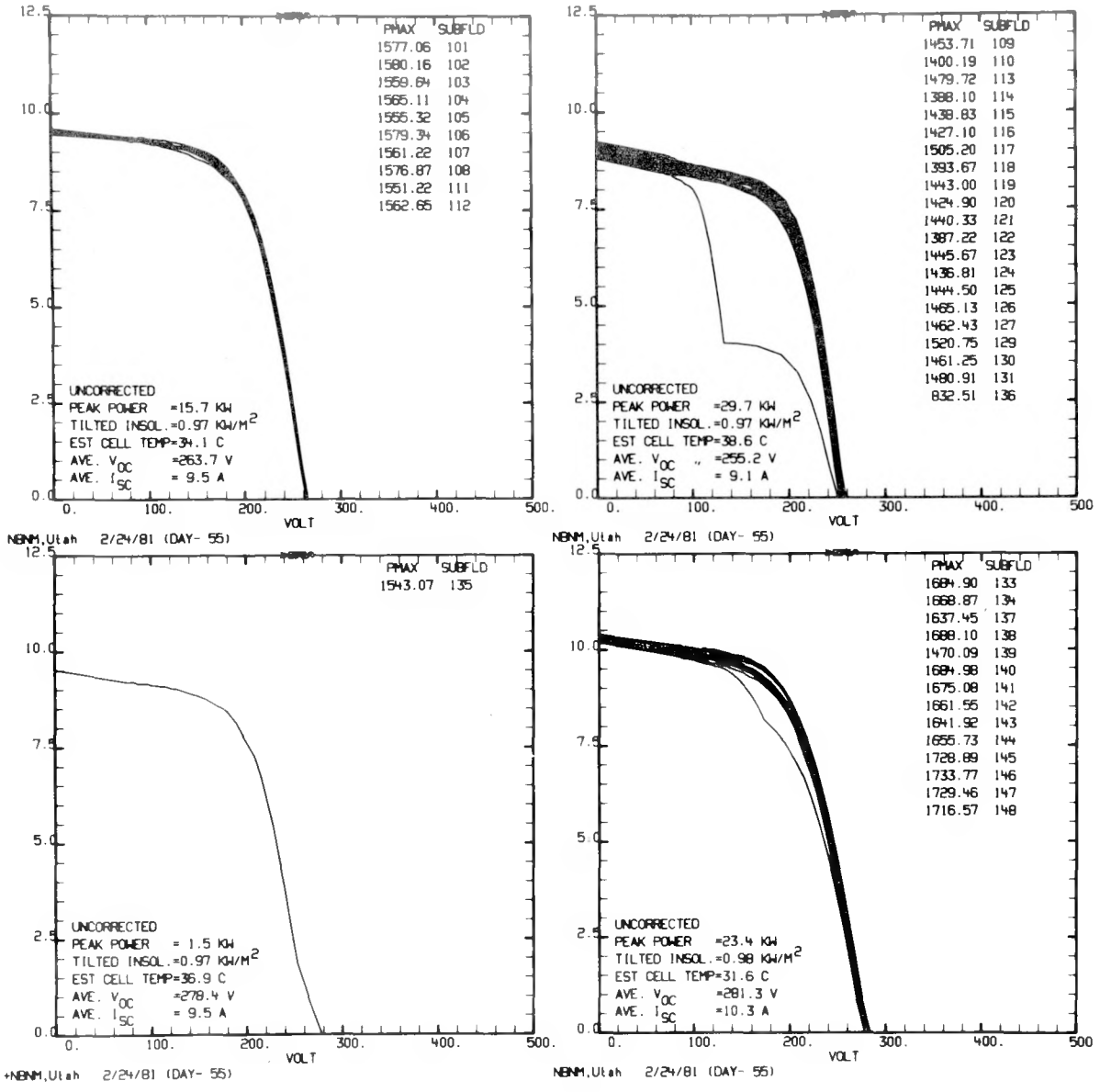

Fig. 5-10. Multiple plots of I-V scans for all array subfields.

5.7 PV System Performance

The performance of the NBNM PV power system is described in the following sections. The first section presents a comparison between computer predictions and observed values for energy and power production and for component and system efficiencies. The second section provides a summary of the overall system and subsystem performance.

5.7.1 Comparison of Predicted and Measured Performance

As part of the design process, the NBNM PV power system was simulated on a computer using analytical models for the array, battery, auxiliary power and inverter. Initial simulation work was done with SOLMET data for Albuquerque, New Mexico. The models used for the array, battery, inverters and auxiliary power source are given in References 13 and 14.

Figure 5-11 presents a comparison of simulated array energy for various insolation conditions and site loadings. The top curve in the figure shows the daily average energy available each month from an ideal array (one which always operates at maximum power with no losses) assuming that the weather is also ideal (clear and constant). The energy available from an ideal array operating in typical weather conditions is shown in the second simulated data curve while the middle curve presents the daily average energy available from a less-than-ideal array operating in worse-than-average weather. The simulations also reflect the energy available from the array when: (1) the array operates at maximum power (4th curve from the top), (2) the array operates below maximum power (bottom curve).

C74-1167

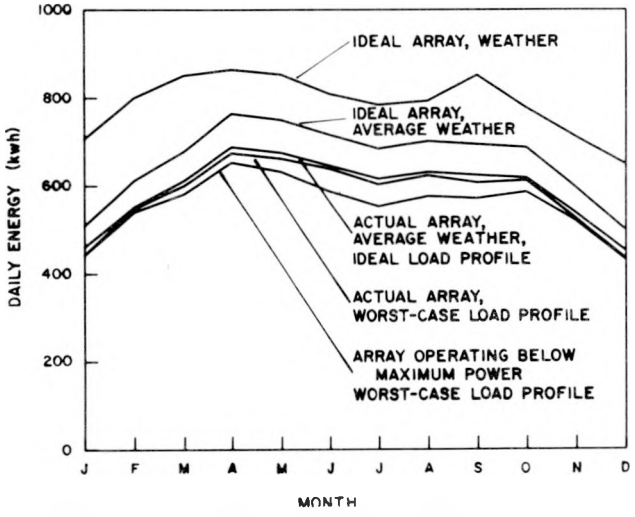

Fig. 5-11. Predicted energy available from array.

A comparison between simulated and measured system energy flow for six months of actual system performance is shown in Table 5-7. As the table shows, actual system loads at NBNM from January through June 1981 were considerably

lower (due to conservation efforts) than originally estimated. Although the individual overhead loads (UPS inverter, PV building) were estimated incorrectly, the total overhead load of 7 MWh used in the simulation agrees very closely with the actual 8 MWh. It is also noteworthy that the percentage of simulated and actual energy that went through the battery agree very closely (56% of the energy input into the actual system went through the battery, compared with a predicted value of 57%).

TABLE 5-7

SYSTEM ENERGY FLOW
(January through June 1981)

	Simulation	Actual
Energy Input Into System		
Array Energy	85 MWh	58 MWh
Auxiliary Energy	10	4
Direct to Load	0	0.3
Intermediate Energy Distribution		
Energy Direct to Inverter	41	27
Energy through Battery then Inverter	54	35
DC Load	87	57
Energy Output from System		
Losses		
Battery	8	5
Inverter	18	14
Loads		
Overhead		
UPS Inverter	5	3
PV Building	2	5
Site	62	35
TOTALS (MWh)		
Total Energy Input	95	62
Total Losses	26	19
Total Loads	69	43

Figure 5-12 presents a comparison between simulated monthly loads data and actual load data collected at NBNM from January through July 1981. According to the results of the simulation, the actual loads measured during this period should fall into the "low load" region, except for the January load. (The January load is categorized as medium.) A load is designated as a low load if it is never necessary to use the diesel backup to augment the

battery state of charge; it is a medium load if occasional diesel usage is required. From February through July, the auxiliary power was never used to boost the battery SOC (it was used only for equalization). In January, however, auxiliary power was occasionally used to boost the SOC as well as for equalization. Thus, January fits into the definition of medium load.

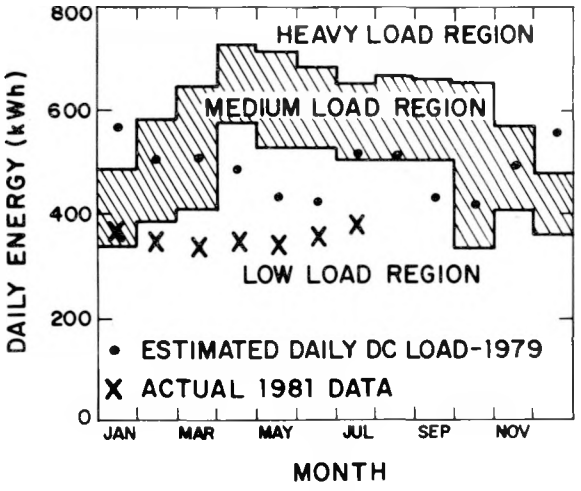

C74-1665

Fig. 5-12. Monthly load categories.

A comparison was also made between simulated and actual effects of system load upon battery SOC. According to the simulation, the battery SOC exhibits certain patterns which depend upon the kind of load the system is carrying; the actual SOC data exhibited similar behavior to that predicted in the simulation. Figures 5-13 and 5-14 show battery SOC, both actual and simulated, for January and April 1981, respectively. January shows the SOC pattern characteristic of a medium load, whereas April shows a light load pattern. This is what was predicted (cf. Fig. 5-12) when varying loads were superimposed on the system for each month of the year. Note that in January the SOC does not go all the way down to 20% as it did in the simulation. This is because it was assumed in the simulation that the generator (auxiliary power) could be turned on any time, day or night. While this is in theory true, in actual operation the generator was typically started late in the afternoon, when people were around to make sure that it worked, even though the SOC was greater than 20%.

5.7.2 Summary of PV System Performance

A large amount of performance data was gathered over an eighteen-month period of operation. These data include information on energy flow within the

C74-1770

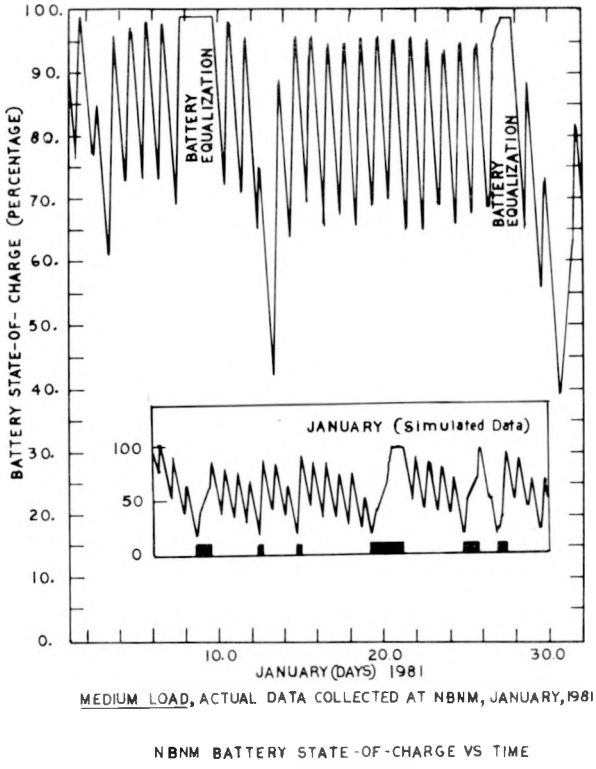

Fig. 5-13. Battery plots.

C74-1769

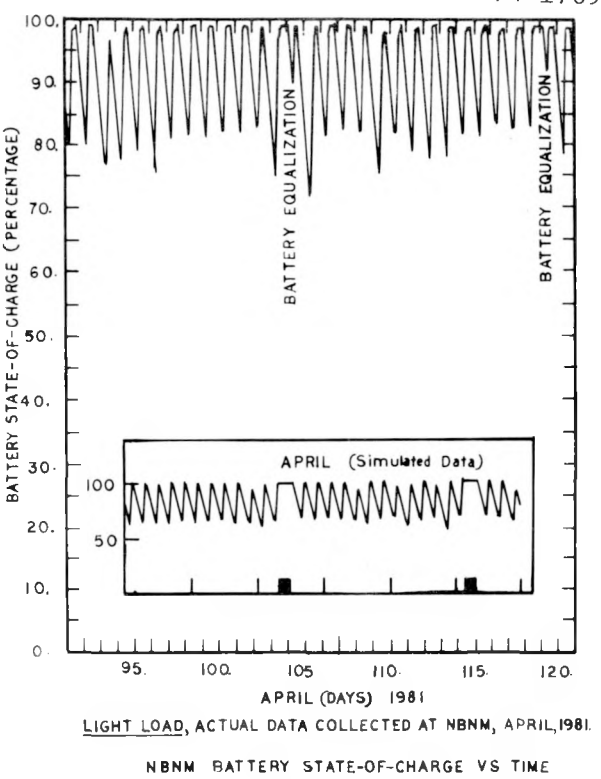

Fig. 5-14. Battery plots.

system, individual component and overall system efficiencies, and performance data for each of the five major subsystems discussed earlier in this report. A summary of the overall PV system performance derived from these data follows.

From June 1980 through October 1981, 90% of the NBNM site load (108,760 kWh of the total 120,844 kWh of site ac energy usage) was supplied by the PV system. This performance of the PV system is consistent with the original goal of sizing the system so as to serve 85 to 90% of the site load with the PV system.

A complete summary of the NBNM site ac energy usage (June 1980 through October 1981) is presented in Table 5-8. A block diagram showing system energy flow during a typical month is presented in Fig. 5-15. Included in this figure are integrated values for various system components, their measured efficiencies and characteristic energy flow.

C74-1668

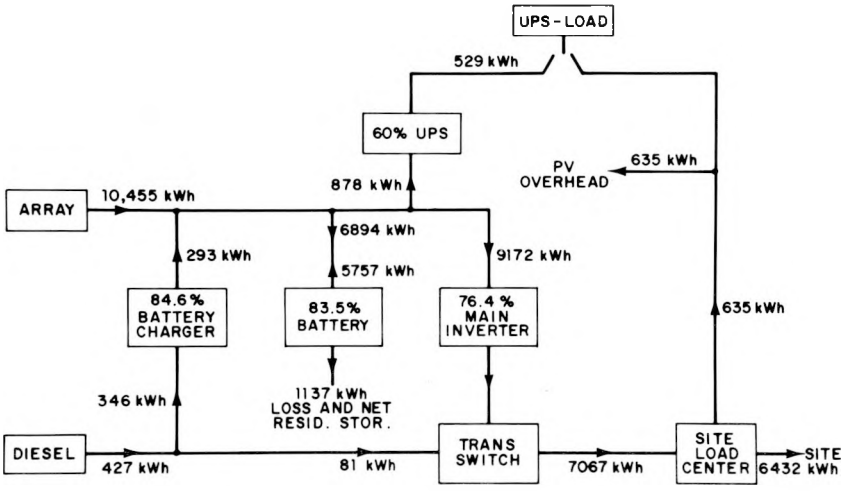

Fig. 5-15. Block diagram of energy flow (2/81).

TABLE 5-8

AC ENERGY SUMMARY
(June 1980 through October 1981)

	1980	1981	Total
Site ac Load (kWh)	53,390	67,454	120,844
Diesel Generator*	33	16	23
PV System*	77	99	90
PV Building*	12	11	11
UPS*	8	8	8

*As percent of site ac load.

NOTE: The sum of the energy produced by the diesel generator and the PV system is greater than 100%. This is due to the energy required for battery equalization and the efficiency of the battery charger and main inverter.

Table 5-9 presents a summary of average component and system energy efficiencies measured at NBNM over a 16-month period (July 1980 through October 1981). The average energy efficiencies for both the battery charger and battery system (85%) agree favorably with manufacturers' ratings, whereas the energy efficiencies of the two inverters--75% and 61%, respectively--are lower than the 85% and 88% ratings quoted for the respective main and UPS inverters. The reason for this difference is that both units exhibit maximum efficiency at full load and zero efficiency at no load, due to the effects

of tare losses. The tare loss of the main inverter is 2.5-3.0 kW; that of the UPS inverter is 400 to 475 W. Both tare losses vary with the input voltage and are highest at the higher voltages. Full-load efficiencies of the inverters are 85 and 88% for the main and UPS inverters, respectively. The load on the main inverter varies from 8 to 20 kW; the UPS load is almost constant at 750 W.

TABLE 5-9

MEASURED AVERAGE COMPONENT AND SYSTEM ENERGY EFFICIENCIES
(July 1980 through October 1981)

	Average Value (%)	Variation (%)
Battery Charger	85	±1
Main Inverter	75	±4
UPS Inverter	61	±3
Battery*	85	±5
Array+	5.4	±1.3
System++	67	±4.5

*Battery efficiency is the ratio of energy released on all discharges to the energy stored on all charges.

+Array efficiency is the ratio of the solar energy falling on the gross array area to the array dc-energy output. Due to array shedding, this efficiency is less than the cell efficiency and will vary seasonally and with the site load.

++System efficiency is defined as the ratio of the ac-load energy delivered by the UPS and main inverters to the dc energy generated by the array and battery charger.

5.7.2.1 PV Array Performance

After 24 months of field operation, the number of PV module failures at NBNM is 56, or 1.2% of the 4500 modules installed there. (A failed module is one which delivers less than 75% of its nominal short-circuit current under the measurement conditions.) Although this is an encouragingly low failure rate, it was found that all but three of the failures occurred in the Motorola modules, and were the result of short circuits between the electrically active cells and the steel substrate used for this module. This is discussed further in Reference 17 as well as in Section 6 of this report.

On several occasions large array outputs, resulting from insolation and temperature extremes, have been recorded. On 11 October 1981, for example, a peak radiation of 1.34 kW/m^2* produced a peak array power of 130.7 kW from the 100-kW peak PV system. Since the battery state of charge was low (72%), all array subfields were on-line and the battery voltage of 257.9 V was close to the maximum power voltage of the array I-V curve. Array temperature, at the time of peak radiation, was 20¼C.

Figure 5-16 presents a bar graph history of maximum array power output during a typical month. As the graph illustrates, a maximum power of 120.2 kW was registered on Day 109 (19 April 1981), a scattered cloudy day, with intermittent bright sunlight breakthroughs.

During January and February 1981, a number of arrays became inoperative following snowstorms. The problem was traced to a group of fast-blow, 15-A fuses that were accidentally used for the lightning-protection fuses on the wires to the array field. The fuses were apparently blown by transient current surges of 16 to 17 A, which occurred when the arrays were switched on and off during a period when the insolation was enhanced by snow albedo and clouds. During this period, insolation peaks of 1.4 kW/m^2 were observed on the array area tilted pyranometer. The 15-A fuses were replaced with medium-speed, 20-A fuses and no further problems occurred. Because of its inherent redundancy, the array system has been quite reliable.

5.7.2.2 Battery Performance

The performance of the lead-acid battery installation at NBNM was closely monitored during the first eighteen months of system operation. Two types of measurements were conducted to monitor the battery performance: physical measurements on the cells themselves and electrical measurements via the data logger.

The physical measurements taken were of individual cell voltage, electrolyte levels and specific gravity readings. These measurements were manually taken

*The phenomenon of unusually high insolation is usually the result of natural concentration of sunlight through apertures in fast-moving scattered clouds. On other occasions, reflections from snowfields surrounding the array have also produced larger-than-normal array outputs.

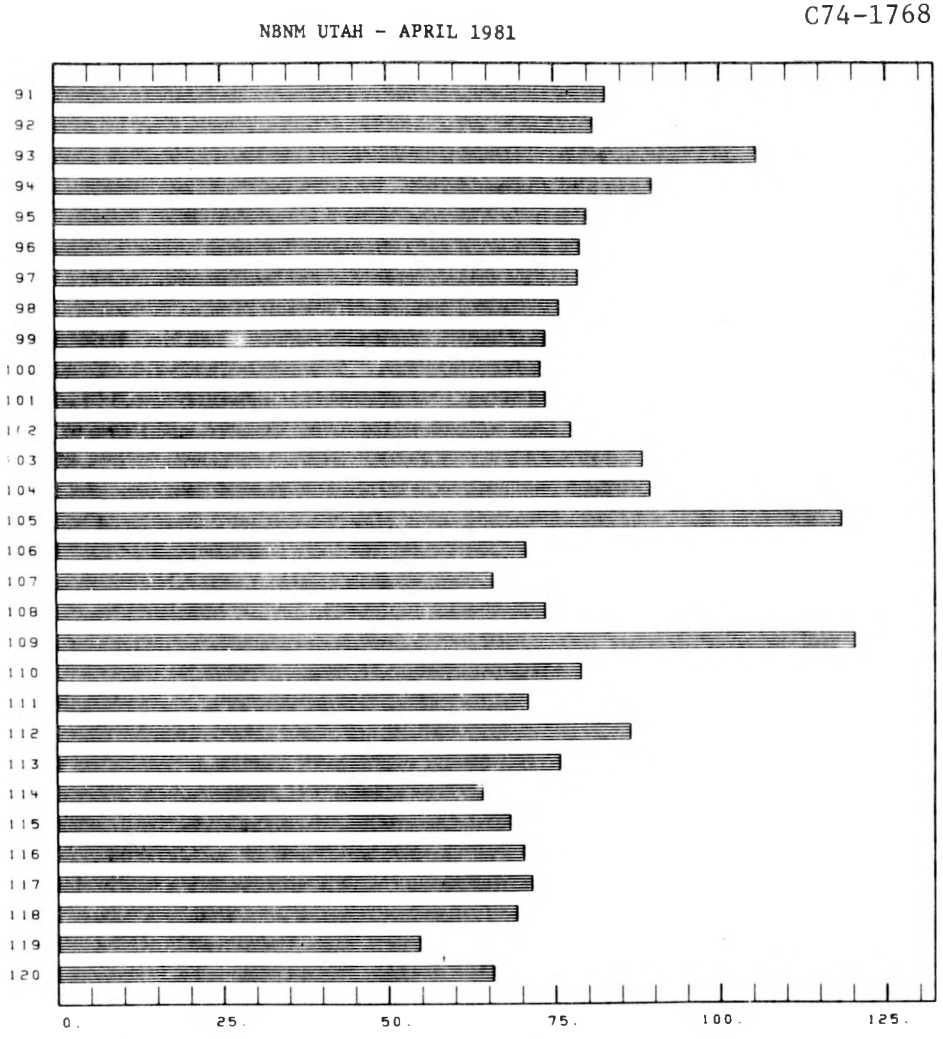

Fig. 5-16. Bar graph of maximum array power.

at the end of an equalizing charge when the battery was in a fully charged state. Readings of 224 cell voltages, done with a voltmeter, could be taken and recorded by two people in less than a half hour. The watering operation required to adjust battery electrolyte levels took about 6 to 8 man hours and, since it should be done with the battery on charge, required extra care. Specific-gravity readings require 3 to 6 man-hours and were performed with the PV system shut down and the battery off-line.

During the first year of operation, two cells in one of the 28 battery modules showed significant deterioration and the module was returned to the manufacturer for service. Since shipping costs are significant, this experience suggests that a battery package with fewer or even one cell might be more cost effective (less shipping weight and more flexibility with spare units).

Electrical measurements, which include battery voltage, current and SOC, were recorded on the data logger at regular 10-minute intervals. Figure 5-17 shows a typical daily plot of battery voltage and current versus time for a sunny day. Note that the battery voltage rises to 280 V by about noon and the battery-charging current drops to a fairly low value of less than 10 A by about 3 p.m. As Fig. 5-18 illustrates, the battery SOC reaches 99% (highest value displayed) at this time.

C74-1533

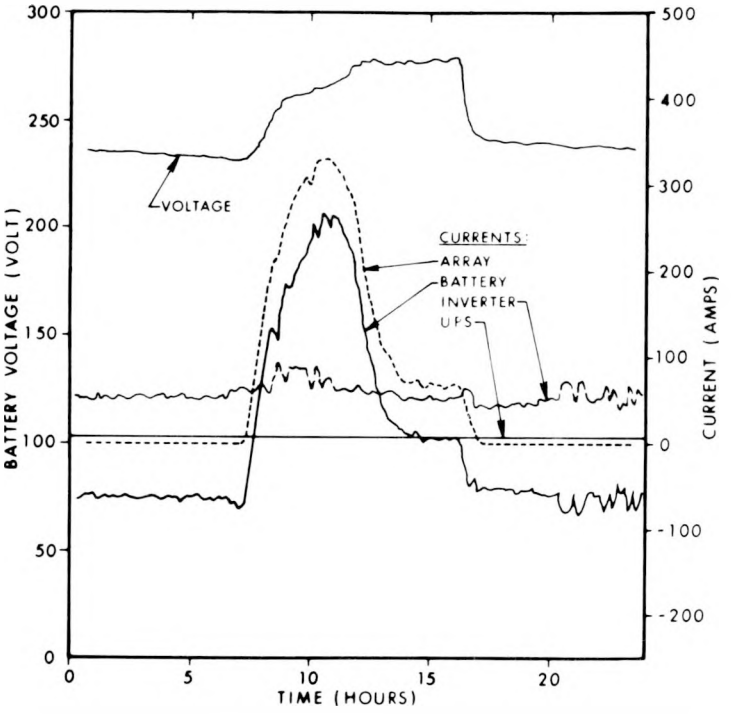

Fig. 5-17. Voltage and current versus time.

In summary, the battery subsystem at NBNM continues to perform satisfactorily. Automatic battery equalization and/or trickle charges, hydrogen recombiners, and other automatic accessories need to be improved in order

C74-1534

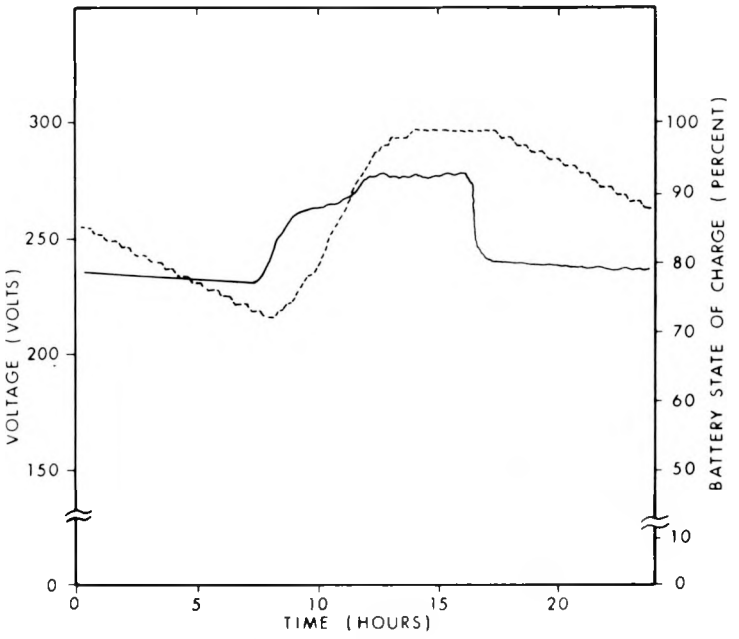

Fig. 5-18. Voltage and SOC versus time.

to cut operating and maintenance costs to a minimum. For example, the amount of energy consumed annually for battery-charge equalization is about 5% of the total PV system output. Additional information on battery maintenance, efficiency and thermal performance is given in References 9, 15 and 16.

5.7.2.3 Power-Conditioning Performance

The principal power-conditioning elements of the NBNM system include two inverters (a main inverter with a capacity of 50 kVA, and a smaller 5-kVA UPS inverter) and a battery charger.

- Inverter Performance

During 18 months of continuous operation, the PV system unscheduled downtime amounted to approximately 7% of the total operating period; the inverters were responsible for almost all of the downtime.

During the initial checkout of the system, four inverter-related problems were encountered: (1) overload of the main inverter due to initial core saturation at turn-on of a large power-distribution transformer, (2) radio noise emanating from the main inverter, (3) sensitivity of the inverter

control circuitry to radio-frequency (450 MHz) energy from a nearby radio-telephone, and (4) malfunction of the small UPS inverter resulting from the very low resistive-source impedance in the large battery. These problems were solved with: (1) a resistive starter to limit initial current, (2) power-line filtering, (3) radio-frequency filtering, and (4) installation of a small resistor in series with the UPS inverter.

The longest main inverter outage (14 days), resulted from a shorted SCR and occurred in November 1980 just before Thanksgiving, when the holiday delayed the arrival of the manufacturer's service representative. An intermittent problem with the inverter which caused blown fuses on startup during cold weather was traced to a faulty SCR. Two subsequent main inverter failures were readily diagnosed over the telephone and repaired by NPS maintenance personnel.

- Battery Charger Performance

The performance of the Ratelco 40-kW battery charger has been excellent. Since installation at NBNM in early 1980, there have been no instances of component problem/failure.

5.7.2.4 System Control Performance

The performance and reliability of the PV power system control elements, which include a manual control panel and a microprocessor-based, automatic-control unit (ACU) for array regulation and other control functions, have been excellent. Routine performance of the five principal tasks accomplished by the ACU has been flawless.

One problem involving the interface between the system control and data acquisition was readily resolved by replacement of a faulty power supply. (The supply had been providing 3 V instead of the required 5 V.)

5.8 Lessons Learned

Lessons learned during the design, construction and operation of the 100-kW NBNM PV system are summarized below. See References 18 through 21 for further discussion of the topics in this section.

5.8.1 Unattended Operation

Despite the considerable complexity of the NBNM system (being a stand-alone ac system and having both a backup diesel and battery-storage unit, it represents an extreme case for flat-plate PV system designs), it was found that extended, unattended operation is feasible. As was the case for the WBNO system, this is due mainly to the enormously flexible and reliable control of the system afforded by the microprocessor-based control unit.

5.8.2 Repair and Maintenance

It is vital that adequate stores of on-site spares be provided, and that up-to-date and identical documentation sets on the system be available both at the site and at the PV system suppliers' facilities so that problems can be solved over the telephone. A full set of system manuals, References 22 through 25, was prepared for this system.

In addition, the NBNM experience showed that an on-site training course is necessary for the operators and the maintainence people.

5.8.3 Simpler Systems

The NBNM system would have been simplified considerably by use of a manual transfer switch (for switching from the PV system to the diesel generator). In view of the limited number of times that this switching is performed, a manual approach is probably preferable.

5.8.4 Mercury Relays for Array Shedding

The mercury relays used at NBNM provide a simple, reliable means for switching sections of the array in and out of the system. They are preferable to transistor switches because the latter, being solid-state devices, are more susceptible to lightning damage.

5.8.5 Batteries

A decision to utilize on-site storage has far-reaching implications relative to system complexity, cost, space/volume requirements and overall system efficiency. If the opportunity presents itself to eliminate this function by a utility-interactive connection, it should certainly be done.

If on-site storage is required to supply electricity on demand at any time, the PV system designer currently has only one option; namely, the use of lead-acid batteries. This being the case, the designer would be well advised to strive for:

1. Very low maintenance (once per year) batteries (the NBNM batteries require service every 2 to 3 weeks, and the recombiner, float-level indicator and air-lift system interfaces could be improved).
2. Batteries of smaller size (each module of the NBNM battery weighs 2400 pounds, which presents significant handling problems).

In addition, every attempt should be made to minimize the size of the battery not only because of cost but also because of energy losses associated with equalization. One way to do this might be to provide storage in alternative ways. For example, if one of the uses of the PV system is for pumping water, storage could be provided by pumping extra water to an elevated resevoir during sunny periods.

5.8.6 Site Energy Audits

Because of their extreme complexity, stand-alone PV systems of the type exemplified by the NBNM system will always be relatively expensive compared with the simpler dc-only systems or ac utility-interactive systems. Accordingly, it is particularly important that all components of the electrical load be critically examined prior to establishing the power rating of the PV system. In the case of NBNM, the audit turned up instances of inappropriate use of electric energy, mainly in connection with the use of resistance heaters (LP gas heaters are usually cheaper, even in a region as remote as Natural Bridges) and carelessness in shutting off lights when they are unneeded.

5.8.7 PV Modules with Metal Substrates

As a result of the NBNM experience with PV cells shorting to the metal case, it has become apparent that either the design of modules with metal substrates must be improved or that the metal substrates should be replaced with a dielectric material. This generic design does not appear in more contemporary modules.

5.8.8 Design Protection Against High PV Array Output

In light of the high insolation peaks recorded at NBNM and at WBNO (1.47 and 1.39 kWh/m^2, respectively), the system designer should ensure that a flat-plate PV system can safely withstand insolation peaks of, say, 1.5 kW/m^2 for a duration of one hour.

5.8.9 Inverters

Improvements are needed in the design of inverters to:

1. Render them more "bullet proof" regarding overcurrent protection,
2. Eliminate the generation of radio-frequency noise, and
3. Provide for simpler, faster replacement of failed components.

5.8.10 Subarray Structures

Although the size of the subarrays was determined on the basis of minimum fabrication and installation cost, it appears in hindsight that insufficient weighting was applied to installation costs. The subarrays at NBNM are relatively large and therefore awkward to handle in the field.

5.8.11 Enhanced Output from Modules

To improve the electrical output of the Spectrolab Block II modules by 8 to 10%, the rear surface of the module was painted white. This white coating internally reflects the light which would otherwise pass through the transparent areas of the module between the cells and scatters it in the encapsulation to provide additional light to the PV cells. This feature has since been incorporated in most commercial glass substrate modules.

Painting the rear surface of Motorola and Arco modules with high-emissivity coatings was investigated (26) in an attempt to reduce module and cell temperatures and hence increase output power.

For silicon solar cells, power output increases about 0.5% for each $1^{o}C$ the cell temperature is lowered. The coatings lowered cell temperature between 2 and $5^{o}C$ so the power output increased only 1 to 2.5%. This was not enough to warrant painting of modules after they were received in the field but might have been cost effective if done at the factory.

REFERENCES

1. Lyon, E. F., et al, "Design of the Natural Bridges National Monument 100-kW PV Power System," 1978 IEEE PV Specialists' Conference, Washington, DC, 5-8 June 1978, COO-4094-20.

2. Peatfield, C. R. and Jarvinen, P. O., "Photovoltaic Applications in the Southwest for the National Park Service," MIT Lincoln Laboratory Technical Report, 28 April 1977, COO-4094-3.

3. Jarvinen, P. O. and Peatfield, C. R., "Photovoltaic Applications for the National Park Service," 12th Intersociety Energy Conversion and Engineering Conference, Washington, DC, 28 August-2 September 1977, COO-4094-11.

4. Jarvinen, P. O., "Natural Bridges National Monument, Utah--Solar Photovoltaic Power System Design," Second National Conference on Technology for Energy Conservation, Albuquerque, NM, 24-27 January 1978, COO-4094-14.

5. Benoit, A. E., "Construction of a PV Power System at Natural Bridges National Monument," MIT Lincoln Laboratory Technical Report, December 1980, DOE/ET/20279-94.

6. Brench, B. L., "Snow-Covering Effects on the Power Output of Solar Photovoltaic Arrays," MIT Lincoln Laboratory Technical Report, December 1979, COO-4094-61.

7. Bucciarelli, L. L., et al, "The Energy Balance Associated with the Use of a Maximum Power Point Tracker in a 100-kW Peak Power System," 14th IEEE PV Specialists' Conference, San Diego, CA, 7-10 January 1980, COO-4094-72.

8. Grossman, B. L., "Simulated Performance of the Stand-Alone Photovoltaic System at Natural Bridges National Monument," MIT Lincoln Laboratory Technical Report, March 1981, DOE/ET/20279-125.

9. Solman, F. J. and Grossman, B. L., "Operating Experience with the Natural Bridges National Monument Photovoltaic Power System," 15th IEEE PV Specialists' Conference, Orlando, FL, 11-15 May 1981, DOE/ET/-20279-135.

10. Lyon, E. F., "The Design and Construction of a 100-kW Photovoltaic Remote Stand-Alone Power System," 1979 Photovoltaic Solar Energy Conference, Berlin, Germany, 23-26 April 1979, COO-4094-54.

11. Lyon, E. F., "A 100-kW Peak Photovoltaic Power System for the Natural Bridges National Monument," ISES Silver Jubilee International Solar Exhibition, Atlanta, GA, 28 May-1 June 1979, COO-4094-46.

12. Hopkinson, R. F., "Safety Procedures for the 100-kW Solar Photovoltaic System at Natural Bridges National Monument," MIT Lincoln Laboratory Technical Report, September 1981, DOE/ET/20279-108.

References (continued)

13. Klein, D. N., "Safety Analysis Report, Natural Bridges National Monument 100-kW PV Power System," MIT Lincoln Laboratory Technical Report, September 1981, DOE/ET/20279-116.

14. Brench, B. L., et al, "Simulation of the Performance of a 100-kW Peak Photovoltaic System," 14th IEEE PV Specialists' Conference, San Diego, CA, 7-10 January 1980, COO-4094-71.

15. Brench, B. L., "Operational Experience in Lead-Acid Batteries for Photovoltaic Systems," 15th IEEE PV Specialists' Conference, Orlando, FL, 11-15 May 1981, DOE/ET/20279-118.

16. Brench, B. L., "Application, Sizing, Testing and Performance of the Photovoltaic Battery Subsystem at Natural Bridges National Monument, Utah," MIT Lincoln Laboratory Technical Report, November 1981, DOE/ET/20279-153.

17. Forman, S. E. and Themelis, M. P., "Materials, Processes and Testing Laboratory Final Report Summarizing Module Performance at MIT Lincoln Laboratory Experimental Photovoltaic Test Sites, 1977-1982," MIT Lincoln Laboratory Technical Report, June 1982, DOE/ET/20279-188.

18. Solman, F. J. and Nichols, B. E., "Design, Construction and Evaluation of Two Large Photovoltaic Power Systems," 1980 Annual Meeting of American Section of ISES, Phoenix, AZ, 1-5 June 1980.

19. Solman, F. J., et al, "The 100-kWp Photovoltaic Power System at Natural Bridges National Monument," 15th Intersociety Energy Conversion Engineering Conference, Seattle, WA, 18-22 August 1980, DOE/ET/20279-98.

20. Solman, F. J., "Photovoltaic System Performance Experience," presented at the 15th IEEE PV Specialists' Conference, Orlando, FL, 11-15 May 1981, DOE/ET/20279-147.

21. Solman, F. J., Bullwinkel, H. J., Doucet, J. D., and Brench, B. L., "A Photovoltaic System with Energy Storage - Natural Bridges National Monument 100-kW System," presented at the AIAA 20th Aerospace Sciences Conference, Orlando, FL, 11-14 January 1982, DOE/ET/20279-171.

22. Coleman, S. D., "Operations Manual for Photovoltaic Power Systems--Natural Bridges National Monument," MIT Lincoln Laboratory Technical Report, February 1982, DOE/ET/20279-142.

23. Solman, F. J., et al, "Maintenance Manual for the PV Power System at Natural Bridges National Monument," MIT Lincoln Laboratory Technical Report, July 1982, DOE/ET/20279-177.

24. Baird, R. H., et al, "System Design Drawings for the PV Power System at Natural Bridges National Monument," MIT Lincoln Laboratory Technical Report, 30 May 1982, DOE/ET/20279-178,

References (continued)

25. Coleman, S. D., Ed, "Power Processing Subsystems for the 100-kWp Solar Photovoltaic Power System at Natural Bridges National Monument in Utah," MIT Lincoln Laboratory Technical Report, July 1982, DOE/ET/20279-180.

26. Raghuraman, P., "On Influencing the Operating Temperatures of Motorola and ARCO Solar Photovoltaic Modules," MIT Lincoln Laboratory Technical Report, October 1979, COO-4094-59.

6.0 MEASUREMENT OF PV MODULE PERFORMANCE AND RELIABILITY

6.1 Introduction

This section summarizes the results of a six-year program of periodic inspections and measurements of PV modules at several Lincoln Laboratory test sites. Specific details are given of module failures and failure rates and of the electrical and physical degradation of modules due to weathering. The section concludes with a summary of lessons learned which it is hoped will be of benefit to designers of improved PV modules.

In this activity, MIT Lincoln Laboratory worked closely with the California Institute of Technology's Jet Propulsion Laboratory (JPL), the latter organization being the source of the PV modules for the evaluation program. Lincoln Laboratory received modules from various manufacturers who had been funded by JPL as part of their large scale procurement activity for DOE. Each module was inspected at the factory of origin by JPL, and an inspection sheet was prepared outlining its physical appearance and workmanship-related anomalies. This information constituted the initial conditions present in the module, and subsequent degradation was measured against these starting conditions (1). Key physical and electrical features for all of the modules involved in this program are given in the appendix to this section.

Module measurements were made at two different types of field sites. One group consisted of complete PV systems, most of which contained a relatively large (measured in kilowatts) PV array. This category includes the following:

25-kWp Mead PV system
1.6-kWp PV system at the Chicago Museum of Science and Industry
15-kWp system at Bryan, Ohio
100-kWp Natural Bridges PV system
7.5-kWp Residential system at Arlington, Texas
25-kWp PV test bed at Concord, Massachuetts
10-kWp PV test bed at Lincoln Laboratory, Lexington, Massachusetts.

The second group included several small sites which were established at selected locations for the purpose of obtaining data on PV arrays only. These include:

New York City, rooftop arrays:	361 W at New York University
	179 W at Columbia University
Summit of Mt. Washington, NH:	88-W array
Cambridge, Massachusetts:	327-W rooftop array.

Data from each of these sites are discussed.

Contributions to this effort were made by the following individuals: Joseph D. Doucet, Leo A. Dube, John A. Farnsworth, Steven E. Forman, John P. Husler, John T. Kelly, M. Patricia Themelis and Thomas H. Warner.

6.2 25-kWp System at Mead, Nebraska

The array field for the Mead system consists of 28 subarrays of PV modules, separated into two rows. The front row consists of 728 silicone-encapsulated Solarex modules, the back row has 1512 silicone-encapsulated Sensor Tech modules. Both module types are from the JPL/DOE Block II procurement.

At Mead, every module in the array field was inspected twice a year for the first two and a half years, and the changes and degradation which the modules underwent in the field were carefully recorded and related to the DOE 20-year lifetime goal. Prior to inspection, each module in the array field was washed, using the techniques for silicone-encapsulated modules described in Reference 2. For the most part, these field-washing techniques left the silicone-rubber outer surfaces of the modules optically clear, and the cells could be viewed easily. During each field inspection, hand-held magnifying glasses were used to examine the solar cells.

The results of four field inspections, conducted in March and September 1979 and 1980, are presented here. A cumulative listing of the types of physical defects observed is presented in Table 6-1. At present there is little or no correlation between many of these defects and electrical degradation. The defects, however, present evidence of the types of real-time changes which can be expected to occur in silicone-rubber-encapsulated modules.

Over half the modules inspected had one or more cracked cells. Many of these cracks were caused by a hailstorm in May 1978, but a significant number were evidently the result of fatigue due to cyclic thermal conditions. A summary of cracked cell data is presented in Table 6-2.

The highlights of these data are:

1. A total of 61% of the Sensor Tech modules had at least one cracked cell while 28% of the Solarex modules had at least one cracked cell.
2. A total of 47% of the cracked cells on Sensor Tech modules had impact cracks caused by hail. The remaining 53% were caused by the positioning of cells over structural ribs filled with silicone rubber. At these positions uneven pressures were applied to the cells during heating and cooling, causing subsequent cracking.
3. A total of 93.4% of the cracked cells on Solarex modules contained impact cracks due to hail. Without the hail damage, the cells in these modules seemed less likely to crack.
4. A total of 2.2% of all the cells on 26 frames were cracked after 27 months of operation.

TABLE 6-1

MODULE PHYSICAL DEGRADATION AT MEAD, NEBRASKA, CUMULATIVE FIELD INSPECTION RESULTS

Time Period: 7/77 - 10/79

Defects	Modules
Module inspected	2080
Edge-seal delamination	1037
Newly cracked cells	1044
Delamination over cells	386
Delamination over or around interconnects (IC)	65
Split encapsulation over IC or cell	54
Protruding IC or cell	35

TABLE 6-2

CRACKED CELL DATA AT THE MEAD TEST SITE

Time Period: 7/77 - 10/79

Mfg.	Modules Inspected	Modules with Cracked Cells	Total No. of Cracked Cells	No. of Impact Cracked Cells	Total No. of Cells
Solarex	676	188	425	397	28,392
Sensor Tech	1404	856	1596	758	61,776
TOTALS	2080	1044	2021	1155	90,168

As is evident from these highlights, the predominant cause of electrically failed modules at Mead has been the cracked cell. Each module is a series assemblage of cells, and it only takes one cell, cracked in the right way, to interrupt the flow of current through this series circuit in the module. A module is considered to be an electrical failure when it produces less than 75% of its nominal short-circuit current under the prevailing conditions. To date, fourteen searches for electrically failed modules have been conducted since system turn-on. The results of these searches are summarized in Table 6-3.

TABLE 6-3

Module Failures at Mead Test Site

Front Row: 728 Modules (Solarex)
Back Row: 1512 Modules (Sensor Tech)

Starting Date: July 1977

Date of Search	Number of Failures Found Front Row	Back Row
October 1977	0	1
November 1977	1	1
February 1978	0	3
March 1978	0	0
July 1978	6	3
September 1978	3	1
February 1979	2	0
March 1979	1	2
July 1979	6	7
October 1979	1	10
July 1980	11	7
October 1980	4	26
March 1981	4	13
September 1981	25	23
TOTALS	64	97

The data of Table 6-3 are plotted in Fig. 6-1, where each data point represents the cumulative percentage of failed modules after a particular period of operation. In 50 months of operation, 161 out of 2240 modules (7.19%) have failed. Since the hailstorm of May 1978, the slope of this curve has been steadily increasing. As indicated in Table 6-2, there are still many cracked cells which have not yet caused modules to fail. In order to disrupt current flow, a crack must penetrate through the entire thickness of a cell. This can happen days or years after the initial cracking.

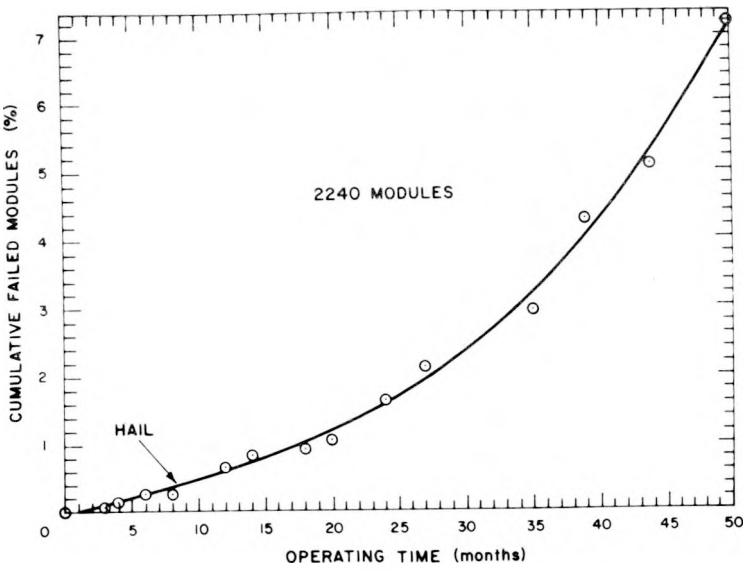

Fig. 6-1. Cumulative percentage of failed modules, Mead, Nebraska.

A large number of newly impact-cracked cells were found on the failed modules removed in September 1981, and it was subsequently learned from site personnel that a second severe hailstorm had occurred in Mead in June, 1981. In an effort to determine the extent of storm damage to the arrays, site personnel measured the short-circuit current of every module in the back row, under high-insolation, warm-weather conditions during October-November 1981. The results were extraordinary: 121 modules (8% of the total number) were operating at less than 75% of the nominal module short-circuit current. Similar measurements for the front row indicated only one additional failure. Clearly the back row modules are more prone to hail damage.

Seven of the Solarex failures found in 1980 and 1981 displayed a different type of failure mode--a pair of broken interconnects on one cell. This type of failure has also been observed at Bryan, Ohio, and Concord, Massachusetts, in the Block III version of this module. It is caused by differential thermal expansion of the polyester substrate, metal interconnects, and silicon cells during diurnal temperature cycling. The likelihood of failure is increased when an inadequate strain-relief loop is placed on an interconnect. Further discussion of this failure mode is included in Section 6.4.

6.3 1.6-kWp System at Chicago Museum

An array of 288 Block I Spectrolab modules was placed on the roof of the Chicago Museum of Science and Industry in July of 1977. The modules used in this array are glass covered and consist of twenty 2-in.-diameter cells potted in silicone rubber and set on the top surface of an aluminum I-beam. Further details are found in the appendix to this section.

These modules were initially assigned by JPL to NASA Lewis Research Center in 1976 and subsequently used in a high-voltage application. Several modules incurred short circuits between cell rearsides or interconnects and the aluminum substrate. The modules were deemed unusable by NASA Lewis and sent to Lincoln Laboratory in early 1977. Three-hundred modules selected from those which had passed a 1500-Vdc "hi-pot" test conducted at Lincoln Laboratory were sent to Chicago. The modules in the array were wired 3 in series by 96 in parallel to avoid high voltages.

The array was visited once a year to search for physical and electrical degradation. In five years of operation, no modules failed electrically. Visual inspections on the roof and in the Lincoln Laboratory Materials, Processes and Testing Laboratory (MP&T Lab) of *in situ* and removed modules showed evidence of delamination between the silicone rubber and the glass cover, the cell and the terminal discs of over half of the modules. Cells with discolored main collectors were also observed on over half of the modules. Little evidence of cell cracking was present.

A soil accumulation study was conducted on 12 modules after the first ten months of exposure. The power loss due to dirt ranged from 2.5 to 4.3% and was completely recovered upon washing. Further details pertaining to physical degradation in these modules are found in References 3 and 4.

6.4 15-kWp System at Bryan, Ohio

This 15-kWp PV system at radio station WBNO became operational in August 1979. The array field consists of 800 Block III, Solarex modules in which the cells are encapsulated in silicone rubber. These modules are almost identical to the earlier Block II version used at Mead.

Searches for electrically defective modules were made in the spring of 1980, and again during the spring and fall of 1981. None were found during the first visit; four were found during the second visit. In two cases, the cause of failure was a pair of broken interconnects. In another case, a cracked cell caused the failure. The cause of failure for the fourth module is unknown. After returning the module to Lincoln Laboratory, retesting showed proper performance under both normal and high-temperature conditions. It is suspected that deterioration or improper connection of module-to-module wiring caused the module to appear as an open circuit on the diagnostic I-V curve for its branch circuit during the field measurement.

In the spring of 1981, I-V curves were made of each branch circuit at the Bryan array field in order to search for electrically defective modules; a total of 42 open-circuited modules were found. Many of these were intermittent in behavior and their output depended very much on temperature. During warm periods the modules exhibited open-circuit failures and during cooler periods continuity was restored. Analysis of each of these modules at the MP&T Lab at Lincoln Laboratory showed that the cause of failure was one or more pairs of broken interconnects. During a similar visit in the fall of 1981, 74 more open circuits were detected. While these modules were not visually examined, it is likely that the cause of failure in most of them was again broken interconnects.

The cause of the interconnect failures is excessive stressing during diurnal temperature cycling. The degree of overstressing was found to be exacerbated if the interconnect contained large amounts of solder and/or sharp bends in the strain relief at the joint. Thus, process control plays an important role in determining failure rate for these modules; it is believed that variations in process control explain the difference between the low failure rates at Mead and the higher rates at Bryan, Ohio. Further details are found in Reference 5.

6.5 100-kWp System at Natural Bridges, Utah

The array for this system, shown in Fig. 6-2, contains 1740 Arco Solar modules in the front of the array field, 2064 Motorola modules in the

center, and 720 Spectrolab modules at the rear. The Arco Solar and Motorola modules were purchased as part of the Block III procurement while the Spectrolab modules are from Block II. All three types are glass covered.

CP267-5524

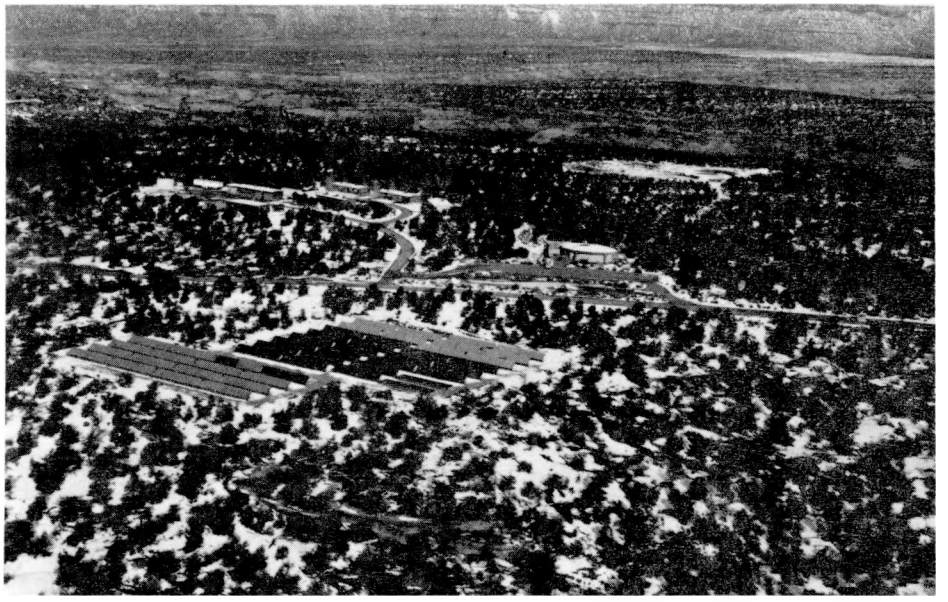

Fig. 6-2. Natural Bridges National Monument aerial view.

Although this system was officially dedicated in June 1980, the array field was installed in January of that year. The array was measured in January 1980, March 1980 and in November of both 1980 and 1981.

Over this measurement period, only 56 out of the total of 4524 PV modules failed. Of these failures, 53 occurred in the Motorola modules and were the result of short circuits between electrically active cells and the metal substrate used in this particular module.

During the same period of operation, only three of the 1740 Arco Solar modules failed electrically. One module became open-circuited when an interconnect solder joint on the rear of a cell failed; the other two failed when cracked cells open-circuited the module. No Spectrolab modules failed.

During January 1980, shortly after installation, it was noticed that the glass covers on 25 of the Arco Solar modules had cracked. Later, in March 1980,

27 more modules were found with cracked cover sheets. Close examination of three modules removed from the site indicated that each crack emanated from a flaw on one of the long edges of the untempered glass. It is believed that the cracks were caused by diurnal temperature cycling, which resulted in excessive tensile stresses at the flaw sites. Subsequent observations in November of 1980 and 1981 revealed no new cracking. However, the polyvinyl butyrate (PVB) along many existing cracks had started to yellow due to moisture penetration. The long-term effect of these cracks on module electrical performance is unknown. Nevertheless the electrical performance of these modules to date continues to be impressive.

More details on the degradation of NBNM modules are found in References 6, 7 and 8.

6.6 7.5-kWp System at Arlington, Texas

The Solar Energy Research Facility at the University of Texas at Arlington (UTA) was selected in 1978 by Lincoln Laboratory as the location for a series of residential experiments dealing with the use of photovoltaic/thermal (PV/T) collectors. Because combined PV/T collectors were not available in multi-kilowatt quantities, the UTA experiment was initiated in November 1978 using separate PV and thermal collectors. The PV array field was composed of 240 Block II modules manufactured by Solar Power, Inc., connected in 24 parallel branch circuits of 10 modules each, for a total peak output power of 7.5 kWp. Each module in the array field was protected by an external diode placed across the terminals in the module terminal box. The system is shown in Fig. 6-3.

Between November 1978 and June 1979, the system appeared to operate with few problems. In March, only two failed modules were found, and each had a single cracked cell which had caused it to become open-circuited. In June, each branch circuit in the array field was short-circuited for washing and visual inspection, which took two to three days. During July and August, the operating currents of several branch circuits were found to be reduced by 40 to 50%, but all branch-circuit, open-circuit voltages were normal. (When one module becomes open-circuited in a branch circuit of 10 modules in series, each with a protective diode, the branch-circuit, open-circuit voltage is reduced by 10%.)

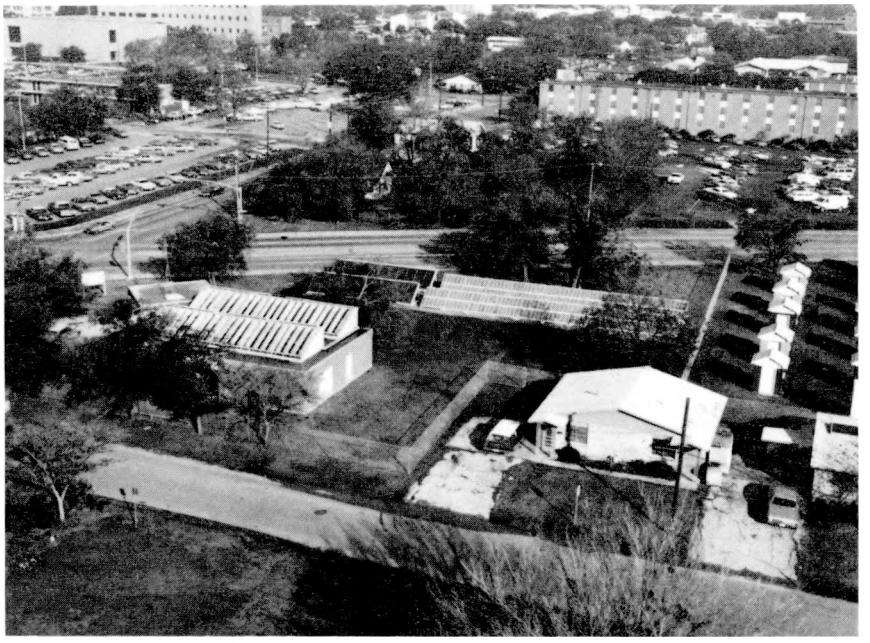

Fig. 6-3. University of Texas at Arlington residential system.

To determine why branch-circuit operating currents were low, the short-circuit current (Isc) of each module in the array field was measured in early September. The results were remarkable: 38 modules (16%) were found with less than 75% of their nominal short-circuit currents. Sixteen spare modules were sent to the site, and branch circuits were rearranged by grouping all normal modules in operative branch circuits and all defective modules (with lower output power) into lower output branch circuits. The short-circuit currents of each module were again measured later in the month. Once again the results were interesting: 38 modules delivered 75% of their nominal short-circuit currents after placing 16 new modules in the system. This meant that 16 more modules failed during September. (Note: Of the new failures, three were found with between 0 and 25% of their nominal Isc, five were found with between 25 and 50%, and eight were found with between 50 and 75%.) Within the next three weeks, seven more failures were found, bringing the total to 63 out of 240 modules (26.2%) since turn-on in November 1978.

Each failed module was found to contain one or more cracked cells, and several of these cracked cells were accompanied by delamination around part or all of the cell periphery. In several cases, evidence of intense local heating was also present. Flash testing of the failed modules using a Large Area Pulsed Solar Simulator* indicated that each module exhibited a low short-circuit current and a normal open-circuit voltage.

It is believed that the onset of most of the module failures at UTA was triggered by shorting the array field in June 1979. This shorting caused local hot-spot heating in modules due to reverse bias operation of cells. The heating was sufficient to cause substrate outgassing and subsequent cell cracking.

In April of 1980, all the modules in the array field were removed because of the large number of failures and were replaced with a second array field containing 640 Sensor Tech, Block III modules. Between April and December 1980, seven of the new modules failed in an open-circuit mode. The cause of the failures was diagnosed as failure by module assemblers at the factory to solder both interconnects to the back of one cell on each module, and it does not appear to be related to the failure mode exhibited by the previous array. Further details are found in Reference 6.

6.7 PV System Test Beds at Lexington and Concord, Massachusetts

The two system test facilities located at MIT Lincoln Laboratory, in Lexington and Concord, Massachusetts, were used for performing experiments in a systems context on various PV components. The former, located on a rooftop at the main Lincoln Laboratory complex, provided a flexible test bed of up to 10-kW capacity for evaluating storage batteries, inverters, data-acquisition equipment, and various types of monitor and control systems. The latter provided a ground-level, 25-kWp array field which was divided into several residential-size fields for use in conducting residential system experiments at the Northeast Residential Experiment Station (NE RES). The former, shown in Fig. 6-4, became operational in May 1977; the latter, shown in the upper right-hand corner of Fig. 6-5, to the north of the NE RES prototype systems, in December 1978.

*Manufactured by Spectrolab, Inc.

CP267-2079

Fig. 6-4. MIT Lincoln Laboratory Rooftop Test Facility.

CP267-6876

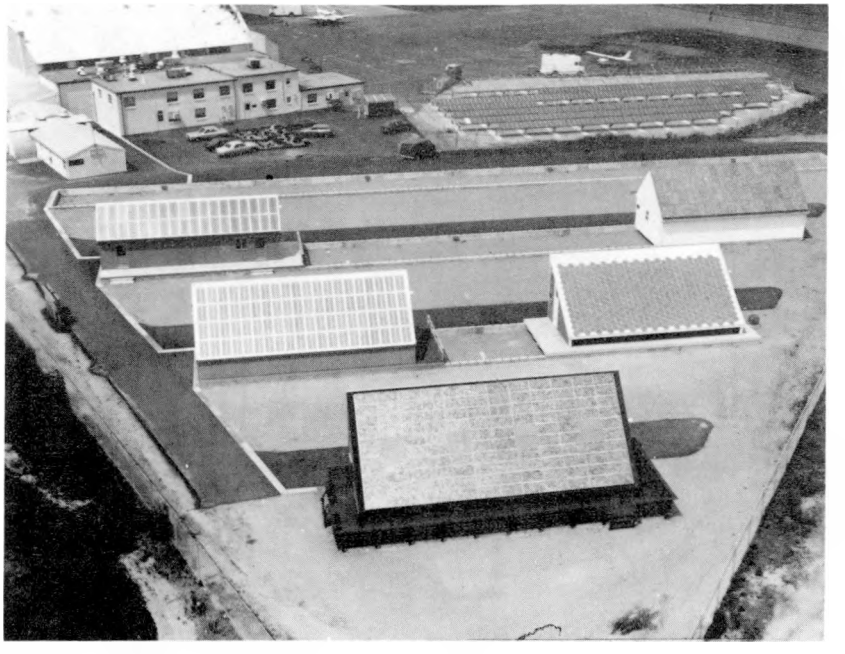

Fig. 6-5. MIT Lincoln Laboratory Residential System Test Facility (upper right corner) and five Northeast Residential Experiment Station systems (foreground).

Because of their experimental nature, these two array fields included a wide variety of modules, specifically: 945 Block I, Spectrolab modules; 64 Block II, Solar Power modules (similar to the original ones installed at UTA); 736 Block II, Sensor Tech modules (similar to those at Mead); and 288 Block III, Solarex modules (similar to those at Bryan, Ohio). The failure modes incurred by the modules were similar to those experienced by similar modules at other Lincoln Laboratory test sites.

Of the 945 Spectrolab Block I modules, 15 failed for one of three reasons: cracked cells, broken solder joints, and shorts between cell string and metal substrate. The Sensor Tech modules from Blocks II and III are quite similar in appearance. Of these modules, which total 1014 for both types, 23 failed for one of two reasons: cracked cells and pairs of unsoldered rearside interconnects.

Of the 64 Solar Power modules, five failed because of cracked cells (4 cases) and broken interconnects (1 case). The large differences in thermal expansion coefficients for the molded fiberboard substrate, the silicon cells, and the plated copper interconnects caused excessive strain in the interconnects which, in turn, caused work-hardening until failure ultimately occurred. Those failures of Solar Power modules attributed to cracked cells occurred in a manner similar to the failures at UTA.

Of the 268 Solarex, Block III modules, 19 failed due to a pair of broken interconnects on one cell on each module. This failure mode was discussed in the sections on Mead and Bryan. Further details can be found in References 9-20.

6.8 Arrays in New York City, Cambridge, MA, and Mt. Washington, NH

In order to gain some insight into module degradation in environments different from those of the sites described above, a variety of modules were placed on the roofs of buildings at New York and Columbia Universities in New York City, on the roof of a building at MIT in Cambridge, MA, and at a weather station atop Mt. Washington, NH. A photo of the MIT array which is typical of the two in NYC is shown in Fig. 6-6, and a photo of the Mt. Washington array is shown in Fig. 6-7.

C74-2197

Fig. 6-6. MIT (Cambridge, MA) rooftop module test site.

CP267-2823

Fig. 6-7. Mt. Washington, NH, module test site.

The NYC and MIT sites provided representative data for urban environments, and the Mt. Washington site provided an extremely cold and windy environment. Interestingly, of the sixty modules used at these sites, only two failed, due to cracked cells. The remainder contained the same types of degradation described earlier.

Most of the data at the urban sites were used for the soil accumulation studies described in the next section. Details of physical and electrical degradation for MIT and Mt. Washington modules can be found in References 8 and 9.

6.9 Soil Accumulation on PV Modules

Over the past five years, on-site soil accumulation measurements were made at all of the test sites discussed previously. Modules with glass covers, silicone encapsulants (RTV and Sylgard), and silicone encapsulants with surface coatings were utilized to conduct these measurements. Short-term results are summarized in Table 6-4. This table provides several insights into the module-soiling problem. First, soiling is the greatest single source of power loss short of failure. This power loss is recoverable, for the most part, after washing. Second, as has been found in the past, glass best lends itself to self-cleaning and hardcoat-covered RTV cleans better than plain RTV.

New York City clearly has the dirtiest of all the selected test environments, with typical losses of 40 to 50% on RTV-covered modules during the test period. The soiling of the hardcoat-covered RTV module can be used to rank order the "cleanliness" of the various test sites: 4.5% power loss at UTA, 5.7% at Lexington, 13.5% in Cambridge and 40.5% in NYC.

Although a comparison of the Arco Solar and Motorola modules indicates that the matted-finish glass cover remains cleaner than the plain glass, this is not the case. For the plain glass modules utilized above, it was found that a silicone residue seeps out from the edges of the module frame onto the plain glass surface, covering the glass over the cells and causing dirt which would normally be washed off by rain to adhere. This has been observed at NBNM, as well as NYC and Cambridge, MA.

TABLE 6-4

MIT LL ENVIRONMENTAL TEST SITES RECENT SOIL ACCUMULATION DATA
(12/78 - 6/79)

Module Type	Percent Power Loss					
	NYU	Columbia	MIT	Lex.	UTA	Neb.
Glass (plain) (Spectrolab, Blk I)	13.9	--	7.2	--	--	--
RTV-615 (Sensor Tech, Blk II)	43.3	42.2	--	8.5	--	9.9
Sylgard-184 (Solarex, Blk II)	52.9	48.1	29.9	--	--	7.2
RTV + hardcoat (Solar Power, Blk II)	40.5	--	13.5	5.7	4.5	--
RTV-615 (Sensor Tech, Blk III)	41.1	43.1	18.5	12.0	--	--
Sylgard-184 (Solarex, Blk III)	47.3	42.7	20.3	9.9	--	--
Glass (plain) (Motorola, Blk III)	9.3	18.1	22.5	5.3	--	--
Stippled-glass (Arco Solar, Blk III)	2.7	4.3	4.2	1.1	--	--

A long-term soil accumulation study was also conducted on the roof of a building at MIT in Cambridge. Two groups of modules with various types of encapsulants were left exposed, with no cleaning, for periods of two years and 9 months and three years, respectively. The data are summarized in Table 6-5. The results were consistent with the other study: glass-covered modules lost the least power while the silicone-rubber-encapsulated modules lost the most. Placing a hard coating over the silicone rubber improves the self-cleaning ability of the module.

TABLE 6-5

SOIL ACCUMULATION STUDY AT MIT, CAMBRIDGE, MASSACHUSETTS

Module Type	Sample Size	Period of Exposure	Percent Power Loss
Block I Spectrolab plain glass	2	3 yrs.	9
Block II RTV Sensor Tech	2	3 yrs.	24
Block II Solarex Sylgard	2	3 yrs.	30
Block II Solar Power, Hardcoat	2	3 yrs.	9
Block III Motorola plain glass	2	2 yrs. 9 mos.	8
Block III Arco Solar stippled glass	2	2 yrs. 9 mos.	0
Block III Sensor Tech RTV	4	2 yrs. 9 mos.	26
Block III Solarex Sylgard	2	2 yrs. 9 mos.	25

More detailed descriptions of the module-soiling problem can be found in References 2 and 21.

6.10 Summary

During the past five years, MIT Lincoln Laboratory has installed over 11,000 PV modules at various test sites in the United States. To date, only about 4% of these modules have failed electrically. Most of these failures are attributable to cells cracked by hail impact, natural weathering, or local intense heating caused by operation in a reverse-bias mode. The remaining failures were caused by failed solder joints, cell/interconnect shorts to ground and broken interconnects.

For the most part, current-generation PV modules have been reliable sources of electrical power at Lincoln Laboratory test sites. At UTA, the module design was such that upon shorting one or more individual cells were forced to operate in a reverse-bias mode. These cells underwent intense local

heating which caused cracking. This behavior caused significant failure, however, only for the modules used at UTA. Other than hail damage, most failures could be eliminated by tighter process control during fabrication and by using better conceived designs.

To date, the greatest single cause of power loss has been soil accumulation, where losses as great as 50% have occurred for silicone-encapsulated modules exposed for seven months in NYC. Glass-covered modules have fared much better. For the most part, these losses are recoverable upon washing. Lessons learned from the MP&T Lab experience are enumerated in Section 6.11. Further details of module performance and degradation at Lincoln Laboratory test sites are presented in References 1 through 20, which include many photographs of the defects described.

6.11 Lessons Learned

Lessons learned during the course of the module performance evaluation program are summarized below.

6.11.1 General Observations

1. Module failure modes and frequency of occurrence were as follows: (a) cracked cells--50%; (b) broken interconnects--32%; (c) shorts to ground--12.8%; and (d) soldering problems--5.2%.
2. Failures in categories (b) through (d) were caused by factory flaws, poor process control, or inherent design deficiencies. This is also true for approximately half the modules in category (a). Thus, it appears that about 75% of the observed failures could have been avoided, and it is likely that such occurrences will become rarer as the industry matures.
3. Wearout was never observed. There does not seem to be any inherent physical, electrical or chemical limitation to prevent a 20-year or even longer life. Varying degrees of maturity relative to this goal were evidenced by the modules tested.
4. Physical degradation, such as discoloration and delamination, is abundantly evident in one or more forms for all designs. While in the short term unrelated to electrical degradation, long-term effects are unknown.
5. No one has devised an accelerated testing method for predicting PV module life.
6. Despite the infancy of the industry, the complexity of the experimental systems involved, and the different wiring and mounting methods used everywhere, no person was injured in any way at any of the listed areas.

6.11.2 Specific Observations

1. Silicone-rubber superstrates are susceptible to hail damage, irreversible power loss from soil accumulation, delamination and exposure of electrical circuitry under thin layers.
2. On the other hand, glass superstrates clean and self-clean easily and exhibit reversible power loss. There is no field data indicating susceptibility to hail damage given that the glass is tempered and edge-treated.
3. Silicone rubber covered with glass is an acceptable encapsulant where cost is not a factor.
4. Metal substrates must be properly insulated from cells to prevent shorts. Also, the substrate must be flat to prevent uneven pressures on cell backs.
5. Fiberglass-base substrates are poor because of large mismatch in thermal expansion coefficient relative to silicon and interconnect materials and because of a tendency to outgas on heating to 100°C or over.
6. Laminated module fabrication has potential although the technique has not yet been mastered. PVB films yellow when exposed to moisture and Tedlar and Mylar films are permeable to moisture.
7. Silicone gel is difficult to contain and tends to seep out of package edges. It is a poor encapsulant.
8. Small flaws left at cell edges during processing almost always develop into cracks which can traverse cells.
9. Redundant interconnection, internal bypass diodes and series-parallel wiring are most effective in enhancing module reliability in the face of cell cracking, broken interconnects and hot-spot heating.
10. The fatigue strength of interconnects as well as their shape must be taken into account during their design.
11. Modules must be able to withstand operation in a short-circuited mode to permit safe maintenance operations.
12. The covered terminal boxes commonly used on module backs rarely prevent moisture penetration, and corrosion-resistant components must be used.

APPENDIX TO SECTION 6

Key Features of Principal Test Modules Electrical Performance*

Module Type	I_{sc} amp	V_{oc} volts	Peak Power watts	Dimensions mm	Physical Features
Block I					
Spectrolab	0.66	11.6	5.45	633 x 124 x 69	Al "I-beam" extrusion substrate 2.3-mm glass over silicone encapsulant 20 cells, 50-mm diameter
Block II					
Sensor Tech	0.58	24.3	10.2	589 x 290 x 25	Stamped Al substrate 3.2-mm silicone encapsulant 44 cells, 56-mm diameter
Solar Power	1.96	23.3	33.9	1168 x 389 x 48	Molded polyester fiberglass substrate 2.8-mm silicone encapsulant 40 cells, 100-mm diameter
Solarex	1.40	23.7	22.0	582 x 582 x 33	Polyester fiberglass substrate, Al frame 2.3-mm silicone encapsulant 42 cells, 75-mm diameter
Spectrolab	1.88	23.2	30.7	1168 x 384 x 36	Formed Al frame 4.3-mm glass over PVB encapsulant 120 cells, 50-mm diameter
Block III					
Arco Solar	1.40	23.2	22.2	1160 x 232 x 36	Formed Al box frame 10-mm glass/PVB/Tedlar laminate 41 cells, 75-mm diameter
Motorola	4.90	7.2	26.5	580 x 580 x 50	Formed stainless steel pan 4.3-mm glass front, silicone gel encapsulant 48 cells, 75-mm diameter
Sensor Tech	0.58	24.7	10.7	582 x 287 x 48	Finned Al extrusion substrate 5-mm silicone encapsulant 44 cells, 56-mm diameter
Solarex	1.40	23.7	21.8	582 x 582 x 33	Polyester fiberglass substrate, Al frame 2.3-mm silicone encapsulant 42 cells, 75-mm diameter

*Based on 100 mW/cm^2 and 28¼C; average values of modules at Southern California sites.

REFERENCES

1. Forman, S. E., "Visual Defects in Terrestrial Photovoltaic Modules," MIT Lincoln Laboratory Technical Report, 21 March 1978, C00-4094-6.

2. Forman, S. E. and Murphy, E. B., "Measuring Dirt on Photovoltaic Modules," MIT Lincoln Laboratory Technical Report, 21 March 1979, C00-4094-37.

3. Forman, S. E., "Endurance and Soil Accumulation Testing of Photovoltaic Modules at Various MIT LL Test Sites," MIT Lincoln Laboratory Technical Report, 28 September 1978, C00-4094-23.

4. Forman, S. E. and Themelis, M. P., "Quarterly Report, Solar Photovoltaic Project, Materials, Processes and Testing Activities for the Period 1 January 1979 to 31 March 1979," MIT Lincoln Laboratory Technical Report, 31 October 1979, C00-4094-60.

5. Forman S. E. and Themelis, M. P., "Materials, Processes and Testing, Technical Progress Report: July, August, September, October, 1981," MIT Lincoln Laboratory Technical Report, February 1982, DOE/ET/20279-173.

6. Forman, S. E. and Themelis, M. P., "Materials, Processes and Testing, Final Report 1977-1982," MIT Lincoln Laboratory, Technical Report, June 1982, DOE/ET/20279-188.

7. Forman, S. E. and Themelis, M. P., "Final Materials, Processes and Testing Progress Report, November, December 1981, January, February, March 1982," MIT Lincoln Laboratory Technical Report, DOE/ET/20279-190.

8. Themelis, M. P., "Final PV Module Degradation Analysis Report," MIT Lincoln Laboratory Technical Report, June 1982, DOE/ET/20279-189.

9. Forman, S. E., "Summary of Field Experience of Photovoltaic Modules at Various MIT LL Test Sites," MIT Lincoln Laboratory Technical Report, 1 April 1979, C00-4094-8.

10. Forman, S. E. and Themelis, M. P., "Quarterly Report for 10/1/78 to 12/31/78 on Photovoltaic Module Performance at Mead, Nebraska, Test Site," MIT Lincoln Laboratory Technical Report, 1 April 1979, C00-4094-40.

11. Forman, S. E. and Themelis, M. P., "Quarterly Report for Solar Photovoltaic Project, Materials, Processes and Testing Activities for the Period 1 January 1979 to 31 March 1979," MIT Lincoln Laboratory Technical Report, 30 June 1979, C00-4094-55.

12. Forman, S. E. and Themelis, M. P., "Technical Progress Report, Materials, Processes and Testing Laboratory for the Period July, August, September, October 1979," MIT Lincoln Laboratory Technical Report, 15 March 1980, DOE/ET/20279-83.

References (continued)

13. Blake, F. A. and Hanson, K. L., "The Hot Spot Failure Mode for Solar Cells," 4th IECEC, 1969 Record, pp. 575-581.

14. Forman, S. E. and Themelis, M. P., "Technical Progress Report, Materials, Processes and Testing Laboratory for the Period November, December 1979, January, February 1980," MIT Lincoln Laboratory, 30 November 1980, DOE/ET/20279-113.

15. Forman, S. E. and Themelis, M. P., "Materials, Processes and Testing Laboratory, Technical Progress Report: March, April May, June 1980," MIT Lincoln Laboratory Technical Report, January 1981, DOE/ET/20279-114.

16. Forman, S. E. and Themelis, M. P., "Materials, Processes and Testing Laboratory, Technical Progress Report: July, August, September, October 1980," MIT Lincoln Laboratory Technical Report, January 1981, DOE/ET/20279-117.

17. Forman, S. E. and Themelis, M. P., "Reliability of Terrestrial Photovoltaic Modules at Various DOE/MIT Lincoln Laboratory Test Sites," presented at the 15th IEEE PV Specialists' Conference, Orlando, FL, 11-15 May 1981, DOE/ET/20279-126.

18. Forman, S. E., "Performance of Terrestrial Photovoltaic Modules at MIT Lincoln Laboratory Experimental Photovoltaic Systems," MIT Lincoln Laboratory Technical Report, 30 April 1981, DOE/ET/20279-140.

19. Forman, S. E. and Themelis, M. P., "Materials, Processes and Testing Activities, Technical Progress Report: November, December 1980, January, February 1981," MIT Lincoln Laboratory Technical Report, 30 April 1981, DOE/ET/20279-160.

20. Forman, S. E. and Themelis, M. P., "Materials, Processes and Testing Activities, Technical Progress Report: March, April, May, June 1981," MIT Lincoln Laboratory Technical Report, December 1981, DOE/ET/20279-172.

21. Hoffman, A. R. and Maag, G. R., "Photovoltaic Module Soiling Studies, May 1979-October 1980," 1 November 1980, DOE/JPL-1012-49.

7.0 DEVELOPMENT OF INSTRUMENTS FOR MEASURING PV SYSTEM PERFORMANCE

7.1 Introduction

In the course of conducting Lincoln Laboratory's PV system testing program, it quickly became apparent that there was a lack of suitable instruments for measuring the performance of PV systems in the field. In particular, there was a need for:

- A pyrheliometer for providing data on the solar resource at a remote, unattended site over extended time periods, and
- A portable measuring unit for determining the current-voltage characteristics of an array in the field.

Development of these two devices is summarized in this section.

Contributions to this effort were made by the following individuals: Matthew E. Buresch, Charles H. Cox, III, Carl H. Much, S. Hardy Prince, Peter L. Rossini, Douglas Smith, David G. Stuart and Thomas H. Warner.

7.2 Development of a Sun-Following Pyrheliometer

A sun-following pyrheliometer mount and control system for support of a solar PV energy program was designed and built (1). The system features the use of a microprocessor for controlling the mount and handling complex control functions required by variations in the apparent motion of the sun. The system is a stand-alone, unattended unit with capabilities for remote diagnosis by telephone.

7.2.1 Capabilities of Sun-Following Pyrheliometer

When viewed over long periods of time from a fixed location, the movement of the sun in relation to the earth is not uniform. For a sun-following pyrheliometer mount to monitor solar energy and weather conditions it must:

1. Point a normal-incidence pyrheliometer at the sun within 1^{o} accuracy.
2. Compensate for day-to-day changes in the sun's motion.
3. Operate unattended while exposed to the weather for up to six months.

4. Accommodate and adjust for power outages and interference with mount motion from external influences (ice, snow).

5. Consume minimal power.

A pyrheliometer mount developed at Lincoln Laboratory incorporates all of these objectives, and has been operating at the research facility's Lexington, Massachusetts, headquarters since late 1978 (Fig. 7-1).

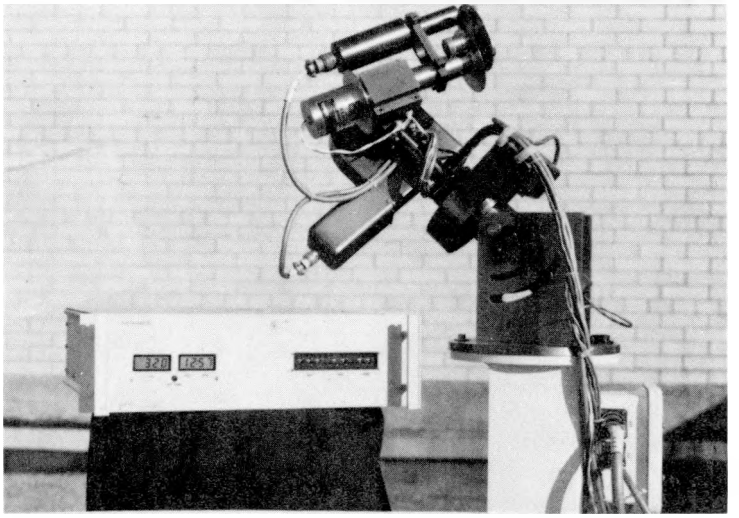

CP267-4514

Fig. 7-1. The sun-following pyrheliometer.

7.2.2 System Description

A polar-axis mount was selected because sun-pointing can be achieved during any one day via rotation about the hour-angle (HA) axis alone (Fig. 7-2). The mount moves at a uniform mean sun rate from 0200 to 2200 hours daily and then stops and returns to the 0200 position. While unwinding, incremental adjustments determined from the sun's ephemeris stored in a read-only memory (ROM) are made in both HA and declination to prepare the mount to follow the sun again during the ensuing day.

The mount, manufactured by the Edward J. Byers Co., of Barstow, California, designed specifically for pyrheliometer pointing with 180:1 worm-gear reduction--one for each axis--is driven by stepping motors using an open-loop configuration with no feedback elements. Each step rotates the mount 0.01^{o}. Since the mount unwinds itself daily, no slip rings are necessary.

A closed-loop sun sensor, activated each noontime, makes small corrections to reduce sun-pointing errors if the sun is clearly visible.

C76-424

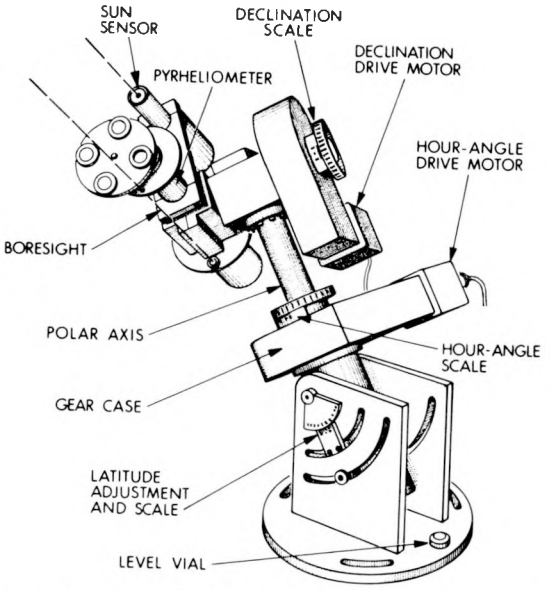

Fig. 7-2. Polar sun-following mount.

Contained within the control package is a temperature-compensated oscillator which supplies a precision reference for the software clock's timing functions that:

1. Controls the pulse frequency applied to the stepping motors during pointing.
2. Determines the time to start the unwind cycle (2200 hours).
3. Provides the date to select the appropriate daily adjustment from memory.
4. Generates a fast pulse rate for the unwind cycle.
5. Determines the time (0200 hours) to resume the mean sun-stepping rate.

Time-of-day and day-of-the-year are displayed on the front panel.

When set up, the mount is aligned properly and pointed at the sun. The control electronics measure the distance from the sun to the reference switch in each axis during the first unwind cycle. This distance varies with site longitude. Each new day starts with respect to the reference switches that enable the mount to start from a known position. If mount rotation is deterred by ice, for example, steps will be lost because of the open-loop driving method.

The control electronics default to a battery-powered condition when a power failure occurs. All control functions are maintained, but "steps" are not sent to the stepping motors, and status reporting is not available. The stepping count is accumulated during the power outage, and an appropriate correction is made when power is restored.

Around noon each day, the sun-sensor output is observed, and any pointing error is corrected by stepping the mount to reduce the sun-sensor error. Corrections thus determined are applied to succeeding days' rewind count, but are limited to $\pm$15 steps.

A sun sensor with several degrees field of view that contains a PV detector and analog/digital circuitry provides 2-bit HA and declination digital-error signals. The error signals indicate when the adjustable error threshold (nominally 0.1^{o}) has been exceeded. An intensity threshold enables the correction to be made only when the sun is bright enough to be clearly visible. Both error signals return to zero only after the pointing error has been reduced to "0" degrees because of built-in hysteresis. The sensor subsystem may be disabled if closed-loop correcting is not desired.

As many future solar PV sites will probably be in remote areas, the microprocessor reports the status of major control functions via a 300-baud RS-232 line. It will often be possible to diagnose problems remotely, eliminating the time and expense involved in visiting the site.

7.2.3 Summary

The microprocessor-controlled, sun-following mount, operating since the fall of 1978, has met all of its design objectives. The open-loop sun-following technique has resulted in errors that are only a fraction of a degree after several weeks of operation. These small errors are reduced even further with the error-sensor enabled.

Although designed to collect solar-insolation data, the controller can be applied to other tasks:

1. Control sun-pointing of PV arrays, solar concentrators or other devices that need to follow the sun.
2. Follow other celestial objects such as the moon, or even satellites.

The microprocessor permits inclusion of all the complex functions required to overcome the shortcomings of earlier versions. Also, far fewer integrated circuits are required than in the hardwired approach. Perhaps most important of all is the flexibility obtained; major changes in system operation can be effected at any time by simply changing the software.

7.3 Development of an I-V Curve Tracer

7.3.1 Introduction

The current-versus-voltage plot of a PV array or module is a powerful diagnostic aid. Many recently built PV installations are in remote locations, presenting the problem of transporting bulky testing equipment. As PV power becomes more common, a service industry will be needed to develop and supply portable diagnostic instruments capable of measuring modules or entire arrays. Extensions of the steady-state dissipative methods presently used for making I-V curves will not be adequate to fill these needs.

A very small and light curve tracer employing a capacitive load can be made. The basic concept is quite simple, as shown in Fig. 7-3. Initially the switch is closed, the capacitor is discharged, and the array is operated at short circuit. When the switch is opened, the array current flows into the capacitor and charges it according to the familiar capacitor equation:

$$V_C(t) = \frac{1}{C}\int_o^t i(\tau)d\,\tau. \qquad (1)$$

As the charging progresses, a data-acquisition system measures the voltage and current of the array and plots them parametrically.

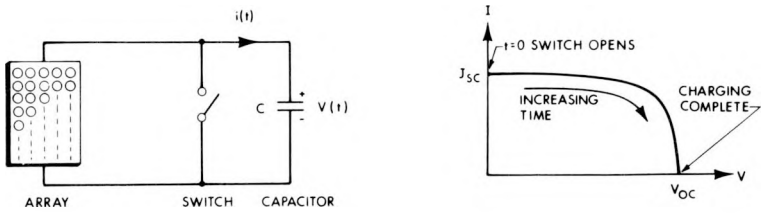

C74-1262

Fig. 7-3. Use of a capacitor to measure the I-V curve: basic capacitive-charging method (left), and resultant I-V curve (right).

7.3.2 Design Considerations

- Capacitor Sizing

This measurement scheme hinges on utilizing a capacitor of the appropriate size. If the array is assumed to have a fill factor of one, Equation 1 can be solved easily. The voltage simply ramps up from zero to the open-circuit voltage, V_{oc}, in a time, T_{scan}. When the array reaches V_{oc}, the current drops to zero and the charging stops:

$$V_{oc} = \frac{I_{sc}}{C} T_{scan}. \qquad (2)$$

This equation can be rearranged to find the capacitor size necessary to produce a predetermined scan time:

$$C = \frac{I_{sc}}{V_{oc}} T_{scan}. \qquad (3)$$

Equation 3 shows that the ratio of short-circuit current to open-circuit voltage is more important than the array power in determining the capacitor size. A minimum scan time should be determined such that the "transient I-V curve" very closely approximates the I-V curve obtained using "steady-state methods." The Large Area Pulsed Solar Simulator* obtains good results with scan times of 2 milliseconds. If a 2000-μF capacitor is chosen, the curve tracer will be able to handle any module or array with:

$$\frac{I_{sc}}{V_{oc}} \leq 1. \qquad (4)$$

This includes all residential arrays and the newer low-voltage, high-current module designs. 1000-μF, 450-V capacitors are available from several manufacturers and are about the size of a 12-oz. soft drink can.

- Power Dissipation

The reason conventional I-V loads are so heavy and bulky is the need for large resistors, heat sinks and fans to dissipate the array power. The capacitor-charging curve tracer has a very low average power dissipation that

*Manufactured by Spectrolab, Inc.

depends only on the capacitor size, open-circuit voltage and frequency of measurement, f_m:

$$P_{avg} = \frac{1}{2} f_m \, CV_{oc}^2 .$$

For example, a 5-kW array at 250 V being measured every 3 seconds would require an average power dissipation of only 21 W with a 2000- μF capacitor.

7.3.3 Implementation

The curve tracer consists of two units, as shown in Fig. 7-4. The data-acquisition unit (DAU), contains all of the power electronics, data acquisition, and short-term memory, along with control electronics to run the measurement. The data display, storage and analysis is performed by an HP-85 desktop computer. The DAU and HP-85 communicate via a standard IEEE-488 instrumentation bus.

Fig. 7-4. Photograph of 10-kW I-V curve tracer showing measurement unit (right) and HP-85 (left).

A block diagram of the system is shown in Fig. 7-5. Initially, switch 1 is closed, while 2 and 3 are open. This allows the capacitor to be charged to a negative voltage. When switch 1 is opened and 2 is closed, a negative voltage will be placed across the array. The I-V curve will actually start in the reverse bias region, proceed through short circuit and continue all the way to open circuit. In this manner the entire forward operating characteristic can be plotted. Once the curve is complete, switch 2 is opened and 3 is closed to discharge the capacitor for the next measurement.

During the capacitor charge-up, the DAU digitizes the voltage and current with 8-bit resolution and stores them in a temporary memory. The range selection is chosen such that I_{sc} and V_{oc} can always be made to lie above 80%

of the full-scale value. This makes full use of the analog-to-digital converter range and reduces quantization errors. When the DAU is idle, it performs an auto-zero function.

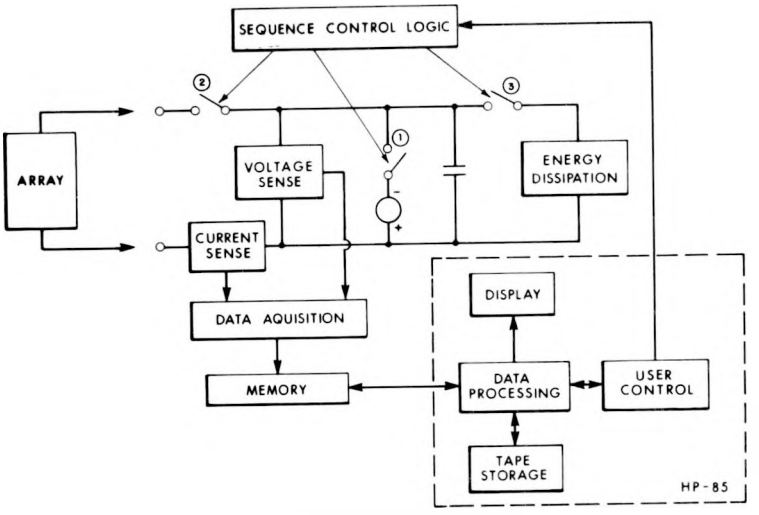

Fig. 7-5. Simplified block diagram of I-V curve tracer.

Since the HP-85 is not fast enough to run the measurement directly, it must wait until the curve is complete and then read the data from the temporary memory in the DAU. Data display, hard copy and magnetic tape storage are all performed by the computer. On-screen prompting and menu format are used to minimize operator errors. All commands to the DAU are generated by the HP-85 and are transparent to the user.

7.3.4 I-V Curve Tracer Performance

A comparison of the I-V curves taken with the capacitive load and a more conventional dissipative load is presented in Fig. 7-6. The curves agree closely, indicating that fast scan times are possible to locate faults in large arrays.

Figure 7-7 shows an I-V curve of an array operating at approximately 7 kW, which could not be measured with a commercially available resistive load.

A comparison of the physical dimensions of the capacitive load with a resistive load of equal rating (10 kW) is shown in Table 7-1. The capactive load is far smaller, lighter and less expensive.

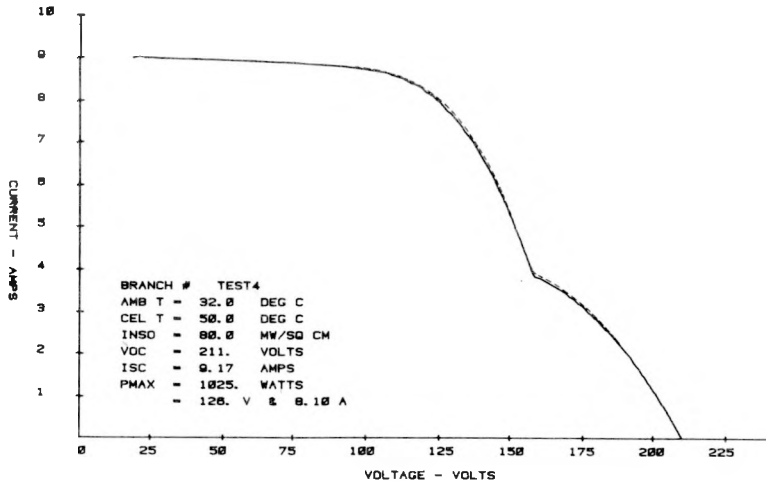

Fig. 7-6. Output of capacitor-load curve tracer (solid line) and resistor load (dotted line).

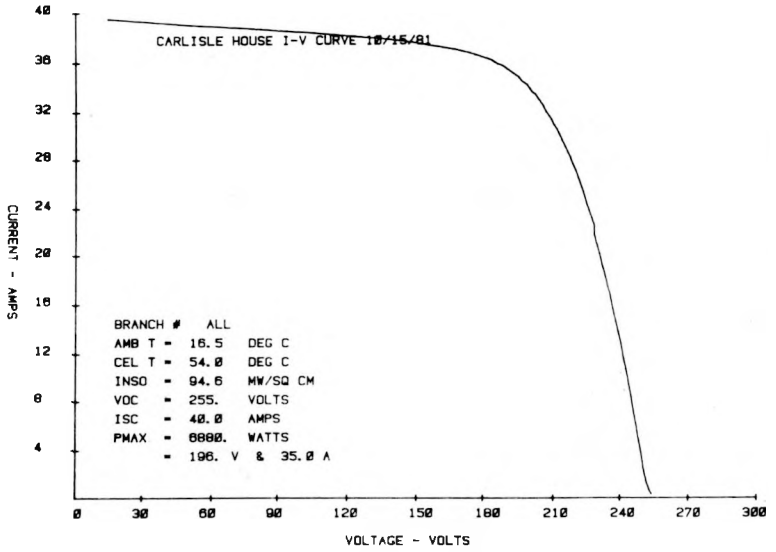

Fig. 7-7. I-V curve of approximately 7.5-kWp array.

TABLE 7-1

COMPARISON OF 10-kW INSTRUMENTS

	Resistive Load	Capacitive Load	HP-85
Weight (lbs)	125	13	20
Size (cu. ft.)	4.3	0.5	1.08
AC Power (W)	240	20	30
Cost ($)	11,000	8,000	4,000

7.3.5 Conclusions

The capacitive load curve tracer offers many distinct advantages over resistive loads for making I-V curves. The required capacitors are available and are not very bulky. Direct comparison of I-V curves taken using the two techniques show negligible difference between them. References 2 through 4 provide further information on this I-V curve tracer and techniques developed for its use.

REFERENCES

1. Much, C. H., Rossini, P. L., Stuart, D. G., "A Microprocessor-Controlled Autonomous Sun-Following Mount for Solar Photovoltaic Energy Planning," Industrial Application of Microprocessors Conference, Philadelphia, PA, March 1979, COO-4094-34.
2. Cox, C. H., III., and Warner, T. H., "Photovoltaic I-V Curve Measurement Techniques," MIT Lincoln Laboratory Technical Report, August 1982, DOE/ET/20279-215.
3. Warner, T. H. and Cox, C. H., III, "A High Power I-V Curve Tracer Employing a Capacitive Load," presented at the Commerical Photovoltaic Measurements Workshop, Vail, CO, 27 June 1981, DOE/ET/20279-156. (Also published in Solar Cell, The Netherlands, December 1982.)
4. Cox, C. H., III, and Warner, T. H., "Swept Measurement of High Power I-V Curves," presented at the 16th IEEE PV Specialists' Conference, San Diego, CA, 27 September 1982, DOE/ET/20279-229.

8.0 BACKGROUND AND OVERVIEW OF RESIDENTIAL PHOTOVOLTAICS ACTIVITY

The residential application of photovoltaics was recognized early by DOE (then ERDA) as being of potential importance; there was little doubt that future demand for such systems would create a large commercial market. However, DOE was concerned about the appropriateness of early field testing of residential PV systems at a time when there was an enormous disparity (approximately a factor of 50) between the cost of the systems and the prices at which they would have to sell in order to be competitive with conventional electricity generation on a life-cycle basis. There also was some question as to whether the Photovoltaics Program as a whole was prepared for an undertaking of this magnitude. For these considerations, the Lincoln Laboratory effort in residential photovoltaics was deferred until late 1978.

Lincoln Laboratory then created a draft plan for DOE based on evaluation of candidate residential PV systems which would be built at three Residential Experiment Stations located in the northeastern, southwestern and southeastern regions of the United States. Although complete in every technical detail of the PV system and its physical integration into a residence-like structure, these prototype systems would not be habitable; only that portion of the structure needed to effect the integration was to be provided. The plan went into effect and the results of the first three years of this activity are shown in Figs. 8-1 and 8-2, which depict the five prototype systems installed at the Northeast Residential Experiment Station (NE RES) in Concord, Massachusetts, and the eight prototype systems at its sister facility in the Southwest (SW RES), respectively. Due to funding constraints, the Laboratory did not proceed with creation of the Southeast Residential Experiment Station (SE RES)*.

The residential activity also included construction and evaluation, at sites apart from the experiment stations, of several residential PV systems:

- PV/thermal residence, Arlington, Texas (inhabited)
- Carlisle PV house, Carlisle, Massachusetts (inhabited)
- PV residence at Florida Solar Energy Center, Cape Canaveral, Florida (uninhabited)
- PV residence in Phoenix, Arizona (uninhabited)
- Three PV residences in Oahu and Molokai, Hawaii (all inhabited).

*DOE has since initiated work on the SE RES through Sandia National Laboratories, Albuquerque, New Mexico.

CP267-6376

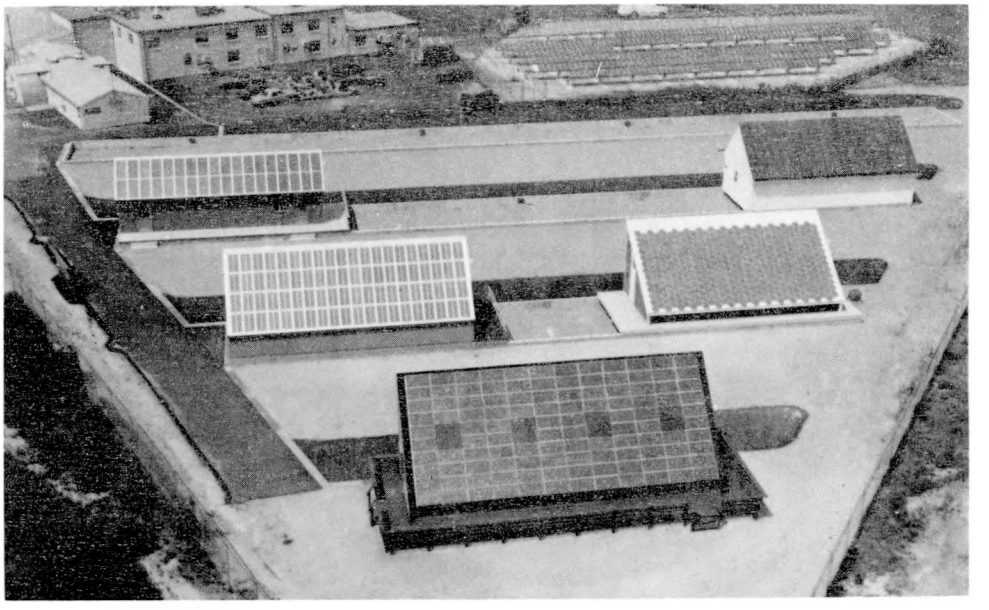

Fig. 8-1. Aerial view, Northeast Residential Experiment Station.

CP267-7122

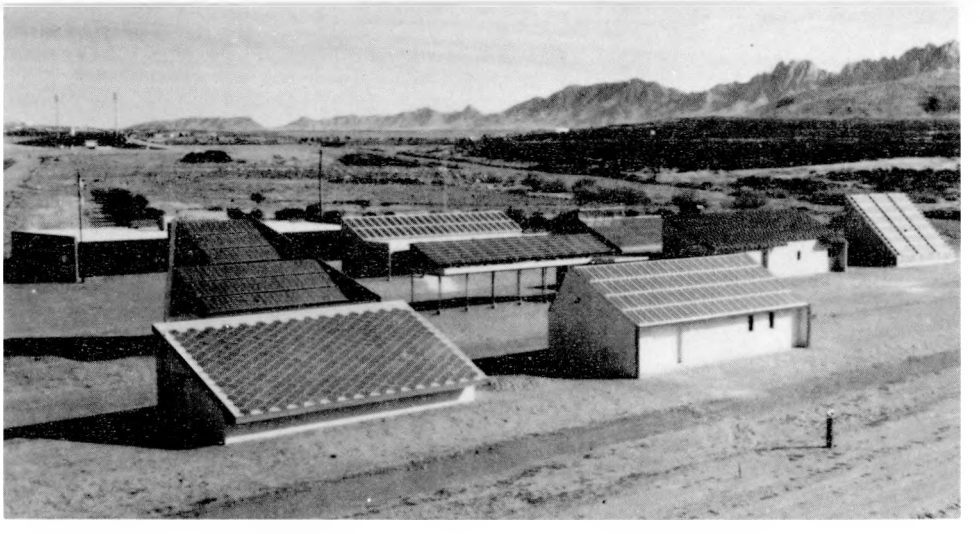

Fig. 8-2. Aerial view, Southwest Residential Experiment Station.

The results of performance measurements on all of these residential PV systems are presented and the data systems which served most of the units are described in Section 11.0.

The residential PV system testing was accomplished by system studies of various types and by technical development of critical components. The system studies, summarized in Section 9.0, included both economic and technical evaluations. Because all of the PV systems used utility-interactive designs (thus eliminating the need for on-site energy storage by providing for two-way power flows with the utility), it was necessary to study not only the performance of each system as an entity, but also its integration and interaction with the electric utility.

Another important aspect of the system studies was Lincoln Laboratory's efforts in the development of codes and standards for residential PV systems. In this work, the Laboratory supported the Solar Energy Research Institute (SERI), which was designated by DOE to provide draft codes and standards for all PV applications, including residential systems. It is noteworthy that one of the results of this activity by Lincoln Laboratory and SERI is a major addition to the 1984 National Electric Code, which sets forth for the first time the minimum safety requirements for a residential PV system (see Section 9.5.5).

Lincoln Laboratory's residential PV activity also included technical development in several key areas (summarized in Section 10.0):

> PV Arrays - Development of PV cells, PV/thermal collectors and roof-mounting methods for PV arrays.
>
> Inverters - Evaluation of candidate residential inverters and development of waveshaping techniques for utility-interactive inverters.
>
> Energy Storage - Use of flywheel energy storage systems for residential applications.

A summary is given in Section 12.0 of the entire Residential Project effort at Lincoln Laboratory. This section also enumerates lessons learned throughout, and concludes with recommendations for future work on residential PV systems.

Lincoln Laboratory withdrew from the DOE Residential Project in June 1982. The Laboratory's responsibilities were then assumed by the Sandia National Laboratories, Albuquerque, New Mexico (Dr. Edward L. Burgess), the MIT Energy Laboratory, Cambridge, Massachusetts (Dr. Edward C. Kern, Jr.), and the New Mexico Solar Energy Institute, Las Cruces, New Mexico (Dr. John Schaefer). The reader is referred to these organizations if additional information is desired beyond that presented in this report and its references and bibliography (Section 13.0).

9.0 RESIDENTIAL PHOTOVOLTAIC SYSTEM STUDIES

In this section, the systems engineering studies done by or under the direction of Lincoln Laboratory are summarized. Four broad types of studies were performed, each with a different objective. They included the following categories:

> Economic Studies - To determine preferred types and sizes of residential PV systems on a regional basis for the United States. Also to determine the necessary economic environment for emergence of economically competitive PV systems.
>
> Integration of Residential PV Systems with the Utility - To determine the effects of PV systems on the utility's distribution system and its generation-capacity requirements and fuel use, as a function of the amount of residential PV generation capacity installed.
>
> PV System Performance Modeling - To develop and validate computer models for predicting the performance of residential PV systems. This effort in turn required the development of modeling techniques on a subsystem-by-subsystem basis.
>
> Codes and Standards - To initate the preparation of necessary codes and standards for residential PV systems, so that such systems can be incorporated in a rational and orderly way into the nation's present and future housing stock.

The studies performed by Lincoln Laboratory are presented in the above order. Implicit in this ordering method is the assumption that the reader is familiar with the components and technical workings of PV and combined PV/thermal systems. If this is not the case, Section 9.3 should be read before proceeding with the other sections of this chapter.

Although the system studies performed by Lincoln Laboratory were extensive, they by no means represent the total effort in this important portion of the overall DOE Photovoltaics Program. For further information, the reader is referred to the following organizations:

> Jet Propulsion Laboratory
> California Institute of Technology
> 4800 Oak Grove Drive
> Pasadena, CA 91109
>
> Sandia National Laboratories
> 1515 Eubank Boulevard, SW
> Albuquerque, NM 87185

Aerospace Corporation
350 East El Segundo Boulevard
El Segundo, CA 90245

Solar Energy Research Institute
1617 Cole Boulevard
Golden, CO 80401

9.1 Economic Studies of Residential Photovoltaic Systems

9.1.1 Introduction

Since 1976 numerous computer-based simulation studies have been conducted under DOE sponsorship in order to investigate the engineering performance and the economics of residential PV systems. The goal of the earliest of these efforts was to understand the optimum configurations of such systems prior to initiation of hardware demonstration or development efforts.

MIT Lincoln Laboratory's involvement in residential studies began with the investigation of combined photovoltaic/thermal (PV/T) systems. Basic to such systems were both thermal solar collectors and PV panels, combined to serve residential heating, hot water and electric demands. Photovoltaic/thermal collectors, which integrate the functions of these single-duty collectors in a single unit, were the focal point of these studies. Optimizations were done to determine the most economical mix of PV, thermal and combined PV/T collectors to serve the demands of a residence.

Once the first-generation prototype PV/T collectors were constructed and evaluated, refined PV/T collectors were designed. Using analytical models of these improved collectors, a worth analysis was undertaken to determine the allowable cost of systems utilizing such collectors, given the value of the thermal and electrical energy they could generate for a residential application. For this particular study, the engineering performance of systems employing the "second-generation" PV/T collectors was simulated at Lincoln Laboratory; the MIT Energy Laboratory was engaged to conduct the worth analysis.

Lincoln Laboratory representatives also participated in and helped guide similar studies conducted by General Electric and Westinghouse under contract to Sandia National Laboratories. Both of these broadly scoped efforts were aimed at evaluating numerous system design options in each of twelve regionally representative U.S. geographical locations.

The studies described above yielded ambiguous results regarding the merits of combined PV/T collector systems and PV systems employing electrical storage (batteries). However, the simplest system, one using only PV modules and a utility-interactive, dc-to-ac inverter, was shown by most studies to be an attractive option in virtually all locations of the country. As a consequence, DOE's Photovoltaic Residential Project focussed on the design, test and evaluation of utility-interactive residential PV systems.

During the period of design and construction of the first prototype residential PV systems, a cost study was undertaken to summarize the status of all PV system related costs. Additionally, the MIT Energy Laboratory was funded to summarize their investigations of residential PV system worth. Finally, an MIT Energy Laboratory review study of existing models for predicting regional housing markets was conducted.

The results of these studies are summarized in the following sections.

Contributions to this effort were made by the following individuals: Charles H. Cox, III, Thomas L. Dinwoodie, Martin Katzman, Edward C. Kern, Jr., Miles C. Russell and Richard D. Tabors.

9.1.2 Worth Analysis of Residential PV Systems

This study, which was performed by the MIT Energy Laboratory (1), estimated the allowable cost for PV systems based on the value of the electrical (and in the case of combined PV/T systems, thermal) energy produced by them. One important cost goal, namely, that for the PV module component, was estimated in 1973 to be $0.50/Wp (in 1976 dollars). This is very nearly the median of allowable costs projected from more refined analyses. These show allowable installed system costs ranging from $1.50/Wp to $4.00/Wp (1980 dollars), depending upon certain critical variables such as the level of solar insolation, the local utility rates, and the locally available tax credit/subsidies (in addition to the federal). Other parameters that are critical but more predictable (and hence embedded in the analysis) are the PV array efficiency, the utility buyback rate, the utility rate escalation, and the homeowner discount rate.

One question that will have a heavy impact on residential PV economics, and that has not been treated widely in the literature, is whether homeowners will be taxed at their ordinary income tax rate for electricity sold to the utility. If so, will it be on the basis of all PV electricity produced (thus requiring 2 meters, as in simultaneous purchase and sale), all PV energy in excess of the instantaneous load, or net energy sold over some pre-established time period (utility billing period, tax period, etc.)? Assumptions here are critical in the final analysis.

It was found that the simplest systems typically are the most enduring. With electricity buyback rates approaching utility prices for the sale of electricity to homeowners, batteries do nothing to enhance the value of photovoltaics. Also, combined PV/T collectors are less desirable than side-by-side systems. New construction applications for a simple utility-interactive system generally were found to offer cost savings over retrofit installations.

In matching industry expected costs with the latest assessment of investor allowable costs, it was projected that the residential market would begin to accelerate around 1990, with activity first in those areas of high solar insolation, high utility electric rates and significant investment incentives (tax credits or others).

9.1.3 Studies of Residential PV/Thermal Systems

Lincoln Laboratory evaluated the economics of using combined PV/T systems as well as separate side-by-side PV and thermal units (2, 3). In particular, consideration was given to use of heat pumps as a means of enhancing these systems by making use of the relatively low-grade heat produced from a combined PV/T collector.

The objectives of these studies were:

- To identify "reasonable" residential PV/T heat-pump system configurations;
- To predict the performance of such systems in meeting residential heating, cooling and electric power demands;
- To compare system performances in northern and southern climates;
- To determine the most desirable systems for each of the two climates.

All economic evaluations were based on anticipated mid-1980s PV technology and prices, and on 1986 system installation.

The TRNSYS simulation program, developed by the University of Wisconsin, was used to predict system energy flows in PV/T heat-pump systems in New York and Fort Worth. The total auxiliary energy required by each system to meet the annual residential space heating, space cooling, hot water and diversified electric loads was calculated.

Two thermal subsystems were studied: a series, or solar-source, heat pump, and a parallel, or ambient-air-source, heat pump. Two electric subsystems were studied: a utility-interactive dc-ac inverter subsystem which diverts excess electric energy generated on site to the utility, and a dc subsystem with on-site electrical energy storage (e.g., batteries) and a "consume-only" utility connection. Four different systems may be configured by permuting these thermal and electrical subsystems. The primary independent variable in all four systems, the total collector area, was varied from 0 to 100 square meters.

The economic analyses used TRNSYS performance results and assumptions for component costs, mortgage rates, marginal tax brackets, general inflation rate, energy escalation rate, and tax incentives to calculate the predicted levelized annual cost of owning and operating the solar system for its assumed 20-year lifetime beginning in 1986.

The results of this study show that:

- Systems employing on-site electrical storage batteries are not economically competitive with utility-interactive systems for a 0.5 utility energy buy-to-sell ratio;
- For the New York (northern) residence, the parallel heat-pump system configuration meets a greater percentage of the total residential loads with solar energy than the series heat-pump configuration for PV/T collector areas less than $\sim$75 square meters;
- A parallel heat-pump system utilizing $\sim$40 square meters of PV/T collectors and providing $\sim$45% of the total residential energy demands represents the most economical PV/T system option of those studied for the New York residence;
- Separate thermal collectors and PV collectors result in systems with costs comparable to those using combined PV/T collectors in the New York residence;

- Due to the availability of low-cost electrical energy during the heating season in the Fort Worth (southern) residence, PV/T collector systems are not cost competitive in this location;
- The most economical system option for the Forth Worth residence is a parallel heat-pump system with approximately 35 square meters of PV collectors, which provides about 48% of the total residential energy demands.

9.1.4 Cost Goals for Residential PV Systems

Studies were performed at the MIT Energy Laboratory (4) and Lincoln Laboratory (5) to determine cost goals for both combined PV/thermal and PV-only residential systems. In the Energy Laboratory study, residential PV/T system costs were derived considering four different conventional energy systems for providing backup heating: all oil, all gas, all electric resistance, and electric resistance hot water with space heating by parallel heat pump. Electric space cooling was also modeled, with the electric utility serving as backup for all electrical needs.

The analysis was separated into two parts. The first was a base case study using conservative market and financial parameters for comparing PV/T economics in three northern locations: Boston, Madison and Omaha. All parameter estimates were for a privately purchased residence, newly constructed in 1986. Three measures were used for establishing allowable costs: system breakeven capital cost, allowable levelized annual costs, and an allowable combined collector cost when compared directly with a side-by-side collector system. In the second portion of this study, the sensitivity of PV/T economics to pertinent physical, market, and financial variables was examined. The difference in economic outlook for PV/T in retrofit applications was also examined.

The results indicate that, for those northern locations modeled, the allowable cost for a combined PV/T collector system is roughly \$10-\$30/m^2 less than that of separate (side-by-side) collector systems, at total array areas between 40-80 m^2. Below this range, allowable costs diverge, benefiting optimally sized separate collector systems. All systems look best when operating against all-electric homes. Retrofit applications seem favorable to newly designed homes, although here there is need to assess alternative retrofit options, such as conservation.

At MIT Lincoln Laboratory, a study of costs associated with the installation and operation of a residential PV system was conducted to determine present and projected (1986) status (5). As a basis for the study, a residential PV-only system design projected for 1986 was assumed, consisting of two principal components: a roof-mounted array and a utility-interactive inverter. The scope of the study encompassed both new and retrofit residential applications employing either silicon or cadmium sulfide PV modules.

Cost estimates were obtained by a survey and study of reports generated by companies and agencies then active in each of the subsystem areas. Where necessary, supplemental estimates were established as part of this study.

The range of estimates for silicon-based systems strongly suggests that such systems will be competitive for new installations and reasonably competitive for retrofit applications. The cadmium-sulfide-based system cost estimates, which are less certain than those for silicon, indicate that these systems will be marginally competitive with silicon-based systems for new construction, but not competitive for retrofit applications. Significant variations from the DOE system price subgoals were found, however, particularly in the areas of array mounting, wiring and cleaning. Additional development work appears to be needed in these areas.

As a result of the estimates compiled for this study, the 1986 DOE goal of $1.60/Wp appears attainable, provided that development efforts under way, such as silicon sheet growth, are successful and that intensive development efforts are initiated in power-conditioner design and array installation.

Several other specific findings are worth noting. The revised estimates of wiring costs indicate that recessed contact, weatherproof quick-connectors should provide a code-acceptable means of interconnecting modules. The disparity between power-conditioner cost estimates should be resolved. One approach would be to apply a uniform pricing methodology, such as SAMICS (Solar Array Manufacturing Industry Costing System developed for the Jet Propulsion Laboratory), in order to separate those components of the disparity which are "real" from those which are "artificial" (in the sense that they stem from different initial assumptions). Costs for installation of the power conditioning are estimated to be well below target, provided all pre-wiring

of disconnects, etc., is performed at the factory. Additional development in both the operation and maintenance areas is projected to produce substantial savings. Professional cleaning of modules is too expensive and self-cleaning or owner spray-type cleaning methods need to be evaluated. Application of redundant cell and module interconnect wiring techniques will reduce the probability of a major failure to a negligible level. All benefits from the above efforts will be nullified, however, if an unwieldy marketing and distribution chain develops. The results of a parametric analysis show that overall markup of 30% is compatible with the 1986 goal, while markups above 60% would seem to put it beyond reach.

9.2 Integration of PV Systems with the Utility

9.2.1 Introduction

Among the most frequently debated issues pertaining to the use of PV systems in the United States is the impact of such systems, either distributed or in central station fields, on the conventional operation of electric utility systems. Although the utility business is fairly evenly divided into three relatively distinct types of operations--generation, transmission and distribution--only generation issues have been the subject of exhaustive research during the past five years. The most intensive debate focused on the relative merits of photovoltaics as compared with more familiar forms of generation; namely, coal, oil and nuclear. In the forefront of this field of study were the Energy and Environmental Systems Division of the Argonne National Laboratory, industrial participants in the Electric Power Research Institute's renewable energy programs, and the MIT Energy Laboratory Utility Systems program. MIT Lincoln Laboratory's participation in this debate included analyses and reviews performed under subcontract by Dr. Martin Katzman.

A second area of research pertains to the impact of distributed PV systems on electric utility operations and was explored in large part by MIT Lincoln Laboratory. These investigations dealt with the physical response of distribution feeders to distributed generation. The first of these studies was conducted under a Lincoln Laboratory subcontract by Professor Jack Fitzer, at the University of Texas at Arlington, and addressed the impact of PV houses on a

specific feeder of the Texas Electric Service Company in the Dallas-Fort Worth area. Subsequent research has been conducted at the Northeast Residential Experiment Station (NE RES) and at the Southwest Residential Experiment Station (SW RES) under their charters to conduct research on the integration of distributed, grid-connected PV systems. These latter experiments have been used to validate theoretical models of feeder voltage control and losses.

Lincoln Laboratory's studies in each of these areas are summarized in the following sections.

Contributions to this effort were made by the following individuals: Jack Fitzer, Martin Katzman, Emanuel E. Landsman, Ervin F. Lyon, Alan R. Millner, Neil E. Rasmussen and F. John Solman,III.

9.2.2 The Impact of Residential Photovoltaics on Utility Generation Requirements

The canonical subdivisions of an electric utility's operation are generation, transmission and distribution. If PV generation is introduced into a utility's operating area, it can reduce the amount of time that conventional generators must run (thereby saving fuel), and it can also eliminate the need for an existing or planned plant (thereby offering a potential capital saving for the replaced capacity).

The question of what fuels would be displaced by widespread PV system application, and the amount and type of generation station capacity which need not be built as a consequence of such PV application, gained considerable significance with the passage of the Public Utilities Regulatory Policy Act of 1978. This law requires that electric utility companies reimburse the owners of solar, wind, hydroelectric and co-generation power-generation equipment for energy fed into the utility grid. Furthermore, such payments are required to be made according to the costs spared the utility as a consequence of receiving energy from the small power producer. This requirement, and its potential revenue consequences, has made the full understanding of "avoided costs" important.

In his summary report Katzman (6) reviewed simulation results from two of the most commonly used electric utility models. These were exercised,

to predict the impact of residential PV systems located at the two Residential Experiment Stations: that on Boston Edison Company owing to the NE RES systems, and that on El Paso Electric Company owing to the performance of the SW RES systems.

Katzman's findings indicate that in both the Boston Edison and El Paso Electric systems, the introduction of PV generation capacity will displace expensive fossil-fuel-fired electric power generation in the late 1980s. Boston Edison's capacity is likely to be at least 55% oil-fired, and the simulations indicate that each peak kilowatt of PV systems in their service area would displace on the order of 1000 kWh of oil-derived electricity each year. In addition, nuclear power generation would be reduced by a smaller amount: namely, 100 to 200 kWh, depending on which simulation model is used. In the El Paso Electric service area, gas-fired generation is likely to account for about 60% of the capacity in the late 1980s, and it is likely that a kilowatt of photovoltaics will displace 1400 to 1600 kWh of electricity otherwise produced from gas. In El Paso there is little oil-fired capacity, but both coal and nuclear plant electricity production would each be reduced 200 to 400 kWh annually by each kilowatt of photovoltaics.

These estimates were developed based on computer simulation models which make slightly different assumptions regarding the future generation-capacity mixes for these utilities. The Argonne methodology is designed to provide capacity-planning guidance to utilities, as it defines the optimal capacity mix toward which they should strive. While their simulation model can handle any capacity mix, the Argonne Energy group in practice assumes that each utility can quickly optimize its capacity mix to produce power most cost effectively. Accordingly, the results of the Argonne group undervalue PV systems by contrasting them with idealized and unattainable utility-generation mixes with little oil- or gas-fired capacity. In his simulations, Katzman assumes that each utility is restricted by the inventory of its current and planned capacity, a seemingly more reasonable representation of the reality of the situation.

The determination of that utility-generation capacity supplanted by a specified amount of PV capacity involves a more complex set of assumptions

and more subjective judgment than the determination of fuel savings. This complexity stems from two distinct features of the problem faced by utilities when they assess the adequacy of their generation capacity.

First, in their present operations, utilities must have on-line at every instant in time sufficient reserve capacity to cover the sudden failure of any active generation plant. For example, the Texas Electric Service Company in the Fort Worth area maintains enough "spinning reserve" to cover the failure of the largest generation plant on-line. Should a 1000-MW nuclear plant be the largest connected generator on-line, then within the entire system there needs to be 1000 MW of capacity on line and spinning, but not loaded, and therefore available instantly should the large nuclear plant trip off-line.

The utility-capacity planner must make such reserve capacity available to the dispatcher, the person responsible for ensuring that sufficient spinning reserve is available at all times, whether the system is fully or lightly loaded. When the system is fully loaded, the problem of maintaining sufficient capacity is more difficult. Planning for capacity to meet system peak loads involves projection of system peaks into the future at least as long as the time required to build additional capacity. New nuclear capacity now requires as much as a ten-year construction period, if not longer, because of current industry problems. The electric-utility-capacity planner's problem is that he cannot realistically predict system peak loads that far into the future. Planning for reimbursement for "capacity not required" because of the introduction of PV systems might require informing a utility ten years in advance that one intends to install PV capacity, thereby allowing the utility time to factor such a commitment into their generation-capacity planning. This perspective of the capacity-credit problem is not the only one, however, because new PV capacity might allow a utility to purchase less existing capacity from neighboring utilities should their loads be increasing and their neighbor have excess capacity. Alternatively, the solar capacity might allow a utility to retire, earlier than planned, their capacity which is least cost effective to own and operate.

Two methods are commonly used to determine the adequacy of a utility's generation capacity. First is the traditional notion of "reserve margin."

Once a utility peak load is known or predicted, a percentage (usually 20%) is arbitrarily chosen to provide for either exceptionally high loads or for generation plant unavailability when the system peak load is encountered. Thus a predicted peak of 20,000 MW for a region or large utility would require 24,000 MW of capacity to maintain this index of utility capacity expansion planning reliability. The second and newer framework for assessing capacity requirements is known as the "loss-of-load probability" approach, or LOLP. In this methodology the loads for an entire year are considered from the perspective of the dispatcher as indicated above. A spinning reserve is maintained, and an hour-by-hour calculation takes into account such factors as forced (unpredicted) and scheduled generation-station outages in the analysis of the probability that the system load exceeds the system-generation capacity in any given hour. Probabilities of overloads are then determined, with target values in the fractions of hours per year. This method, as a substitute for the simple 20%-reserve-capacity approach, is favored for assessing PV system effects on utility-capacity expansion. This occurs because the PV system output at the very instant of the system peak load might be either very large or very small. Since PV-generation systems have such variable output, it would not be prudent to sample their power production for just one hour during the course of an entire year. In doing so one might either overrate or underrate PV system-induced capacity displacement effects. The LOLP approach considers an entire year, and the probabilities of electric system overload at times of low, intermediate and peak system loads. One non-intuitive conclusion of the Katzman studies on capacity displacement is that enhancement of utility system reliability is accomplished by PV systems mostly by reducing the likelihood of overload during the long periods of intermediate loads when scheduled outages for maintenance reduce system-generation capacity, rather than during periods when the system load approaches its peak.

For the Boston Edison system, each kilowatt of PV capacity reduces the need for conventional capacity by approximately one-half kilowatt for the first 10% penetration of photovoltaics. (Penetration is defined as the peak PV capacity divided by the system peak load.) At higher levels of penetration, the marginal effect of additional photovoltaics diminishes rapidly, such that

at 30% penetration, the cumulative capacity savings for a kilowatt of photovoltaics is only one-third of a kilowatt of conventional capacity. In the El Paso Electric system, the corresponding values are a 50% credit for the 10% penetration and a 40% cumulative credit for penetrations in the 30% range. The higher credits in the Southwest arise from the probabilistically greater coincidence of high loads and high insolation.

Katzman reached three general conclusions about avoided fuel and capacity costs associated with PV systems. First, fuel savings dominate the total "avoided costs" passed on to the owner of the PV system, according to the Public Utilities Regulatory Policy Act of 1978. Capacity accounts for only from 5 to 15% of total "avoided costs." Second, the marginal savings in both fuel and capacity diminish with increasing PV capacity. As Katzman states it, "This follows from the facts that increased penetration saves increasingly cheaper base and intermediate fuels and that increased penetration saves a decreasing amount of capacity" (Reference 6, p. 18). Third, and finally, the worth of PV systems in the El Paso Electric Company service area exceeds those in the Boston Edison Company service area, owing primarily to the higher insolation in the Southwest; in both cases expensive oil and gas fuels, rather than less expensive coal, would be displaced.

9.2.3 The Impact of Residential Photovoltaics on Utility-Distribution Systems

9.2.3.1 Effect of PV on Feeder Capacity

To assess the effects of PV generation on utility feeders, case studies were made of two existing utility-distribution feeders. These studies included computer simulations as well as measurements to confirm predictions. The first of the studies (7) was performed on a modern (7.2/12.5 kV) distribution feeder (#3511) belonging to the Texas Electric Service Company (TESCO). The second study (8) was done on a feeder of older design which operates at a lower (2.4/4.16 kV) voltage. It is located in Concord, Massachusetts, and is feeder #23 of the Concord Municipal Light Plant (CMLP). This feeder serves the Northeast Residential Experiment Station (NE RES).

A detailed data base providing line and customer monthly loads existed for the TESCO feeder and permitted detailed computer simulations to be made,

assuming various numbers of PV systems on the feeder. The line was instrumented at the substation to provide voltage and load data, and the PV generation was modeled after the performance of the PV system at the University of Texas at Arlington (UTA) solar house in Arlington, Texas (see Section 11.4.1).

The Concord feeder was modeled in less detail, but was subjected to a number of experimental measurements using the facilities at the NE RES to check model predictions against actual measurements.

Figure 9-1 shows the output power of the utility-interactive PV system at the UTA solar house. This was for a clear day in July, and peak output occurred near noon. Figure 9-2 shows the demand at the substation for the same day as well as the changes in demand as a function of the market penetration of PV systems (the percentage of customers with PV systems). Each PV system was assumed to provide a power profile identical to the one at the UTA solar house. The reduction in load during the daylight hours is quite obvious, but the peak load which occurs at about 1800 hours is not significantly reduced. The dashed curve at the bottom of Fig. 9-2 shows the demand profile for 11 November 1980 to be considerably less than the demand on 31 July 1980,

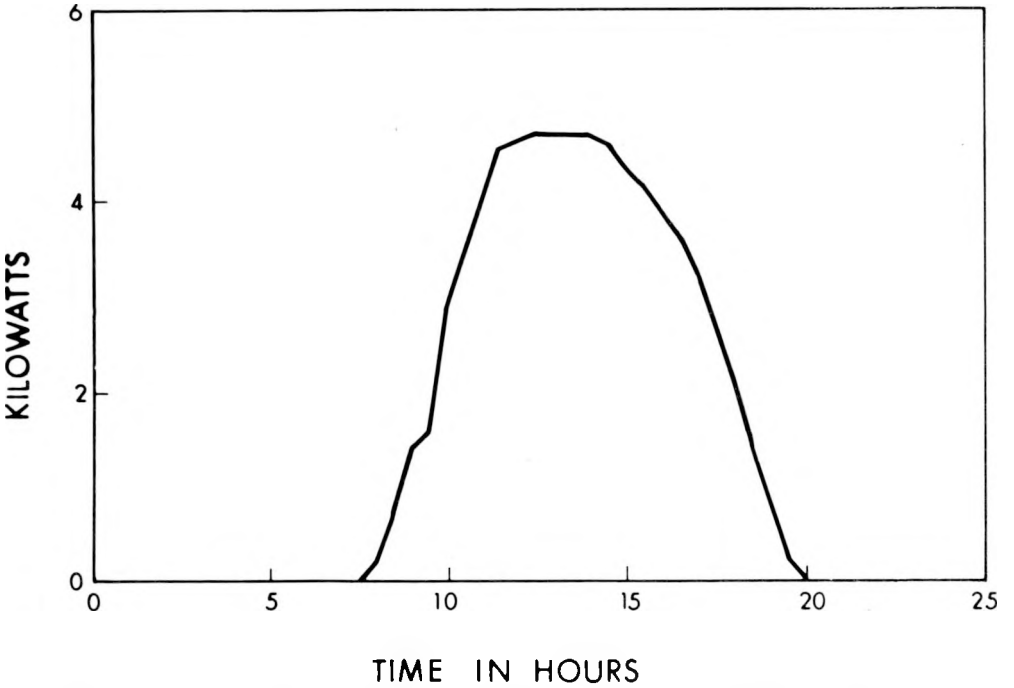

Fig. 9-1. Power output versus time of day for the UTA Solar House utility-interactive PV system on Thursday, July 31, 1980.

which was heavily influenced by air conditioning. For market penetrations above 40%, reverse power flows might occur on such light load days. When PV penetration is likely to become relatively large, this possibility should be considered in the design of protective equipment for the feeder.

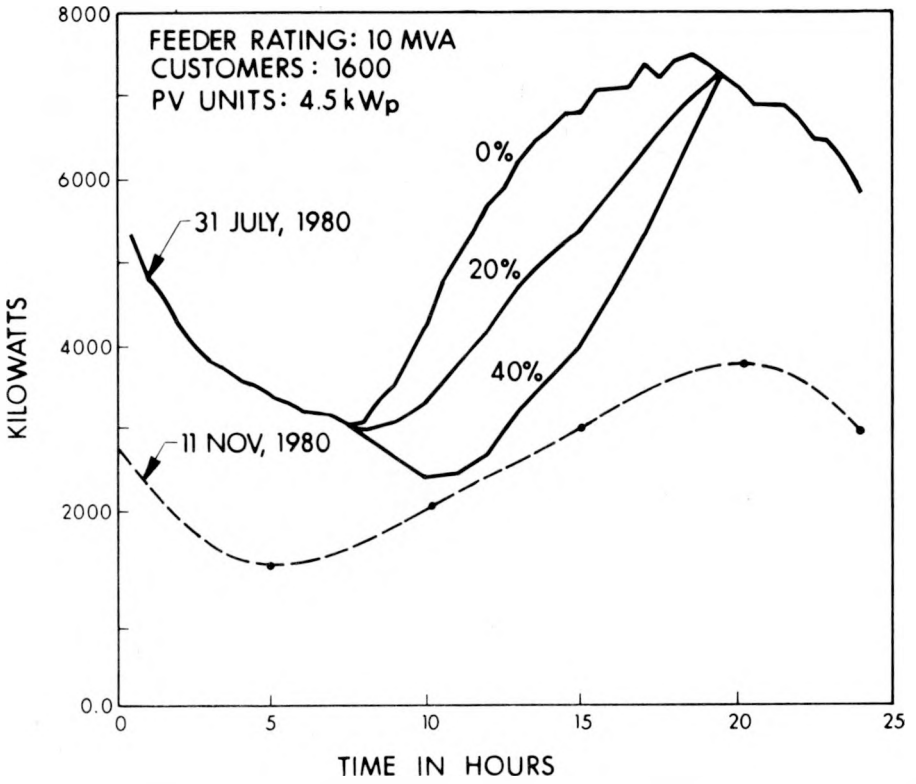

Fig. 9-2. Demand at TESCO substation for feeder #3511 with and without distributed PV systems for July 31, 1980. Demand for November 11, 1980 is shown for comparison.

Figure 9-3 shows the effect on the voltage at the end of the TESCO feeder as a function of penetration and inverter power factor. Note that for a PV inverter power factor of about 0.85, there is very little change in the voltage profile with large amounts of injected PV power (market penetration). Higher power factors produce a voltage boost and lower power factors reduce the end-of-line voltage. The range of end-of-line voltages that would occur as a function of feeder load without PV system operation is shown at the right. For market penetration of PV systems below about 40%, the voltage variations that occur with normal load changes exceed the effects of the PV systems.

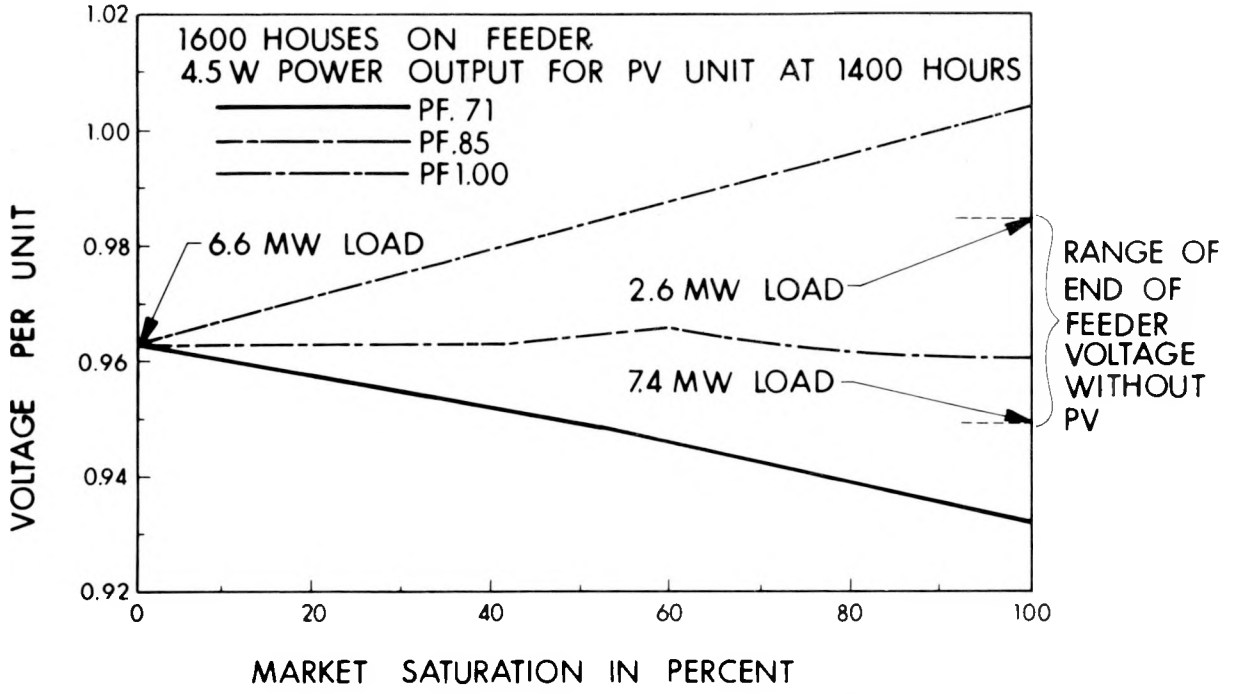

Fig. 9-3. Voltage in per unit at the end of TESCO feeder #3511 on Thursday, July 31, 1980 at 14:00 hours as a function of PV market saturation and inverter power factor.

9.2.3.2 Effect of PV Feeder Losses and Substation Load Reduction

Figure 9-4 shows the apparent power as seen by the substation and the line losses as a function of market penetration for inverters with unity power factor.

In all the cases studied, the PV generation produced a reduction in distribution line losses. Since line losses are reduced, the net reduction in load seen at the substation is larger than the amount of PV power injected. On a 7.2/12.4 kV system, this bonus can be 2 to 3%.

The line losses are reduced even more dramatically on the lower voltage feeder of the CMLP since such losses are greater in lower voltage distribution systems. In this case, the substation load is reduced by between 10 to 30% more than the amount of injected PV power, depending on feeder load, with the benefits greater at heavier loads.

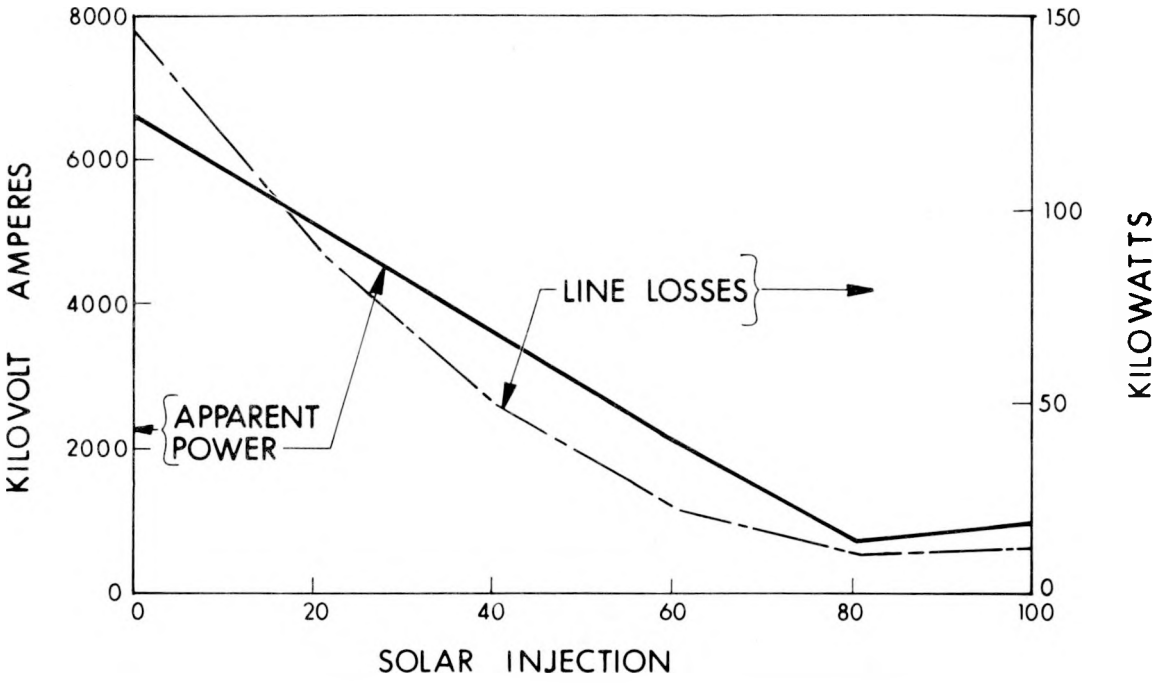

Fig. 9-4. Apparent power at TESCO substation and feeder losses for Thursday, July 31, 1980 at 14:00 hours. PV inverter PF = 1.0.

9.2.3.3 Effect of Inverter Harmonics on Feeder Voltage and Current

The effect of harmonics produced by PV inverters needs to be considered in the context of ambient harmonic levels and their effect on utility equipment and customer loads. The simplest type of PV inverter developed to date uses a line-commutated bridge of silicon-controlled rectifiers (SCRs) to convert the dc power from the array to ac power for injection into the ac line. Landsman (9) has made extensive measurements on the output current spectrum as a function of power level for a commercial unit. Further refinements of such units and improved inverter designs using, for example, "wave-shaping techniques" (10), will provide PV inverters with much less harmonic content than the values based on Landsman's measurements used in this study.

Preliminary utility standards are based on the belief that if harmonic voltage levels are kept below 5 to 10% no disturbance of customer loads is

likely to occur. Simulations done on TESCO feeder #3511 indicate that the harmonic voltages will be about 1.5% of the fundamental for a market penetration of 20%, and that no adverse effects are likely to occur.

Measurements of harmonic voltage and currents were made on the CMLP feeder #23 near the substation. The measured ambient harmonic voltages without PV injection are less than 1.3% for the fifth harmonic and even less for other harmonics. Figure 9-5 shows typical voltage and current waveforms. Table 9-1 lists the magnitudes of the respective current and voltage harmonics. Note that the harmonic currents can be quite high without changing the voltage waveform due to the low source impedance of the utility.

For further information concerning design of inverters for utility interactive use, the reader is referred to Section 10.6 of this report.

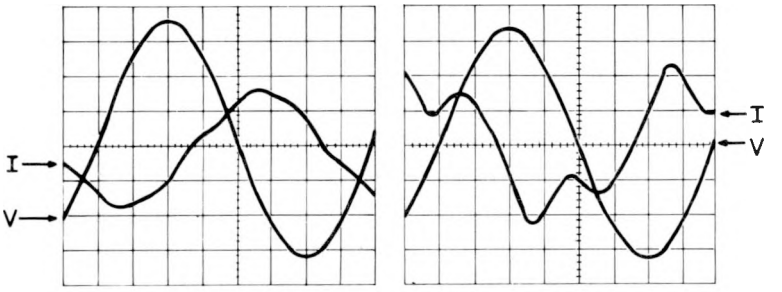

Fig. 9-5. Voltage and current waveforms measured on CMLP Circuit 23 at Pole 17 (near substation).

TABLE 9-1

HARMONICS MEASURED ON CMLP CIRCUIT 23 AT POLE 17
(May 14, 1982 between 2 and 4 p.m.)

Parameter Measured	Harmonic Content in Percent — Harmonic									
	2	3	4	5	6	7	8	9	10	11
A-Phase Voltage[1]	0	0.7	0	1.3	0	0.2	0	0	0	0
A-Phase Current[2]	0.1	3.0	0.1	3.0	0	0.4	0	0.3	0	0
C-Phase Current	0.2	3.4	0	3.4	0	0.1	0.2	0.1	0	0.1
Neutral Current	0.5	15.0	0.1	4.0	0.2	1.0	0.1	--	--	--

[1] B and C phase voltages had similar harmonic content.

[2] B phase current harmonics were similar to A and C phase.

9.2.3.4 Effect of PV on Utility Operation

While the effects on utility operations from PV generators are likely to be minor, good line-design practice would suggest that the installation of new PV generation should be assessed using techniques similar to those now used for interfacing new customers and loads. Several areas of concern have been discussed by Fitzer (7) and Shelton (8); they include conductor voltage drops (primary and secondary), reactive-power compensation, overcurrent protection, 3-phase load balance, backup-circuit connections, and safety of customers and utility-service personnel. Conductor voltage drops and reactive-power compensation have been discussed in the previous section. This section will discuss the remaining topics.

Overcurrent Protection

Distribution feeder overcurrent protection may be implemented at several locations on a feeder from the substation out to individual transformers. Substation protection can range from fuses on each of the three phases to more elaborate protective relaying for control of the substation circuit breakers.

The protective relays at the substation trip the feeder circuit breaker on individual line overcurrent as well as on unbalanced line currents. Unbalanced line currents are sensed by monitoring the neutral current, which should be a small fraction of any line current in a balanced 3-phase system. Since line imbalance provides a sensitive indication of line faults, normal distribution system practice is to equalize loads among the three phases. For this reason efforts should be made to balance both the amount of PV generation and the loads on each of the three phases.

Overcurrent protection devices located out on the distribution feeder include fuses and circuit breakers, as well as multishot version of fuses and circuit breakers.

Fuse and circuit breaker trip ratings are coordinated in an attempt to sectionalize the line in the event of fault. Fuse values from the substation outward are sized progressively smaller so that a fault near the end of the line will blow only the closest fuse and leave other fuses upstream unblown.

This limits the area of outage. To improve the reliability of service, multiple-shot fuses and circuit breakers are used to provide more than one attempt to clear a fault (for example, by burning off a fallen branch), and the time intervals between reclosings are sufficiently long to extinguish arcs.

The contributions to fault currents by utility-interactive PV systems are inherently limited by several factors. First, a PV array has a limited short-circuit current; second, the ac output current of an inverter is limited by internal protective circuits which are necessary to protect its power semiconductors from overcurrent. The result of these two factors is that the maximum fault current possible from a PV system is only a few percent larger than its normal output current at full power.

A study (7) was done on a 7200-V feeder to determine the effect of a 40% PV penetration on fault current. The maximum increase in fault current on single-phase branches was found to be about 3%. In essence, almost all of the short-circuit current delivered to a fault is sourced from the substation, and the magnitude of this current is limited only by line and substation transformer impedances.

The increments of fault currents that can be attributed to PV sources appear to be too low to affect coordination of the individual phase overcurrent relays and fuses. In a radial distribution system, the tripping levels of upstream protective devices are usually a hundred percent (or more) higher than the tripping levels of downstream devices, and the few percent increase in fault currents due to PV sources cannot affect this coordination. In fact, the small increase in fault currents due to PV system contributions is generally lower than the precision to which the protective devices can be set.

In general, protective devices are sensitive to the magnitude of fault current and not to the direction. However, some types of substation protective relays may have to be rearranged when PV market penetration becomes large enough to cause reverse power flow at the substation, but it is unlikely that this potential problem will occur in the foreseeable future.

Interconnections with Backup Circuits

Standard utility practice is to provide backup circuits which can be connected by switches to pick up groups of customers in order to provide

continuity of service during periods of construction, maintenance or emergency circuit repairs. If load balance is maintained with new PV generation, this practice should not be adversely affected by PV sources. In fact the presence of PV generation may help to reduce low voltage problems which often occur under emergency conditions.

Safety During Maintenance

Virtually all utilities perform maintenance on their overhead distribution systems by means of live-line techniques, obviating any need to shut down equipment for this purpose. Underground equipment which may require de-energization generally has sufficient switching capability to sectionalize and insure separation from all power sources.

Utility accessible and lockable disconnect switches on inverters may have some use for localized repairs at the distribution tranformer level. In general, however, selective grounding of de-energized cables and transformers could readily be incorporated into maintainance procedures. The location of PV units must be clearly marked on circuit maps and nearby poles. Grounding of de-energized cables and equipment will prevent injury should a PV unit accidentally start up into a de-energized line (9,11).

Emergency Repairs

In the case of a major failure involving damage to the distribution equipment or lines, conventional live-line techniques may not be feasible. In those cases it becomes necessary to separate the section of line from all possible sources, test for voltage, and solidly ground all conductors before working on the circuit. All open switches are tagged and locked to prevent unauthorized closing.

It is impractical to expect a line crew to find, open, and tag a large number of PV inverters in order to prevent accidential energization of the line. Design of the inverters to prevent absolutely startup without line energization (11) and close attention by the utility personnel to the testing and grounding procedure should provide adequate protection from this potential problem.

9.3 Analytical Models for PV System Technical Performance

9.3.1 Introduction

In this section, work done at Lincoln Laboratory on development of analytical models of residential PV systems is discussed. Most of this work was focused on PV utility-interactive systems (as opposed to combined PV/thermal), because the economic studies done at Lincoln Laboratory and elsewhere indicated that this is the preferred system.

In order to model a complete system accurately, detailed knowledge of each subsystem is needed. Accordingly, a "bottoms-up" approach was followed wherein models were developed and tested for each important element of the system. Then complete systems were modeled, and the predicted performances from the models were compared with actual performances as measured in the five residential PV prototype systems at the NE RES. These activities are summarized.

For information on modeling residential PV systems employing combined PV/thermal collectors, the reader is directed to References 12 and 13, which cover this subject in great detail.

Contributions to this effort were made by the following individuals: Louis L. Bucciarelli, Barbara L. Grossman, George W. Hart, Susan D. Hendrie, Ervin F. Lyon, Pattabiraman Raghuraman, Miles C. Russell and Duncan B. Sheldon.

9.3.2 General Framework for Simulation

The present work describes a TRNSYS program, which is the general framework for simulation of the prototype PV energy systems that has been developed at Lincoln Laboratory. TRNSYS (standing for Transient System Simulation) is a computer simulation program package developed at the Solar Energy Laboratory of the University of Wisconsin at Madison (14).

Figure 9-6 shows the basic elements of a utility-interactive residential PV energy system. For simulation purposes, each system is divided into its major functional components, which are individually described with computer models:

1. A simple, time-dependent, thermal model of an array. This computes cell temperature, given insolation, ambient temperature and wind speed;

2. A model of an array's dc current-voltage characteristics as a function of insolation and cell temperature;
3. Models of the electrical characteristics of the dc side of commercial power conditioners (devices which convert dc to ac);
4. Models of power-conditioner ac output, given the dc input.

C74-1652

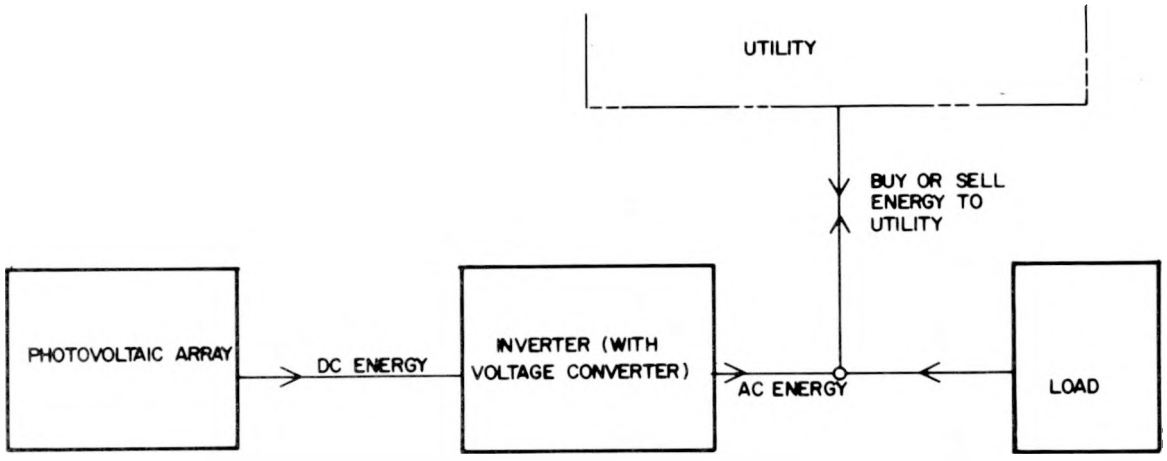

Fig. 9-6. Basic elements of a utility-interactive PV energy system.

A TRNSYS-compatible subroutine was written for each of these components. All of the component models and the entire TRNSYS simulation were calibrated and verified against measured thermal and electrical performances of residential prototype systems at the NE RES.

Figure 9-7 shows the organization of the simulation. The independent variables, which can be classified into weather data and load data, are the physical quantities needed to run the simulation. The weather data determine the performance of the PV energy system (inverter ac output), while the load data determine whether energy must be bought from or sold to the utility.

TRNSYS allows all of the inputs and outputs depicted in Fig. 9-7 to be interconnected flexibly, and sees to it that the different subroutines are called as often as necessary until all variables converge to stable values. TRNSYS also provides simple mechanisms for converting units allowing, for example, a subroutine written with inputs and outputs in SI units to be

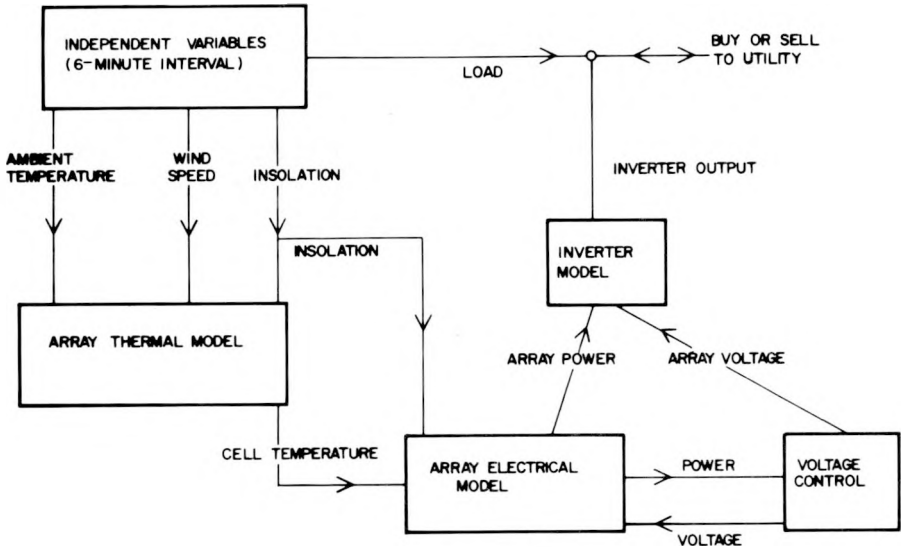

Fig. 9-7. Organization of simulation.

connected with a subroutine using English units, with no internal changes to either subroutine. In addition, TRNSYS provides subroutines that perform standard calculations, e.g., a radiation subroutine which computes the insolation on a tilted surface given the insolation on a horizontal surface.

TRNSYS also provides a time frame for the simulation. The results obtained from the simulation which are described in the following sections and in References 15 and 16 were obtained with 24-hour simulations at six-minute intervals based on weather and residential load data that were measured at the NE RES. These simulations were used for calibrating and checking the validity of the analysis. Other runs were made over a year-long period at hourly intervals using Typical Meteorological Year (TMY) and SOLMET data. These were used for projecting annual estimates.

A data unit subroutine provides the simulation with values for the independent variables (see Fig. 9-7), indicating the six-minute measurements recorded by the NE RES data-acquisition system. These variables are ambient temperature, wind speed, tilt insolation and house load. These data can be provided for any of the five prototype systems, on any day that the system was operating normally. The data unit also provides several other channels of

information which are used for comparison purposes when checking the validity of the simulation, such as the measured array voltage, and the inverter's input and output power.

9.3.3 PV Array Thermal Model

The purpose of the thermal model is to estimate accurately the array cell temperature as a function of insolation, ambient temperature and wind speed. Following the method of Stultz and Wen (17), the model assumes that the equilibrium cell temperature varies linearly with insolation. As Reference 15 describes in detail, the slope of the line is a function of wind speed and decreases as the wind speed increases. A particular slope is calculated by an exponential interpolation between three known points. These points are determined either by measurements from an existing array or by a detailed energy balance calculation.

The temperature calculated in this way is not the actual cell temperature, but the steady-state cell temperature, that is, the temperature that the array would reach were it given enough time to attain thermal equilibrium. Based on an exponential model of temperature change, a simple formula is used to determine the dynamic cell temperature as a function of the calculated steady-state temperature and a previous value of the dynamic cell temperature.

9.3.4 Electrical Models

Details of the modeling of the electrical components of the PV systems and discussion of the results are available in Reference 16. The electrical properties of the array are modeled by a subroutine which inputs the cell temperature, tilt insolation, and operating voltage, and outputs the array current and power. The basis for this routine is the TRW model (18) of an array's current-voltage characteristics at a specified insolation and temperature. The JPL model (19) is used for translating the I-V curve to arbitrary insolations and cell temperatures. Figure 9-8 indicates how the array's I-V characteristics vary as a function of insolation. Figure 9-9 shows the dependence on cell temperature.

The voltage at which an array operates is determined by the power conditioner connected to it. The Abacus inverter attempts to find the

precise voltage at which the array power is maximized, by either a search or a "pilot-cell" mechanism. The Gemini inverter approximates the maximum power voltage by imposing a simple I-V relationship upon the array.

C74-1639

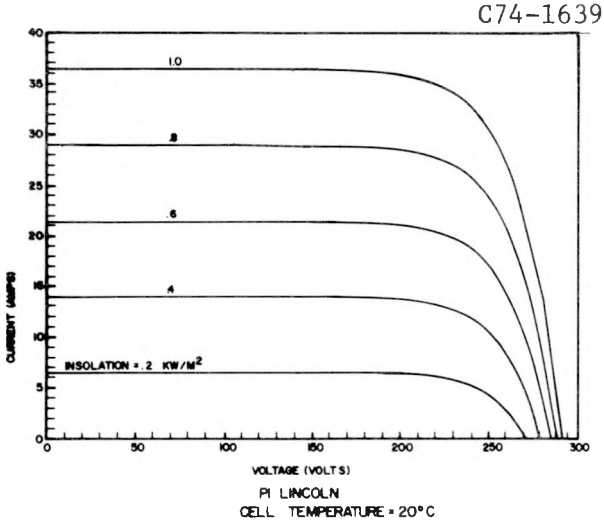

Fig. 9-8. Variation of I-V curves as a function of insolation.

C74-1638

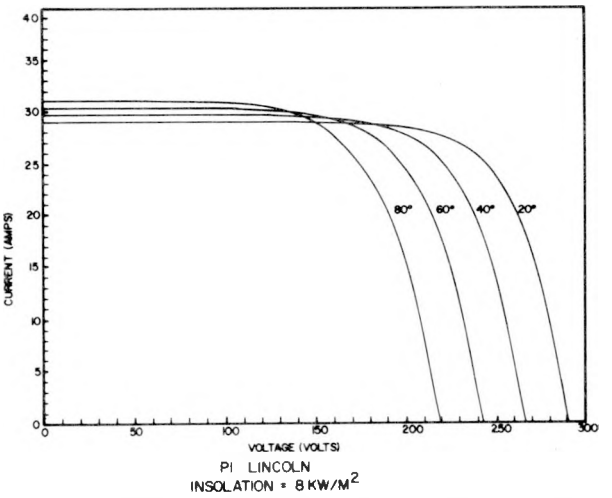

Fig. 9-9. Variation of I-V curves with cell temperature.

The output of the inverter is determined as a function of the array power and voltage. Figure 9-10 shows a measured curve of efficiency (ac output power/dc array power) as a function of the two dc variables. A subroutine was written to perform a two-dimensional linear interpolation between the measured data.

C74-2040

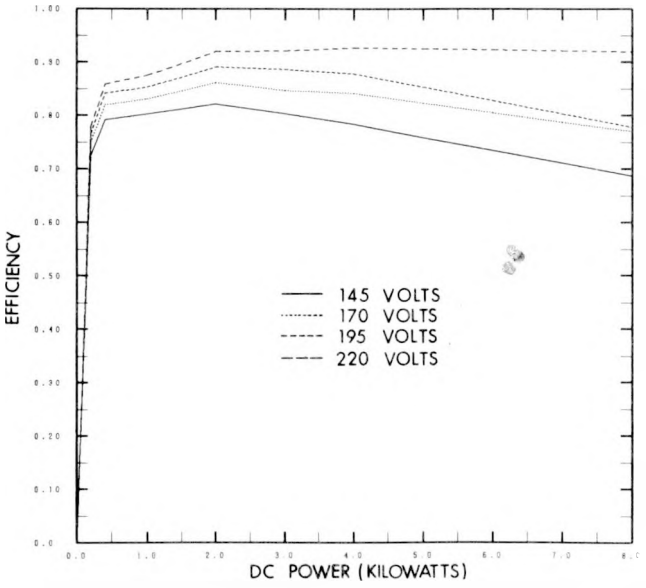

Fig. 9-10. Efficiency of Gemini inverter (with transformer) as a function of dc power and voltage.

Utility interaction is initially performed by a simple subtraction process. If the house load exceeds the inverter output, the difference is purchased from the utility. If the inverter output exceeds the load, the difference is sold back to the utility. This result is then modified by a correction factor which accounts for the details of the energy interaction within the simulation timestep. The difficulties in calculating utility interaction are described in Reference 20.

9.3.5 PV System Model

After the components of the residential PV energy system were modeled, they were calibrated and tied together as a TRNSYS simulation. The simulation is organized about a sequence of timesteps. For each timestep, the program reads in the independent weather variables and calculates the dependent system variables, such as cell temperature, array voltage, array power and inverter output power. Integrated quantities such as total energy are summed together at each step.

This is not the only way to organize a simulation. Many simulations (see, for example, Reference 21) reduce the number of calculations necessary by grouping together timesteps which share some common property, and perform one calculation which is valid for all of those times. For example, if 20 of the 8760 hours in a year could be found with the same insolation, ambient temperature and windspeed, one calculation could be made to determine an output power valid for all of those hours. Then 20 hours multiplied by that power level can be added into the total yearly energy. Similarly, all other combinations of ambient conditions can be taken up in turn, until the entire year is accounted for. This type of organization can reduce the number of timesteps that are considered, and eliminate many repeated calculations. Variations on this method increase the number of timesteps to be grouped together by allowing looser equivalence relations rather than strict equality. All timesteps at which some independent variable falls in a certain range can be grouped together, using the midpoint of the range in the calculations. Other methods group according to time of day; collating all "one-o'clocks" together, for example. Invariably some of the weather and dependent system parameters are not constant when timesteps are grouped together in these methods. Therefore either an average value or a probability distribution of the parameters is often used in the calculations.

These shortcut methods and others can all be made valid and reasonably accurate. The factor which determines if they should be used is whether or not they are sufficiently accurate to serve the purpose for which they are constructed. The NE RES simulation is organized as a "marching forward in time" type for a number of reasons, one of which is that the time simulation was designed to be as accurate as possible in modeling the operational details of each system component. It is used in evaluating various design options, such as voltage-control strategies and thermal-mounting methods. Small differences in electrical output are often the result of such design variables. It was desired to minimize errors that are introduced by the use of averaging, or the substitution of separate probability distributions. Any classing together of nonidentical timesteps introduces these errors to some extent, but it is very difficult to estimate the magnitude of their effect on the final results of interest. This problem is compounded by the fact that different parameters need to be evaluated, and it is convenient to have a single simulation remain suitable for new tests. In addition, the timestep organization is expedient because TMY, SOLMET and NE RES weather data arrive in a time-stream format, so no reorganization of the data is required. Finally, timestep by timestep comparison of the simulation predictions and NE RES prototype measured performance allows quick location of errors and inaccuracies.

9.3.6 Comparison of Measured and Predicted Performance

Four basic components of the PV system simulation require validation: the thermal model of the array, the I-V characteristics of the array, the dc side of the power conditioner, and the power-conditioner efficiency. These are each discussed in turn. The thermal model is described in greater detail in References 22 and 23; the electrical components in References 24 and 25. In all cases, the models were validated by comparing predictions against measured performance of the prototypes at the NE RES.

9.3.6.1 Array Thermal Model

As was discussed in Section 9.3.3, cell temperature is basically calculated as an increase above ambient which is linear in insolation:

Cell Temp = Ambient Temp + k * insolation.

This temperature is adjusted somewhat to allow for the fact that the array is generally not in thermal equilibrium. The slope k varies with windspeed, having a maximum value at zero wind. As the wind velocity increases, k decreases to approach a limiting value exponentially. Parameters for each prototype, which define how k varies with wind, were determined by measurement.

This method seems to predict daytime cell temperature quite accurately during the spring, summer and fall months. It is generally within two degrees of the measured temperature. At night and in the winter, however, certain errors arise. Figures 9-11 through 9-15 compare the predicted and measured cell temperature for the five NE RES prototypes on five nonwinter days. The measured values are an average of four sensor readings which are distributed across the array. The simulated temperature is calculated from measured values of insolation, ambient temperature, and wind speed.

C74-1914

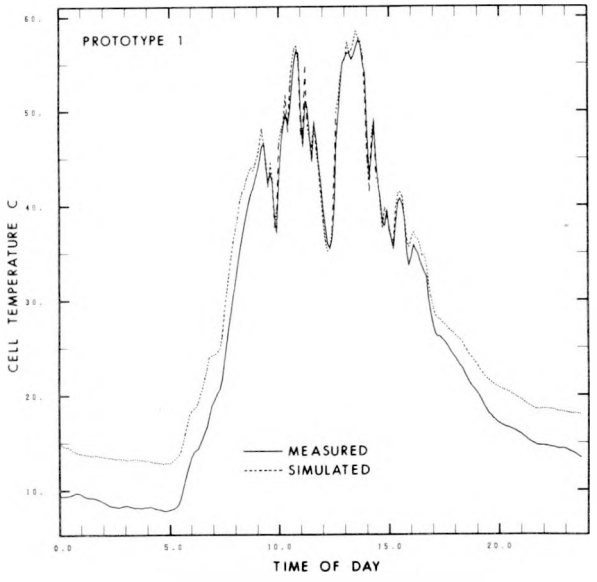

Fig. 9-11. Comparison between measured and computed cell temperature for Lincoln array.

C74-1906

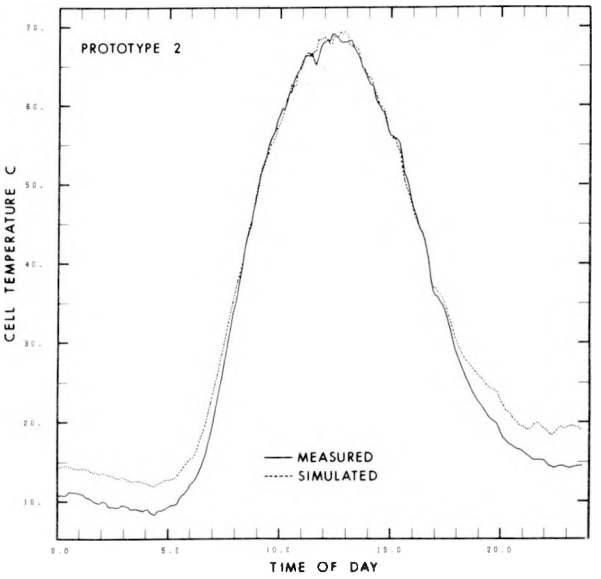

Fig. 9-12. Comparison between measured and computed cell temperature for Lincoln array.

C74-1912

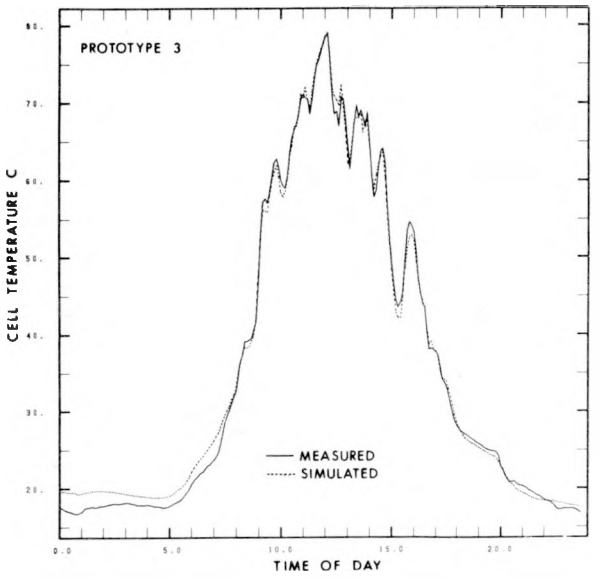

Fig. 9-13. Comparison between measured and computed cell temperature for GE array.

C74-1910

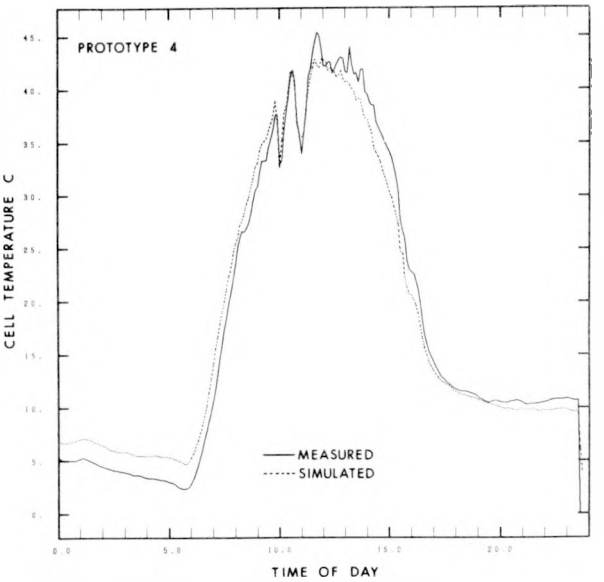

Fig. 9-14. Comparison between measured and computed cell temperature for TriSolarCorp array.

C74-1911

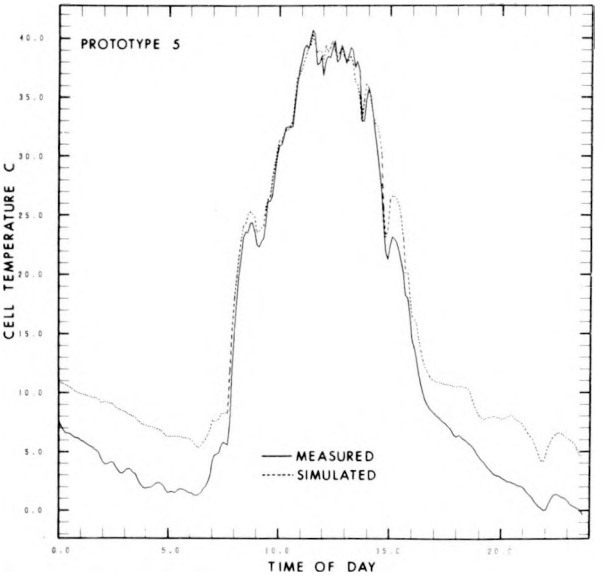

Fig. 9-15. Comparison between measured and computed cell temperature for Solarex array.

It can be seen that the nighttime temperatures are significantly in error by up to 5°C. The simulation predicts a cell temperature equal to ambient when the insolation is zero. The actual array temperature is below ambient, however, due to radiation cooling. The sky temperature varies with cloud cover, so the difference varies from day to day. This discrepancy has no effect on the simulation outputs, of course, because no PV energy is generated at night.

The model fails in a more significant way when there is a spread of temperatures across the roof. The model assumes a single temperature for the entire array. The actual array, depending on its mounting and cooling arrangement, can vary widely from that ideal. Each of the NE RES prototype arrays is monitored with four separate temperature sensors distributed across the array. The four temperatures recorded are averaged together to arrive at the measured cell temperature shown on the comparison plots in Figs. 9-11 through 9-15. Generally the four readings agree within 5 to 10°C during the daytime and within two degrees at night. Figure 9-16 shows the four separate readings of the TriSolarCorp array on a day which shows an extreme case of variation. There is a difference of 20°C between the hottest and coolest points measured. This results from a nonuniform air temperature in the attic space behind the array. There is a natural temperature gradient causing the modules along the ridge to operate at a temperature ten to fifteen degrees above that of the modules along the eave. In addition to this, there is a gradient increasing from west to east along the length of the attic caused by an induced air flow. There is a thermostatically controlled attic exhaust fan which can be seen in Fig. 9-16 to be operating between approximately 9:15 and 12:15 on this day. Because of this variation, the measured cell temperature must not be taken too literally; it is merely an average. It is not clear which temperature within the range of temperatures recorded should best be used as the norm against which to calibrate the simulation.

In the winter, two other effects result in a discrepancy between the simulation and the measured values. One problem is that insufficient (or no) thermal insulation between the living quarters and the array results in

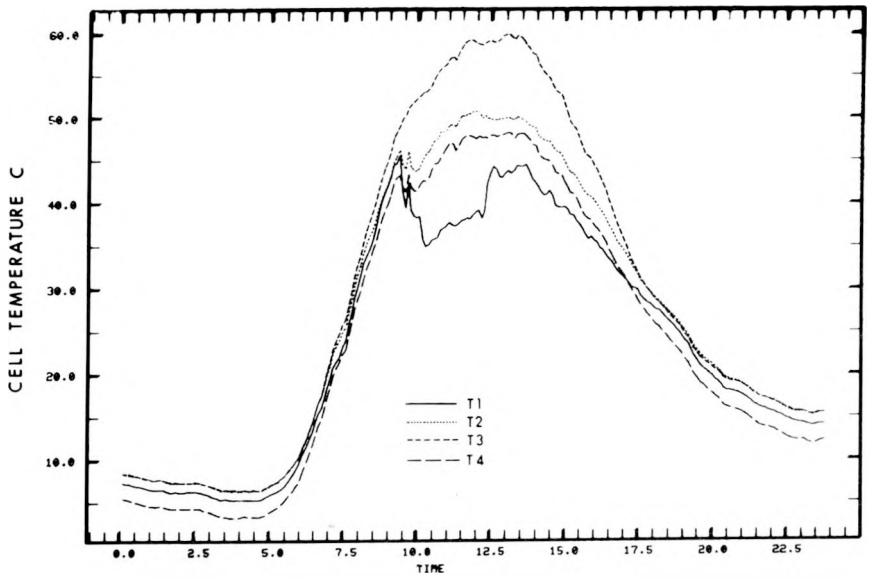

Fig. 9-16. Measured temperature variation across TriSolarCorp array.

a higher than predicted cell temperature because heat lost through the roof heats the array. On the coldest days this produced approximately a five-degree increase at the NE RES prototypes. Figure 9-17 compares the predicted cell temperature, based on nonwinter measurements of k, with the measured cell temperature, which can be seen to be seven or eight degrees higher.

A much more significant error results from snow and ice accumulations on the array. Figure 9-18 shows how wet snow tends to lock the array at $0^{\circ}C$. Generally, snow blocks insolation from the array, leading to colder than predicted cell temperatures. This effect is only of academic interest because the reduced insolation has a direct effect on the electrical output which is far more significant than the indirect effect which results from predicting an incorrect cell temperature. Figure 9-18 also shows that there can be a one-degree calibration error in the sensors.

Finally, it must be pointed out that when calibrating or verifying the cell temperature predicted by the simulation, it should be compared to the cell temperature measured when the array is actually producing electric power. Conservation of energy requires that the energy which appears as the electrical output of an operating PV system shows up in some other form if the

C74-1909

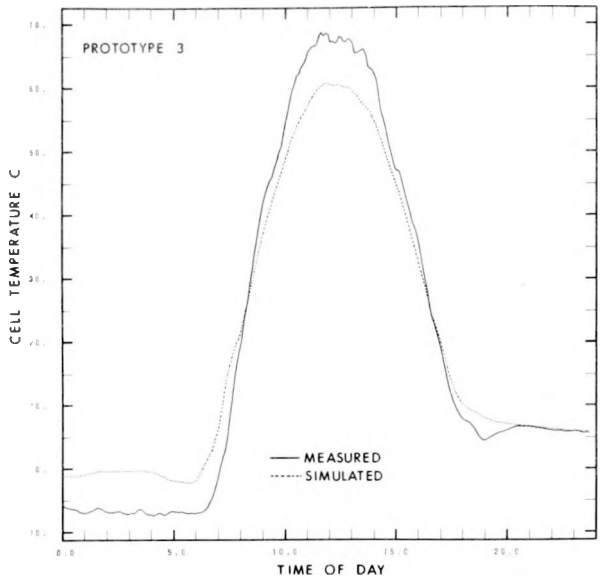

Fig. 9-17. Comparison between measured and computed cell temperature for GE array on winter day.

C74-1935

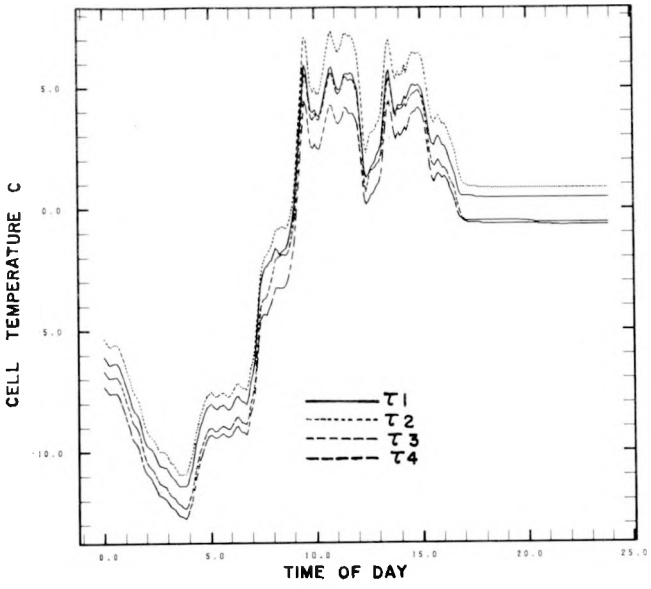

Fig. 9-18. Effect of snow and ice on cell temperature of Lincoln array.

system is turned off. Figure 9-19 shows a five-degree increase in cell temperature resulting from a failure of the power-conditioning unit in the TriSolarCorp system. Change in insolation, ambient temperature and wind speed did not contribute to this rise.

C74-1933

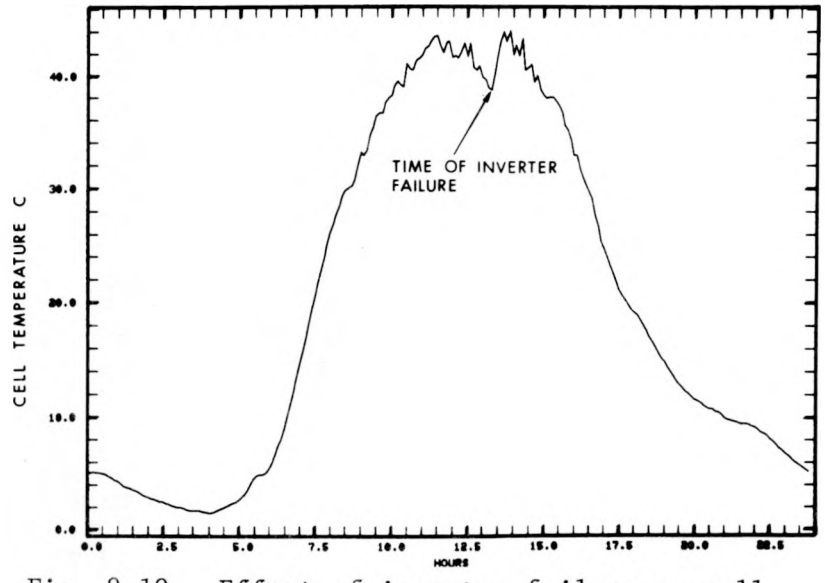

Fig. 9-19. Effect of inverter failure on cell temperature of TriSolarCorp array.

9.3.6.2 PV Array Current-Voltage Characteristics

This model requires data defining three points from a measured I-V curve of the array to be modeled: the open-circuit voltage, the short-circuit current, and the maximum power point (26). The model fits an exponential curve to these points and interpolates between them to provide a complete I-V curve in analytical form. Figure 9-20 compares an I-V curve taken from one string of the Lincoln array with the TRW model based on the three marked points. The simulated curve can be seen to pass properly through the three given points, but the curve is not of the exact shape required. This error remains uncorrected in the simulation.

The curve of Fig. 9-20 is only applicable at one particular insolation level and cell temperature. The simulation uses the JPL model (27) to translate this curve for arbitrary insolations and temperatures. This model shifts the given curve left or right, and up or down, as a function of these two variables, but does not alter its shape. Figure 9-21 shows a sampling of measured I-V curves paired with the translations of Fig. 9-20 that the model predicts for the corresponding insolation and cell temperatures. The error in the shape of Fig. 9-20 remains visible in some of these curves.

9.3.6.3 PV Array Voltage Control

The simulation is capable of operating with three distinct array voltage control strategies: fixed voltage, maximum-power-point tracking, and a hybrid method used by the Windworks Gemini inverter. None of the prototypes at the NE RES has an inverter which is operated in a true fixed-voltage mode. There are three Abacus inverters, which are designed to maximum-power-point track, and two Geminis*. The curve of Fig. 9-22 shows the basic shape of the dc current-voltage characteristics which the Gemini inverter imposes on the array. The point at which the curve begins to rise, and the point where it levels off, can be set manually on the inverter, and are parameters to the modeling subroutine. The scattered points of Fig. 9-22 are measured values of current vs. voltage which were used to calibrate the model.

---

*In the summer of 1982, new inverters were installated as indicated: one Abacus Sunverter (pilot-cell control), one DECC (maximum-power-track), one American Power Conversion Corporation Sunsine (maximum-power-track), one Acheval Wind Electronics SILCI (quasi-constant voltage) and one Windworks Gemini (quasi-constant voltage).

C74-2048

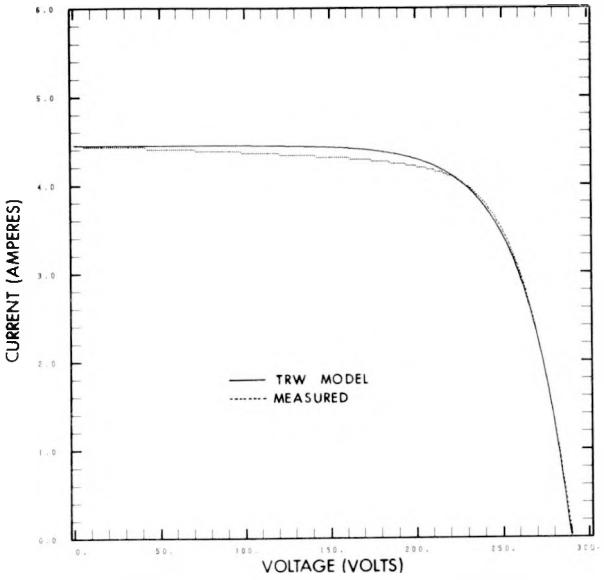

Fig. 9-20. Comparison of measured and simulated I-V curve.

C74-1904

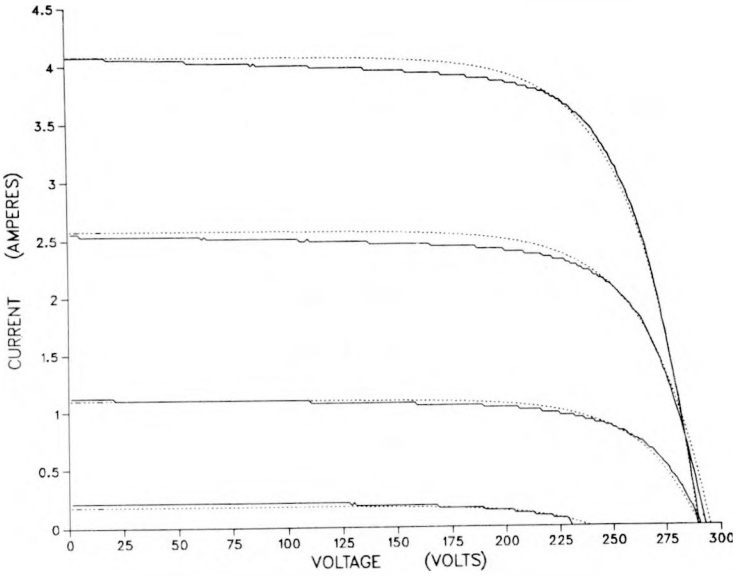

Fig. 9-21. Comparison of I-V curves for various insolation and cell temperatures of the Lincoln array from measurements and the JPL model.

C74-2039

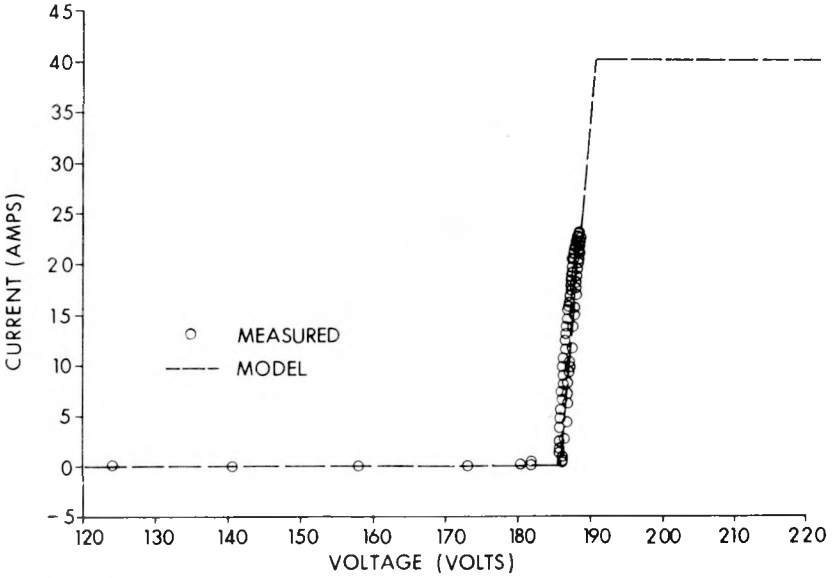

Fig. 9-22. Current-voltage control characteristics of the Gemini inverter.

Figure 9-23 shows how the Gemini varies the array voltage across time and the corresponding voltage that is predicted by the simulation. The discrepancies that occur at times of low insolation arise from slight calibration error or instability in the hardware which measures the tilt insolation. The simulated inverter is very sensitive to insolation, and "wakes up" before there is sufficient light/PV energy to awaken the actual inverter. Although this appears to be a serious discrepancy, it actually results in a negligible power difference because the insolation is so low at these times.

The Abacus inverters attempt to find the maximum-power-point voltage for the array. Prior to December 1981, they used a searching method which resulted in oscillations around the true maximum power voltage. Figure 9-24 compares the array voltage selected by the inverter with the calculated maximum power voltage. The significant difference between the model and the measured voltage is attributed to the fact that the inverter was not effectively tracking the maximum power point.

C74-2047

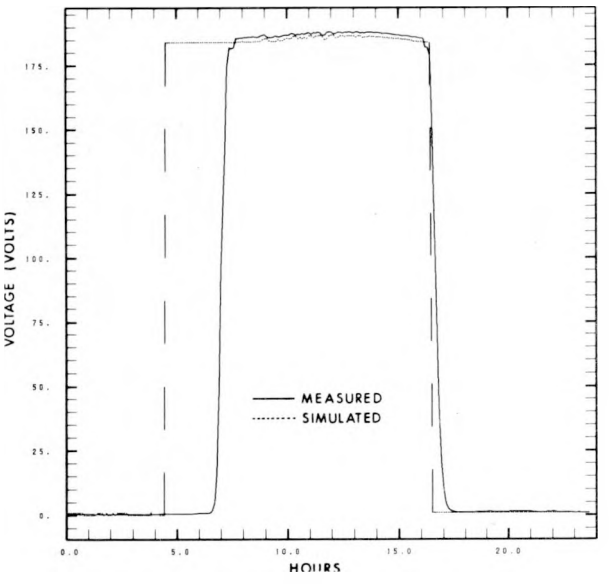

Fig. 9-23. Measured and simulated array voltage for Gemini inverter.

C74-1920

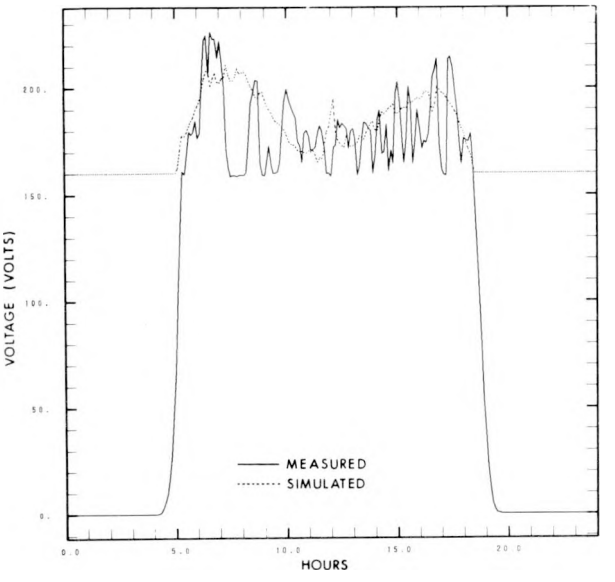

Fig. 9-24. Measured and calculated voltages for an Abacus inverter with "searching" maximum-power-point tracker.

During December 1981, the Abacus inverters were modified to use a pilot-cell approach. The array voltage was set to a fixed multiple of the open-circuit voltage of one cell (or module). For this to work, the multiple must be properly set. Figure 9-25 shows the array voltage calculated in this manner with the predicted maximum power voltage of the Westinghouse array. They differ at sunrise for a short period before the inverter wakes up.

The various aspects of the array modeling discussed above can be checked together by comparing the array dc power with the predicted array power across time. Figure 9-26 makes the comparison for the TrisolarCorp prototype for the same day as Fig. 9-23. A total electrical output of 18.6 kWh was predicted, compared to a measured output of 18.2 kWh. The exact value varies from day to day, but this error of 2.2% is not atypical.

C74-2046

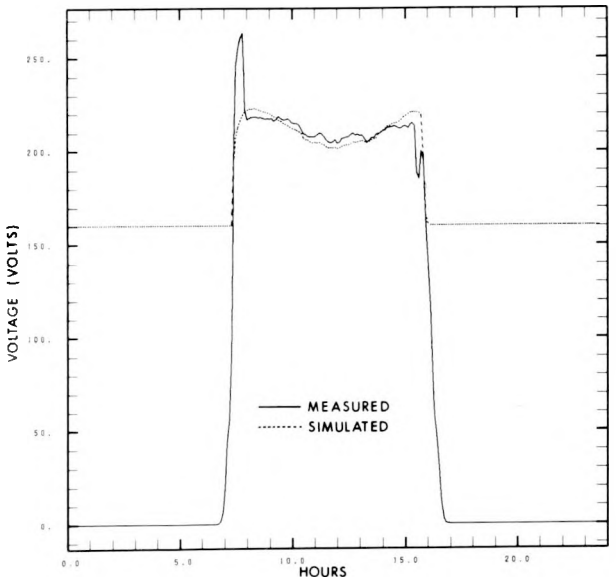

Fig. 9-25. Measured and calculated voltages for Abacus inverter with "pilot cell" maximum-power-point tracker.

C74-2045

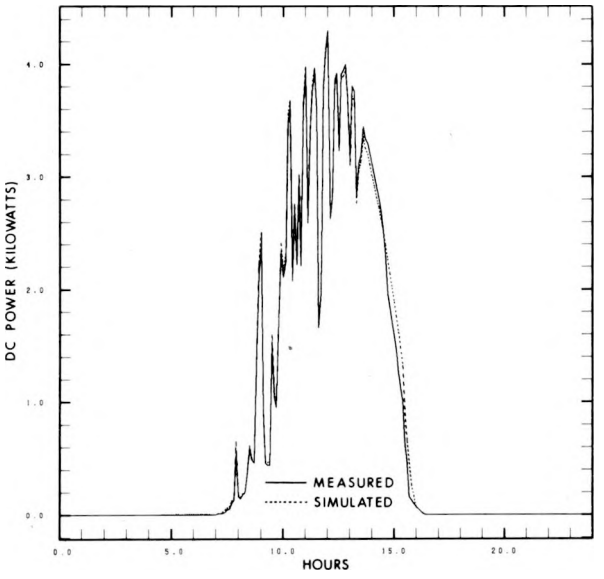

Fig. 9-26. Comparison of measured and calculated dc power output from TriSolarCorp array.

Figure 9-27 shows the measured and predicted dc power for the Westinghouse array on the same day that is shown in Fig. 9-25. The measured and predicted energy outputs are 29.8 and 29.0 kWh. There is a 2.8% error.

C74-2044

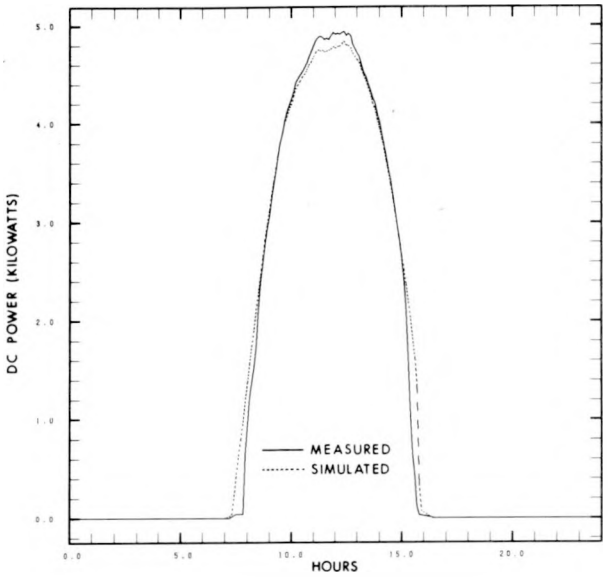

Fig. 9-27. Comparison of measured and calculated dc power output from Westinghouse array.

9.3.6.4 Inverter Efficiency

The efficiency of the two inverters modeled is calculated as a function of dc power and dc voltage. A set of measurements was taken over the operating range of powers and voltages that can be expected. These values are shown in Fig. 9-28 for the Gemini inverter, and in Fig. 9-29 for the Abacus. The inverter model is given a voltage and power level and interpolates within the given efficiency data. The output power is then calculated as the input power times the interpolated efficiency.

The measured ac output of an inverter can be compared with the predicted power as they vary in time. Figure 9-30 compares the measured and predicted inverter output of the TriSolarCorp array for one day. Figure 9-31 does the same for the Westinghouse array. There is a 3.3% error in the TriSolarCorp case and a 4.7% error in the Westinghouse case.

C74-2040

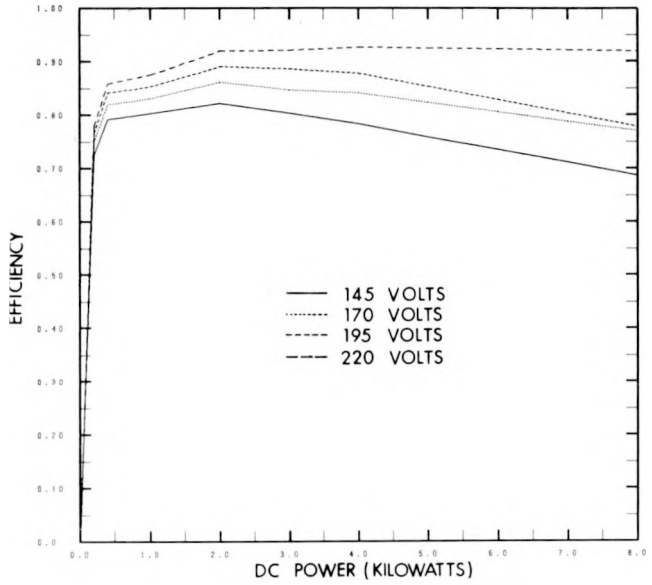

Fig. 9-28. Efficiency of Gemini inverter (with transformer) as function of dc power and voltage.

C74-2041

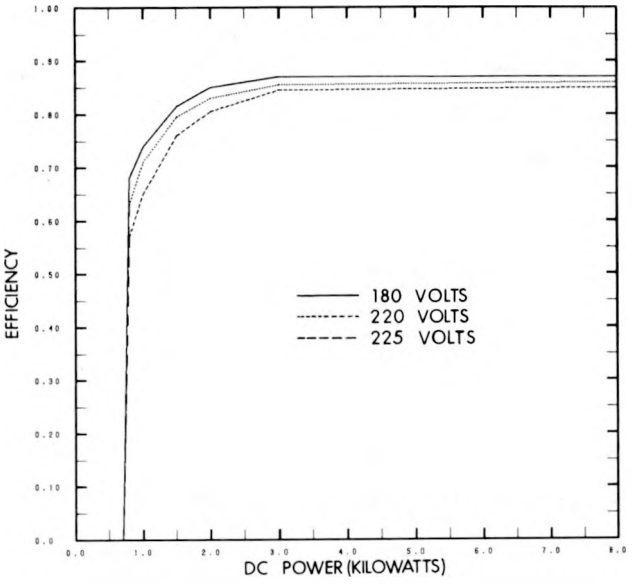

Fig. 9-29. Efficiency of Abacus inverter as function of dc power and voltage.

C74-2043

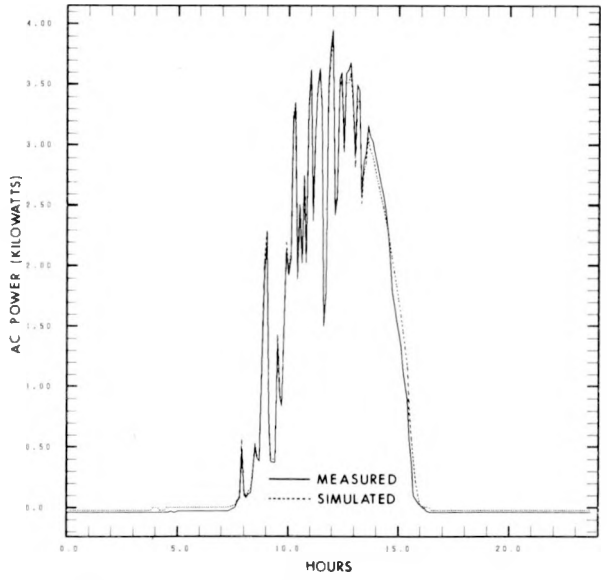

Fig. 9-30. Comparison of measured and calculated ac power output of TriSolarCorp array with a Gemini inverter.

C74-2042

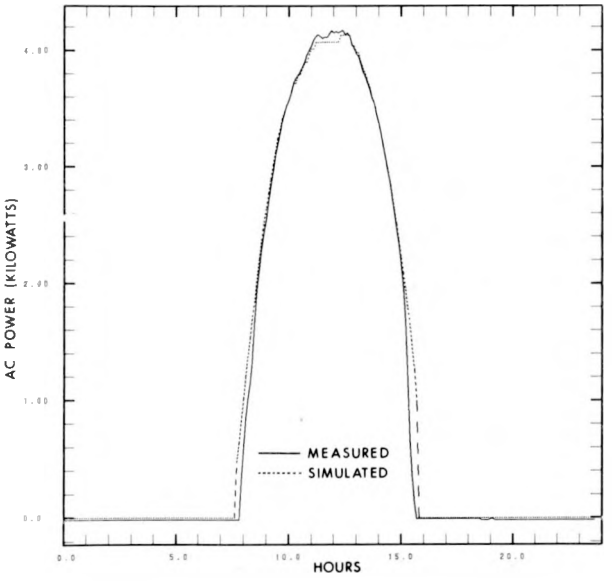

Fig. 9-31. Comparison of measured and calculated ac power output of Westinghouse array with an Abacus inverter.

9.3.6.5 Overall Accuracy of System Simulations

In summary, it is possible to predict residential utility-interactive PV system output consistently within a 5% error. Since the error in the data-gathering system can be up to 5%, these models are as accurate as the equipment can verify.

9.4 The PV Array/Power-Conditioner Interface

9.4.1 Introduction

A typical residential PV system contains two major subsystems: the PV array and the power conditioner. The power conditioner is designed to set the dc voltage at which the array operates. This raises the question of how operating voltage should be set. With additional complexity (and thus cost), the power conditioner can be made to vary the operating voltage such that the maximum possible amount of electric power is always extracted from the array. As an alternative, the conditioner can operate at a fixed voltage, thereby losing some electric energy and incurring some financial loss, but also demanding a less complex and therefore cheaper unit. How much energy would be lost by fixed voltage operation? How will the inevitable occurrences of array degradation affect the choice of voltage control? A study was done to answer these and other pertinent questions (28).

To study the array/inverter interface, a program of computer simulation and experiment was followed. Through computer-simulation studies, the efficiency of a variety of array/power-conditioner-interface strategies was examined. Through the use of simulations based on statistically typical U.S. weather data, the effects of the different array-operating strategies with different PV arrays and in different geographical areas were predicted. This information was presented in a format designed to aid manufacturers and designers in making economic and technical tradeoffs as they design the array/inverter interface for PV systems. Among the array/inverter-interface issues examined through computer simulations were: 1) the choice among several different array operating-point-control stategies, 2) the effect of array degradation on the choice of operating-point-control strategy, 3) the determination of the

optimal relative sizes of the array and power conditioner, and 4) the prediction of the annual operating efficiency of the power conditioner. Techniques were also developed for estimating the maximum voltage that a power conditioner must be designed to withstand.

Most of the experimental program was designed to ensure that the computer simulation accurately reflected real PV-array behavior. During a five-week period, weather data and I-V curves from an operating PV array were collected and stored. The resulting data base fully characterized actual array electrical behavior as seen by the power conditioner. With these data, the computer simulations were calibrated and validated, and error limits were determined.

Reference 28 presents the basic information needed to design the interface between a terrestrial flat-plate PV array and its power-conditioning subsystem. It also details the methodology of the study so other researchers can extend and improve the work as the PV industry matures and new arrays and power conditioners become available.

Contributions to this effort were made by the following individuals: Howard M. Branz, Charles H. Cox, III, and George W. Hart.

9.4.2 Computer Models and Validation

Computer simulation of residential PV systems was used to investigate array energy output from various systems using different array-operating strategies. The simulation program was initially developed to model the prototype systems at the Northeast Residential Experiment Station (NE RES), using measured weather data. This simulation uses TRNSYS (29), a solar simulation control program devised at the University of Wisconsin, augmented by Lincoln Laboratory solar subroutines (see Section 9.3). Figure 9-32 is a flowchart of the simulation.

The program simulates the behavior of PV systems in different geographical locations based on the SOLMET or Typical Meteorological Year (TMY) hourly weather data tapes provided by the U.S. National Oceanic and Atmospheric Administration (NOAA), (30,31). Each hour, a radiation-processing routine determines the insolation incident on an array tilted at the latitude of the site from the SOLMET value of the total insolation on a horizontal surface. The solar-cell-operating temperature is computed for the hour using a linear-temperature-rise model developed by Stultz and Wen (32).

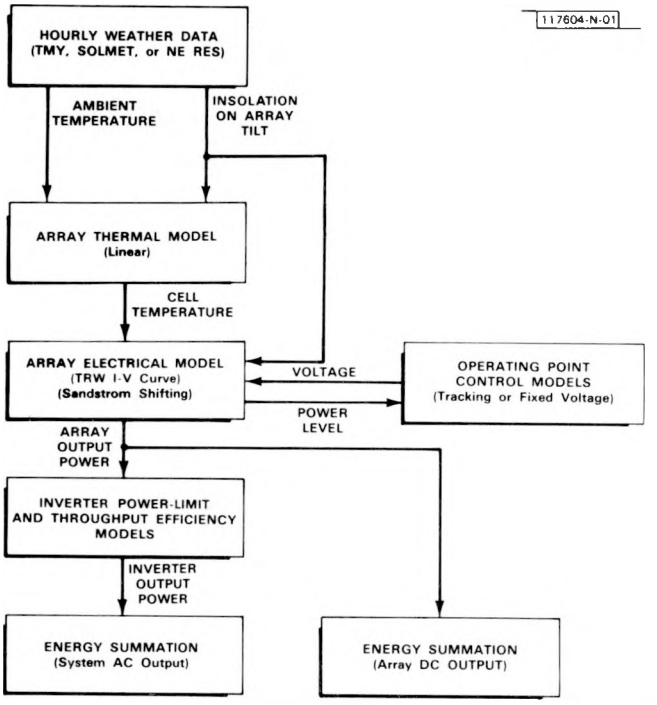

Fig. 9-32. Flowchart of PV system simulation program.

Given a cell operating temperature and tilt insolation, the hourly array I-V curve is computed using the TRW solar cell model (33) and translated using a method following closely that of Sandstrom (34). From this I-V curve, the simulation can determine the hourly array power output to any inverter. The inverter models available include fixed-voltage operation at any voltage, and unlimited-range, or limited-range, maximum-power-point tracking. The maximum-power-point tracker steps through the tracking range in 1-V steps and computes the power output at each voltage to find the maximum power point for the hour.

Two different types of user-determined power limits are also available in the inverter model. The simulated inverter can either shut down completely or deliver energy at the power limit during any hour that the array output power exceeds the inverter power limit.

The simulation sums the hourly energy output over any time interval to determine system energy production totals. It can also compute the energy output distribution as a function of output power for characterization of the array output.

The accuracy of the computer simulation components was checked by comparing measured values of key system variables from the Lincoln Laboratory NE RES prototype with values predicted by the simulation.

Figure 9-33 shows four measured and four simulated I-V curves. Each simulated curve is a translation of the reference I-V curve to the insolation and cell temperature that was measured as the actual I-V curve was swept. While these curves have the same fundamental shape, there is a slight difference in current at voltages lower than the maximum-power-point voltage. This difference is small, however, compared to the changes in shape that were made to the curve to simulate the effect of various array parameters, such as fill factor. Thus the error introduced by the inaccurate shape of the model I-V curve is very small; and it can be seen that the simulation models the translation of real I-V curves very well.

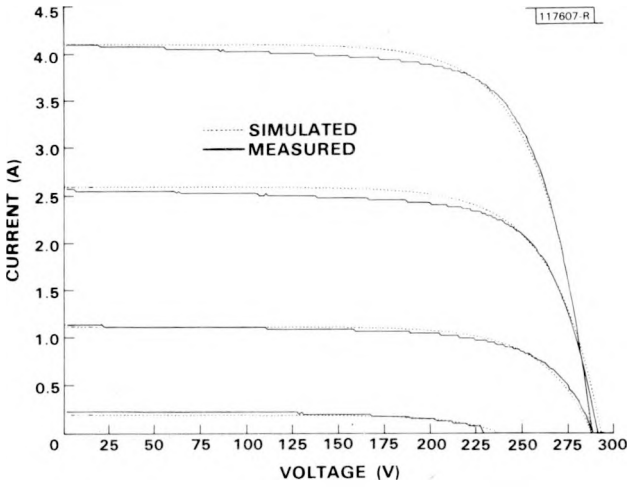

Fig. 9-33. Pairs of measured and simulated I-V curves at four combinations of insolation and cell temperature.

9.4.3 Array-Operating-Point Control Strategies

As the array I-V characteristic shifts with changing insolation and cell temperature, the maximum power point moves. The desire to follow the short-term variations in array maximum power point and to accommodate long-term shifts due to array degradation has led PV designers to develop maximum-power-point-tracking algorithms.

Ideally, a maximum-power-point tracker has unlimited range and an accurate tracking algorithm. Existing maximum-power-point trackers usually can follow the optimum voltage only within a limited operating window, and the algorithms of some are easily misled. (For example, one maximum-power-point tracker used at the NE RES loses between 5 to 10% of available array energy, even when operating with a full-power array on a sunny day.)

Concern about the performance, expense and reliability of maximum-power-point tracking has motivated the following examination of the worth of alternative array-operating strategies. Among the alternatives covered in Reference 28 are fixed-voltage, limited-range tracking, and pilot-cell tracking. The results of the investigation of fixed-voltage operation for both fully operational and degraded arrays are presented here.

9.4.3.1 Fixed-Voltage Operation with Fully Operational Arrays

The simplest alternative to maximum-power-point tracking is array operation at a single fixed voltage.

In order to quantify the annual loss of available array energy that results from fixed-voltage array operation and to establish a method for finding the best fixed voltage of array operation, extensive computer simulations were performed. The simulations encompassed 26 U.S. locations and included many different PV arrays and mounting methods. In these simulations, it was assumed that the array was neither degraded nor shaded, and that the maximum-power-point-tracking algorithms employed were ideal. The simulations show that less than 5% of the annual available PV system energy will be lost with fixed-voltage operation, depending on the system, its geographical location, and the accuracy with which the fixed voltage is set.

Figure 9-34 shows the amount of energy that would be delivered by the baseline residential PV system using two different operating strategies in both Albuquerque, New Mexico, and Boston, Massachusetts. The horizontal lines show the annual available energy that could be delivered by this system with maximum-power-point-tracking operation in both locations. The curved lines show the energy delivered in each city by the system as a function of the fixed voltage employed. There is, in each city, a best fixed voltage (BFV)

at which the array can be operated. At the BFV in Boston, only about 19 kWh of 1200 kWh, or about 1.6% of the available energy, is lost. For operating voltages within about ± 15 V of the BFV, less than 5% of the available energy is lost, but if the array is operated 25 V above the BFV, over 10% of the available energy is lost.

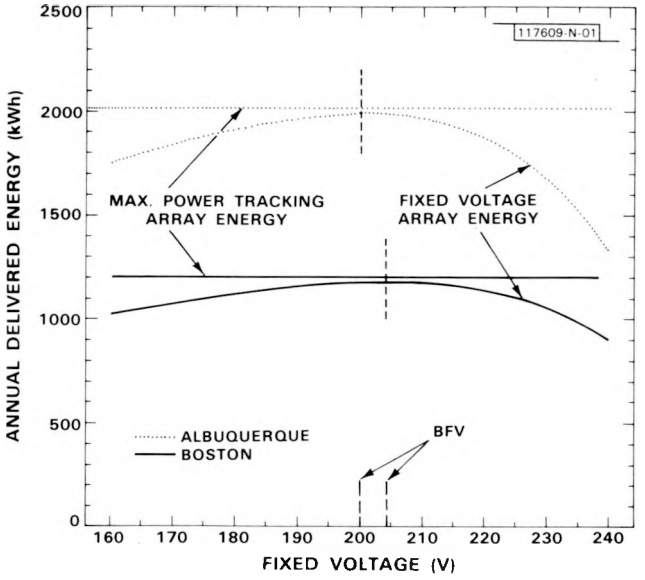

Fig. 9-34. A comparison of the energy output as a function of fixed operating voltage and the total available array energy.

These results--a very small energy loss when operating a BFV and a rapid increase in losses when operating more than 25 V above the BFV--are typical for all 26 locations studied.

In addition to the dependence of the results on local weather, there is a dependence of the energy loss on the exact PV array that is simulated. For most normal arrays, in terms of parameters such as operating temperature, fill factor, etc., the deviation from the results discussed above is quite small, and these system values are indicative of the energy loss that can be expected due to fixed-voltage operation of a PV array.

9.4.3.2 Fixed-Voltage Operation with Degraded Arrays

Though less than 5% of the annual available energy is lost by operating most flat-plate PV arrays at fixed voltage, there is the concern that the unpredictability of I-V curve shape under array degradation and shadowing,

and the resulting variations in maximum-power-point voltage, will force inverter manufacturers to install maximum-power-point-tracking inverters in their systems. It is true that fixed-voltage operation will sacrifice available energy from degraded arrays, but the results of computer simulations presented in Reference 28 show that in most cases degraded PV arrays do not give maximum-power-point tracking a significantly larger annual energy advantage over fixed-voltage operation than that offered by tracking with healthy arrays. Certainly there are some array degradations that result in larger energy collection penalities for fixed-voltage operation, but much of the array degradation that is most costly for fixed-voltage operation is so severe that array repairs would be required under most reasonable maintenance strategies.

The subject of PV array degradation is complex because of the many array design approaches in use. Instead of examining selected array failures, a large set of the I-V curves that may result from degradation were analyzed without regard to the particular array or array failure that produced them.

Several I-V curves are pictured in Fig. 9-35. Field experience (35) indicates that this set of curves, called "single-glitch" I-V curves because they result from a single module or interconnection failure, is the most frequent result of array degradation of residential-size PV arrays. Curve C is the result of an actual array degradation while curves A and B are included for illustrative reasons.

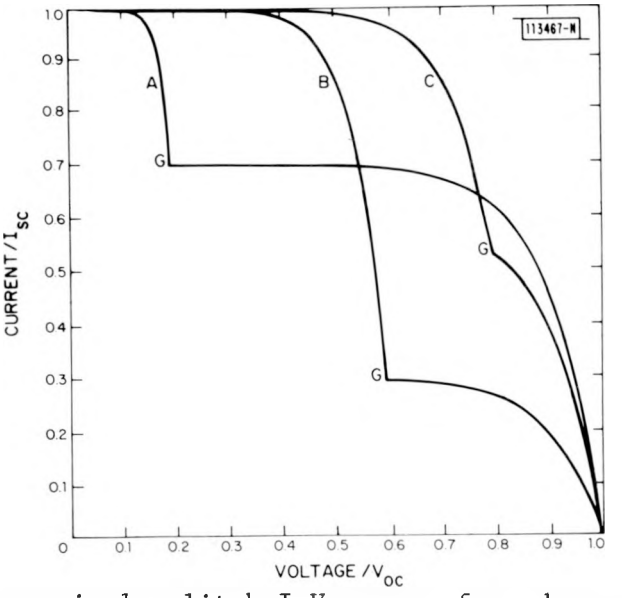

Fig. 9-35. Three single-glitch I-V curves from degraded PV arrays. Each I-V curve can be uniquely represented by the location of its glitch-point.

To adapt the TRNSYS-based annual simulation program to degradation studies, a mathematical model of single-glitch I-V curves was devised, based on how changes in insolation and cell temperature affect degraded I-V curves.

A hypothetical array with in situ, nominal operating cell temperature (NOCT') of 46.5°C and Boston TMY weather data was used for all the degradation studies. Under in situ, standard operating conditions (SOC'), the 3.5-kWp hypothetical array has an open-circuit voltage of 200 V, a short-circuit current of 25 A and a fill factor of 0.70. This array was simulated in its healthy state and under degradations resulting in 64 different single-glitch I-V curves having the same open-circuit voltage and short-circuit current. Annual simulations of the healthy array showed that 160 V is the BFV of the array in Boston and that 1.6% of the annual available energy is lost by fixed-voltage operation at 160 V. In the field, the BFV will be calculated and set, and will not be changed as the array degrades, so the operating voltage was held at 160 V for all the fixed-voltage degradation simulations.

The total annual available energy from the full-power system in the Boston TMY is 5090 kWh. The energy loss when operating a degraded array under fixed voltage can be broken down into two components. The available energy loss is independent of the array control strategy; it is due to the loss of a portion of the array. The operating-control energy loss depends upon the array control strategy; it is zero for maximum-power-point tracking and increases for other control strategies, such as fixed-voltage operation.

To explore the available energy losses, Fig. 9-36 shows the total available energy of this array after degradation for all degradations that result in single-glitch I-V curves. Figure 9-36 and subsequent figures convey information about a continuum of possible single-glitch degradations of a given PV array by use of the following observation: the entire first quadrant I-V curve of a single-glitch, degraded array may be uniquely represented by the location of its glitch point. Thus, a given point in the I-V plane can be used to represent an array whose degraded I-V curve has its single-glitch at that point. In Fig. 9-36, the annual available energy of each of 64 degraded arrays was mapped against the location in the I-V plane of the glitch point of the array at SOC, and from these points a contour plot of the annual available energy was

made. Each contour shows the glitch points of the set of degradations that result in equal energy collection from the array by an ideal, unlimited-range, maximum-power-point tracker. The undegraded I-V curve of the array is indicated by the bold I-V curve drawn onto Fig. 9-36. The glitch points of the degraded I-V curves simulated span the region enclosed by the dashed line.

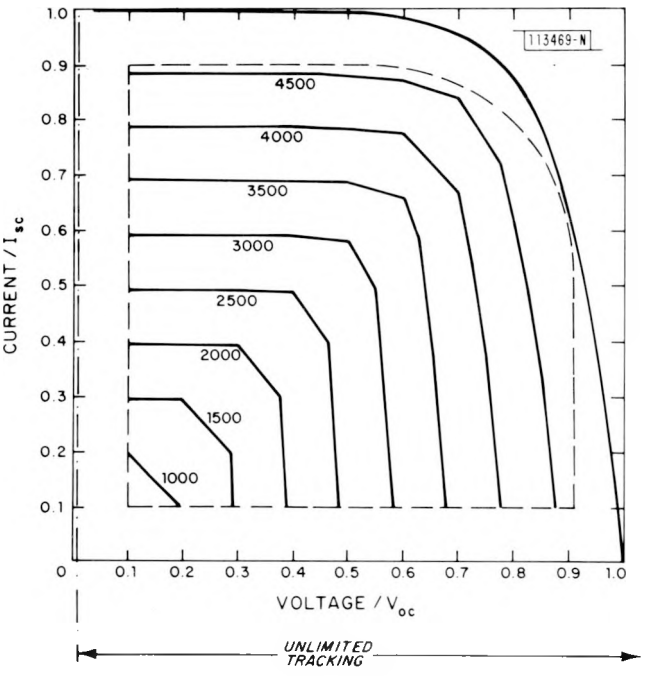

Fig. 9-36. Total available energy from single-glitch I-V curves plotted at the glitch-point location in the I-V plane. Glitch points with equal available energy are connected by the contours shown.

The annual energy lost by any single-glitch I-V curve can readily be determined by simply normalizing its I_{sc} and V_{oc} to the scale of Fig. 9-36 and reading off the loss at the location of the glitch point. For example, if the I-V curves of Fig. 9-35 were laid over Fig. 9-36 and their axes matched, the annual available energy from curves A, B and C could be determined directly from the contour map at the I-V curve glitch point. Accordingly, the total available energy in Boston from an array with the I-V curve A (Fig. 9-35) is 3550 kWh, from an array with curve B, 3100 kWh, and from an array with curve C, 4400 kWh. Curve B is the worst of the degradations shown. With unlimited-range,

maximum-power-point tracking, it can be seen that the worst glitches are those that eliminate the greatest area from under the undegraded I-V curve.

To determine the effect of control strategy on energy loss, simulations were run with a fixed-voltage inverter set to the BFV of 0.8 x V_{oc}; the resulting system collected 5010 kWh from the undegraded array. Figure 9-37 shows the annual energy that will be collected from the array if it is operated at the BFV under any single-glitch state of degradation. The annual energy from each simulated system was mapped against the location of the glitch point in the I-V plane and from these points the contour plot was made. As was the case above, the percent energy loss for any given single-glitch I-V curve can be determined directly by simply normalizing its I_{sc} and V_{oc} to the scales of Fig. 9-37, then reading off the percentage loss at the glitch-point location. If, for example, the I-V curves of Fig. 9-35 were used, it could be seen that curve A results in a fixed-voltage energy output of 3500 kWh, curve B results in an energy output of 1500 kWh, and curve C results in an energy output of 3500 kWh.

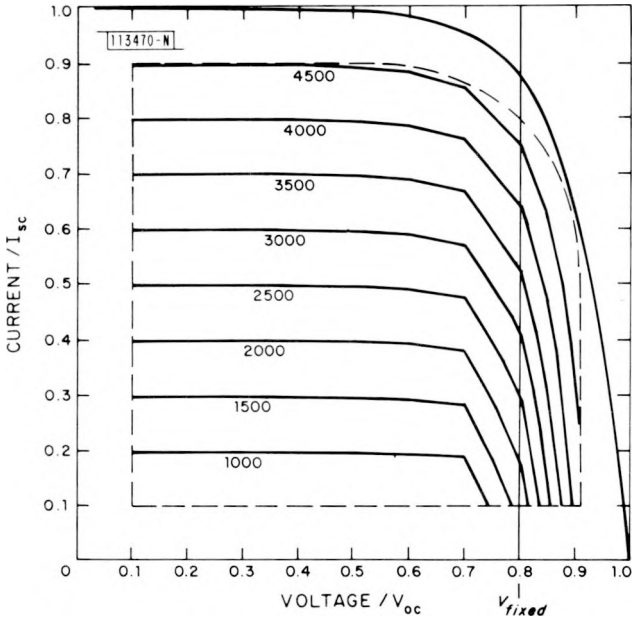

Fig. 9-37. Total energy collected by operating an array with single-glitch degradation at the BFV of the undegraded array.

To assess the importance of maximum-power-point tracking degraded arrays, the information in Figs. 9-36 and 9-37 is combined in Fig. 9-38 to show the percentage of the available energy lost with fixed-voltage operation. This energy loss, PL, is computed according to the formula:

$$PL = \frac{E_{\text{max power}} - E_{\text{fixed V}}}{E_{\text{max power}}} \times 100\%$$

where $E_{\text{max power}}$ is the energy collected from the degraded array with ideal maximum-power-point tracking and $E_{\text{fixed V}}$ is the energy collected at the BFV of the undegraded array. For each simulated system, PL was mapped against the location in the I-V plane of the glitch point of the array, and from these points a contour plot of PL was made. With the undegraded curve, 1.6% of the available energy is lost with fixed-voltage operation. By using the I-V curves of Fig. 9-35, it can be seen that less than 3% of the available energy is lost through fixed-voltage operation on curve A, about 52% on curve B, and about 21% on curve C. A large set of degradations exists which results in an energy loss of less than 3% for fixed-voltage operation. These degradations include curve A of Fig. 9-35 and any other degradation for which the glitch-point lies outside the 3% contour of Fig. 9-38. Figure 9-39 shows the percent energy loss with fixed-voltage operation at the undegraded systems BFV relative to the energy collected with the limited-range, maximum-power-point tracking to which real PV systems are limited. Again, the percent energy loss is plotted at the array's I-V-curve glitch point. It is clear from these figures that limiting the range of the voltage tracking to which fixed-voltage operation is compared decreases the number and variety of array degradations that handicap fixed-voltage operation.

The above contour plots and others given in Reference 28 make possible the estimation of the energy losses after array degradation due to various dc-operating-point control strategies. The glitch-point coordinates of the I-V curve of any degraded array can be determined as a fraction of V_{oc} and I_{sc}, and the resulting energy loss with different operating strategies can be assessed. Several design examples are given in Reference 28.

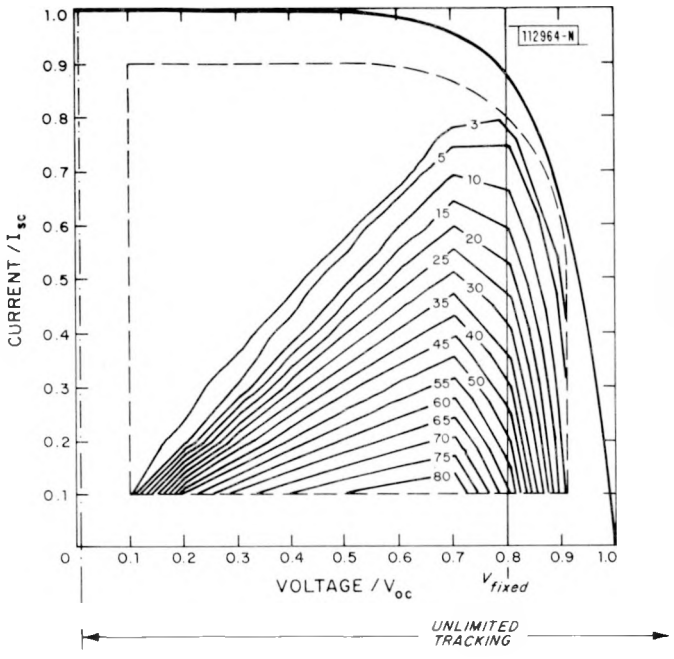

Fig. 9-38. Percent of available energy lost (PL) with operation at the undegraded array's BFV relative to unlimited range maximum-power-point tracking.

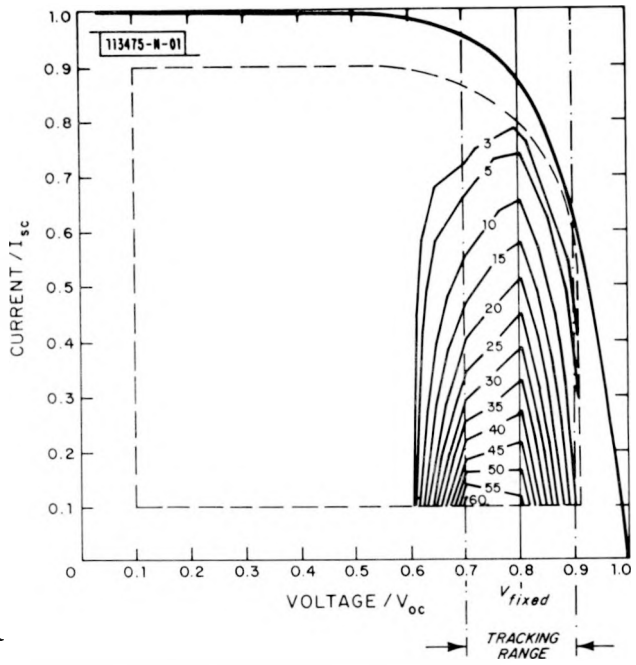

Fig. 9-39. Percent of available energy lost (PL) with operation at the undegraded array's BFV relative to maximum-power-point tracking over the range indicated.

Most failures for which Fig. 9-38 shows a large energy collection advantage for maximum-power-point tracking over fixed-voltage operation are actually severe degradations that cut sharply into the total available energy from the array. To emphasize this, the contours of Fig. 9-36 were rescaled and the results shown in Fig. 9-40. This figure shows the percentage of the available energy of the healthy array which could be collected with an ideal maximum-power-point tracker operating on the degraded arrays. Except for remote-site applications, fault detection and repairs are likely on any array delivering less than 80% of the energy it would have delivered when new and healthy. Comparison of the 20% degradation loss contour of Fig. 9-40 with the additional fixed-voltage loss of available energy shown in Fig. 9-38 shows that most of the degradations that disadvantage fixed-voltage operation would probably be quickly repaired.

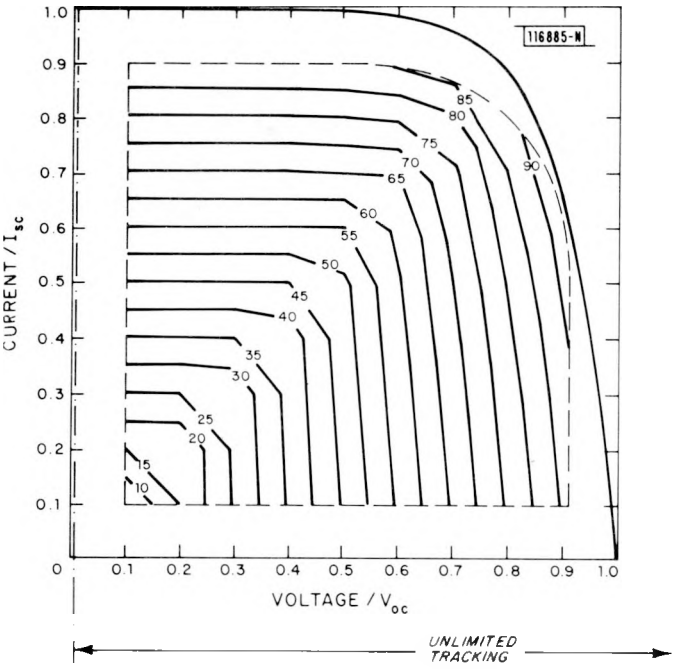

Fig. 9-40. Percent of available energy of the undegraded array which could be collected with an ideal maximum-power-point tracker operating on degraded arrays.

A final caution about maximum-power-point tracking must be made: there are no commercial PV maximum-power-point trackers capable of operating on glitched I-V curves as reliably as does the tracker of this simulation. Existing trackers are generally "satisfied" to find a single local maximum in the power-versus-voltage curve; they do not compare the power at the two peaks of a glitched curve to be certain to operate on the larger peak. The probable failure of real trackers to get all the available energy from degraded arrays reduces still further their presumed advantage over fixed-voltage operation on degraded arrays.

9.4.4 Conclusions

Given a reasonable array-wiring design, periodic I-V curve testing, effective maintenance, and avoidance of regular serious shadowing, there is no reason why considerations of degradation should force the adoption of

maximum-power-point tracking on a PV system that would otherwise operate economically at fixed voltage. If, however, shadowing will be severe, frequent I-V curve tracing forgone, and little maintenance expected, maximum-power-point tracking of the array is advisable.

9.5 Development of Codes and Standards

9.5.1 Introduction

As is the case for any consumer product, PV power systems need to be defined in terms of codes and standards in order for them to be utilized routinely. Lincoln Laboratory, along with DOE's other principal contractors in the National Photovoltaic Program, participated in the development of such codes and standards in a variety of activities, all of which are summarized below.

Contributions to this effort were made by the following individuals: Steven E. Forman, David N. Klein, William H. MacLachlan, Ervin F. Lyon, Emanuel E. Landsman, Miles C. Russell and Thomas H. Warner.

9.5.2 Development of Interim Performance Criteria

During 1978, legislation passed by the Congress of the United States set funds for use in studying, developing and assisting in the commercialization of terrestrial PV systems. Part of this legislation mandated the development of performance criteria and standards as means to clarify the terminology used by the PV community and to provide guidance in the testing and evaluation of PV system components.

When the Solar Energy Research Institute (SERI) was established, part of its mission was to organize and lead a team of professionals from the PV community to develop Interim Performance Criteria (IPC) for Photovoltaic Energy Systems.

This team was tasked to identify, develop and promulgate performance criteria and test methods for PV solar energy conversion systems, and to enhance further the goals of the federal PV program by accelerating the commercialization of PV systems. The final performance criteria developed were to be used as the basis for standards development by voluntary consensus

standards organizations as well as to provide a common base for both manufacturers and purchasers to use in evaluating and characterizing performance traits of interest.

The work was divided into three parts and assigned in late 1978 to the following organizations:

Jet Propulsion Laboratory:	Array Subsystem
MIT Lincoln Laboratory:	Power Conditioning, Monitoring and Control, Storage and Cabling Subsystems
Sandia National Laboratories:	PV Systems.

Typically, performance criteria were segmented into three parts: 1) a criterion statement, 2) an evaluation statement, and 3) a commentary statement. The criterion statement qualitatively addressed the user need or expectation for a given element. It was a general statement of what the element would be able to do, and did not provide any levels of performance. The evaluation statement listed test methods and other information on which conformance with the criterion could be evaluated. The commentary statement provided the background and the rationale for the selection of the criterion and/or evaluation.

Each criterion, evaluation, and commentary statement was included under the following performance attributes:

- Electrical
- Thermal
- Mechanical/Structural
- Safety
- Durability/Reliability
- Installation, Operation and Maintenance
- Building/Site.

The end result of Lincoln Laboratory's work is contained in the document "Interim Performance Criteria for Photovoltaic Energy Systems,"SERI/TR-742-6541, published by SERI in December 1980. This document contains the final criterion, evaluation and commentary statements developed for each performance attribute as well as the names and affiliations of all contributors.

9.5.3 Development of IEEE Standards for PV Systems

Rationale for IEEE Standards

The main objective of IEEE is the advancement of the theory and practice of electrical engineering, electronics, radio, allied branches of engineering or related arts and standards. The issuing of technical standards is an important means by which IEEE can carry out its objectives.

Accordingly, the Photovoltaics Standards Coordinating Committee was established within the IEEE, and four subcommittees were created with the following interests:

Storage Systems

- Sizing of batteries for PV systems
- Installation and maintenance of battery systems for PV

Power Conditioning Devices

- Baseline PCU specification for small power producers
- Harmonics injection and measurements
- System sizing
- Grounding
- Assembly of PV guideline specs

Photovoltaic Systems

- Performance ratings, calculations, and criteria as related to power and energy
- Utility interface for residential and intermediate load applications

Cell/Array

- Fault-tolerant and fault-resistant designs of modules
- Recommended practice for measurement of the operational integrity of PV arrays in PV power generating systems
- Recommended practice for the location, removal and replacement of defective modules in PV generating systems.

Using the IPC document discussed in Section 9.5.2 as a baseline, members of the IEEE subcommittees proceeded to draft documentation according to the IEEE Standards Manual.

Lincoln Laboratory has provided inputs to Cell/Array and Photovoltaic Systems subgroups as follows:

Cell/Array: "Practice for Measurement of the Operational Integrity of PV Arrays in Photovoltaic Power Generating Systems" and "Practices for the Location, Removal and Replacement of Defective Modules in Photovoltaic Generating Systems," both by Dr. S. E. Forman.

Photovoltaic Systems: In the PV systems subgroup, Laboratory personnel participated in preparing the draft of "IEEE Standard for Terrestrial Photovoltaic System Power Test and Power Energy Performance Ratings." The basic purpose of this document is to provide a standard procedure for determining the achieved electrical power and energy performance of installed and operating flat-plate solar PV power systems.

9.5.4 Development of Underwriters Laboratories Standards for Inverters

In order to encourage the commercial acceptability of residential PV systems, the homeowner needs assurance of the safety of the system as well as the option of being able to purchase insurance protection for the system. For many home products, both these objectives are met by having them receive Underwriters Laboratories (UL) approval. In order for UL to approve a product, it must have on file an evaluation procedure, termed a "Standard for Safety", tailored relatively close to the product. Since no UL standard exists for residential PV inverters and since it normally requires several years to establish a standard, Lincoln Laboratory contracted with UL to initiate such activity. The work began with UL coming to Lincoln Laboratory to inspect inverters from two manufacturers. Based on this review, a draft standard was composed. Following revision, it was applied to an inverter from a third manufacturer to verify the completeness and appropriateness of its requirements. The draft standard will now follow the normal UL procedure for adoption of a standard: industry review, revision and issuance. With such a standard in place, inverter manufacturers will be able to submit their units for approval.

In addition to the UL safety standard, a collection of recommended test procedures for inverters has been written by Lincoln Laboratory. It provides

guidance as to what tests are appropriate for an inverter, but does not specify the degree of acceptability, or lack thereof, for the test results.

9.5.5 Revision to 1984 National Electric Code

The advent of the federal residential PV program brought with it the need for PV systems to comply with the National Electric Code (NEC) upon installation in residences. Since the 1981 NEC does not cover the unique characteristics of a PV system, it was necessary that a new chapter be developed to cover that subject for the NEC. Accordingly, Lincoln Laboratory contracted with UL to develop the needed chapter.

After several cycles of internal review, a document, "Article 690--Solar Photovoltaic Systems" (Draft - August 1981), was provided for further review by other organizations involved in the PV Program prior to its anticipated publication in September 1983.

9.5.6 Development of Safety Inspection Guidelines for PV Residences

Until "Article 690--Solar Photovoltaic Systems" is published in September 1983, there will be no formal code which deals strictly with solar PV installations. Since it is anticipated that a number of private residences will be equipped with PV power-generating systems, a means must be provided by which a qualified individual can assess these systems prior to, during, or after installation in order to ensure that proper precautions have been taken to mitigate any potential safety hazards.

Accordingly, Lincoln Laboratory under contract to SERI, developed interim safety-inspection guidelines for assessing the safety of a residential PV system until more formal documentation is available from code-generating groups.

A first draft of "Safety Inspection Guidelines for Photovoltaic Residences," written by Dr. Steven Forman and David Klein, was provided to UL and the International Association of Electrical Inspectors in December 1981. Their comments were incorporated in a second draft which was sent to individuals for review in early February 1982. Subsequently, the proposed Article 690 was released in the NFDA Technical Committee Report for comment prior to the May 1983 NFDA meeting where final balloting will take place.

REFERENCES

Section 9.1.2

1. Dinwoodie, T. L., "Residential Photovoltaic Worth: A Summary Assessment of the MIT Energy Laboratory," MIT Energy Laboratory Report No. MIT-EL-82-005.
2. Kern, E. C., Jr., and Russell, M. C., "Hybrid Photovoltaic/Thermal Solar Energy Systems," MIT Lincoln Laboratory Technical Report, 27 March 1978, COO-4577-1.
3. Russell, M. C., "Solar Photovoltaic/Thermal Residential Systems," MIT Lincoln Laboratory Technical Report, 28 December 1979, COO-4577-9.
4. Dinwoodie, T. L., and Kavanaugh, J. P., "Cost Goals for a Residential Photovoltaic/Thermal Liquid Collector System Set in Three Northern Locations," MIT Energy Laboratory Report No. MIT-EL-80-028.
5. Cox, C. H., III, "Residential Photovoltaic Systems Costs," 15th Intersociety Energy Conversion Engineering Conference, Seattle, WA, 18-22 August 1980, DOE/ET/20279-96.

Section 9.2.2

6. Katzman, M. T. and A. C., "Economic and Financial Analysis of Residential Photovoltaic Systems: The Impact of Solar Photovoltaics on Utilities - Final Report," under subcontract to MIT Lincoln Laboratory, February 1982, DOE/ET/20279-185.

Section 9.2.3

7. Fitzer, J., Dillon, W. E., Rojas-Negrete, C. R., Chen, B-K., "Impact of Residential Utility-Interactive PV Power Systems on the Utility," prepared by University of Texas at Arlington under contract to MIT Lincoln Laboratory, August 1982, DOE/ET/20279-222.
8. Shelton, P. S., Solman, F. J., and Nichols, B. E., "Effect on the Utility Feeder of Utility-Interactive Inverters at the Northeast Residential Experiment Station," MIT Lincoln Laboratory Technical Report, August 1982, DOE/ET/20279-221.
9. Landsman, E. E., "Analysis and Test of Line-Commutated Inverters for Use in Photovoltaic Power Systems," MIT Lincoln Laboratory Technical Report, February 1981, DOE/ET/20279-115.
10. Landsman, E. E., and Rasmussen, N. E., and Cox, C. H., III, "A DC to AC Inverter Based on Waveshaping," MIT Lincoln Laboratory Technical Report, June 1982, DOE/ET/20279-191.
11. Landsman, E. E., "Loss of Line Shutdown for a Line-Commutated Utility-Interactive Inverter," MIT Lincoln Laboratory Energy Systems Engineering Technical Note, March 1981, DOE/ET/20279-128.

References (con't)

Section 9.3

12. Russell, M. C., "Photovoltaic/Thermal Residential System Designs," MIT Lincoln Laboratory Technical Report, December 1979, COO-4577-9.

13. Sheldon, D. B., and Frank, S. M., "Retrofitting Residences with Photovoltaic/Thermal Collector Systems," presented at the 16th Intersociety Energy Conversion Engineering Conference, Atlanta, GA, 9-14 August 1981, DOE/ET/20279-131.

14. Klein, S. A., et al., "TRNSYS--A Transient System Simulation User's Manual," University of Wisconsin-Madison, 1979, Engineering Experiment Station Report No. 38-10.

15. Hart, G. W. and Raghuraman, P. "Residential Photovoltaic System Simulation: Thermal Aspects," Proceedings of the ASME Solar Energy Division Fourth Annual Technical Conference, Albuquerque, NM, DOE/ET/20279-183.

16. Hart G. W., "Residential Photovoltaic System Simulation: Electrical Aspects," MIT Lincoln Laboratory Technical Report, June 1982, DOE/ET/20279-207.

17. Stultz, J. W. and Wen, L. C., "Thermal Performance Testing and Analysis of Photovoltaic Modules in Natural Sunlight," Jet Propulsion Laboratory, California Institute of Technology, 29 July 1977, LSSA Project Task Report 5101-31.

18. Luft, W., Barton, J. R. and Conn, A. A., "Multifaceted Solar Array Performance Determination," TRW Systems Group, Redondo Beach, CA, February 1967.

19. Jet Propulsion Laboratory, Solar Cell Array Design Handbook, Vol. 1, Section 9.2, reproduced by U.S. National Technical Information Service, U.S. Department of Commerce, Springfield, VA, N77-14193.

20. Hart, G. W., "The Effect of Data Sampling Rate on Utility Interaction Calculations," MIT Lincoln Laboratory Technical Report, October 1982, DOE/ET/20279-212.

21. Bucciarelli, L. L. and Grossman, B. L., "A Comparison of Two Techniques for the Simulation of PV Systems," Proceedings of the 2nd Annual Systems Simulations and Economics Analysis Conference, San Diego, CA, 23-25 January 1980, COO-4094-72.

22. Hart, G. W., and Raghuraman, P., "Simulation of Thermal Aspects of Residential Photovoltaic Systems," MIT Lincoln Laboratory Technical Report, June 1982, DOE/ET/20279-202.

23. Hart, G. W., and Raghuraman, P., "Residential Photovoltaic System Simulation; Thermal Aspects," Proceedings of ASME Solar Energy Division Fourth Annual Technical Conference, Albuquerque, NM, April 26-30, 1982, DOE/ET/20279-183.

References (con't)

24. Hart, G. W., and Raghuraman, P., "Electrical Aspects of PV System Simulation," MIT Lincoln Laboratory Technical Report, June 1982, DOE/ET/20279-207.

25. Hart, G. W., "Residential PV System Simulation: Electrical Aspects," Proceedings of 16th IEEE Photovoltaic Specialists Conference, San Diego, CA, September 28-October 1, 1982, DOE/ET/20279-233.

26. Luft, W., Barton, J. R., and Conn, A. A., "Multifaceted Solar Array Performance Determination," TRW Systems Group, Redondo Beach, CA, February, 1967.

27. Jet Propulsion Laboratory, Solar Cell Array Design Handbook, Volume 1, Section 9.2, reproduced by National Technical Information Service, U.S. Department of Commerce, Springfield, VA, #N77-14193.

Section 9.4

28.. Branz, H. M., Hart, G. W. and Cox, C. H., III, "The Photovoltaic Array/Power Conditioner Interface," MIT Lincoln Laboratory Technical Report, August 1982, DOE/ET/20279-170.

29. University of Wisconsin, Solar Energy Laboratory, "TRNSYS a Transient Simulation Program," June 1979.

30. National Oceanic and Atmospheric Administration, National Climatic Center, "SOLMET User's Manual and Final Report," Volumes 1 and 2, No. TD-9724, February 1979.

31. National Oceanic and Atmospheric Administration, National Climatic Center, "Typical Meteorological Year User's Manual," May 1981, No. TD-9734.

32. Stultz, J. W. and Wen, L. C., "Thermal Performance Testing and Analysis of Photovoltaic Modules in Natural Sunlight," 29 July 1981, JPL LSSA Project Task Report 5101-31.

33. Luft, W, Barton, J. R. and Conn, A., "Multifaceted Solar Array Performance Determination," TRW Systems Group, Redondo Beach, CA, February 1967.

34. Sandstrom, J. D., "A Method for Predicting Solar Cell Current-Voltage Curve Characteristics as a Function of Incident Solar Intensity and Cell Temperature," Sixth Photovoltaic Specialists' Conference, Vol. I., pp. 199, March 1967.

35. Forman, S. E., "Using Measurements to Detect Electrical Problems In Operational Photovoltaic Arrays," SERI Commerical Photovoltaic Workshop, Vail, CO, 27-29 July 1981, DOE/ET/20279-149.

10.0 RESIDENTIAL PV TECHNOLOGY DEVELOPMENT

10.1 Introduction

In this section, Lincoln Laboratory's efforts in developing new components for residential PV systems are summarized. The activity is concerned with three major elements of a residential PV system: (1) the PV cells, modules, array and integration with the roof of a residence, (2) the dc-to-ac inverter and associated system-control and utility-interconnection equipment, and (3) on-site storage. With regard to PV arrays, summaries are given of development of PV cells which contain built-in bypass diodes. Also, the development of combined PV/thermal collectors and solar cells is discussed. Finally, the various types of roof-mounting techniques possible for residential PV applications are summarized.

The inverter effort includes evaluation of residential inverters available from industry, as well as a summary of development of the so-called waveshaping inverter.

In the category of storage, the Laboratory's work relating to development of a flywheel storage system is summarized.

As was the case in the systems studies previously discussed, there are many other organizations involved in the development of PV components for residential and other applications. In the storage area, the reader is referred to DOE's Division of Energy Storage and to the Lawrence Livermore Laboratory, who co-sponsored the Lincoln Laboratory flywheel effort, along with the DOE PV Program. Sandia National Laboratories, Albuquerque, should be contacted for additional information on development of inverters and on overall residential-PV-system designs. The Jet Propulsion Laboratory has a large DOE-funded program under way concerned with the development of low-cost PV modules for residential and other applications.

10.2 Development of PV Cells with Self-Contained Bypass Diodes

10.2.1 Background Information

The PV modules used for residential and other multikilowatt applications consist of series strings of individual cells, an example of which is shown in

Fig. 10-1a. The operating point of each cell is determined by the intersection of the string current, I_o, and the cell's I-V curve. As shown in Fig. 10-1b, in a fully operational array this intersection occurs in the first, or power-producing, quadrant. It is common during array operation for the short-circuit current, I_{sc}, and consequently the entire I-V curve of an individual cell, to be reduced. This can occur on a temporary basis in the case of shadowing of the cell; on a moderate-term basis, when dirt accumulates between washings; or on a permanent basis, when cells crack. In any of these cases, the cell operating point will still be the intersection of the string current and the cell's I-V curve. However, when I_{sc} is less than I_o, the intersection will be in the second, or power-dissipating, quadrant, as is also shown in Fig. 10-1b. The reverse breakdown voltage, V_{br}, of a PV cell is rarely a controlled parameter, but it is usually in the range of -15 to -50 V. For string currents on the order of 1 A, this implies a power dissipation of 15 to 50 W*. Under normal conditions, the defective cell region would need to dissipate less than 10 W, assuming a 10% PV-area efficiency. The occurrence of excess power dissipation was termed "hot spot" heating by Blake and Hanson (1) when they first reported it. The result of the excess heating generally is outgassing of the encapsulant and/or breaking of the cover glass (2). For a more complete discussion of the work summarized below, see Reference 3.

C74-2165

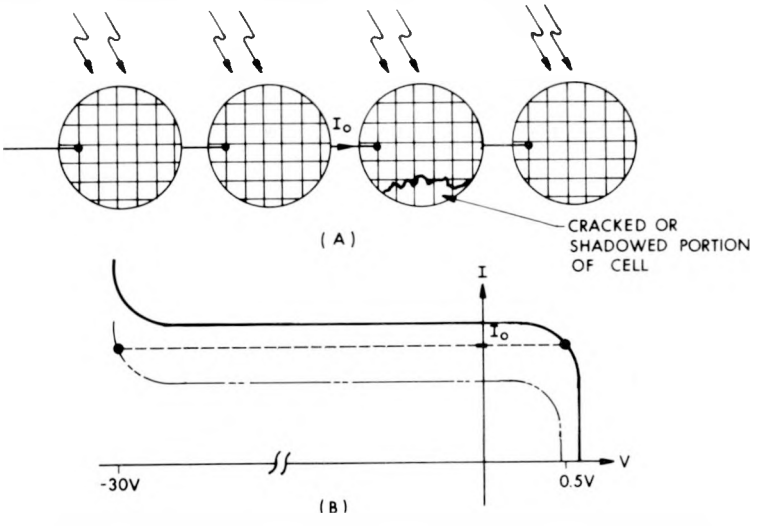

Fig. 10-1. (a) Series-connected string of PV cells operating at current I_o; (b) intersection of constant current I_o with I-V curve of full (solid) and defective (dash-dot) cells.

*This translates to 6 to 20 times the thermal dissipation during normal operation of an undegraded cell.

The common approach to limiting excess power dissipation has been to reduce the cell reverse breakdown voltage, V_{br}. To do this without reducing the cell's efficiency requires a device with low reverse conductance and high forward conductance. A diode, connected in antiparallel to the cell, meets these criteria. At present it is generally not feasible to place such a bypass diode around every cell within a module; consequently, groups of cells or even whole modules are bypassed with a single diode (4). In other cases where bypassing of individual cells has been provided, the cost considerations have been discouraging. Diamond (5), for example, proposed an "integral" diode that is basically a conventional PV cell onto which a separate diode chip has been bonded in the fashion of a hybrid integrated circuit. Giuliano et al. (6) discuss a similar approach, except that the diode chip is placed on the back of the PV cell.

Beyond cost, there is a more fundamental limitation to these approaches: all the protection is contained at a single location rather than distributed throughout the PV cell. Therefore, if the bypass diode becomes inoperative--for example, because of a break in its interconnect--all protection to the cell is lost. Ideally the protection should be distributed throughout the cell and implemented in a manner that is still operational even after the cell becomes damaged, since this is when protection will be needed. In addition, the method should not reduce cell efficiency and should require only a minimum of additional processing steps.

The approach pursued below is to divide the cell wafer into two regions: a main area for the PV cell and an auxiliary area for the bypass diode. Locating the bypass diode around the periphery of the wafer, as shown in Fig. 10-2, results in distributing both the bypass protection and the power dissipation. The potential impact on cell efficiency comes in two ways: reduction of the PV-cell area and reduction of the bypass-diode-leakage current. The sacrifice in active area need not be significant (1 to 2%). The limiting factors are the current density through the bypass diode and the resolution of the process by which the isolation between the two regions is made.

With previous approaches using discrete or chip diodes, the PV cell's reverse breakdown has been limited to approximately 0.6 V. Based on the reasoning given in Reference 3, limiting the reverse breakdown to between 2 to 3 V should be sufficient.

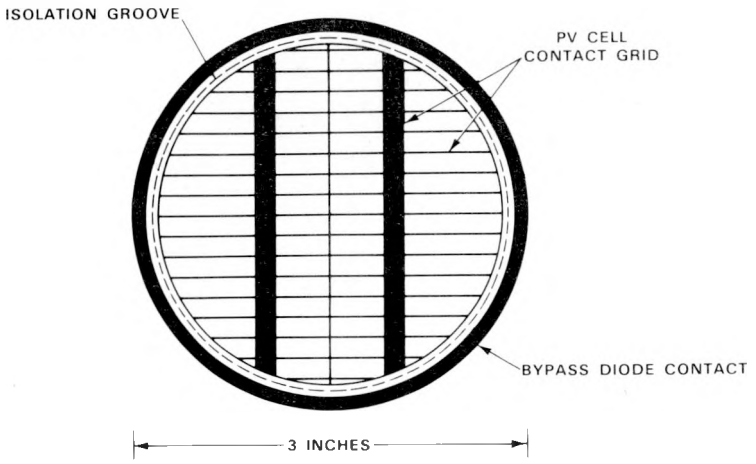

Fig. 10-2. Layout of wafer including peripheral-diode region isolated from central PV-cell region. (The bypass-diode contact is shown in expanded scale for illustration.)

Two methods for implementing the peripheral-bypass diode will be discussed. The first uses a standard diode; the second a backward diode. The standard diode approach requires only one low-resolution isolation step but adds to the interconnect complexity. The backward diode requires an additional doping step while permitting normal interconnections to be used.

Contributions to this effort were made by the following individuals: Charles H. Cox, III, Robert W. Mountain and Donald J. Silversmith.

10.2.2 Utilization of a Standard Diode

An edge view of a PV cell augmented by a standard diode to provide the bypass protection is shown in Fig. 10-3a. For specificity, a p-on-n cell is shown, but all the following holds equally well for the reverse polarity. At the start of processing, the isolation groove is not present. Fabrication of the PV cell proceeds as usual with the p+ doping on the entire front of the wafer. Metallization, using a pattern modified to include the peripheral-diode contact, and AR coating if desired, also proceed as usual. Finally, the peripheral diode is isolated from the central PV area by an isolation-groove etch between the PV cell and the peripheral diode. The two principal requirements for the isolation groove are that it be deep enough to cut through the p+ dopant and that it produce a minimum of junction damage. High resolution

is not required. Hence the isolation can be achieved during the same etching process that is often used to remove the degenerate junction around the edge of the wafer.

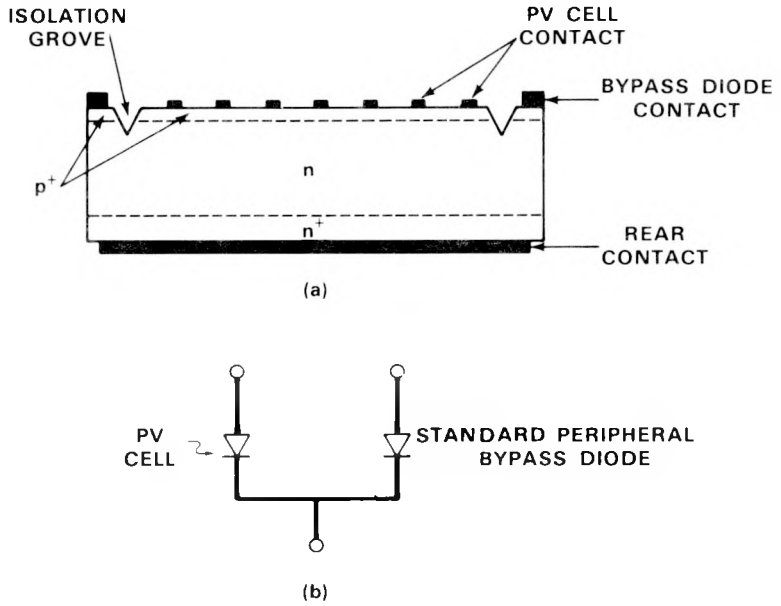

Fig. 10-3. (a) Edge view and (b) schematic of PV cell with a standard diode in the peripheral location for bypass protection.

Schematically, the wafer can be represented as shown in Fig. 10-3b. Since the bypass diode was produced by the same process that produced the PV cell, both diodes have the same reverse breakdown. When the PV portions of several wafers are wired in series, as shown in Fig. 10-4a, achieving low V_{br} will require connecting the bypass diode in antiparallel with the PV cell. The problem in doing this is the common cathode connection provided internally by the n+ back surface field region. Even if one were to groove-etch through the n+ region, the bulk n- region would still provide a shorting connection on the order of < 10 ohms.

An alternative is to use the peripheral diode located on one cell to provide protection for the next cell in the series string, as indicated in Fig. 10-4b. Thus, simplifying the cell processing has forced a slight additional complexity of interconnection.

A measured I-V curve from one of the cells is shown in Figs. 10-5a and b. Illumination at Air Mass 1 was not available, hence all measured curves were

made with a source approximately 0.02 AM1. Reverse breakdown is seen to be at about -15 V. Connecting the peripheral diode of one cell across the succeeding cell produced the I-V curves shown in Figs. 10-6a and b. The short-circuit current of the combination was unchanged from that of the PV cell itself. The V_{br} of the combination is $\sim$0.6 V, about a factor of 4 below the minimum V_{br} voltage discussed above and about a factor of 30 below the non-bypassed PV cell.

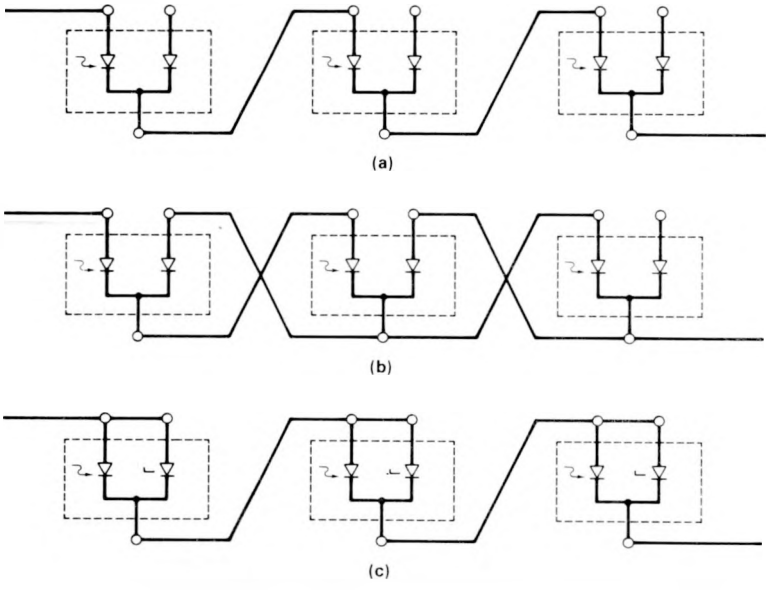

Fig. 10-4. Series interconnection of PV cells: (a) without bypass protection, (b) with standard diode and (c) with backward diode bypass protection.

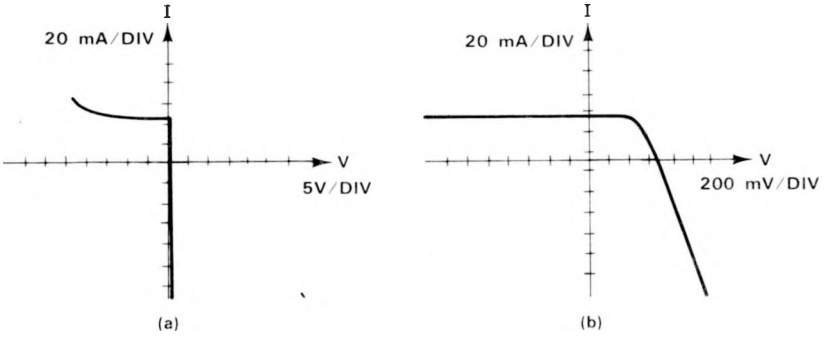

Fig. 10-5. I-V curve of PV cell without bypass protection emphasizing (a) reverse breakdown and (b) forward-conduction regions.

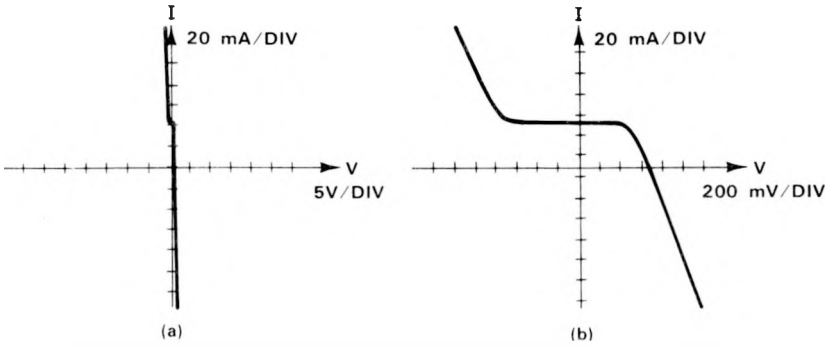

Fig. 10-6. I-V curve of PV cell with standard diode-bypass protection at (a) full and (b) expanded scales.

10.2.3. Utilization of a Backward Diode

Although the standard diode-protection scheme uses a simple wafer-fabrication process, the difficulty of a complex interconnection method remains. Thus, a means was sought for providing the desired protection through the reverse conduction of a parallel-connected diode. As was indicated by the discussion in Section 10.2.1, a reverse breakdown voltage of 2 to 3 V is required.

Figure 10-7 shows a comparison of the I-V curves of three types of diodes. The curves are plotted using the current-polarity convention normally used for PV cells. With breakdown voltages greater than about 6 V, the dominating mechanism for current conduction is avalanche multiplication. For low to moderate doping concentrations in the range 10^{15} to 10^{18} impurities/cm^3 (low doping side of junction), conventional diodes exhibit the sharp breakdown shown by the dashed line in the figure. Increasing the doping concentration to, say, $10^{19}/cm^3$ reduces the breakdown to a few volts but the predominant current-conduction mechanism becomes quantum-mechanical tunneling. The backward diode, shown by the solid curve, is an example of such a diode; it is commonly used as a low-level RF detector and mixer (see, for example, Reference 7). Increasing the doping concentration still further, until both sides of the junction are just degenerated, results in an Esaki, or tunnel, diode (dash-dot curve in the figure). Tunneling is still the dominant current mechanism, but the minimum voltage at which tunneling begins is actually

around 0.1 to 0.2 V positive (see, for example, Reference 8). For the purposes of PV-cell-bypass protection, a peripheral diode with the I-V curve of a backward diode would be satisfactory.

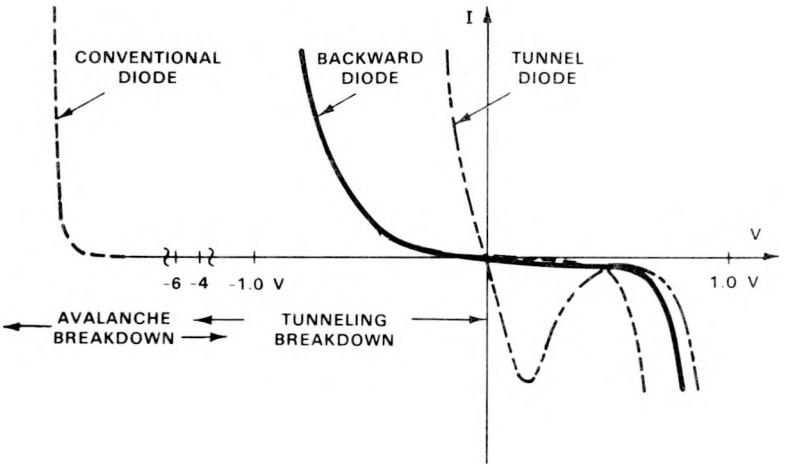

Fig. 10-7. Comparison of I-V curves for conventional (dashed), backward (solid) and tunnel (dash-dot) diodes.

The two principal constraints for producing a good backward diode are an abrupt junction and an appropriate doping density. For the calculations, a one-sided abrupt junction was assumed.

As developed in Reference 3, for a 3-in. wafer, a tunnel current density between 0.1 and 1 A/cm^2 and reverse breakdown voltage in the range 1 to 3 V result in a doping density in the range 1-2 x $10^{19}/cm^3$ on the lightly doped side. The other side should have approximately an order of magnitude greater doping density, as is typical of abruptly doped layers.

Wafers used for PV-cell fabrication usually have low resistivity (e.g., less than 10 Ω cm, and doping of about $10^{15}/cm^3$). Using wafers of lower resistivity and hence higher background doping would result in narrower depletion widths, thereby reducing cell efficiency. Thus, to achieve the doping density required for the backward diode will require adding an additional "buried" layer. An edge view of the resulting structure is shown in Fig. 10-8a. For processing reasons, this cell is shown as an n-on-p design, the opposite of the layout used for the conventional cell. The n+ layer above the PV portion

and the n++ layer above the peripheral diode could be the same and hence applied in the same step. The junction between the n++ and the p+ regions in the peripheral region needs to be abrupt. Consequently a process capable of producing such junctions, for example, ion implantation, must be used.

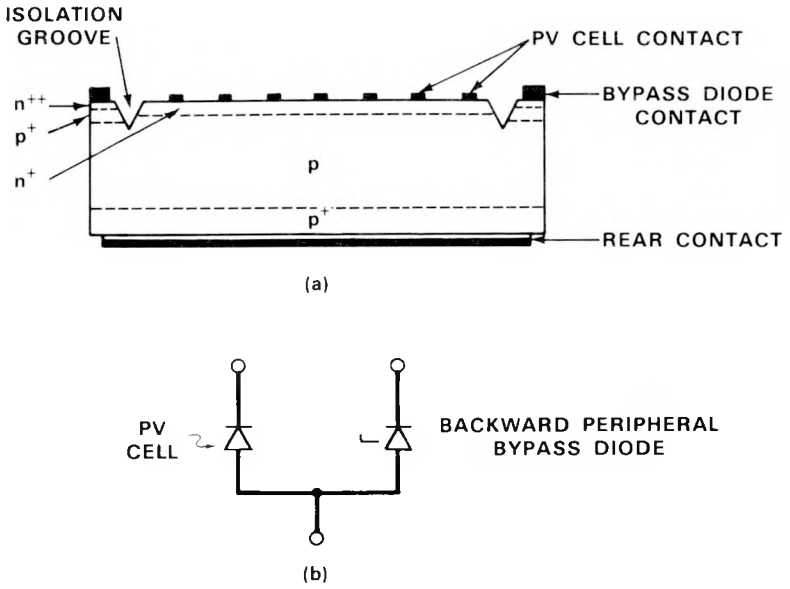

Fig. 10-8. (a) Edge view and (b) schematic of PV cell with a backward diode in the peripheral location for bypass protection.

The schematic representation of the wafer is shown in Fig. 10-8b. With the low reverse breakdown of the backward diode, its cathode may be tied directly to the cathode of the PV cell. The series interconnection of a PV cell with backward-diode protection is therefore identical to the interconnection of regular, unprotected PV cells as shown in Figs. 10-4c and 4a, respectively.

All of the implantation schedules were determined using the SUPREM model developed at Stanford University. The requirements for high doping levels and an abrupt junction force utilization of the model in a domain that is at or beyond its capabilities. If the resulting doping densities err on the high side, a tunnel diode will be made, causing an undesirable shunting of some of the photogenerated current. Therefore, the first processing run was a conservative one.

An I-V curve of a PV cell, with and without the first-cut backward diode connected, is shown in Fig. 10-9. Operation of the PV cell in the first quadrant is virtually unaffected by the addition of the backward diode. In fact an I-V curve of the backward diode itself indicated no forward tunneling current. Reverse breakdown of the PV cell alone was measured to be more than -150 V; the addition of the backward diode reduces the reverse breakdown to approximately -15 V. The predicted voltage for an abrupt junction with the desired doping level was about -2 V. Although the breakdown voltage of the experimental diode as fabricated was reduced by an order of magnitude, it is still higher than desired.

C74-2194

Fig. 10-9. I-V curve of PV cell with backward diode-bypass protection: (a) expanded scale indicating first-quadrant operation with and without the backward diode connected in parallel and (b) normal scale indicating reverse breakdown of the PV cell with and without the backward diode.

Work is in progress to characterize the doping profile that was obtained with the first-generation process. This information will permit the establishment of process modifications necessary to fabricate a backward diode with a breakdown in the 2-to-3-V range. Still the present results indicate that achieving a significantly lower reverse breakdown can be done with a simple additional implant. The complexities normally associated with fabrication of a "true" backward diode (in the RF sense) do not carry over to the present case because of the relatively loose requirement on reverse breakdown voltage.

10.2.4 Conclusions

Two methods for providing reliable, integrated, reverse bypass protection for PV cells were investigated. Both were based on locating a bypass diode around the periphery of the cell and both occupy neglible (1 to 2%) surface area. In one implementation, the forward conduction of a conventional diode, connected in antiparallel across the PV cell, provides the protection. In the other, the low reverse breakdown of a backward diode connected in parallel with the PV cell is the protective device. The conventional diode approach requires only a trivial addition (silicon-etch step) to the processing sequence, but additional interconnections between cells are needed. The backward diode uses standard interconnects but requires an additional doping step in the peripheral diode region as well as an isolation etch. The additional doping parameters were found to be significantly less critical than when fabricating such a diode for RF use.

10.3 Development of Combined Photovoltaic/Thermal Collectors

10.3.1 Background Information

At Lincoln Laboratory, a residential combined photovoltaic/thermal (PV/T) collector development program began in the fall of 1978 with a joint procurement, by Lincoln Laboratory and Sandia Laboratories, of three full-size prototype PV/T collectors. These early units served as a starting point for the eventual understanding and assessment of the PV/T collector concept. The collectors were tested for both thermal and electrical performance (11,12) and were analyzed (13,14) to gain a thorough understanding of collector operation under varying ambient environments. The results of testing indicated that the collectors were performing poorly, motivating the development of a second generation of PV/T units. Full details of this program are provided in Reference 15.

The second-generation PV/T units were of both air and liquid type and included production-ready designs, experimental designs, and a number of novel, proof-of-concept designs. Novel collector concepts included a two-phase Freon unit, an unglazed collector, and a dual-flow liquid unit, which provided for

direct cell-to-fluid contact both above and below the cells. In the process of the development work, two analytical models for flat-plate PV/T collectors were formulated and served as mainstays of the redesign work. One of the models simulated collectors that employ air as the transfer fluid, and the second simulated collectors that employ a liquid, such as one of the glycol mixtures or water, as the transfer fluid. In the process of developing the second-generation collector designs, a number of novel component concepts were also investigated. These included an evaluation of the viability of thermal-diode optical coatings and convection-suppression surfaces for use with, or in place of, the traditional glass collector cover plates. Photovoltaic cell/absorber plate combinations with a broadband, high-absorptance property were also studied and subsequently fabricated for use in both air and liquid collector units. A variety of transfer-fluid flow methods were investigated in a search for flow geometries with enhanced heat-transfer potential between the PV cells and circulating collector fluid.

Contributions to this effort were made by the following individuals: Joseph W. Chludzinski, Susan D. Hendrie, Edward C. Kern, Jr. Pattabiraman Raghuraman, Miles C. Russell and Duncan B. Sheldon.

10.3.2 The Early Photovoltaic/Thermal Units

The early PV/T collector units were procured by competitive bid under a DOE solicitation. Three designs were procured, with Sandia and Lincoln Laboratory each obtaining two collectors of each design for testing and evaluation.

The early PV/T units were fabricated by two PV module manufacturers--ARCO Solar, Inc. and Spectrolab, Inc.--and were based on two distinctly different design philosophies. ARCO, designing an air- and a liquid-type collector, chose to rely on the known manufacturing techniques of the solar thermal collector industry. The two ARCO PV/T collector designs were extensions of existing, commercially available air and liquid solar thermal collectors. The solar thermal units thus required only minor design changes to convert them to PV/T units. This method provided ARCO with thermal designs already optimized for cost and ease of manufacturing, which could, with little extra

effort, be put into volume production at a later date. ARCO chose Solaron Corporation's air-type thermal collector and Solargenics Incorporated's liquid-type thermal collector as starting bases, and ARCO installed their own commercially available PV cells for the two units.

Spectrolab, alternatively, chose to design its air-type PV/T collector from the start for the PV/T application. Both manufacturers used off-the-shelf components wherever possible.

The three collector designs are shown in Figs. 10-10 through 10-12. All employ one or two transparent top surface covers above the PV cells to provide a weather barrier and to minimize heat losses. A low-iron glass was used for this purpose in all of the designs except the ARCO air PV/T, which employed glass as an upper outside cover and a layer of Teflon fluorocarbon (FEP) film sheet as the inner cover surface. Both the low-iron glass and FEP cover sheet are designed for high transmission, each having transmissivities of 92% over the visible and infrared portions of the solar spectrum.

C74-1705

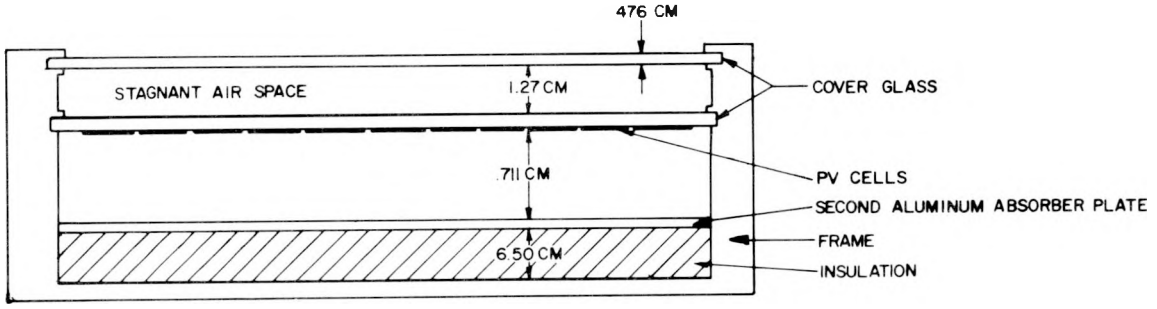

Fig. 10-10. Spectrolab air PV/T collector.

C74-1704

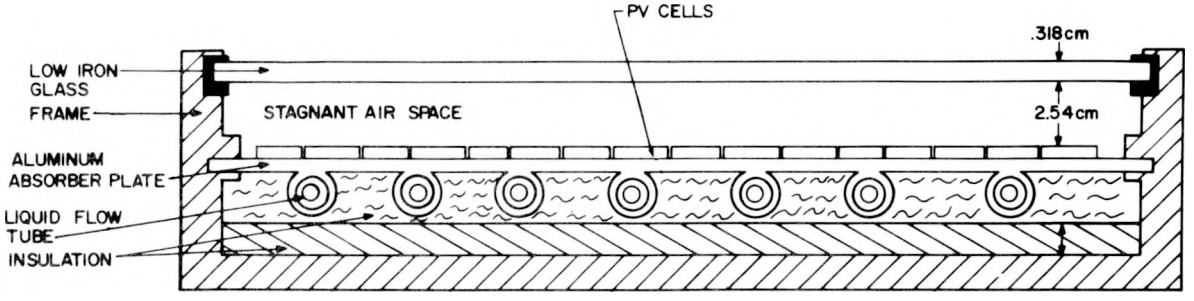

Fig. 10-11. ARCO liquid PV/T collector.

C74-1703

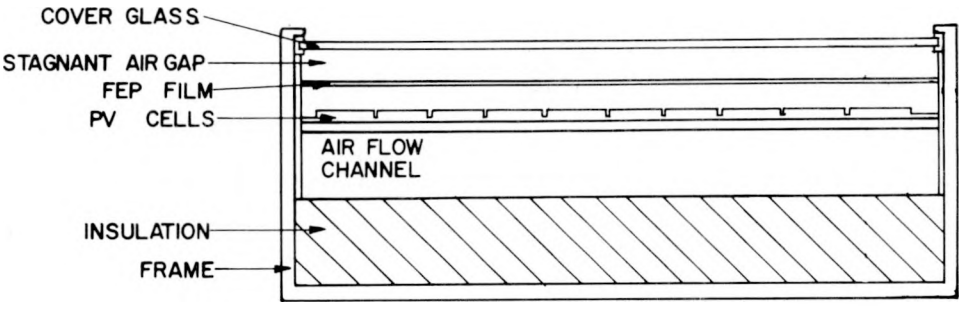

Fig. 10-12. ARCO air PV/T collector.

Early collector electrical characteristics are shown in Fig. 10-13. The results of collector thermal performance testing are presented in Figs. 10-14 and 10-15 for the ARCO liquid and Spectrolab air collectors. In the figures, collector thermal efficiency is plotted for collector operation with and without concurrent PV conversion at the maximum power point. The curves were generated numerically by a first order least squares fit to the measured data.

C74-892A

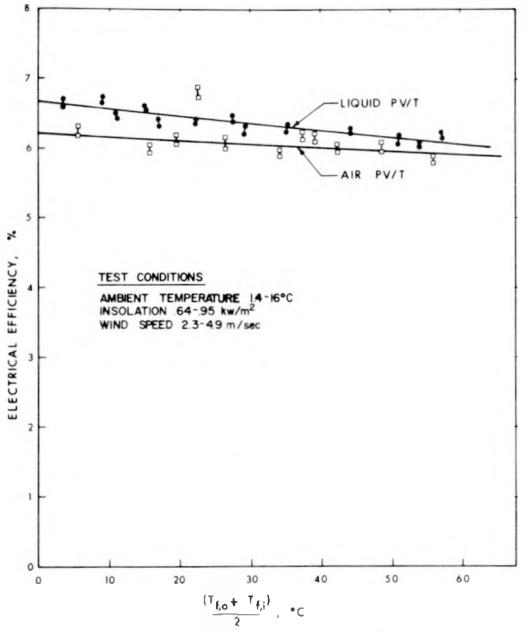

Fig. 10-13. ARCO liquid and Spectrolab air maximum power point PV/T electrical performance.

C74-491B

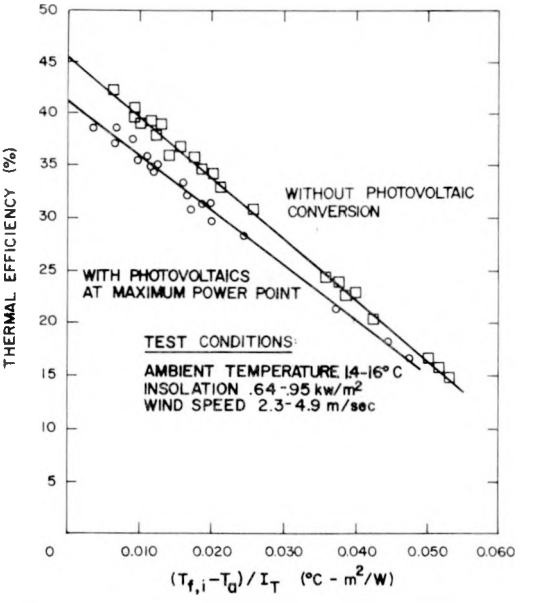

Fig. 10-14. ARCO liquid PV/T collector thermal performance.

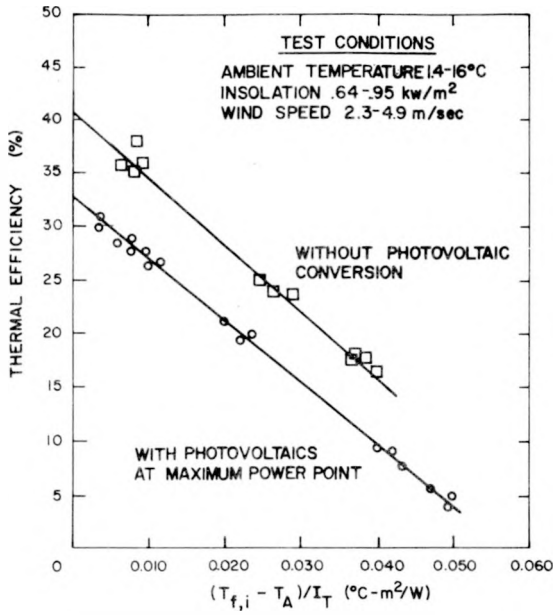

C74-495A

Fig. 10-15. Spectrolab air PV/T collector thermal performance.

After extensive testing in accordance with the ASHRAE 93-77 standards, the early PV/T collectors were seen to have PV conversion efficiencies comparable to the Block II PV modules*, on an area basis, and thermal efficiencies 30 to 40% below those for commercially available solar thermal collectors. Based on temperature-coefficient and loss-coefficient calculations, a number of areas where substantial performance improvements could be made were evident. Although at some fluid temperatures the electrical efficiencies of these early units were within the range of values seen for PV modules, at the estimated PV/T system NOCT operating conditions PV/T electrical efficiencies were a low 6.1 and 6.3%. In addition, newer, improved PV modules became available as a result of the aforementioned JPL Project, and, without further design improvements, the PV/T units would quickly fall well below the electrical performance of even the worst of the newer PV modules.

10.3.3 Development of Second-Generation Photovoltaic/Thermal Collectors

The second-generation PV/T collectors considered here fall into three categories. In the first category are experimental units, which showed

*The DOE/JPL Low-Cost Solar Array Project 1977 PV module procurement was Block II. This represented the state-of-the-art in PV module design in the United States at that time.

substantial promise, but were not yet ready to be field tested. These units were to be completed for laboratory testing and then reworked if the tests proved them viable. The second category includes production-ready collector units, which were ready for field tests and testing in a full-scale PV/T system. Upon successful testing in the field, the production units would then be ready for production and use in a residence. The final category of second-generation units consists of those collectors which illustrate novel concepts. These collectors were developed to test a single concept, without consideration as to how that concept would be integrated into a working unit. Upon successful testing, these novel concepts were next to be built into full-scale units as experimental collectors and then, in the final design phase, redesigned once more as production-ready units.

Two collectors were designed and fabricated as production-ready units and two as experimental units. It is not a coincidence that liquid-type units were chosen for the production-ready collectors, since long experience with this kind of unit in the solar thermal industry made available a wide range of tested design techniques and material components, all of which were well defined and documented. The experimental units were both of the air type, a workable though less frequently used alternative. The novel-concept designs investigated a new top glazing surface system, a new flow method for liquid-type collectors, and the use of a two-phase transfer fluid.

10.3.3.1 Production-Ready Collector Designs

Two liquid-type, production-ready collectors were fabricated for Lincoln Laboratory by the Spire Corporation, a PV module manufacturer. It was believed that a commercial PV manufacturer would build a collector employing assembly techniques which could be easily integrated into a production line. In addition, experience with various fabrication processes enabled Spire to choose reliable and field-tested components and assembly techniques for the collectors (see Fig. 10-16).

10.3.3.2 Experimental Photovoltaic/Thermal Collector Designs

Two experimental collectors were built, both using air as the transfer-fluid medium. The designs incorporated a broadband thermal absorptance method

C74-1675

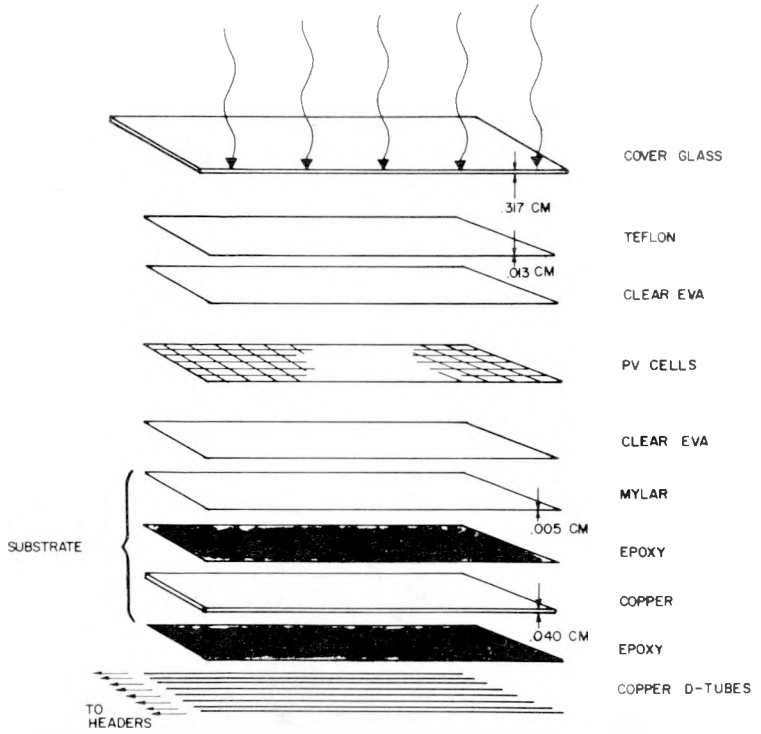

Fig. 10-16. Internal components of production collector designs.

and novel air-flow duct geometries. The basic dual glazing and absorber design which was used in the early Spectrolab air PV/T collector was used again, with alterations to accommodate the more complex flow-channel geometries.

10.3.3.3 Novel Collector Concept Designs

In the design of the experimental and production units, a number of new concepts came forth. These concepts, not ready to be integrated into full-scale units, were first built as subscale prototypes for testing. Three concepts were investigated: a two-phase PV/T collector unit, a dual-flow-path, direct-contact liquid unit, and an unglazed air PV/T collector which employed a heat diode film and gridded top surface in place of the traditional cover glass heat barrier.

10.3.3.4 Testing of Second-Generation Photovoltaic/Thermal Collectors

The full ASHRAE 93-77 test sequence was completed on the two production collectors. Results yielded ASHRAE thermal efficiency curves for operation

with maximum-power-point PV conversion under a variety of ambient conditions. Maximum-power-point electrical efficiency curves were also generated at these conditions and current-voltage curves were measured. Curtailment of Lincoln Laboratory's PV/T project prevented completion of much of the development activity. The experimental air-type collectors were never completely fabricated and hence were not tested as such. The two gridded-back cell/glass panels fabricated by Applied Solar Energy Corporation and by the Spire Corporation were completed, however, and current-voltage curves run for each. Numerical simulations of these units were employed to produce thermal and electrical efficiency curves for each.

Of the novel-concept designs, only the dual-flow liquid design was built and tested. The unglazed concept was studied in depth, but not completed as a design. The two-phase unit was built and assembled into a test loop, but testing was not completed.

The Lincoln Laboratory/Spire and Solar Design Associates/Spire production collector performance curves are shown in Figs. 10-17 and 10-18. The efficiency curves are the result of a linear least squares fit to data obtained while collectors were operating outdoors with concurrent thermal and maximum-power-point PV collection. From the Fig. 10-17 curves, maximum thermal efficiency values are 55% for the Lincoln Laboratory unit and 48.9% for the Solar Design Associates unit, indicating substantial improvement gains over the early ARCO liquid unit.

The lower electrical output of the Solar Design Associates unit reflects the smaller cell aperture area of this collector. The Lincoln Laboratory unit also benefits from the cell-texturing treatment, which further reduces surface reflection losses over the standard antireflection film coating.

The experimental air collector design cell/glass panels were tested outdoors, without accompanying collector housing. From computer simulations using the data, electrical efficiency curves for the two units were drawn, predicting the output of the full collector units (Fig. 10-19).

C74-1681

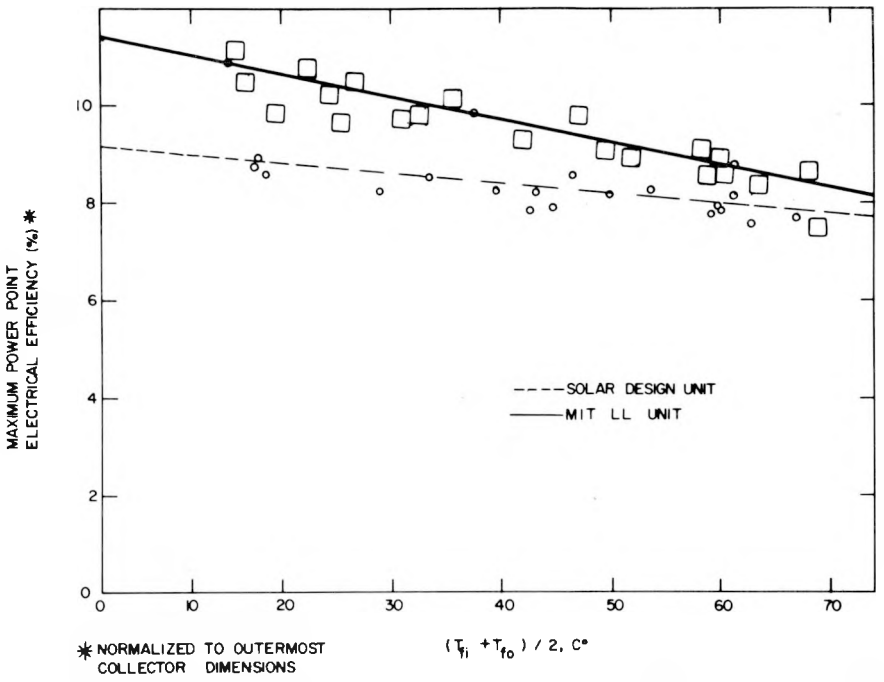

Fig. 10-17. Thermal performance of production collectors with concurrent PV operation.

C74-1353A

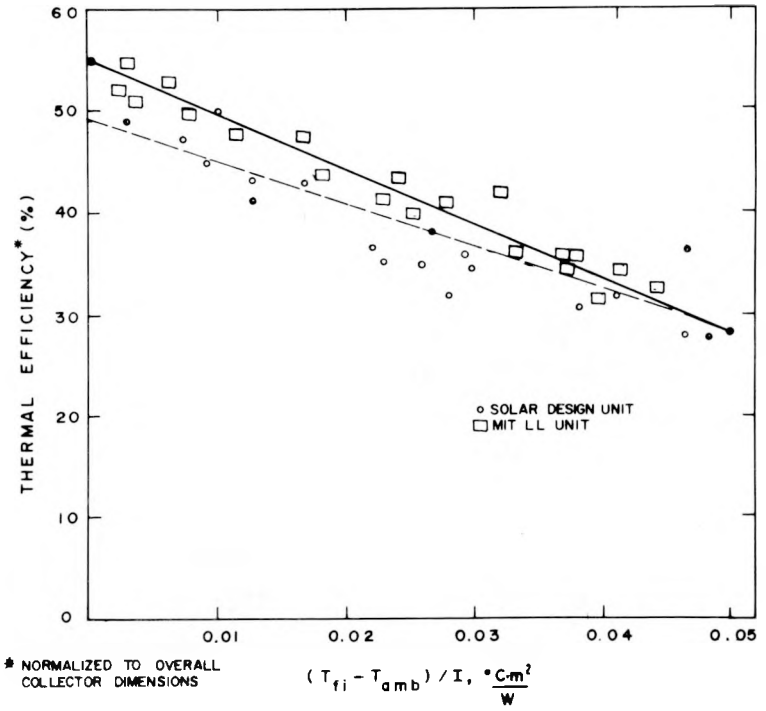

Fig. 10-18. Electrical performance of production collectors.

C74-1019A

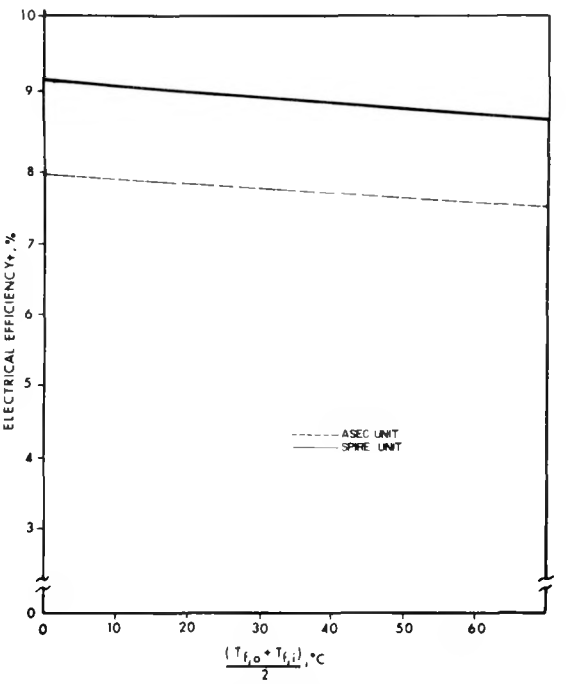

Fig. 10-19. Predicted maximum power point electrical efficiency for experimental air collectors.

The large discrepancy in the output power of the two panels is a result of the large difference in panel area: 0.47 m^2 versus 1.18 m^2. The efficiency calculation normalizes this difference. Projected thermal performance curves are shown in Fig. 10-20 for the full collectors operating with simultaneous thermal and maximum-power-point electrical energy collection. Maximum thermal efficiency values of 40.5 and 42.0%, respectively, are predicted, indicating respective performance gains of 21 and 26% over the early Spectrolab air collector.

10.3.4 Conclusion

Testing of the second-generation production collector designs discussed above demonstrated that PV/T collector performance can be made to approach that of comparable single-functioning solar thermal and PV module counterparts. In addition, the experimental air, dual-flow and unglazed PV/T collectors all showed substantial promise.

C74-1018A

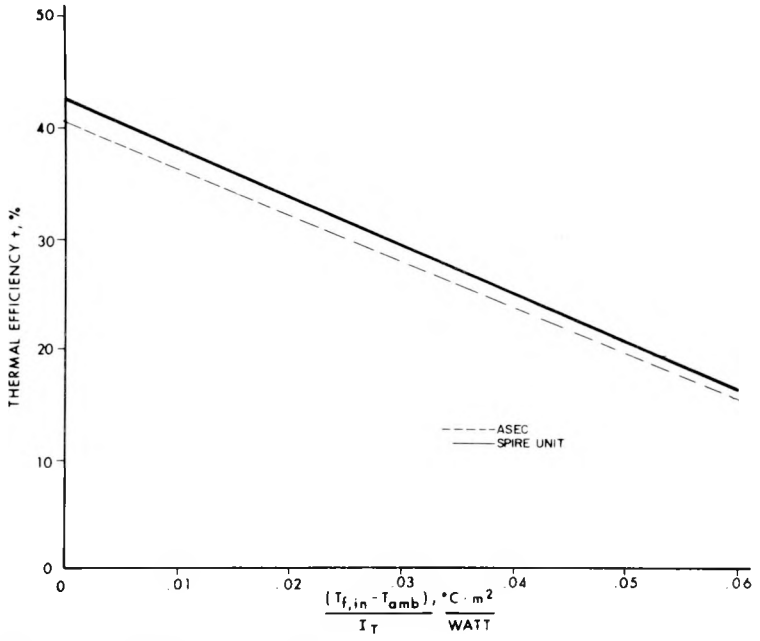

Fig. 10-20. Predicted thermal efficiency with concurrent PV operation for experimental air collectors.

The ultimate viability of the PV/T unit will be decided, however, not merely by collector output, but by the ability of the PV/T system to match both the thermal and electrical loads of residences.

10.4 Development of Solar Cells for Photovoltaic/Thermal Collectors

10.4.1 Background Information

In the design of combined PV/T collectors, where both thermal and electrical output is desired, attention should be given to the entire solar spectrum. For example, the range of wavelengths from 0.36 to 2.3 μm encompasses 98% of an air mass 1 (AM 1) solar spectrum. Comparing this range with the PV cell response range, which ends at 1.1 μm*, indicates that there is a range of energies of potential use to a PV/T collector that is not used in a simple PV collector. In fact, the present design of PV cells results in this energy being rejected by either a PV or a PV/T collector.

*The response range ends at 1.1 μm because the photocurrent arises from carriers generated when a photon with energy greater than the band gap of silicon is absorbed. For silicon, the band gap is 1.1 eV which corresponds to a wavelength of 1.12 μm.

To determine the extent to which the spectral range beyond 1.1 μm can contribute to the performance of PV/T collectors, Table 10-1 was prepared from the data of Thekaekara (16) for the four solar spectra listed across the top of the table. Each of the spectra was integrated over various wavelength intervals, all of which start at 1.1 μm and extend to the longer wavelength listed in the first column of the table.

TABLE 10-1

INTEGRATED FRACTION OF VARIOUS SOLAR SPECTRA

Fraction of Energy Between 1.1 μm	Blackbody 5762°K	AMO	AM 1 Turbulence 1	AM 1 Turbulence 2	AM 2 Turbulence 1	AM 2 Turbulence 2
1.25	0.054	0.058	0.058	0.057	0.063	0.069
1.5	0.112	0.124	0.099	0.102	0.107	0.117
1.75	0.149	0.168	0.154	0.161	0.182	0.205
2.0	0.173	0.194	0.171	0.178	0.199	0.244
2.25	0.189	0.210	0.190	0.198	0.222	0.252
2.5	0.200	0.222	0.202	0.211	0.237	0.271
3.0	0.213	0.238	0.205	0.214	0.238	0.272
4.0	0.234	0.251	0.215	0.225	0.251	0.288

Upon examining the results, it can be seen that 22 to 29% of the total solar spectrum is contained in the wavelength interval between 1.1 μm and infinity. As a practical matter, it is only necessary to consider the response of materials out to 2.0 or 2.5 μm since 80 to 90%, respectively, of this energy is contained within these wavelength ranges. The implication of these results for PV/T collectors is that at least 22% of the solar spectrum available for thermal energy collection exists at wavelengths which cannot contribute to the PV output and which present PV cell designs with back surface metalization that reflects back toward the sky.

The effect of collecting this energy on PV/T performance is manifest via the increased solar absorptance of the cell. The net energy absorbed by the cell per unit collector area, E_c, can be expressed as:

$$E_c = \alpha_c \tau_g I p \qquad (1)$$

where:

α_c = cell absorptance - visible
τ_g = glass transmittance
I = insolation
p = cell area packing factor.

Thus the energy absorbed is linearly proportional to cell absorptance.

To describe PV/T designs that make use of the energy beyond 1.1 μm, it will be necessary to explore briefly the optical properties of silicon as a function of wavelength. For this purpose consider a flat piece of silicon, many wavelengths thick, (so that interference effects can be neglected) suspended in air, which has polished surfaces (so that specular reflection dominates). The reflection and transmission of this sample can be calculated through application of the Fresnel formulae [see, for example, Jenkins and White (17)]. If θ_1 is the angle of incidence in the first medium, and θ_2 is the angle of the transmitted ray in the second medium, then the reflections for the perpendicular, R_s, and parallel, R_p, polarization planes are given as follows:

$$R_s = \frac{\sin^2(\theta_1 - \theta_2)}{\sin^2(\theta_1 - \theta_2)} \qquad R_p = \frac{\tan^2(\theta_1 - \theta_2)}{\tan^2(\theta_1 - \theta_2)} . \tag{2}$$

Unpolarized light, which is dominant in sunlight, can be modeled as having equal amounts of the two polarization components. Thus the reflectance to sunlight is simply the arithmetic average of the two reflectances given above:

$$R = \frac{R_s + R_p}{2} . \tag{3}$$

First, consider the case where $\lambda < 1.1\,\mu$m. The reflection from the top air-silicon interface can be calculated by application of the above formulae. For the later comparison with experimentally measured results, θ_1 was chosen as 10^o; the resulting reflectance was 30.9%. Since light of these wavelengths has corresponding energies greater than the band gap of silicon, any light transmitted into the cell is absorbed within a few hundred microns of the surface. Thus, no light is transmitted through the cell. These results, together with experimental measurements, are shown in the left half of Fig. 10-21.

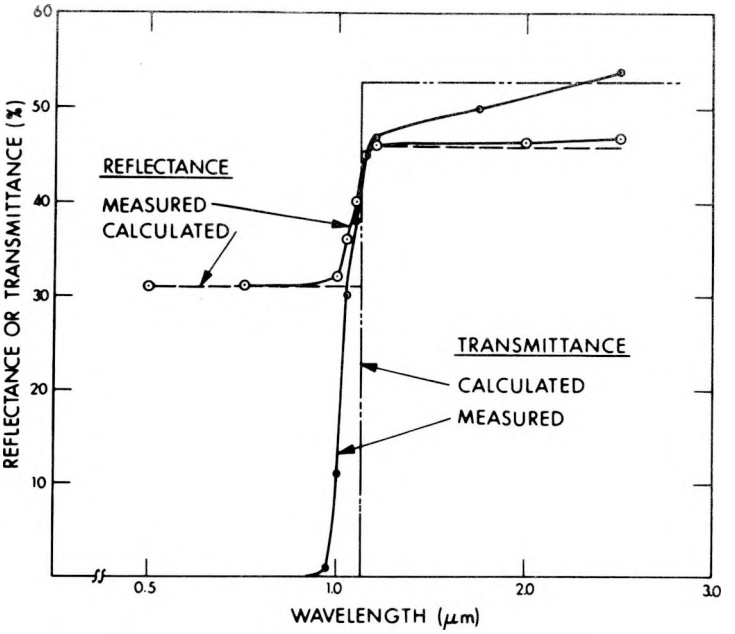

Fig. 10-21. Reflectance and transmittance of a bare silicon wafer in air. Incidence Angle $Q_1 = 10^{\circ}$.

Next, consider the case where $\lambda > 1.1\,\mu m$. Again, 30.9% of the incident light will be reflected when the light first encounters the silicon. However, this will not be the total reflectance because there now exists another path for reflected light. Since silicon is transparent for these wavelengths, light travels through the silicon until it encounters the back silicon-to-air interface. At this juncture, some of the light is reflected while the remaining is transmitted. The reflected light travels back up to the top air-silicon interface where some is reflected back into the silicon and some is transmitted to be counted now as reflected light. Summing all such components, the reflectance is:

$$R_T = R + (1 - R)^2 \sum_{n=0}^{\infty} R^{2n - 1} \qquad (4)$$

and the transmittance is simply:

$$T = 1 - R_T \, . \qquad (5)$$

Evaluation of these latter two formulae for the case R = 0.309 yields:

$$R_T = 0.46 \quad \text{and} \quad T = 0.53 \, .$$

These results compare well with the experimental measurements as shown on the right of Fig. 10-21.

Contributions to this effort were made by Charles H. Cox,III and Pattabiraman Raghuraman.

10.4.2 PV/T Cell Design

The implications of the above findings for the design of PV/T collectors can be understood with reference to 10-22a. This shows a cross section of a PV cell constructed from the piece of bare silicon discussed above. Appropriate amounts of positive (P) and negative (N) impurities (dopants) have been introduced in order to form a P-N junction. Electrical contact to either side of the junction is made through a grid pattern of aluminum on the top and a fully aluminized bottom surface. The transparency of silicon for $\lambda > 1.1$ μm together with the high reflectance of aluminum (typically $\sim 95\%$) means that most of the energy in the waveband 1.1 to 2.1 μm is reflected back out of the solar cell. Figure 10-23 shows the results of measurements made on this solar cell. An analysis similar to the one carried out above for the piece of bare silicon has been performed, but, with the inclusion of a rear metal reflecting layer, two modifications are necessary. One is that the reflectance at the top, air-silicon interface, R, is not necessarily equal to the bottom silicon-metal interface, R_2. Second, the metal aluminum is an absorbing medium, hence its index of refraction is complex and a more sophisticated version of equation (2) is required. Tackling the later case first, at normal and near normal incidence a simple approximation is available:

$$R_s = R_p = \frac{(n_1 - n_2)^2 + k_2^2}{(n_1 + n_2)^2 + k_2^2} \qquad (6)$$

where: n_1 = index of refraction of silicon
n_2 = index of refraction of aluminum
k_2 = extinction coefficient of aluminum.

In absorbing materials, unlike transparent materials, the wavelength dependance of n and k cannot be neglected. Reference 18 gives values of n and k for evaporated aluminum, as used in solar cells, in the wavelength range of interest. The resulting values of the silicon-aluminum reflectance, R_2, can be calculated

using equation (6) assuming the index of refraction for silicon is 3.5. The other case requires a more general form of equation (4), as developed in Reference 19; it is given by:

$$R_T = \frac{R_1 + R_2 - 2R_1R_2}{1 - R_1R_2} . \qquad (7)$$

C74-1024

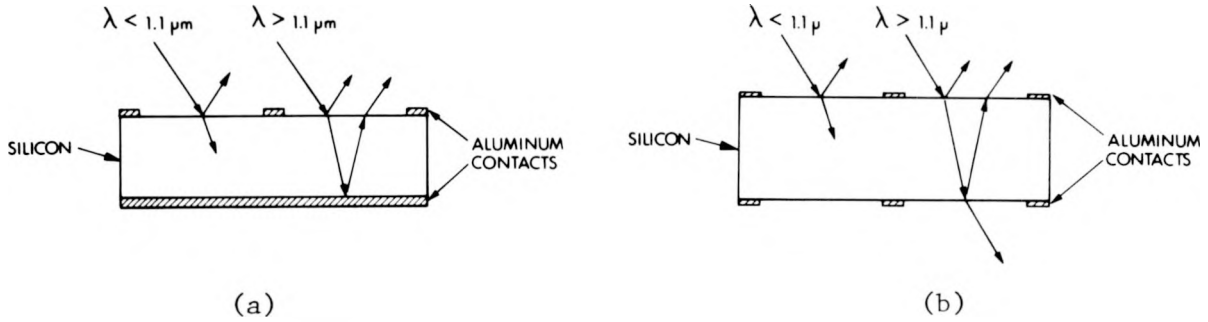

(a) (b)

Fig. 10-22. Contrast of the optical performance of silicone: (a) with full metal back and (b) with a gridded metal back.

C74-1025A

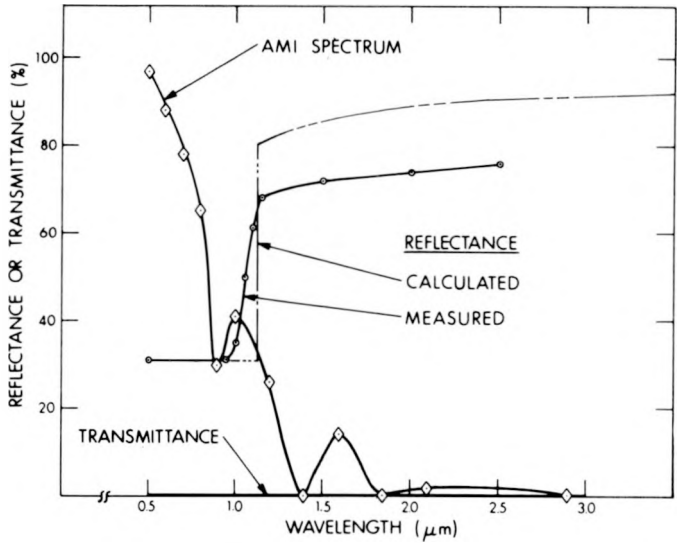

Fig. 10-23. Reflectance and transmittance of a silicon wafer with a full metal back.

For $\lambda < 1.1\,\mu m$, both the calculated and measured results indicate that the reflectance remains the same as was the case with no rear surface reflection. This is reasonable since for these wavelengths the silicon is

absorbing, and no radiation reaches the rear surface. For $\lambda > 1.1\,\mu m$, the reflectance rises to a value greater than that without the reflective back, but approximately 10% below the calculated curve. That the two curves have the same shape suggests that the difference is due to the fact that the rear surface was not polished as highly as the front surface; thus, the rear surface reflection has a significant diffuse component whereas the modeling assumed no such component. As a reference, the AM-1 spectrum is also plotted in this figure. It has been scaled such that its peak corresponds to 100%.

From the above analysis, it was found that approximately 20 to 25% of the solar spectrum is reflected back out of a typical silicon solar cell due to the highly reflective metal backing placed on the cell as an electrical contact. This energy, though useless for the generation of electricity, could, if captured, contribute to the thermal output of a PV/T collector. In order to capture this long wavelength energy, there are two apparent options: one could leave the back surface metallization on the cell and provide a mechanism for capturing the reflected energy above the cell or, alternatively, one could, to the maximum extent possible, remove the metallization, thereby allowing the radiation to pass through the cell and to provide a mechanism for capturing the energy below the cell. The former approach would increase the temperature of the cell and members above the cell, thereby increasing the loss of energy through the top of the collector. As this loss is already great, every effort should be made to minimize it; consequently, the latter course was pursued, namely, removing the cell back metallization.

10.4.2.1 Cell Back Metallization

A straightforward approach to reducing the area covered by the back metallization, and thereby the reflection caused by it, would be to substitute a grid or finger metallization pattern on the back similar to the one presently used to make contact on the front surface of the cell. If, as is shown in Fig. 10-22b, this rear grid pattern is the same as the front one and is co-aligned with it, then the rear grid will contribute negligible additional reflection beyond that already incurred by the front grid pattern (for normal incidence, at least).

To explore the effects of a gridded rear contact on the cell electrical output, three cells, differing only in the manner described below, were prepared (19). Curve A of Fig. 10-24 shows an I-V curve of a solar cell with full metallization on the back. As a figure of merit for comparing the various cases, the fill factor (FF) will be used:

$$FF = \frac{I_{mp} V_{mp}}{I_{sc} V_{oc}} \tag{8}$$

where: $I_{mp}(V_{mp})$ = current (voltage) at maximum power point
I_{sc} = short-circuit current
V_{oc} = open-circuit voltage.

For the above cell, FF = 0.761. Replacing the full metallization on the back surface with a gridded contact results in the I-V curve B shown in Fig. 10-24. Unfortunately, the fill factor was reduced to 0.404, or a 53% reduction; i.e., roughly half of the available electrical output was sacrificed by going to a gridded back contact.

C74-1027

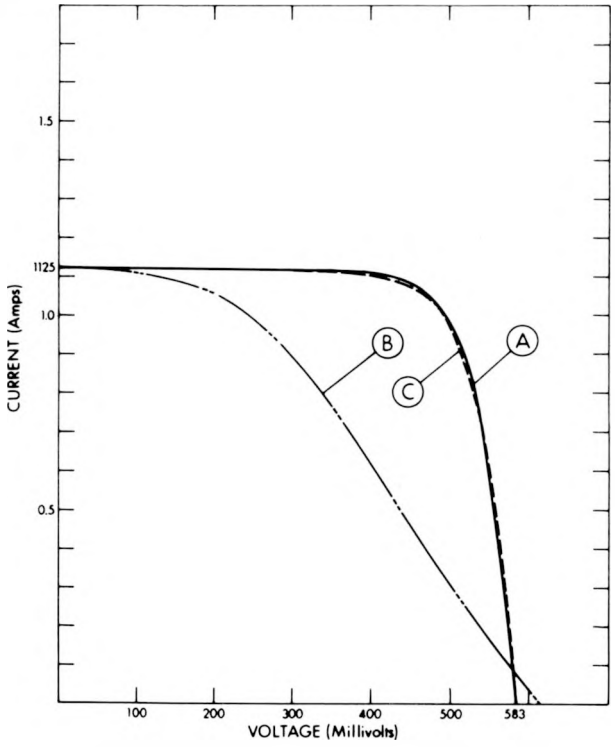

Fig. 10-24. Measured current versus voltage (I-V) curves for three cell configurations: (a) full metal back, and gridded metal backs without (b) and with (c) a back surface field.

The reason for the drastic decrease stems from an increase in the resistance between the rear contact and the semiconductor junction--where the electrical current is being generated--when the back contact is reduced from full metal coverage to a gridded arrangement*. Fortunately, this resistance can be decreased to the level with full metallization by placing a heavily doped layer, e.g., a P+ layer in an N-on-P cell, at the back of the cell. In fact, there is an additional reason, in terms of increased carrier collection efficiency, for incorporating such a heavy doping layer, which is usually referred to as a back surface field (BSF) [see, for example, Mandelkron and Lamneck (20)].

An I-V curve measurement on a cell having both a gridded back contact and a heavily doped layer is shown in Fig. 10-24c. The fill factor has been restored to 0.750, virtually equal to the value obtained with a full back metallization.

Careful selection of a dopant is required. In an N-on-P design, aluminum is commonly used as a P-dopant. Diffusing in aluminum should increase the reflectivity that removal of the metallization was attempting to decrease. Such an effect has been reported by Giuliano and Wohlgemuth (21). Thus boron, another common P-dopant, should be used in order to preserve the transmittance of silicon.

10.4.2.2. Reflection Loss Reduction

As results have suggested, the reflection losses from untreated silicon surface(s) in air are 31% and 46%, depending upon whether the wavelength is less than or greater than 1.1 μm.

Two general techniques may be employed to reduce these losses: anti-reflection (AR) coatings, and surface texturizing. With the former technique, a thin film coating is placed onto the silicon, and the index of refraction

*This does not imply, for example, that if the top gridded contact were replaced with a visibly transparent, full metallization, the cell output would increase substantially. Inherent to the design of a solar cell is heavy doping of the semiconductor material (an N+ layer in the case of an N on P cell) just below the top contact grid. In addition to other functions, this N+ layer acts as a conductive layer just within the top surface of the cell, thereby permitting an increase in the distance required between metal contacts for a given level of series resistance.

lies between that of air and silicon. With proper choice of the film thickness and its reflective index, it is possible to make the reflection from the film-silicon interface destructively interfere with the light reflected from the air-film interface, thereby canceling out the reflected component.

Although this method theoretically has the advantage of allowing complete cancellation of the reflection loss, it is capable of doing this in the strict sense for only one wavelength and one angle of incidence. In order to explore the effectiveness of an AR film for various incidence angles and wavelengths, calculations based on the Fresnel formulae were performed. Expressions for the two reflected components are given in Table 10-2; multiple interlayer reflections were taken into account as was done in the development of Equation (4). These equations were combined via vector addition to yield the resultant reflected amplitude. The AR film was designed to have minimum reflectance at a wavelength λ_o and normal incidence. The results of these calculations are presented in Fig. 10-25 where reflectance is plotted as a function of incident angle with wavelength as a parameter. For comparison, the reflectance of an uncoated piece of silicon is also included. In all cases the piece of silicon was considered semi-infinite in depth so reflection from the back silicon-air interface could be neglected. The range of wavelengths covered, $1/2\ \lambda_o$ to $2\lambda_o$, is slightly less than that covered by the solar spectrum. Although the AR film always does better than the uncoated surface, it is considerably less effective over a reasonable range of incident angles, e.g., out to 50^o, as the wavelength varies off from λ_o.

TABLE 10-2

FORMULAE FOR CALCULATION OF REFLECTION FROM AN AR-COATED SURFACE

	Magnitude	Angle
Air-film interface	$R_{AF}(\theta_A)$	θ_A
Film silicon interface	$(1 - R_{AF}(\theta_A))^2 . \sum_{N=0}^{\infty} R_{FS}^{N}(\theta_F)\ R_{AF}^{N-1}(\theta_A)$	$\frac{(180)\ (\lambda_o/\lambda)}{(\cos\ \theta_F)}$

θ_A incident angle in air

θ_F incident angle in film

$R_{AF}(\theta_A)$ average Fresnel reflectance at air-film interface

$R_{FS}(\theta_A)$ average Fresnel reflectance at film silicon interface.

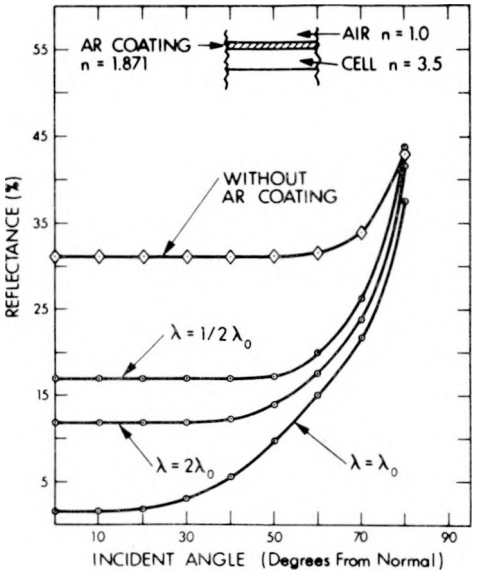

Fig. 10-25. Reflectance from an AR-coated, semi-infinite silicon wafer versus incident angle with wavelength as the parameter.

With the texturing technique, the surface is roughened so that incident light undergoes more than one air-silicon reflection before being reflected back into space. Such techniques avoid the wavelength dependence of AR coatings, but the dependence on incident angle remains. Although one might conceive of many different "texturing" patterns, there is one pattern that is particularly easy to obtain with silicon. As has been demonstrated by Arndt, et al. (22), regular tetrahedral pyramids can be formed on the surface of a properly oriented piece of silicon using an anisotropic etch. The texture, then, arises from exposing portions of the surface of selected crystal planes resulting in a highly regular surface pattern. Estimates of the reflectance from such a surface can be accomplished by straightforward application of geometrical optics and the Fresnel formulae. The results of these calculations, for a semi-infinite piece of silicon, together with the previous result for a polished surface, are plotted in Fig. 10-26. The disjointed shape of the textured reflectance curve is due to the decreasing number of internal reflections as the incidental angle increases. For a narrow range of low incident angles, there are three reflections before the light escapes the surface; there is then a broad midrange, from about 10 to 50°, where the light undergoes two reflections and finally a third range, for incident angles beyond 55°, where only one reflection occurs.

C74-1022

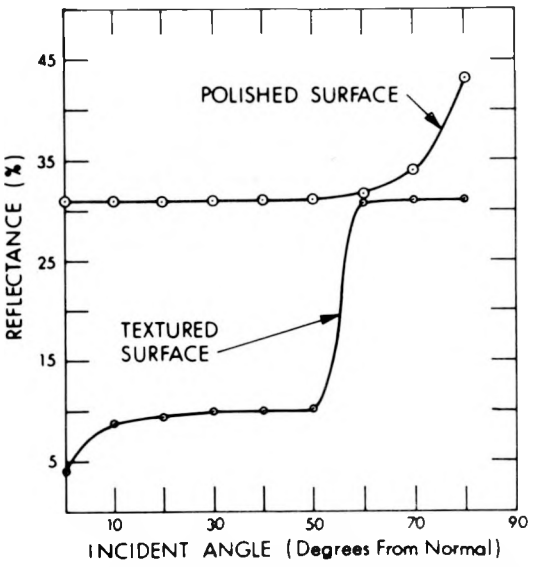

Fig. 10-26. Reflectance from a textured surface, semi-infinite silicon wafer versus incident angle.

A comparison of the two methods indicates that over the range of from 0^{o} to 50^{o}, which is the wavelength range of interest, the textured surface is better than a single AR coating. Equal or superior performance is possible if multiple-layer AR coatings are used. However, cost and durability issues could discourage such an approach.

Although the AR coating and the texturizing are aimed at accomplishing the same end, a subtle distinction exists between them for wavelengths that must be transmitted through the cell. This distinction stems from the fact that the choice of an optimum AR coating at one surface is largely independent of the choice of an optimum coating at the other surface. In the case of texturizing, however, applying this process to one surface requires applying it to the other, in order for light to be transmitted through the cell. The reason is that light which enters the cell via a textured surface will strike the other, planar, surface at an angle greater than the critical angle. Thus this light will be totally internally reflected. To permit passage of light through a cell with a textured surface, then, requires the other surface to have an identical texture. This is readily accomplished with the anisotropic technique, since the texture is directly related to the crystal structure and solar cells are often made from single crystal material.

Estimating the improvement in PV/T collector performance afforded by using gridded back cells requires a simulation program, a collector design, and specific values for all the parameters involved. All of this material is covered in an article by Cox and Raghuraman (23). Figure 10-27, based on their work, shows the estimated thermal and electrical efficiencies for an air PV/T collector with conventional and gridded back PV cells. The thermal efficiency (η_T) has improved by slightly more than five percentage points over the entire ΔT ($\Delta T = T_i - T_A$) range investigated. The electrical efficiency is unaffected for low ΔT, but is decreased by approximately 0.5% for high ΔT. The dominant reason for the decrease is due to the slightly higher operating temperature of the more efficient collector.

C74-2009

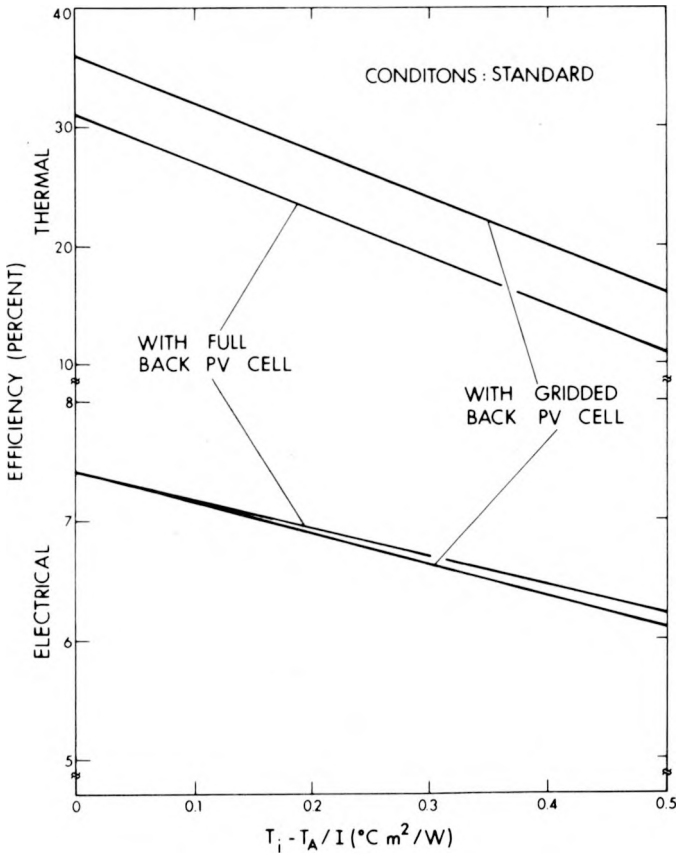

Fig. 10-27. Thermal and electrical efficiencies for the advanced prototype, air PV/T collector.

10.4.3 Conclusions

In conclusion, analysis and testing have shown that reduction of the back metallization to a grid similar to, and aligned with, the front metallization grid will permit radiation that would otherwise be reflected to be absorbed by the thermal portion of the PV/T collector. In order to avoid degradation of collector electrical performance with increased resistance, a heavily doped layer needs to be added to the back of the cell. In addition a more broadband reflection-reducing means should be employed. Two techniques for reducing the reflection losses over the broad solar spectrum have been investigated: antireflection (AR) coatings and surface texturizing. A multiple-layer AR coating is required to surpass the performance of a texture etch. The AR coating may be applied to one or both silicon surfaces; the texture etch must be applied to both. A simulation of a second-generation air PV/T collector design indicates that a 5% improvement in thermal efficiency with a negligible decrease in electrical efficiency is possible.

10.5 Method for Roof-Mounting Photovoltaic Arrays

10.5.1 Introduction

In early, intermediate-size PV system experiments such as those discussed in Sections 2 to 6 of this report, it was found that materials and construction costs were very high for typical ground-mounted PV array support structures. The fundamental requirement of a ground-mount structure for a flat-plate array is to provide a fixed (or possibly adjustable) tilt support. Such structures are typically made of steel and are anchored in poured concrete footings, resulting in high costs.

Since cost is a primary determinant of the future viability of residential PV systems, ground-mounting was abandoned in favor of roof-mounting. The synergism in this arrangement is obvious: a roof is tilted at a near-optimum angle for maximizing the annual insolation on the PV array, and a typical residence's roof is sufficiently large and strong to hold an optimally sized PV array. In addition, little or no additional structure is required to support a PV array on a roof.

The specific requirements of an array roof-mounting design, four generic roof-mounting approaches, and examples and performance of actual installations utilizing these approaches are discussed, based on Lincoln Laboratory experience at the Northeast and Southwest Residential Experiment Stations.

Contributions to this effort were made by the following individuals: Anthony A. Augustine, John T. Kelly, Jr., Burt E. Nichols and Miles C. Russell.

10.5.2 Requirements of an Array Roof-Mounting Design

The design of the PV array-mounting system is influenced by a number of specific requirements and considerations which are discussed below.

Roof Strength: PV panels typically weigh between two and four pounds per square foot, including their frames. This presents only a small increase in the load which a typical roof is designed to bear, and standard roof structures are expected to be adequate for supporting the additional weight of a PV array. It is prudent, however, to determine the roof's load-bearing capability, which is a function of beam size, span, spacing, tilt angle, and specific properties of the beam material. The actual roof loading expected from all sources--wind, snow and PV array--may be estimated and compared with the design load of the roof to determine the roof's margin of safety under maximum loading conditions.

Physical Access for Removal: The array-mounting design must provide for a simple, safe means of removing the PV modules in order to facilitate both the original installation and replacement of failed or damaged modules. For cost considerations, a minimum of special equipment should be required to accomplish such module removal.

Insolation Enhancement: The albedo of the horizontal surface directly "in front" of the roof-mounted PV array significantly affects the amount of reflected insolation which impinges on the array. Under some circumstances, this factor may be controlled to benefit the energy production of the system. For example, reflective white gravel may be used to cover a horizontal roof or roof section which lies south of the PV array itself. Most often, however, the albedo of the surface is uncontrolled and dictated by ground cover or adjacent structures.

Aesthetics: For a system to be marketable, it must be aesthetically acceptable. Although this area is open to subjective judgment, it is prudent to consider shape, size, color, texture, and patterns when designing a roof-mounted and highly visible PV array. A rectangular, dull-finished, earth-colored PV array will probably be most appealing to the public. To date, this effect has not been totally achieved, due primarily to the dissimilarity between the appearance of the circular solar cells and the interstitial background. Additionally, the cross-hatching of typical module and array aluminum framework is visible and difficult to disguise. The trend in PV module design, however, is to employ square- or rectangular-shaped solar cells, which present a more uniform, pleasing appearance when densely packed in a PV module. In addition, module frames may be anodized a dark color resembling that of the PV cells, thereby softening the aesthetic impact of the array.

Cost: One factor that often works against other considerations is the inherent cost of the PV array-mounting system. Any mounting concept must ultimately be capable of achieving the necessary cost goals for economically viable residential PV systems. Both the mounting hardware and installation costs associated with a particular array mount, as well as any credit for displacing standard roofing materials, must be considered in the overall design of a roof-mount system.

10.5.3 Four Generic Roof-Mounting Approaches

The four generic methods for roof-mounting a PV array--stand-off, direct, integral and rack--are discussed below.

10.5.3.1 Integral Array Mounting

An integrally mounted PV array (Fig. 10-28) takes the place of the roof--shingles, felt and sheathing--and is mounted directly on the roof rafters. The major concern with such a mounting scheme is the assurance of an effective long-term weatherseal. Due to the quantity of displaced sheathing and roofing material, this method results in a relatively low cost.

C74-977

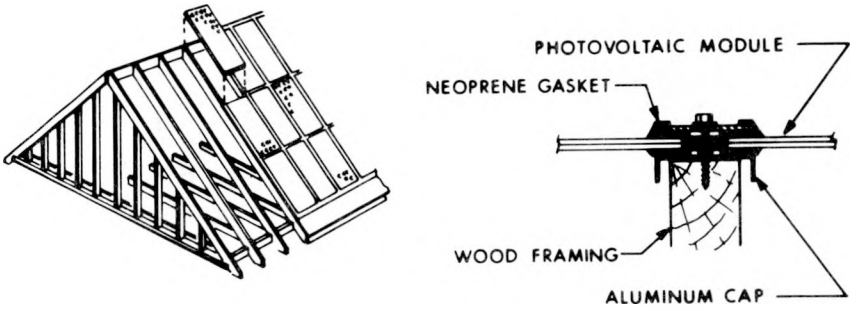

Fig. 10-28. Integral mount.

10.5.3.2 Direct Mounting

Using the direct-mount method (Fig. 10-29), the PV modules are flush-mounted directly on the roof felt, replacing the standard asphalt shingles. Just as with an ordinary roof, these "shingles" overlap one another to provide an effective weatherseal. The PV modules or their frames may be secured to the roof.

C74-978

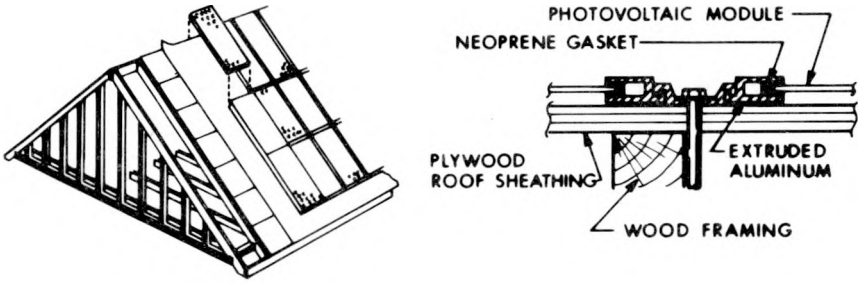

Fig. 10-29. Direct mount.

10.5.3.3 Stand-Off Mounting

PV panels can be mounted several inches above and parallel to a standard roof surface; this is called the stand-off mount (Fig. 10-30). In this system, penetration of the roof surface is made only to secure the mounting rails to the roof, and sealing is accomplished with flashing. The PV modules do not provide the weatherseal.

In theory, by mounting the PV array above the roof, air is free to circulate to both the top and bottom sides of the modules. This design was expected to enhance heat transfer from the array to the benefit of system efficiency. In

reality, however, systems employing stand-off mount arrays at the Northeast Residential Experiment Station did not have sufficient space between the module and the roof surface to promote convection-cooling adequately. Additionally, what little space was present was cluttered with impediments to free air flow such as frame members and wiring. Improved designs are expected to enhance cooling much more effectively.

C74-976

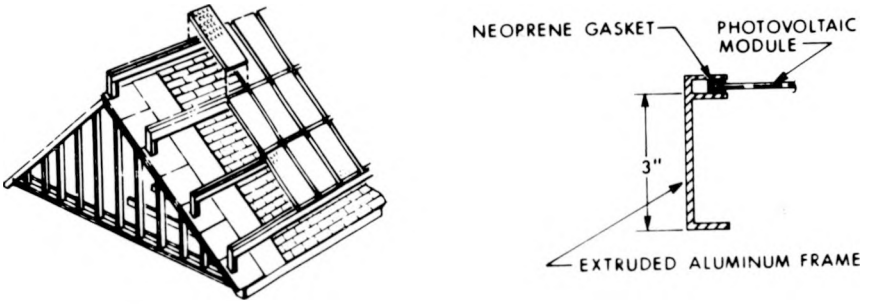

Fig. 10-30. Stand-off mount.

10.5.3.4 Rack Mounting

A rack would typically be used to ground-mount a PV array; the frame or rack would provide a support for the PV array tilted at the appropriate angle. Since most residential roofs have slopes in the range from 18 to 30°, mounting a PV array on such a roof and at the roof slope will result in a near-optimum tilt for solar access. A rack mount is not required for such an installation. The roof-mounted rack, therefore, is primarily applicable in areas such as the arid Southwest, where flat-roof construction is common but a PV array tilt of 20 to 30° is desirable.

10.5.4 Prototype System Installations

As is discussed in detail in Section 11, thirteen prototype residential PV systems have been built and tested: five at the Northeast Residential Experiment Station (NE RES) and eight at the Southwest Residential Experiment Station (SW RES), shown in Figs. 10-31 and 10-32, respectively. In addition, a lived-in house containing a roof-mounted PV system was built in Carlisle, Massachusetts, with funding from DOE for the PV system. All of these systems utilize various versions of the four mounting types discussed above.

CP267-6876

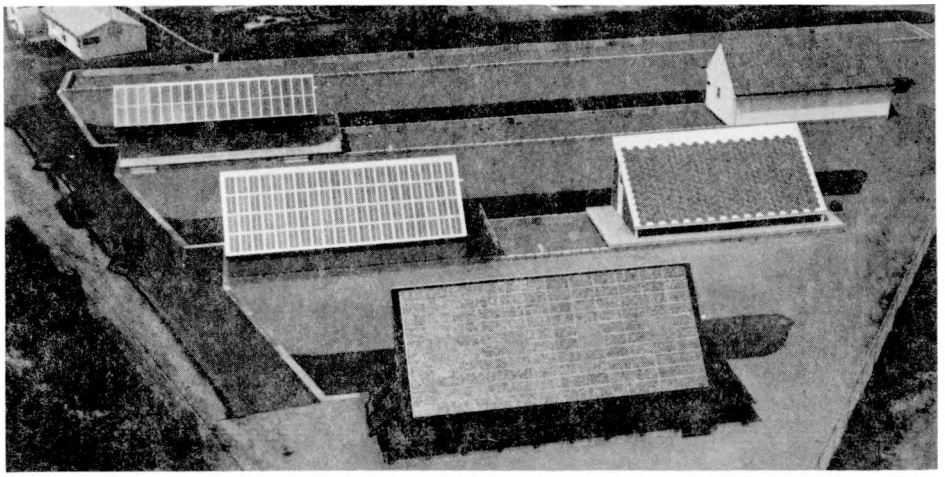

Fig. 10-31. Aerial view of the Northeast Residential Experiment Station, Concord, Massachusetts.

CP267-6985

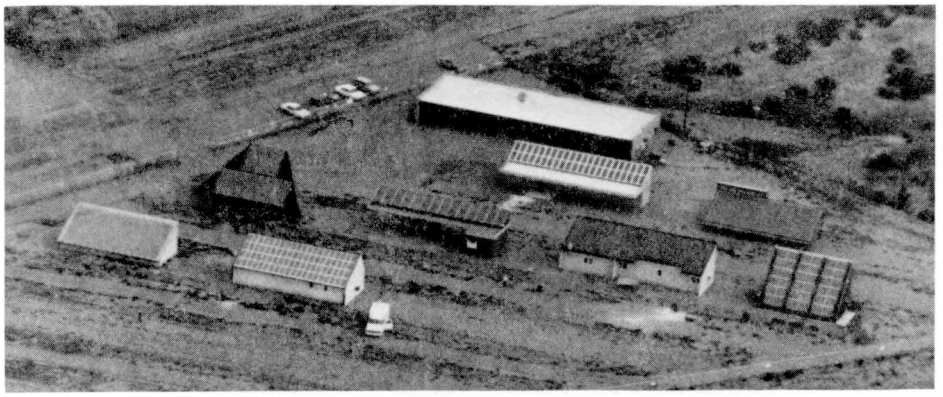

Fig. 10-32. Aerial view of the Southwest Residential Experiment Station, Las Cruces, New Mexico.

A breakdown of the number of systems in each mounting type category is shown below.

Mounting Method	Number of Systems
Rack	1
Stand-Off	5
Direct	3
Integral	4

Interesting features of some of these systems are highlighted in the following subsections.

10.5.4.1 Carlisle House Stand-Off Mount

Figure 10-33 shows the PV array installation on the Carlisle PV house located in Carlisle, Massachusetts. In this particular stand-off mount system, brackets with rollers are attached to the PV module frame. The roller brackets hold adjacent modules together in a vertical column. During the installation sequence, a pulley-crank arrangement is used to hoist and hold a module in position on the track while another module is bolted on. This process allows an entire column of PV modules to be rolled up or down the roof much like a garage-door system.

The inherent costs associated with this roller method are relatively high, due to the quantity of hardware required and the lack of any credit for displacing roofing material. The concept, however, provides for module replacement without climbing on the roof.

CP267-6422

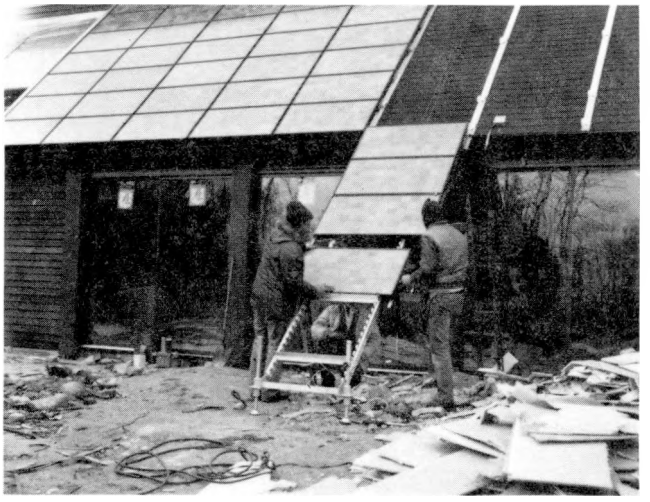

Fig. 10-33. The Carlisle PV house, stand-off mount.

10.5.4.2 General Electric Direct Mount

The General Electric prototype system at the NE RES is shown in Fig. 10-34. The "shingle" modules are direct-mounted on the roof surface, overlapping to provide the roof's weatherseal. Since these modules are hexagonal, specially designed shingles are used to flush out the roof edges.

Because no framing material is required and the standard roof shingles are displaced, a direct-mounting system is expected to have moderate cost.

A direct-mount array may operate as much as 20°C hotter than other mounts under full sunlight, since only the top sides of the modules are exposed to the air for convective cooling.

CP267-6593

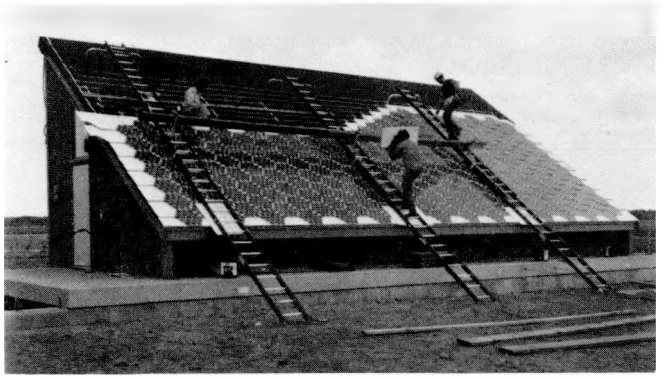

Fig. 10-34. The General Electric Prototype at the NE RES.

10.5.4.3 TriSolarCorp Integral Mount

Figure 10-35 shows the back side of the TriSolarCorp integral mount modules on the NE RES prototype system. PV modules with an edge gasket are mounted directly on roof rafters spaced 32 in. apart. An aluminum hold-down strip overlaps the edge of adjacent columns of modules and is screwed into the rafter. A silicone sealant is applied along horizontal butt-joints and is backed by a strip of tape. In this system, the modules provide mechanical strength for the roof and act as the weatherseal.

All standard roofing materials--sheathing, roofing felt, and asphalt shingles--have been displaced by the PV array, resulting in a relatively low cost for this method.

Directly beneath this PV array is an attic space. Thermostatically controlled ventilation provided in this space to enhance array cooling keeps operating temperatures lower than those of any other array at the NE RES.

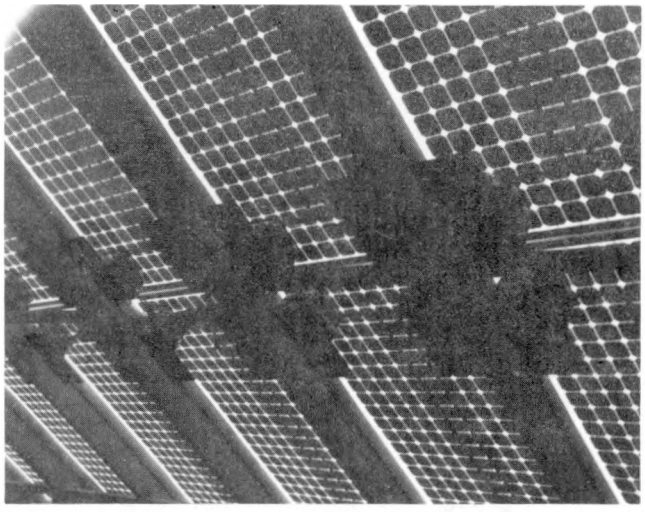

CP267-6231

Fig. 10-35. TriSolarCorp integral mount modules (backside).

10.5.4.4 TEA Rack Mount

The picture (Fig. 10-36) shows such a southwestern flat-roof installation. There is full access to the module electrical junctions and to the front and rear sides of the modules for module removal and maintenance. Circulation of air on both front and rear array surfaces will help maintain relatively low operating temperatures. This mount, however, requires considerable framing and mounting hardware, and is expected to result in above-average cost.

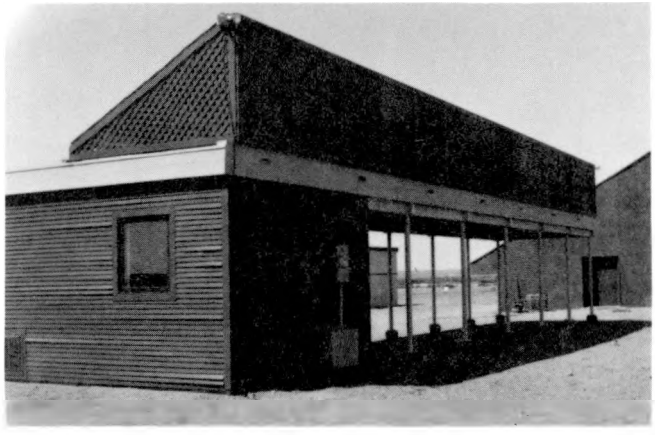

CP267-6623

Fig. 10-36. TEA prototype, SW RES, rack mount.

10.5.5 Mounting Method Cost Breakdown

During construction of the prototype systems, all costs associated with the physical installation of the array were tabulated. Table 10-3 summarizes

these costs, which are grouped according to generic mounting method. All costs are normalized by the as-installed array area.

From the table it can be seen that the cheapest installations are the direct-mount arrays. This is primarily due to the reduced amount of mounting hardware required for these installations as compared to the other installations.

TABLE 10-3

ARRAY INSTALLATION COSTS*

	Array Area (m^2)	Installation materials ($/$m^2$)	Installation Labor ($/$m^2$)	Displaced Roofing materials and Labor ($/$m^2$)	Total Cost ($/$m^2$)
Rack					
TEA	49.4	62.06	47.61	0	109.67
Stand-Off					
MIT LL	91.0	59.14	26.74	0	85.88
Carlisle	98.4	49.15	18.23	0	67.38
Solarex (NE)	70.1	20.16	64.41	0	84.57
BDM	54.0	15.48	14.67	0	30.15
FSEC	62.5	30.40	80.80	0	111.20
Direct					
GE (NE)	76.8	11.51	11.51	9.90	13.12
GE (SW)	76.8	6.45	12.11	9.90	8.66
Integral					
TSC (NE)	47.2	16.27	29.49	18.84	26.92
TSC (SW)	58.0	15.24	27.79	18.84	24.19
West.	71.0	112.79	48.34	18.84	142.19

*Excluding the photovoltaic modules themselves and wiring.

10.6 Development of Inverters for Residential PV Systems

10.6.1 Introduction

At the start of Lincoln Laboratory's effort in development of residential inverters, only two such products were commercially available, and their characteristics were different. One of the products is relatively simple, inexpensive and highly reliable, but its poor current waveform and power factor raised concerns about it adversely affecting the utility feeder to which it would connect. The other unit is complicated, relatively expensive, and unreliable, but its current waveform and power factor were of much higher quality. Details of Lincoln Laboratory's evaluation of these units and others which appeared later are given in References 24 through 27.

Contributions to this effort were made by the following individuals: Joseph W. Chludzinski, Charles H. Cox, III, Joseph D. Doucet and Emanuel E. Landsman, Ervin F. Lyon, Burt E. Nichols,Neil E. Rasmussen and Michael C. Wong.

10.6.2 Classification of Inverter Approaches

As part of the Laboratory's effort to develop inverters, they were studied from the vantage point of the functions performed by the inverter and the order in which these functions are performed, with an eye toward determining whether there were any potentially attractive inverter technologies which were not being pursued (28). This study is summarized below.

The ideal utility-interactive inverter provides a constant-amplitude, (in an RMS sense), single-frequency sinusoid, bidirectional output current from a variable amplitude, unidirectional input current. It is apparent that three basic and separate functions* are being performed:

Inversion (I)
Regulation (R)
Waveshaping (W).

An inverter can be classified according to the order in which the functions are performed in passing from the dc-to-ac side. If two functions are combined, an upper horizontal line joins them. All six possible sequences are listed in Table 10-4, followed by usable combinations for inverters and their embodiments.

Three of the above functional orders have not been used by inverter manufacturers. The basic version of the RWI or WRI topology would be a dc-dc converter for average power control, and a waveshaping stage that would produce something similar to a full wave rectified sinusoid, followed by inversion. A logical embodiment would be to combine the regulation and waveshaping into one dc-dc converter stage and call it a $\overline{WR}$.

---

*Numerous auxiliary functions are also incorporated into modern inverters. Some of these are protective and some pertain to organized start-up and shut-down. Although they are important, they are not basic to the inversion process and therefore will not be discussed here.

TABLE 10-4

CLASSIFICATION PERMUTATIONS

Basic Type	Derived	Embodiment
IRW	$\overline{\text{IRW}}$	Square wave/ferro
	$\overline{\overline{\text{IRW}}}$	Quasi-square wave/ filter
IWR	New	
RIW	RIW	Prereg/inverter/filter
	$\overline{\text{RIW}}$	Prereg/step wave
	$\overline{\overline{\text{RIW}}}$	Same as $\overline{\overline{\text{IRW}}}$
RWI	New	
WRI	New	
WIR	WIR	Line commutated

The IWR topology would use an inverter stage followed by a waveshaping stage. The output would be sinusoidal but unregulated. A tap-switching autotransformer regulator, which is a commercial item, would then follow.

A comparison of the new approaches showed that the WRI approach offers many advantages. The practical capability of a transistor used in a dc-dc conversion stage is greater than the capability of the same device used in an inversion stage. The use of single-power transistor as a pulsewidth modulated dc-dc stage for waveshape and regulation, followed by an SCR or transistor inverter stage, would use the best capabilities of both devices. The inverter SCRs need only operate at 60 Hz, thus keeping switching losses low. The transistor preregulation stage can be made to have subcycle response and, if voltage levels are over 100 V, the efficiency penalty paid for handling the power twice can be minimized. The unit would be a current source and would operate in a free-run mode with no response delay for transients. The dc-dc conversion stage need not be bidirectional if unity power factor operation can be guaranteed. If isolation is required, it can easily be accommodated by replacing the four full-bridge SCRs with two and a transformer used in a parallel inverter topology. A remaining problem is to arrange reliable commutation of the SCRs at all operating conditions. Therefore, a device

capable of active turnoff, such as a transistor or GTO may be better suited to this application. Alternatively, some small inductive power factor may be required in order to allow the inductor current to decrease sufficiently fast near current-zero, but some distortion would necessarily remain.

10.6.3 Development of Waveshaping Inverter

In light of its potential advantages, the Laboratory undertook the development of a waveshaping inverter, which is an embodiment of the WRI approach discussed above. This development activity is discussed in Reference 29 and is summarized in the following section.

10.6.3.1 Waveshaping Inverter Design

Figure 10-37 shows a block diagram containing the principal components of a waveshaping inverter. Between the dc and ac filters lie the combined waveshaping-regulation ($\overline{WR}$) stage and the inversion (I) stage. Below all this are the various major portions of the control stage.

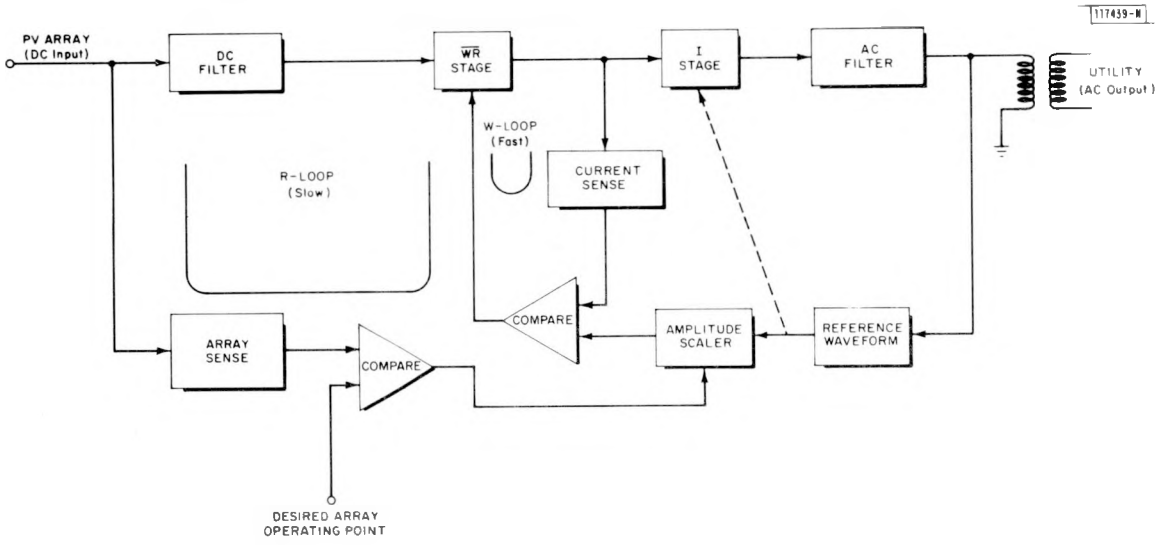

Fig. 10-37. Block diagram of a waveshaping inverter.

Since the $\overline{WR}$ stage performs two functions, its output, as measured by the current sense, is used as input to two control loops. The fast loop performs the waveshaping function; i.e., within a half cycle of the line frequency, numerous corrections are fed back to the $\overline{WR}$ stage in order to shape

the dc current into a half sinusoid. The slow loop performs the regulation function; i.e., over a period of many cycles of the line frequency, the difference between the average value of the current being drawn from the array and the desired average current is used to readjust the average current drawn from the array. The desired average current would depend upon the array loading control strategy chosen by the PV system designer; maximum-power-point tracking and constant voltage operation are two common options. The reference for the waveshaping loop is derived from the ac line voltage waveform.

Conceptually, the I stage would be either the self- or forced-commutated variety. In practice, the forced-commutated method is preferred, thus it requires an input from the reference waveform generator.

The filters on both ends reduce the ripple in two different parts of the spectrum. The dc-side filter reduces the 120-Hz ripple that the inverter would impose on the array; the ac-side filter reduces injection into the utility of the switching ripple (nominally around 20 kHz) that the waveshaping stage introduces.

Although inverters suitable for residential systems eventually need to handle powers in the 2 to 10 kW range, power semiconductor devices for both the $\overline{WR}$ and I stages are readily available only at the 1-kW level, so this level was chosen as being one of credible size for experimental evaluation and one which would not be difficult to implement.

10.6.3.2 Waveshaping Inverter Performance

A photograph of the prototype is shown in Fig. 10-38. Figure 10-39a shows the current and the voltage at the output of the $\overline{WR}$ stage. Figure 10-39b shows the I stage output current and utility voltage. The high-frequency switching noise has been filtered out using a capacitor.

Measurements of the efficiency versus power level of the prototype are shown in Fig. 10-40. The peak efficiency is nearly 90%.

CP267-6117

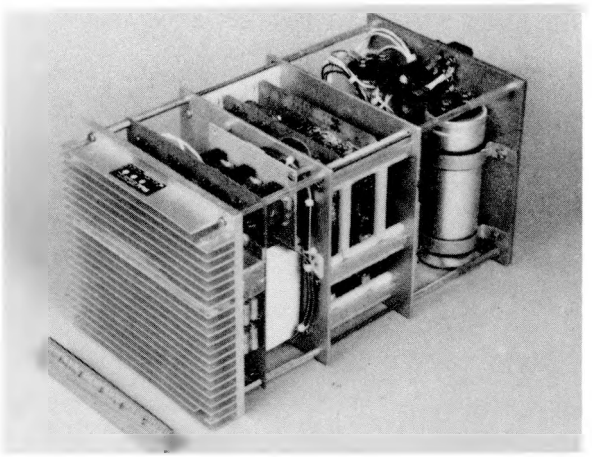

Fig. 10-38. Experimental inverter: The $\overline{WR}$ stage is at the far end, the control stage is in the middle, and the I stage is near the front of the photograph (with heat sink).

C74-2029

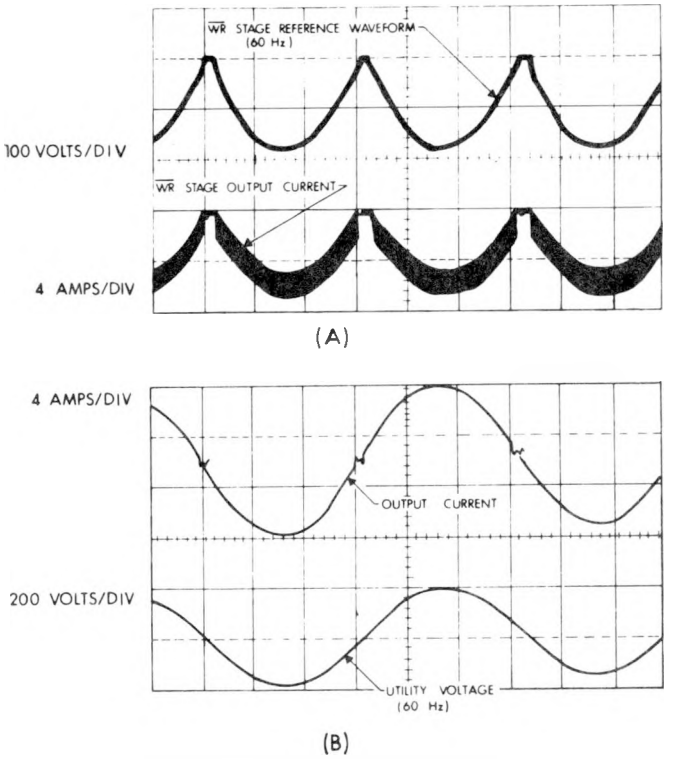

Fig. 10-39. Oscilloscope measurements of some waveforms of the experimental inverter: (a) voltage (top) and current at the output of the $\overline{WR}$ stage, (b) current (top) and voltage at the I stage.

C74-1291

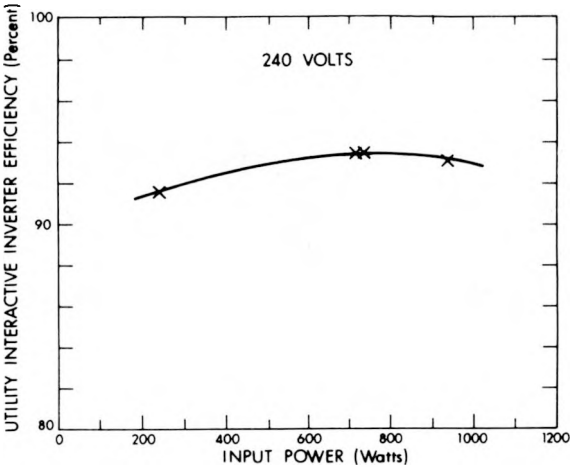

Fig. 10-40. Plot of measurements of efficiency versus dc power level for the experimental inverter.

10.6.3.3 Waveshaping Inverter Manufacturing Costs

Commercial feasibility depends on both technical and economic factors. At present, the DOE cost goals for residential inverters are stated in terms of $/Wp.

Table 10-5 shows allowable inverter costs, C_{pi}, for a range of efficiencies, with the baseline case of η = .90 highlighted. It is interesting to note that for efficiencies less than about 74%, the inverter must be free. From the prototype inverter efficiency curve (Fig. 10-40), the average power efficiency over all power levels is around 93%, so C_{pi} = .30.

TABLE 10-5

VARIATION IN INVERTER SELLING PRICE AS A FUNCTION OF EFFICIENCY

$\eta_{dc\ to\ ac}$	C_{pi} ($/Wp)
1.00	.40
.95	.33
.90	.25
.85	.18
.80	.10
.734	.00

As a first order estimate of the costs for producing a waveshaping inverter, a parts list from the prototype inverter, suitably scaled to the 5-kW level, can be used. This should produce an upper bound on the cost since several expensive items, such as modular power supplies, were used in the prototype that would not be used in production equipment. The resulting total suggests that on the basis of raw materials alone, a waveshaping inverter can be built in moderate quantities for .10 \$/W. The selling price, C_{pi}, must clearly reflect the contributions of assembly, profit, and overhead. A reasonable assumption is that the sum of these factors would result in a selling price that is triple the raw parts cost. Under this assumption, the resultant inverter price would be 0.30 \$/W.

10.6.4 Conclusions

A review of the basic operations that a dc-to-ac inverter must perform--inversion, regulation and waveshaping--indicates that one of the untried combinations appears to be attractive to implement. Measurements made on the experimental 1-kW breadboard of a waveshaping inverter confirmed the theoretical performance predictions: an efficiency of 92%, current harmonic distortion below 2%, and a power factor of 1. Some of the issues that arise in advancing the design to one more suitable for a commercially viable product were investigated. Primary among the issues were power level and cost, both of which appear solvable.

In the control section, a number of functions, mainly concerned with permitting fully automatic operation, remain to be implemented. Their design, although relatively straightforward functionally, will require some effort in order to insure trouble-free operation. Although it is generally assumed that a power factor of 1 is the ideal, a recent study (29) indicates such may not be the case. The design of a non-unity power factor waveshaping inverter would be difficult at best (and impossible at worst).

Eventually, mass-produced inverters should consist of about a dozen components. A typical breakdown might be as follows:

Power semiconductors	4-8
Energy storage elements	2-4
Control and drive circuits	1-2
Input and output switchgear	2
Total	10-17

In considering design revisions, preference should be given to implementations that would permit the level of integration indicated above.*

10.7 Development of Flywheel Energy Storage for Residential Photovoltaics

10.7.1 Introduction

Under joint funding from DOE's Divisions of Energy Storage and PV Energy Systems, Lincoln Laboratory developed a solar PV flywheel storage and conversion system which would store the electrical output from a solar PV array and convert the stored mechanical energy to 60-Hz ac power as required. The residential system concept is shown in the artist's sketch, Fig. 10-41. The flywheel unit acts as a complete interface between a solar PV array and an ac load, thus performing the dc-to-ac inversion function in addition to providing storage. Key elements in the approach include the use of extremely low-loss magnetic bearings, maximum-power-point tracking of the PV array, integrated motor-generator and output power conditioning of the stand-alone cycloconverter or utility-interactive inverter type, and selection of a configuration tolerant to rotor imbalances by suspending the rotor from a flexible quill. The development effort is discussed in detail in Reference 30.

C74-1899

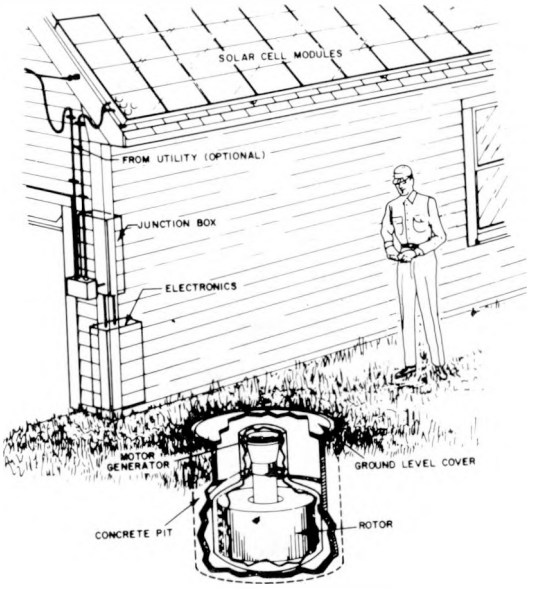

Fig. 10-41. Residential photovoltaic flywheel system.

*American Power Conversion Corporation of Burlington, MA, has further developed the waveshaping-inverter concept and now offers both a 2-kWp and 4-kWp commercial versions whose technical performance meets expectations. Its present price in low volume production is $2.00/W for a 2-kW unit and $1.25/W for a 4-kW unit.

The project included the following major tasks:

- To design a flywheel storage system suitable for use in a PV-powered residence.
- To perform manufacturing cost studies and user-worth studies of residential and 100-kW load center units.
- To build and test a 1/10-scale working residential system capable of operating in either a stand-alone or utility-interactive mode, and to evaluate experimentally its performance and efficiency over a range of residential loads and off-design conditions.

Contributions to this effort were made by the following individuals: Bronwyn L. Brench, R. Duncan Hay, Philip O. Jarvinen, Alan R. Millner, Neil E. Rasmussen and Neil Sullivan.

10.7.2 Flywheel System Design

A full-size, 40-kWh residential flywheel storage system was designed (Fig. 10-42). Subsequently, manufacturing cost estimates based on this design were prepared by three industrial contractors, and the economics of using flywheel energy storage were studied by the MIT Energy Laboratory (31). From these studies, it was found that flywheel systems are economically competitive with battery/inverter systems for the same PV application.*

As was discussed in Reference 30, the design shown in Fig. 10-41 was evaluated to determine its ability to withstand seismic loading resulting from earthquakes. It was found that flywheel systems possess resistance to earthquakes comparable to that of the buildings they would service, even in the worst earthquake regions of the United States.

10.7.3 1/10-Scale Prototype Flywheel System

A fully operational 1/10-scale prototype flywheel energy storage unit was built which was capable of operating either in a stand-alone mode or in a utility-interactive mode. The 1/10-scale unit was identical to the 40-kWh full-scale design with the exceptions, for ease of testing, that the quill

---

*As was discussed in Section 9, PV systems which operate interactively with the utility and thus require no on-site storage are generally less costly than systems which require on-site storage. Thus, economic competitiveness of flywheels as mentioned above applies to those situations where a utility hookup is not available.

C71-1055

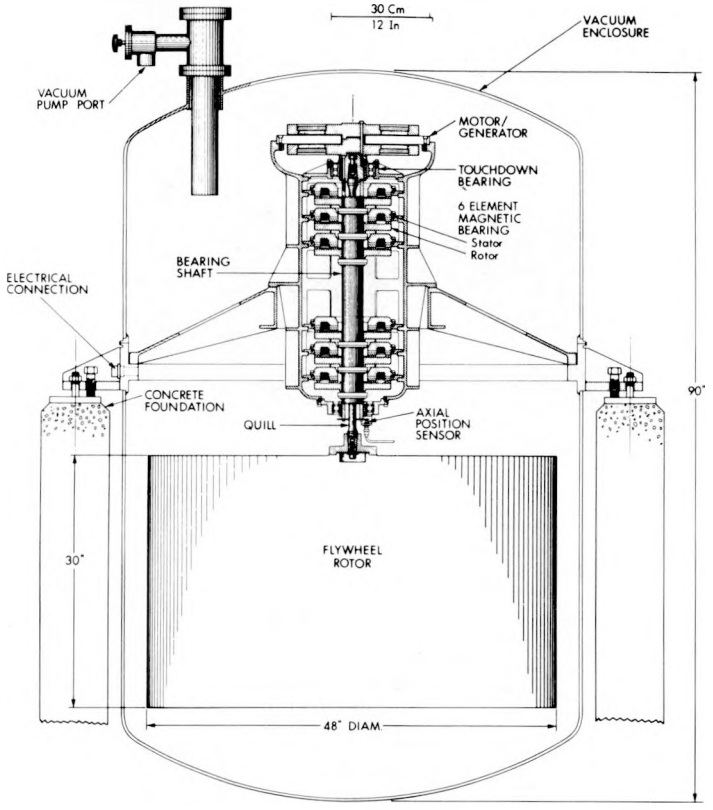

Fig. 10-42. 40-kWh residential flywheel energy storage unit.

shaft supporting the rotor was not telescoped inside the magnetic bearing shaft, and the motor-generator was mounted below the magnetic bearing (Fig. 10-43). A cut-away view of the 1/10-scale experimental flywheel is shown in Fig. 10-44, and a photograph of the six-element prototype magnetic bearing is offered in Fig. 10-45. The axially active, radially passive magnetic bearing supported a 400-pound steel rotor which stored 1 kWh of energy when spun to 15,000 RPM. A complete electrical system was designed and fabricated to handle all electrical and control functions between the PV array and the electric service panel of a residence (Fig. 10-46). Power-conditioning equipment of both the stand-alone cycloconverter and utilty-interactive types was constructed (Fig. 10-47). The excellent output power waveform quality of the inverter (less than 2% of total harmonic distortion) is shown in Fig. 10-48.

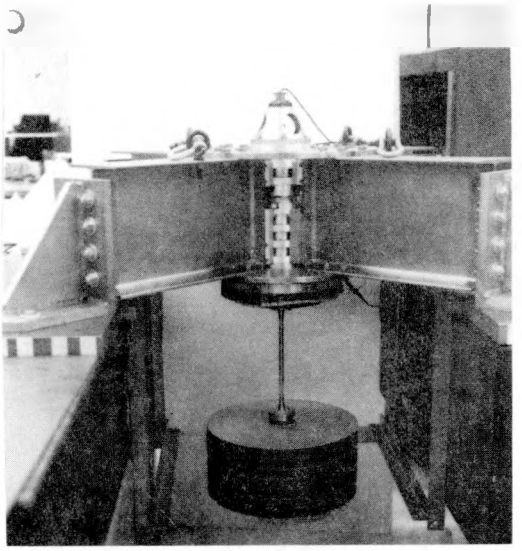

CP267-5403

Fig. 10-43. 1/10-scale prototype flywheel system.

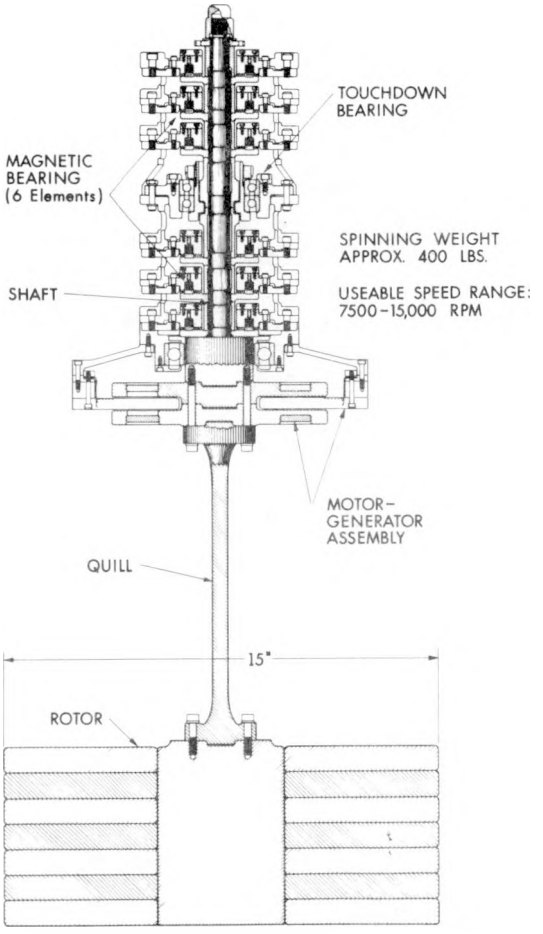

C71-1020

Fig. 10-44. Cutaway, 1/10-scale experimental flywheel.

CP267-5346

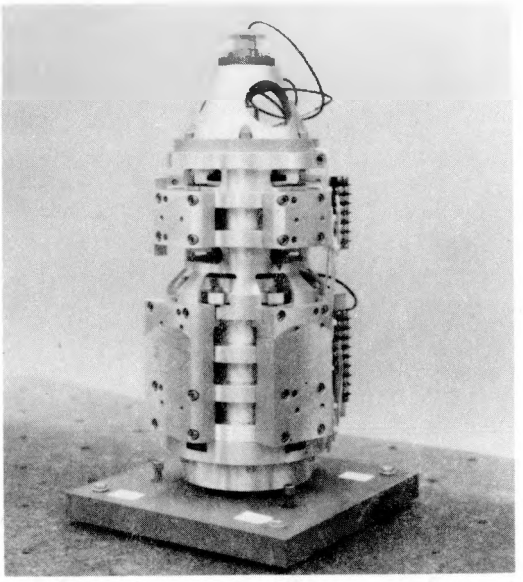

Fig. 10-45. Photograph, six-element prototype magnetic bearing.

C74-1108A

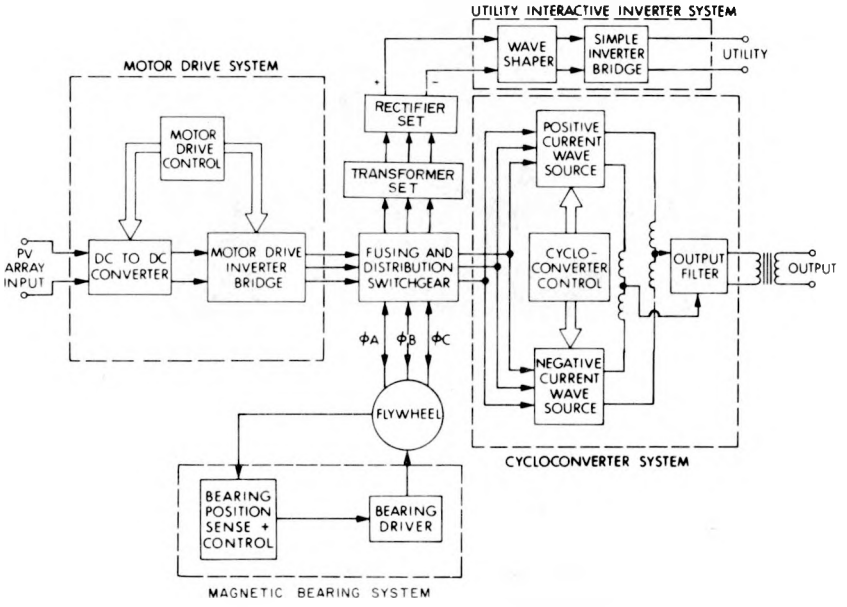

Fig. 10-46. Diagram of 1/10-scale flywheel unit electrical system.

CP267-6117

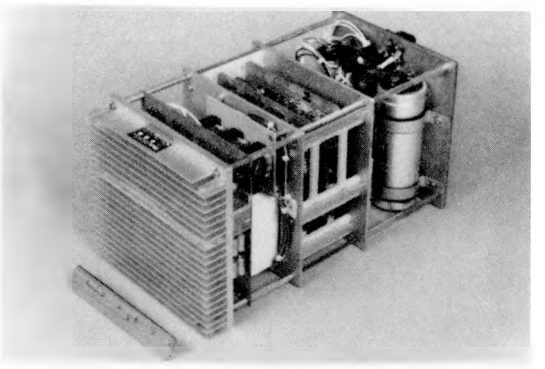

Fig. 10-47. 1 kW utility-interactive inverter.

OUTPUT POWER .75 KW

C74-1009

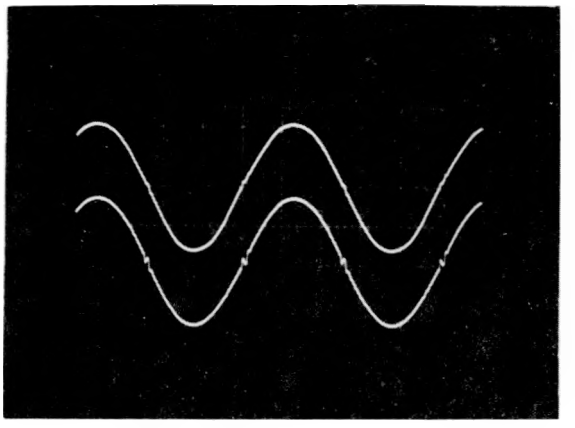

UPPER TRACE - UTILITY VOLTAGE
LOWER TRACE - UTILITY CURRENT

Fig. 10-48. Utility-interactive inverter output power waveform (less than 2% total harmonic distortion).

10.7.4 Measurements on 1/10-Scale Prototype System

Careful measurements were made on the 1/10-scale prototype flywheel unit to determine the overall in-out electrical storage efficiency and the component power-transfer efficiencies when the unit was operating in either a utility-interactive mode or a stand-alone mode. A measurement accuracy of $\pm 0.5\%$ was achieved through use of calibrated power meters and by conducting the tests in a hard vacuum of 10^{-6} to 10^{-7} torr to eliminate rotor aerodynamic friction drag effects and associated data corrections. The measured in-out storage efficiency of the utility-interactive inverter flywheel unit was 82% for a storage time of one hour and 80% for a 10-hour storage time (Table 10-6). The stand-alone cycloconverter-equipped flywheel unit exhibited efficiencies of 67% for a one-hour storage time and 65% for 10-hour storage time (Table 10-7). For comparison, battery-inverter systems for the same application have storage efficiencies of ~67%.

TABLE 10-6

MEASURED EFFICIENCY - UTILITY-INTERACTIVE MODE*
300 Watts In
500 Watts Out

Component	Flywheel Speed: Efficiency (percent) 10,000 RPM	12,000 RPM	13,500 RPM
DC-to-converter	98.7	99.1	99.5
Motor electronics	94.2	94.3	93.0
Motor	98.9	98.2	97.5
Generator/rectifier	95.0	96.9	96.7
Utility-interactive inverter	93.4	92.5	92.1
Tare loss (per hour)	0.2	0.3	0.4
Overall In-Out Efficiency			
(1-hour storage time)	81.4	82.0	80.0
(10-hour storage time)	79.9	79.8	76.9

*Efficiencies determined with 300 W (dc) input power levels and 500 W (ac) output power levels.

TABLE 10-7

MEASURED EFFICIENCY - STAND-ALONE MODE

300 Watts In
500 Watts Out

Component	Flywheel Speed: 7500 RPM	10,000 RPM	12,000 RPM	13,500 RPM
	Efficiency (percent)			
DC-to-DC converter	98.1	98.7	99.1	99.5
Motor electronics	94.0	94.2	94.3	93.0
Motor	98.6	98.9	98.2	97.5
Generator/cycloconverter	76.6	72.5	70.0	68.0
Tare loss (per hour)	0.1	0.2	0.3	0.4
Overall In-Out Efficiency				
(1-hour storage time)	69.5	66.5	64.0	61.1
(10-hour storage time)	68.9	65.3	62.3	58.9

Total spin down tare losses were found to be a maximum of 4 W at 15,000 RPM and to decrease linearly with RPM below 15,000 RPM (Fig. 10-49). This represents a loss of less than 1/2 of 1% of the stored energy per hour.

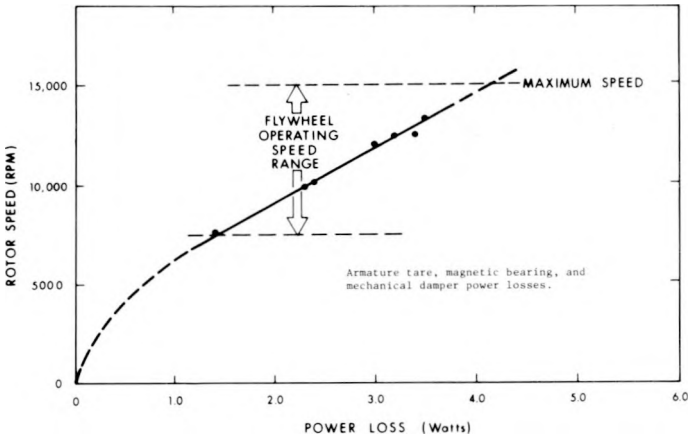

Fig. 10-49. Spin-down tare loss.

10.7.5 Advanced Prototype Flywheel Unit

An advanced prototype flywheel storage unit (Fig. 10-50), with a simplified two-element magnetic bearing to reduce costs (Figs. 10-51 and 10-52), and a composite rotor (Fig. 10-53), was designed, fabricated and tested. The composite rotor which was provided by DOE weighed 123 pounds and stored 1 kWh at 15,000 RPM. The primary material in the rotor was a Kevlar/epoxy composite. The

rotor was originally designed for a vehicular application. The advanced prototype test program was undertaken for two reasons: (1) to determine the effects of rotor flexibility on the operation of the magnetic bearing; (2) to assess the need for additional external damping requirements of an advanced composite rotor, arising from internal hysteresis effects, in comparison with those for a steel rotor. (The development of low-frequency whirl modes due to internal hysteresis effects in the test of the 1/10-scale prototype steel flywheel system, and their elimination by the addition of external damping, had been shown earlier (30) to be an important consideration in the design of any flywheel system.)

These tests were only partially completed when the rotor failed (Fig. 10-54). Testing had been performed up to speeds of 12,000 RPM, as compared with the design goal of 15,000 RPM. The failure is believed to be the result of a fatigue situation in the rotor support spokes.

CP267-6950

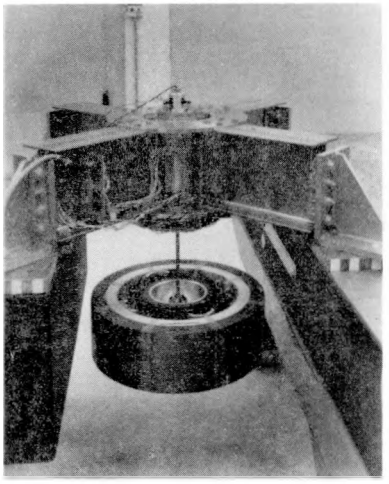

Fig. 10-50. Advanced prototype flywheel storage unit.

CP267-6942

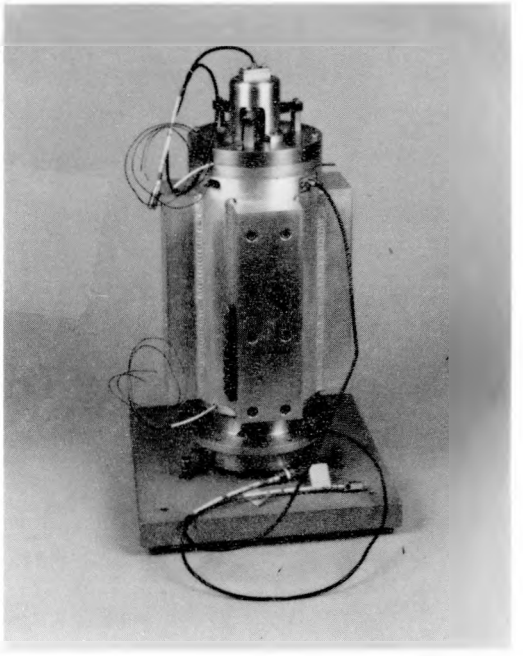

Fig. 10-51. Simplified two-element magnetic bearing.

C74-1480

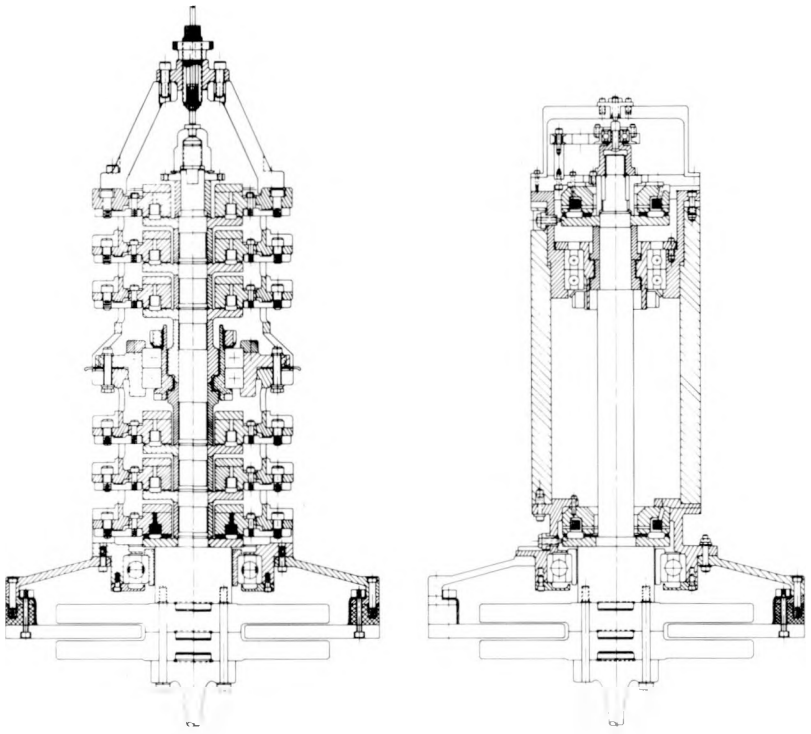

Fig. 10-52. Original six-bearing design (left) compared with new two-bearing design (right).

CP267-6338

Fig. 10-53. Composite rotor.

CP267-7084

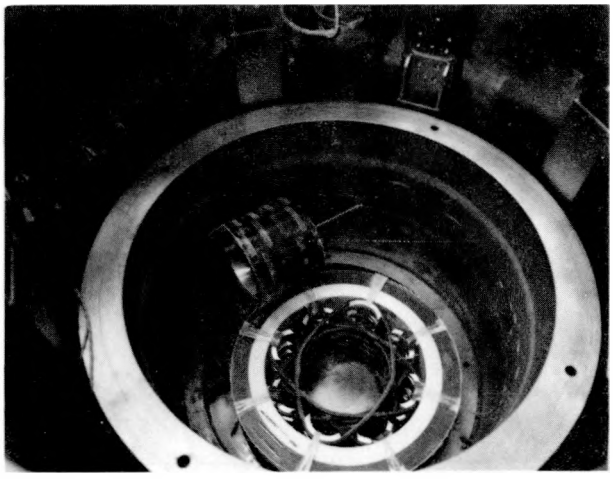

Fig. 10-54. Composite rotor in containment vessel following its failure.

10.7.6 Conclusions

On the basis of the Laboratory's technical development of flywheel systems and system studies of their usage in a residential PV application, the following conclusions may be drawn:

1. Given modest production quantities (thousands per year), flywheel energy storage units would be economically equal if not superior to conventional lead-acid and advanced battery storage.
2. Techniques are available for building efficient and reliable magnetic suspension systems which are sufficiently rugged to withstand earthquake loadings.
3. Further development and testing is required to mitigate the harmful effects of composite rotor hysteresis on system stability.

REFERENCES

Section 10.2

1. Blake, F. A. and Hanson, K. L., "The 'Hot-Spot' Failure Mode for Solar Arrays," Proc. IEEE 1969, pp. 575-581.

2. Forman, S. E. and Themelis, M. P., "Performance and Reliability of Photovoltaic Modules at Various MIT Lincoln Laboratory Test Sites," Proc. of IEEE PV Specialists' Conference, 1980, pp. 1284-1289.

3. Cox, C. H., Silversmith, D. J. and Mountain, R. W., "Reduction of Photovoltaic Cell Reverse Breakdown by a Peripheral Bypass Diode," Proc. 16th IEEE PV Specialists' Conference, San Diego, CA, 27-29 September 1982, DOE/ET/20279-228.

4. Ross, R. G., "Flat-Plate Photovoltaic Module and Array Circuit Design Optimization," Low-Cost Solar Array Project Workshop Proc., JPL, March 1980.

5. Diamond, R. M., "Advanced Developments of Integral Diode Solar Cells," Proc. IEEE PV Specialists' Conference, 1972, pp. 196-200.

6. Giuliano, M., et al., "By-pass Diode Design, Application and Reliability Studies for Solar Cell Arrays," Proc. IEEE PV Specialists' Conference, 1981, pp. 997-1000.

7. Shurmer, H. V., "Backward Diodes as Microwave Detectors," Proc. IEEE, Vol. III, No. 9, 1964, pp. 1511-1516.

8. Lesk, I. A., et al., "Germanium and Silicon Tunnel Diodes - Design, Operation and Application," Proc. IRE Ucscon, 1959, part 3, pp. 9-31.

9. Sze, S. M., Physics of Semiconductor Devices, 2nd Edition, John Wiley and Sons, New York, 1981.

10. Moll, J. L., Physics of Semiconductors, McGraw Hill, New York, 1964.

Section 10.3

11. Hendrie, S. E., "Evaluation of Combined Photovoltaic/Thermal Collectors," presented at the ISEE International Congress and Silver Jubilee, Atlanta, GA, 1979.

12. Hendrie, S. D. and Raghuraman, P., "A Comparison of Theory and Experiment for Photovoltaic/Thermal Collectors," presented at the 14th IEEE PV Specialists' Conference, San Diego, CA, 1980, COO-4094-74.

13. Raghuraman, P., "Analytical Prediction of Liquid Photovoltaic/Thermal Flat Plate Collector Performance," MIT Lincoln Laboratory Technical Report, 29 November 1979, COO-4094-66.

References (continued)

14. Raghuraman, P., "Analytical Prediction of the Performance of an Air Photovoltaic/Thermal Flat-Plate Collector," MIT Lincoln Laboratory Technical Report, 30 April 1980, DOE/ET/20279-93.

15. Hendrie, S. D., "Photovoltaic/Thermal Collector Development Program--Final Report," MIT Lincoln Laboratory Technical Report, March 1982, DOE/ET/20279-168.

Section 10.4

16. Thekaekara, M. P., "Data on Incident Solar Energy," The Energy Crisis and Energy from the Sun, M. P. Thekaekara, Ed. Proc. Symposium on Solar Energy Utilization, Washington, DC, 30 April 1974.

17. Jenkins, F. A. and White, H. E., Fundamentals of Optics, 4th Ed. McGraw-Hill, NY, 1976, p. 523.

18. Gray, D. E., American Institute of Physics Handbook, 3rd Edition, McGraw Hill, New York, 1972, p. 6-124 to 6-125.

19. Cox, C. H., "Modifications to Solar Cells for Use in Photovoltaic/Thermal Collectors," in press, Solar Cell.

20. Mandelkorn, J. and Lamnect, J. H., "Advances in the Theory and Application of BSF Cells," Proc. 11th IEEE PV Specialists' Conference, Phoenix, AZ, 6-8 May 1976, p. 36.

21. Giuliano, M. and Wohlgemuth, J., "The Gridded Back Contact and Its Effect on Solar Cell Performance," 15th IEEE PV Specialists' Conference, Kissimmee, FL, 12-15 May 1981.

22. Arndt, R. A., Allison, J. F., Haynos, J. G., and Meutenberg, A. Jr., "Optical Properties of the COMSAT Non-Reflective Cell," Proc. 11th IEEE PV Specialists' Conference, Phoenix, AZ, 6-8 May 1976.

23. Cox, C. H. and Raghuraman, P., "Design Considerations for Flat-Plate Photovoltaic/Thermal Collectors," submitted for journal publication.

Section 10.6

24. Landsman, E. E., "Analysis and Test of Line-Commutated Inverters for Use in Photovoltaic Power Systems," MIT Lincoln Laboratory Technical Report, February 1981, DOE/ET/20279-115.

25. Landsman, E. E., "Evaluation Tests of Abacus 6-kVA Utility-Interactive Inverter," Energy Systems Engineering Technical Note, September 1981, DOE/ET/20279-145.

26. Nichols, B. E., "Evaluation of Recent Residential Inverters," MIT Lincoln Laboratory Technical Report, June 1982, DOE/ET/20279-205.

References (continued)

27. Landsman, E. E., "Loss of Line Shutdown for a Line-Commutated Utility-Interactive Inverter," MIT Lincoln Laboratory Energy Systems Engineering Technical Note, March 1981, DOE/ET/20279-128.

28. Landsman, E. E., "Classification and Technical Review of DC-AC Inverters for Use in PV Power Systems," MIT Lincoln Laboratory Technical Report, April 1979, DOE/ET/20279-125.

29. Landsman, E. E., Rasmussen, N. E. and Cox, C. H., III, "A DC to AC Inverter Based on Waveshaping," MIT Lincoln Laboratory Technical Report, June 1982, DOE/ET/20279-191.

Section 10-7

30. Jarvinen, P. O., "A Flywheel Energy Storage and Conversion System for Photovoltaic Applications - Final Report," MIT Lincoln Laboratory Technical Report, March 1982, DOE/ET/20279-159.

31. Dinwoodie, T. L., "Flywheel Storage for Photovoltaics: An Economic Evaluation of Two Applications," February 1980, MIT Report No. MIT EL-80-002.

BIBLIOGRAPHY FOR SECTION 10.3

1. Wolf and Martin, "Performance Analysis of Combined Heating and Photovoltaic Power Systems for Residences," University of Pennsylvania Report, Philadelphia, PA, 1975.

2. Kuzay, Malilk and Boer, "The Solar Collectors of Solar One," Institute of Energy Conversion Report, University of Delaware, Newark, DE.

3. Russell, M. C., "Solar Photovoltaic/Thermal Residential Systems," MIT Lincoln Laboratory, Lexington, MA, 1979, DOE Report COO-4577-9.

4. "Conceptual Design and System Analysis of Photovoltaic Systems," Westinghouse Corporation/DOE Report ALO-2744-13, Westinghouse Corporation, Pittsburgh, PA, 1977.

5. "Conceptual Design and System Analysis of Photovoltaic Systems," General Electric Co./DOE Report ALO-3686-14, General Electric Company, Philadelphia, PA, 1977.

6. Cox, C. H. and Raghuraman, P., "Design Considerations for Flat-Plate Photovoltaic/Thermal Collectors," submitted for journal publication.

7. Dinwoodie and Kavanaugh, "Cost Goals for Residential Photovoltaic/Thermal Liquid Collector System Set in Three Northern Locations," MIT Energy Laboratory Report, MIT Energy Laboratory, Cambridge, MA, October 1980, 80-0-28.

8. Cox, C. H., "Design of Solar Cells for Use in Photovoltaic/Thermal Collectors," presented at the ASME Winter Annual Meeting, Washington, DC, 1980, p. 12, DOE/ET/20279-97.

9. Nowlan, M. J., "Design and Fabrication of Air and Liquid Cooled Photovoltaic/Thermal Collectors," prepared for Lincoln Laboratory by Spire Corporation as subcontractor, March 1981, DOE/ET/20279-162.

10. Aiello, W. A. and Raghuraman, P., "Performance of a Combined Photovoltaic/Thermal, Flat-Plate, Liquid Collector," presented at the ASME Heating and Cooling Operational Results Conference, Reno, NV, May 1981, DOE/ET/20279-111.

11. Raghuraman, P. and Kon, D., "On Reducing Convective Losses from Cover Glazings of Solar Thermal Collectors," presented at the ASME Winter Annual Meeting, Washington, DC, November 1981, DOE/ET/20279-146.

11.0 RESIDENTIAL SYSTEMS TESTS

11.1 Background Information

An important element of DOE's National Photovoltaic Program (1) was the development of grid-connected PV applications such as residential PV systems. Accordingly, Lincoln Laboratory was asked by DOE to prepare an implementation plan for residential PV activity (2). The resulting plan was based on establishing Residential Experiment Stations in the Northeast, Southwest and Southeast. The Northeast Residential Experiment Station (NE RES) in Concord, Massachusetts, and the Southwest Residential Experiment Station (SW RES) in Las Cruces, New Mexico, began operations in 1980 and 1981, respectively. A Southeast Residential Experiment Station was initiated by DOE in September 1982, following the conclusion of Lincoln Laboratory's involvement in the system activities of the National Photovoltaic Program.

Each of the Residential Experiment Stations of the Solar Photovoltaic Residential Project was designed to meet two basic objectives: residential PV system development and evaluation. The following sections summarize information contained in two reports (3,4) which provide complete results of testing and evaluating prototype residential PV systems at the NE and SW RESs, respectively.

Five prototype residential PV systems were built at the NE RES during the 1980-1981 period, followed by eight systems at the SW RES; none of the prototypes is habitable. Each prototype system consists of a roof-mounted PV array, sized to meet at least 50% of the annual electrical demand of an energy-conserving house, and an enclosed structure to house the remainder of the PV system equipment, test instrumentation and work space. Each prototype structure is the minimum size building which can accommodate the PV system.

Each RES also contains a residential data system with extensive data collecting, formatting and reducing capability. The data systems were designed to be compatible with telephonic transmission of digital data from locations physically remote from the RES. Accordingly, each RES also serves as a data collection and reduction center for other PV experiments, such as measurements relating to utility interaction and performance monitoring of experimental PV residences located in the region of the particular RES.

Development and evaluation of the uninhabited prototypes at the Experiment Stations was augmented by installing and evaluating experimental PV systems in residences located at various places off the Experiment Station sites. Seven such systems were constructed, of which five are inhabited; they are located in the following places:

University of Texas at Arlington, Arlington, TX (inhabited)
Carlisle, MA (inhabited)
Three systems in Hawaii (inhabited)
Cape Canaveral, FL (uninhabited)
Phoenix, AZ (uninhabited).

The development and evaluation activity relating to all of these PV systems is summarized in the following sections. Section 11.2 deals with the systems at the NE and SW Residential Experiment Stations. The data systems which serve the RESs (and, in the case of the NE RES, the Carlisle PV House) are described in Section 11.3. Finally, the seven experimental residences mentioned above are described in Section 11.4.

Contributions at the NE RES were made by the following individuals: Alfred E. Benoit, Henry J. Bullwinkel, Matthew E. Buresch, Joseph W. Chludzinski, Joseph D. Doucet, Harvey A. Fenton, George W. Hart, John T. Kelly, Jr., Edward C. Kern, Jr., Peter C. Mahoney, Carl H. Much, Burt E. Nichols, Vincent J. Pybus, Miles C. Russell and Michael C. Wong.

Contributions to the Lincoln Laboratory effort at the SW RES were made by the following individuals: Harvey A. Fenton, James W. Harrill, Peter C. Mahoney, Carl H. Much, Burt E. Nichols and Miles C. Russell, and by New Mexico State University personnel under the leadership of John F. Schaefer, Director of the Southwest Residential Experiment Station, and Harry B. Zwibel, Director of the New Mexico Solar Energy Institute.

11.2 Prototype Systems at the Northeast and Southwest Residential Experiment Stations

11.2.1 Northeast Residential Experiment Station (NE RES)

At the NE RES located in Concord, Massachusetts, five prototype systems are under test. To gauge quantitatively the ability of the prototype systems to meet residential load demands, five residences in the vicinity of the NE RES (monitored houses), representative of the occupancy and loads found in the area, were equipped with instrumentation which continually records the residences'

electrical energy consumption. Telephone lines carry load information from these monitored houses to the NE RES where the data are recorded. One of the monitored houses provides a common programmable load profile for all prototype PV systems--thereby simulating an actual residential electrical load and permitting side-by-side comparison of the prototypes under essentially identical load conditions.

The extensive data system at the NE RES also monitors the performance of the five prototype systems and the site meteorological conditions. The data are then analyzed, reduced and published in monthly reports (5-16). Additional information on the retrieval, processing and dissemination of data collected by the residential data system is given in Section 11.3

In addition to the routine operation of the prototype systems, special tests of limited duration were conducted. The goals of such tests were to characterize the electrical performance of the systems and their components, and to verify proper operation of the systems under both normal and abnormal operating conditions. The prototype system evaluation procedures are described in Reference 17.

Figure 11-1 is an aerial view of the NE RES. The site became operational with the installation of the first of five prototype systems in November 1980, and consists of the five prototype systems and space in the facility building (at the top of the photograph) for offices and data system equipment. Meteorological instrumentation is mounted on the facility building roof.

CP267-6876

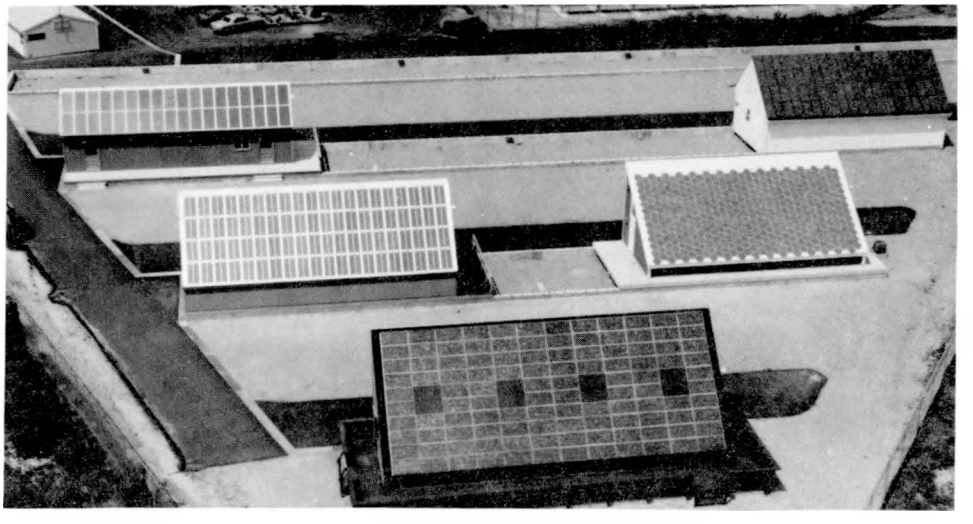

Fig. 11-1. Aerial view of NE RES.

The NE RES is located approximately fifteen miles northwest of Boston, Massachusetts. The latitude is 42.46°N, the longitude is 71.30°W, and the elevation is 131 feet.

Record extreme temperatures	-12°F, 102°F (Logan Airport)
Annual heating degree days	5620°F days
Annual cooling degree days	660°F days
Annual average relative humidity	67%
Annual average rainfall	37 in.
Annual average snowfall	48 in.
Annual total horizontal insolation	1271 kWh/m^2.

The five prototype systems at the NE RES present a diversity of PV modules, array sizes/powers, array roof-mounting techniques, array electrical configurations, and inverters. Table 11-1 lists the general system features. For additional information on the prototypes, see the final report on the NE RES prototypes (3), and the final reports written by the manufacturers of the prototypes (18-21).

TABLE 11-1

NE RES PROTOTYPE SYSTEMS: PHYSICAL FEATURES

System Supplier	PV Module Manuf.	PV Array* Area(M^2)	PV Array Peak Rated Power(kW)	Array Tilt Angle(Deg)	Array Mounting Method	Power Cond. Manuf.	Power Cond. Manuf. Rating(kW)
GE	GE	76.8	6.6	33.7	Direct	Abacus	6(AC)
MIT LL	Solarex	84.9	6.8	45.	Standoff	Windworks	8(DC)
Solarex	Solarex	68.4	5.0	40.	Standoff	Abacus	6(AC)
Westinghouse	Arco Solar	69.2	5.1	45.	Integral	Abacus	6(AC)
TriSolarCorp	ASEC	47.2	4.8	45.	Integral	Windworks	8(DC)

*Area of active modules only.

11.2.1.1 Evaluation of NE RES Prototypes

Over the past year and a half of residential PV system testing and evaluation, insights were gained into how the systems work, how they fail and how often they do either. The five systems were evaluated from engineering performance, safety and cost standpoints, and what follows is a summary of some of the significant lessons learned at the NE RES, to provide a record of past experiences as well as to focus attention on any system design weaknesses or areas where further study and experiment are required.

- PV Array Reliability - The PV arrays are more reliable than the power conditioners to which they were originally connected. Further, most module failures are benign; that is, a system will continue to operate with one or even several failed modules.
- Power Conditioner Performance - Some of the second-generation power conditioners--which were developed largely due to deficiencies found in the units originally installed in the prototype systems--exhibit improved reliability and performance.
- Maximum-Power-Point Tracking - The performance of the Abacus maximum-power-point tracker at actually following the PV array maximum power point was very poor. The pilot-cell control, which replaced the maximum-power-point tracker, is a superior array-controlling circuit. Ideal maximum-power-point tracking yields only marginal increases in annual PV energy production over fixed-voltage operation, at the expense of additional circuitry and complexity.
- Array I-V Curve Measurement - Array I-V curves are a fundamental measurement which must be made to characterize a PV array and also to diagnose a module failure condition. Instruments to make these measurements were designed and built by the Laboratory as they were not available commercially at the time.
- PV Array Rating - Determining the rating of a PV array is difficult and challenging given the variation in cell temperature across an array, the difficulty in measuring an accurate cell temperature, the uncertainty associated with using a pyranometer insolation reference, and the soiling of the array top surface.
- Power Degradation from Soiling - At the NE RES array, power degradation due to accumulation of natural airborne soilants over a one-year period was so small that it was impossible to determine from I-V curve data, due to the measurement uncertainties arising from inherent limitations of the pyranometer, non-uniformity of module temperatures in an array, and variations in meteorological conditions from one measurement to the next.

- Array Maintenance: Finding Module Failures - The time required to locate a failed module in an array is highly dependent upon the array wiring configuration, and the level of wiring accessibility. Arrays with a small number of modules and electrical access to each module are easier to diagnose than arrays with a large number of modules and limited electrical access.

- Peak Array Power Output - Maximum array power output was measured in the months of February or March and maximum energy production was measured in April or May. The maximum array power was as high as 1.3 times the peak rated power.

- Peak Solar Irradiance - Tilt irradiance as high as 1.37 kW/m^2 has been measured at the NE RES and can be expected in other sites as well. Higher values have been measured (approaching 1.5 kW/m^2) at other Lincoln Laboratory field sites.

- Array Maintenance: Washing - Array washing was accomplished easily by a professional window washer using standard equipment and procedures. Total labor involved averaged three and a half man-hours per array.

- Snow - Snow on the PV arrays is a common wintertime occurrence. Snow shedding occurs at unpredictable rates and in unpredictable patterns. Worst-case snow cover events during the evaluation period resulted in reduced system output for two and a half days. Pilot-cell array control is vulnerable to occlusion of the pilot cell by snow. During array snow-cover conditions, the pilot-cell-controlled systems often operated erratically or not at all, depending upon the relative cell/array snow cover. Snow infiltration into an attic space beneath a PV array did occur, but was a result of architectural design inadequacies, and was not the fault of the PV array.

- Safety - The sole safety-related event in the entire Lincoln Laboratory Program occurred during installation of the Solarex array. One workman was installing the Unistrut™ frames on the roof which eventually would hold the Solarex modules. The frames were hoisted up to a staging platform and the pieces installed one at a time into a rectangular grid pattern. While on the staging, the workman was testing the uniformity of the frame rectangles by holding a module-sized sheet of glass up to each frame. The glass slipped, the workman tried to recover it, and both fell to the ground. The glass was broken and the workman bruised and shaken. The lesson learned here is simple--never work alone, and do not risk personal safety in order to save falling equipment.

- PV Array Operating Temperatures - PV-array operating temperatures vary widely among the five systems' mounting methods. In one array, temperature variation from module to module as high as 25°C was observed. One of the future areas of investigation at the NE RES is the modification of array installations to enhance passive cooling.

- Cost - Minimizing materials reduces array installation costs dramatically. This is likely to be a necessary system feature to insure future economic viability. Investigation of low-cost retrofit mounting methods should be pursued. Present PV system costs are dominated, however, by the PV array price. This item has the greatest leverage over system economics.

Of interest to system designers are the system performance extrema experienced over a twelve-month operating period. Records of such extrema were kept for the five NE RES prototype systems and are summarized in Table 11-2.

Note that the General Electric, Solarex and Westinghouse prototypes have not operated during all months and therefore may not show extrema values for some quantities as high as would be expected based on comparison with the other systems.

TABLE 11-2

SYSTEM PERFORMANCE EXTREMA

	General Electric*	MIT Lincoln Laboratory	Solarex*	TriSolarCorp	Westinghouse*
PV ARRAY					
Peak Rated Power (kW)	6.6	6.8	5.0	4.8	5.1
Days Power Exceeded Rated Power	2	69	12	43	21
Total Days of Operation	139	422	60	475	133
Peak Measured Power (kW)	6.9	9.0	6.3	6.0	6.4
Irradiance (kW/m^2)	1.05	1.20	1.30	1.26	1.26
Cell Temperature (^oC)	17.5	23.8	36.9	30.0	21.7
Date	1/17/82	3/2/82	4/18/82	2/18/82	2/18/82
Peak Irradiance (kW/m^2)	1.37	1.26	1.30	1.29	1.26
Date	4/18/82	4/18/82	4/18 + 3/20/82	4/18/82	2/18/82
NOCT (^oC)	60.8	54.4	54.3	47.5	58.3
Max. Meas. Cell Temp. (^oC)	80.0**	80.0**	68.1	59.4	65.8
Irradiance (kW/m^2)	1.28	1.18	1.30	0.89	0.91
Ambient Temp. (^oC)	29.5	32.5	9.6	27.7	27.6
Date	7/6/81	7/7/81	3/20/81	7/31/81	7/31/81
Max. Energy Output (kWh/day)	37.2	49.5	32.4	30.5	29.4
Insolation (kWh/m^2-day)	7.2	7.0	7.4	6.9	6.5
Date	6/31/81	4/14/82	4/14/82	5/13/81	7/10/81
Avg. Monthly Output (kWh/day)	29.4	30.5	21.7	20.2	20.7
POWER CONDITIONER					
Peak Measured Power (kW)	5.7	8.3	5.3	5.6	5.4
Date	1/17/82	3/2/82	4/18/82	2/18/82	2/18/82
Max. Energy Output (kWh/day)	30.2	45.0	27.6	27.8	24.6
Date	6/13/81	4/14/82	4/14/82	5/13/81	7/10/81

* System not operative all months.

** Maximum sensor reading possible. Actual value may have been higher.

The array peak rated power (array maximum power at 1000 W/m^2 irradiance and a cell temperature of 25^oC) is shown as the first entry in Table 11-2. Following this is the number of days when the measured array power exceeded this peak rated power. As can be seen from the table, the two systems that operated for twelve full months, Lincoln Laboratory and TriSolarCorp, achieved higher-than-rated power many times: 69 for Lincoln Laboratory and 43 for

TriSolarCorp. The occurrences of higher-than-rated array power happen only between late September and mid-April. They are a regular and frequent condition in all the included months except December. For example, the Lincoln Laboratory array exceeded rated array power on each of 13 days in February 1982, 15 days in March 1982, and 11 of the first 18 days of April 1982. The TriSolarCorp prototype exhibited a similar pattern: 10 days in February, 13 days in March, 8 days in April. There are several further observations that can be made:

- A greater number of higher-than-rated array power incidences occur between the winter solstice and the vernal equinox, than between the autumnal equinox and the winter solstice (i.e., there are more occurrences on the "spring side" than the "autumn side" of the solstice). This is due to lower prevailing ambient, and therefore PV cell, temperatures in those spring-side months, and a greater percentage of clear-sky, high irradiance days, as well as some enhancement due to reflections from snow.
- Conversely, higher-than-rated array powers have never been measured during the summer months, principally due to the high ambient and cell operating temperatures.
- Despite the lack of operating data for a complete 12-month period, it appears that the direct-mount PV array will register many fewer higher-than-rated array power days than the other systems. This is not unexpected, since the direct-mount array typically operates hotter than either the standoff or integral arrays.

It is also of interest to note the magnitude of the highest recorded array power for each system. For the Lincoln Laboratory array, the peak measured power is 9.0 kW, which is 32.4% more than the peak rated power. The other systems have recorded peaks approximately 25% greater than their ratings, except for the General Electric prototype which was not operating during the prime, peak-power-producing months. The ratio of the peak measured, or expected, power to the peak-rated power is of interest to those designing PV systems as it affects component sizing, circuit fusing, and array-voltage/current-control strategy. From the results cited above, it seems likely that a 25 to 30% increase over the peak rated power can be expected in this region of the country.

Of similar interest is the peak irradiance on the array surface. The highest recorded tilted irradiance was 1370 W/m^2, measured in April on the

General Electric (33.7° tilt from horizontal) array. Irradiance of this magnitude occurs only when there is significant enhancement due to diffuse irradiance from reflective clouds, in addition to unattenuated direct irradiance.

11.2.2 Southwest Residential Experiment Station (SW RES)

The Southwest Residential Experiment Station (SW RES) was established by the New Mexico Solar Energy Institute (NMSEI) with technical support from Lincoln Laboratory, and has been in operation since October 1980 on the New Mexico State University campus in Las Cruces, New Mexico (Fig. 11-2). The 3.26-acre site contains a Photovoltaic Center and eight prototype systems. The Center, a 3,000-square-foot, passive-solar-heated building funded by the New Mexico Energy Research and Development Program, houses offices, a visitor center, a shop, and the residential data system used to monitor the performance of prototype systems and the energy demand profiles of several existing residences in the Las Cruces area.

CP267-7122

Fig. 11-2. Aerial view of SW RES.

The SW RES is located at a latitude of 32° 17'N, a longitude of 106° 45'W, and an elevation of 3,930 feet above mean sea level.

Annual average temperature range	$43.7^{o}F - 76.5^{o}F$
Annual heating degree days	$3,200\ ^{o}F$-days
Annual cooling degree days	$1,600\ ^{o}F$-days
Annual average precipitation	8.4 in.
Annual average relative humidity	40%
Annual total horizontal insolation	$2,135\ kWh/m^2$.

The Prototype Systems at the SW RES

There are eight residential PV prototype systems at the SW RES. As was the case with the NE RES prototypes, each prototype is based on a specific residence design, and the PV system is identical to that designed for the residence in all respects: structural, mechanical, electrical and thermal. Table 11-3 lists the general features of the eight prototype systems. For additional information on the prototypes, see the report on the SW RES (4), and the final reports written by the manufacturers of the prototypes (22-29).

TABLE 11-3

SW RES PROTOTYPE SYSTEMS: PHYSICAL FEATURES

System Supplier	PV Module Manuf.	PV Array* Area(M^2)	PV Array Peak Rated Power(kW)	Array Tilt Angle(Deg)	Array Mounting Method	Power Cond. Manuf.	Power Cond. Manuf. Rating(kW)
ARTU	Arco Solar	55.2	4.9	45.	Standoff	Windworks	8(DC)
Arco Solar	Arco Solar	91.6	7.4	25.	Direct	Windworks	8(DC)
BDM	Motorola	54.0	4.5	35.	Standoff	Abacus	6(AC)
GE	GE	76.2	6.7	27.	Direct	Abacus	6(AC)
Solarex	Solarex	70.2	5.1	26.	Standoff	Abacus	6(AC)
TEA	Motorola	49.4	4.3	26.	Rack	Abacus	6(AC)
TriSolarCorp	ASEC	58.0	5.3	30.	Integral	Windworks	8(DC)
Westinghouse	Arco Solar	75.2	5.5	30.	Integral	Abacus	6(AC)

*Area of active modules only.

11.2.2.1 Evaluation of SW RES Prototypes

Experience gained by evaluating the eight prototype systems at the SW RES has been similar to that of the NE RES. The large number of systems at the SW RES has proven valuable for evaluating the merits of a diversity of components, array roof-mount concepts, array-cooling schemes, and power-conditioning

units, as well as the interaction among the systems. The following partial list of lessons learned is summarized from Reference 4. For additional performance information, see the monthly performance summaries prepared by the SW RES (30-37).

- Array Temperatures - Array-mounting methods and module design both heavily impact array-operating temperature and, hence, array efficiency. Both factors are believed to require substantial further work.
- Supplemental Cooling - One of the two cooling methods employed in SW RES prototypes has potential for being cost-effective, one apparently does not. Work continues to quantify the effects and performance of each.
- Shipping Costs - The ASEC modules on the TriSolarCorp prototype incorporated 4-in.-deep junction boxes on the rear substrate. Although they were convenient for the electrician, these boxes dramatically increased shipping costs. Their size required that each pair of back-to-back modules be separated by four inches of packing material (rigid foam); resulting in each shipping container being filled with about 85% foam and 15% module. Shipping costs, Los Angeles to Las Cruces, were approximately $3,000, roughly 60 cents per installed watt. The Motorola modules, on the other hand, are about 1-in. deep and were efficiently packed 10 to a carton. Shipping for these modules was $213, Phoenix to Las Cruces. Clearly, the mass-marketed module of the future will either have a slim junction box or code-approved connectors without a junction box.
- Fauna Under Standoff Arrays - On one occasion an owl was found trapped under the ARTU standoff array. A group of modules was lifted and the bird escaped. It was suspected that the owl entered at the roof peak and could not exit at the array foot because of a narrower gap. Future array-mount designs should prevent such occurrences.
- Reflective Roofing Aggregate - It has been confirmed that the white roofing aggregate used in the TriSolarCorp prototype can enhance array performance, but not greatly. A generalized life-cycle/cost-effectiveness study is planned.
- Wiring Costs - Prior to the Critical Design Review, one contractor chose to interpret the NEC very rigorously. The contractor's interpretation was that use of coaxial cable (normally used in radio-frequency applications) with appropriate connectors was the most attractive and acceptable mechanism to accomplish intra-array wiring. Parts cost alone would have exceeded $3,000. After redirection to search for a less costly approach, cost was reduced to about $250.
- Solarex Cap Strips/Battens - It was learned that the 1-1/2-in.-wide plastic battens on the Solarex standoff array cannot be reused. It was further learned that the color (light blue) changed markedly in less than six months of exposure to the New Mexico sun. If array maintenance

involving module lifting or removal is necessary, the result will be aesthetically displeasing unless either all battens are replaced or unused replacement battens have been allowed to age similarly. A redesigned batten with better weathering characteristics may allow reuse.

- Array Installation - There was clear manifestation of a significant learning curve improvement associated with all array installations. For example, the first few modules on the BDM prototype averaged 12 minutes installation time each; the last, about 4-1/2 minutes each.

- Diagnostic Wiring - At NMSEI's request, the GE prototype was fitted with special diagnostic wiring. A special #18-gauge sense wire was run from each row of shingles to an interior junction box. SW RES erred in this installation. Because of the extensive paralleling in the GE array, the resistance associated with these wires of varying length precludes accurate measurement of block current and, therefore, realistic I-V curves. Either heavier or equilength wires should have been required; either would allow meaningful comparison, row to row. It is not yet clear whether such special diagnostic wiring will or should be incorporated in a mass implementation of residential PV systems. If it is, such factors as discussed here should be considered.

- Wind Direction and Array Temperature - An exceptionally strong correlation between wind direction and array temperature was found in the TSC and ARTU implementations. In areas with a strong annual prevalent wind pattern, it may be worthwhile to attempt to capitalize on this phenomenon.

- Wind During Installation - The TSC array was installed at the beginning of the Las Cruces windy season (average wind speeds 7-9 MPH). Array installation was not severely slowed (about 9 man-hours were estimated as lost; total installation labor was 109 hours), but only because of the extra effort of the installation team and the acquiescence and enthusiasm of all involved parties (it was the first SW RES array). If forecasts of 25-square-foot modules being the most cost-effective are correct, then it can be speculated that installation will be avoided during such conditions.

- Owner's Manuals - An owner's manual was not called for as a specific deliverable in the eight prototype systems procurements. More important, not a single one of the eight vendors proposed to furnish an owner's manual. When prompted, most of the eight agreed that it would be appropriate. To date, however, only three have provided acceptable documents. Such manuals will be necessary for future system installations to insure that system owners are well informed.

- Post-installation Cleaning - Following a dust storm shortly after the TEA array installation, finger and palm prints all over the TEA array were noticed from 50-foot distances. A subsequent washing eliminated the marks. In dusty areas such as Las Cruces, it is clear that a post-installation cleaning will be mandatory.

- Energy Loss in Isolation Transformers - Based on the performance of the two Gemini-associated isolation transformers at the SW RES, which consume on the order of 1 kWh per day, it is concluded that either their use not be made mandatory or that investment in more efficient units will probably be life-cycle justified.

- Inverter/Array Rating - Experience with the ARCO system (7.4-kWp array, 8-kW Gemini inverter) suggests that an inverter must be able to tolerate array outputs as high as 1.4 times the peak rated value in the Las Cruces climate (compare to 1.3 times for Boston).

- Inverter Protective Circuitry - SW RES staff strongly believe that all inverters should incorporate protective circuitry, including out-of-voltage and out-of-frequency sensors. Nonetheless, no matter how sophisticated each single inverter's circuitry is, there are potential scenarios in which no single inverter in an aggregate will be able to discern presence of the utility. Thus, utility linesmen should not take it for granted that all inverters on a downed line are inactive, and should both check and ground the feeder according to usual practice.

- Component Ratings - Care must be taken to size properly all the protective circuit elements in the PV system. One subcontractor installed underrated (in voltage) fuseholders and fuses in the array summing junction box. Following an inverter failure that left the array shorted, one of the fuses opened, but an arc struck from fuse end to fuse end. It appears that the arc did not extinguish until conducting components were eroded to a critical distance. Later, a second subcontractor arrived on site with underrated fuses in his summing/junction box. These were upgraded prior to installation.

- Intra-array Wiring - From observation of array-installation activity these conclusions are drawn:

    1. Modules should have bypass diodes installed as shipped from the factory.
    2. Modules should have polarized, plug-in connections.

  The basis for these conclusions is a comparison of the labor hours reported by Solarex and TEA for wiring their corresponding SW RES prototype arrays. Solarex reported a wiring materials cost of $615 and 30 hours of labor. TEA reported $1,085 and 117 hours. It was observed that the actual Solarex wiring effort on-site was substantially less than 30 hours, whereas the 117 hours reported by TEA was almost entirely on site. The principal difference in these costs, which normalize to 21¢/W and 66¢/W, respectively, is attributable to the Solarex modules' integral-bypass diodes and quick-connectors. On the TEA array, it was necessary to remove two Motorola junction box covers, install diodes and connections, replace covers, and make intra-array connections. This is believed to be a significant cost driver.

- Array Maintenance Access - Most of the subcontractors' weakest performance was associated with providing well thought out guidance and/or means for gaining physical access to arrays. As of this writing, one contractor has yet to provide a maintenance ladder for his system.

- Inverter Operating Environment - The ambient temperature ranges specified for three of the inverters at the SW RES are as follows:

Abacus:	$0^{o}C$ to $40^{o}C$
Gemini:	$0^{o}C$ to $40^{o}C$
DECC:	$-18^{o}C$ to $43^{o}C$

  For applications in the Southwest desert, the upper limit must be increased since ambient temperatures routinely exceed $40^{o}C$ in many areas, and unconditioned spaces such as garages and equipment rooms can exceed $50^{o}C$. For equivalent reasons, the lower limits of the Gemini and Abacus must also be extended.

- Importance of Realistic Operating Environment - The great majority of Abacus failures occurred at low-irradiance periods, either during morning wake-up, evening shutdown, or cloudy periods. In hindsight it is easy to say the manufacturer should have cycled the dc power supply, which was probably used to qualify the production inverter, several thousands of times instead of several tens or hundreds of times to check out more fully the wake-up/shutdown circuitry. The point here is that a field test, with real solar irradiation on an array, revealed a deficiency that a relatively thorough laboratory-environment qualification test did not.

11.3 Residential Data System

11.3.1 Introduction

A data system records the performance of the Residential Experiment Station (RES) prototypes, monitored houses, and experimental PV residences located near the RES. To fulfill the requirements of the program, the data system:

- Acquires data from all sensors at each site every 5 seconds, and records on magnetic tape the average or peak value from each sensor every 6 minutes for up to about 800 sensors.
- Saves the 5-second readings for selected channels as a frequency distribution of the values, and records the distribution every 4 hours.
- Communicates 6-minute averages of the sensor values to a variety of on-line recipients in a variety of formats.
- Measures the electrical power consumption at a monitored home, and imposes that load on specific prototypes in virtually real time.
- Accommodates the addition, modification or removal of single sensors or entire sites without human intervention on the data system.
- Displays data values at all levels of the system.

- Makes possible the recording of 5-second readings in time order.
- Makes possible the acquisition of RES data coordinated with the taking of I-V curves at a prototype under computer control.

Contributions to this effort were made by the following individuals: Alfred E. Benoit, Henry J. Bullwinkel, Harvey A. Fenton, Carl H. Much and Burt E. Nichols.

11.3.2 System Description

The data system is a concentrating, three-tier, distributed processing computer system (Fig. 11-3). Control from the central system processor (CSP) fans out through data-concentrator units (DCUs) to data-acquisition controllers (DACs). Information funnels in from the DACs through the DCUs to the CSP and then to the system output device, a magnetic tape recorder, and any other output devices that might be attached. Data from a selected residence DAC are also passed to each prototype DAC which uses them to compute and apply load commands. Further information on the system is given in Reference 38.

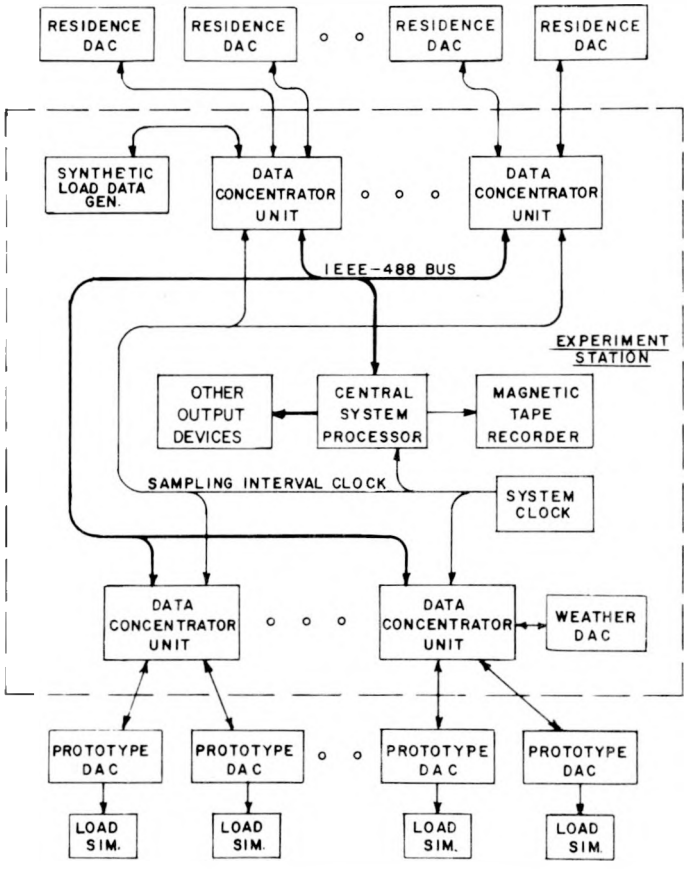

C74-478A

Fig. 11-3. Data system block diagram.

Each data system level, i.e., the CSP, DCUs and DACs, is independent. Each device is a stand-alone processor that continues to function locally despite failure or power outages elsewhere in the system. Each level determines which of its subordinates are on-line. Also, at power-up, devices at each level try to notify the next level up of their presence, but move into steady-state operation regardless of acknowledgment. DACs and DCUs can be added or removed at any time while the rest of the data system continues to operate normally.

System timing is centralized. A single clock keeps track of the time of day and provides sampling time interval interrupts used throughout the system. This synchronizes all levels, resulting in simultaneous sensor readings, and permits changing the sampling interval, presently set at 5 seconds, at one central place.

After sampling the data once every five seconds, the data system then computes an average value for each parameter using a 6-minute averaging period. It should be noted that this provides a factor-of-ten increase in detail over what is currently available from other solar data bases. For example, the SOLMET data base supplied by the U.S. National Climatic Center, National Oceanic and Atmospheric Administration, derives from data sampled once per hour. Lincoln Laboratory conducted experiments to determine whether the 6-minute averaging period was sufficiently short to provide good accuracy (39). In these experiments, the data system was temporarily modified so as to store all of the 5-second data, rather than the 6-minute averaged data. Subsequently, utility-interaction calculations were made from data recorded from one of the NE RES prototypes, in which the amounts of energy supplied to and bought from the utility were determined. Using no averaging (e.g., the 5-second data) as the criterion, the calculations were repeated for ever-increasing averaging intervals. The experiment showed that use of a 6-minute averaging period typically results in errors of less than 8 or 9% in such calculations. On the other hand, it was found that a one-hour averaging period can result in errors as great as 25%.

Emphasis was put on purchasing standard hardware whenever possible to eliminate hardware development time and to allow for vendor maintenance. A

Hewlett-Packard 9845T desktop computer serves as the CSP. Because suitable off-the-shelf units were not available to serve the somewhat specialized functions of the DCUs and DACs, the next best solution was adopted. They are built as microcomputers using the STD bus standard and use complete standardized boards for as many functions as possible. The tape drives are Kennedy 9000 IBM-compatible tape systems.

11.4 Experimental PV Residences

11.4.1 University of Texas at Arlington Residential PV System

11.4.1.1 Introduction

As part of Lincoln Laboratory's Solar Hybrid Energy Project, a grid-connected residential system was installed at the University of Texas at Arlington (UTA) Solar Energy Research Facility, in Arlington, Texas, about halfway between Dallas and Fort Worth (Fig. 11-4).

Contributions to this effort were made by the following individuals: Jack Fitzer, Edward C. Kern, Jr., Miles C. Russell and F. John Solman, III.

11.4.1.2 System Description

The UTA experiment was designed to test various system concepts using both solar PV and solar heating collectors. Since roof-mounted solar heating collectors already were installed at the site, the PV array had to be ground-mounted, as was a second set of flat-plate solar heating collectors (to the west in Fig. 11-4). Details of the system design are provided in Reference 40.

CP267-4531

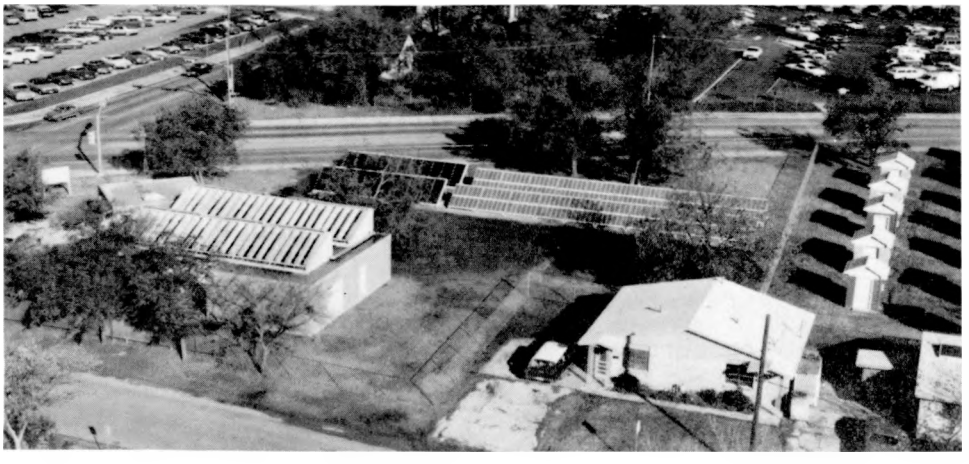

Fig. 11-4. Aerial view of UTA Experiment.

Although the system test at UTA met many of its objectives regarding the design and operation of combined PV/T systems (41), the truly significant contribution of this project lies in the area of integrating photovoltaics and the electric utility grid. The Texas Electric Service Company (TESCO) serves the site and cooperated in this first attempt to tie a PV system to the grid. The Mechanical Engineering Department at UTA, in particular Mr. Steven Kugle, provided the required site management during the design, installation and evaluation of the system configurations tested. Work on the UTA system began in the spring of 1978 with a contract award to UTA to assist Lincoln Laboratory in system installation and testing. Ground-mounted array structures were designed and procured by Lincoln Laboratory, then shipped to UTA along with a power-conversion unit and the modules needed for the array. The modules used were made by the Solar Power Corporation and purchased under the Block II procurement by the Jet Propulsion Laboratory's Low-Cost Solar Array Project during 1976-1977. The power conditioner used was a Gemini model PCU-80-1 manufactured by Windworks, Inc. A conventional isolation transformer was used for electrical isolation of the array from the utility.

During the course of the experiments at UTA, the array of 240 Solar Power Corporation modules failed, apparently owing to hot-spot heating effects caused by the short circuiting of the array field for washing and inspection during June 1979. With module failure defined as degradation leading to operation at less than 75% of nominal power, 63 modules (26.2%) failed during the first ten months of operation, mostly during the summer of 1979 following the washing/inspection. Additional details are provided in Section 6.9.

During the fall and winter of 1979-1980, the failed modules were removed from the array, and the remaining good modules were used to maintain as many good complete strings as possible. Finally, in March 1980, the array of Solar Power modules was completely removed and replaced with modules made by Sensor Technology, model number 20-10-1646. As these are smaller, 640 modules were used to fill the array field which had a nominal rating of 6.4 kW. One problem with the new array is that the modules have exposed contacts on the back surface, leading to an electric-shock hazard. The danger was alleviated with a fence and a wire-mesh screen covering the back surface of the array.

A Gemini inverter is used in the UTA system. During the initial period of operation, this inverter exhibited a control instability at dc currents below 5 A when the amount of sunlight was low. This problem was corrected in December 1979 by revising the control circuitry. The isolation transformer used in the system was changed after approximately one year of operation so that experiments could be performed with an improved transformer. During the first year of system operation, the conventional transformer averaged a throughput efficiency of 90.6%. When the losses associated with this transformer's operation became apparent, Lincoln Laboratory undertook a development effort with the Allied Chemical Corporation to build a more efficient transformer using Allied's amorphous metal (METGLAS^{TM}) for the transformer core material. After testing the prototype unit at Lincoln Laboratory, it was shipped to UTA and installed as part of that system. The improved transformer's throughput efficiency was determined to be 96.6%.

The performance of the PV system during the second year of operation of the UTA experiment (September 1979 to August 1980) is summarized in Table 11-4.

TABLE 11-4
UTA SYSTEM PERFORMANCE SUMMARY 9/79 to 8/80

Insolation	1849 kWh per sq. meter	
Array output (dc)	9500 kWh	(4.7%)
Inverter output (ac)	7869 kWh	(82.8%)
Transformer output (ac)	7132 kWh	(90.6%)
Direct utilization (ac)	3897 kWh	(54.6%)
Feedback to utility (ac)	3235 kWh	(45.4%)

Reference 42 is the most complete source of information on the design revisions and performance of the UTA system during Lincoln Laboratory's involvement.

Research conducted at the UTA site on the operation of grid-connected PV systems provided valuable insights for Lincoln Laboratory when it undertook the design of the Residential Experiment Stations in Concord, Massachusetts, and Las Cruces, New Mexico.

11.4.2 Experimental PV Residence at Carlisle, MA

11.4.2.1 Introduction

An experimental, all-electric, solar PV, lived-in house was built in Carlisle, Massachusetts. Energy-conservation features, passive solar heating, solar domestic hot water collectors, and heat-pump space heating, combined with the PV power system that is coupled to the electric utility, give a balanced design for a potentially energy-self-sufficient residence. Figure 11-5 is a photograph of the house; Reference 43 presents a comprehensive description of the house and equipment.

Contributions to this effort were made by the following individuals: Edward C. Kern, Jr., Burt E. Nichols, Edward Ralowicz, Miles C. Russell, F. John Solman, III and Michael C. Wong.

CP267-6863

Fig. 11-5. The Carlisle PV house.

11.4.2.2 System Description

Floor-to-ceiling, double-glazed sliding glass doors (350 ft.^{2}) allow sunshine to warm the living room, dining area and family room. A 4-in.-thick, tile-covered concrete slab floor (15 cubic yards) stores heat absorbed from the sun. A wood-burning fireplace in the center of the living room provides heat which is stored in a massive 3 x 12-ft. section chimney. Double-studded

outer walls have eight inches of insulation plus one inch of rigid foam under the siding. There are twelve inches of insulation in the ceiling, and eight inches of insulation under the floors. Triple-glazed small windows on the east, north and west walls complete the low-heat-loss structure. Earth berming and foam insulation against the foundation's outer walls also keep heat loss to a minimum. The predicted net heat loss coefficient for the house is 4 BTU/DD/ft.^{2}, which is about two and a half times better than conventional houses. The total livable space for the family is 3000 ft.^{2}, not including garage, utility room, basement or attic areas.

Much of the space heating comes from the south windows and the slab and is augmented by a 38,500 BTU/hr., air-to-air, dual-compressor heat pump with a low-pressure air circulation system for the entire house. Supply registers are on the floor near the outer walls, and return air enters at the top of the chimney and travels down a chase in the masonry core to the air handler, picking up chimney heat on the way. The low-speed fan may operate continuously to circulate the passively heated air throughout the house. South-facing clerestory windows along the ridge line provide passive solar gain. In the summer, these windows are shaded by an overhang and may be opened for natural convective ventilation and cooling. When the passive heating, fireplace and heat pump are inadequate, heat is provided by electric resistance heaters in the air system.

Primary domestic hot water is provided by 100 ft.^{2} of roof-integrated solar collectors coupled to a 120-gal. storage tank via a heat exchanger. Additional heat is provided from the heat pump de-superheater, when available. Emergency water heating is provided by electric resistance heaters. The solar collectors and de-superheater system should provide 75 gal. of hot water per day (annual average), or 90% of the hot water requirements.

The modules are mounted on the roof on tracks. Each row of 7 modules is bolted together with a wheeled bracket, and the assembly is rolled up onto the roof. This arrangement permits easy removal of modules for inspection and replacement. Figure 11-6 shows the installation techniques. The 9 strings are paralleled and fed to a Windworks dc-to-ac inverter.

Under full sunshine conditions at nominal temperature, the PV array can produce 7.3 kW of power; in the summer heat, somewhat less power and in the

winter cold, somewhat more power is available. The electric service is divided into one 200-A feed for the normal house loads, including kitchen, laundry and heat pump, and one 200-A feed for the resistance space and water heaters. Fig. 11-7 shows the utility and load connections.

CP267-6422

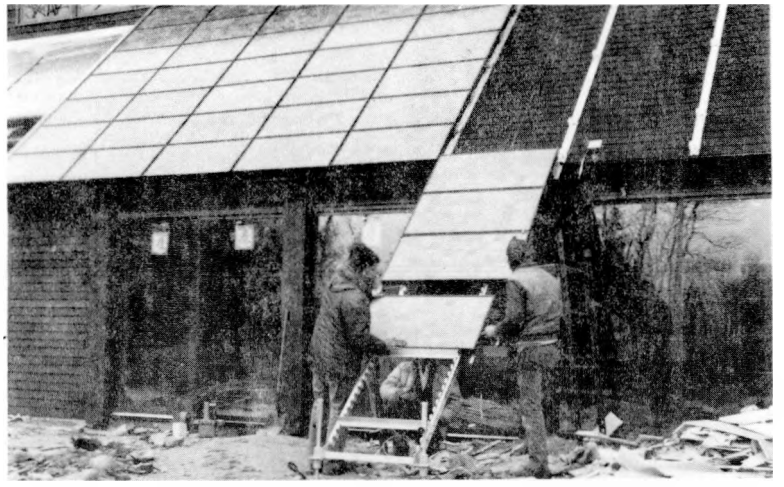

Fig. 11-6. Installing the PV modules.

C74-1283

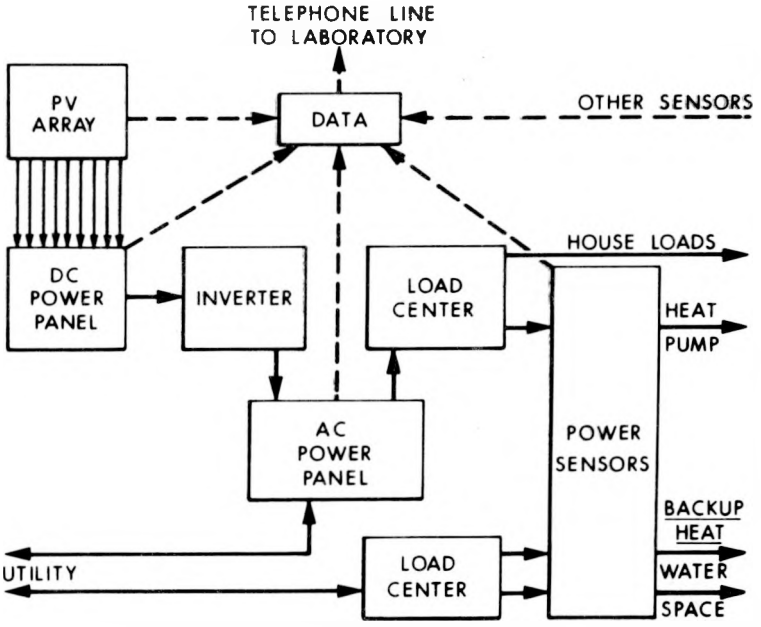

Fig. 11-7. Carlisle house utility and load connections.

The predicted heat loss for the house was 3.5 kWh/DD; at moderate temperatures, the electric energy used for heat pump operation was less than half this figure, showing good performance of the heat pump. At low temperatures,

when the heat pump no longer was efficient and resistance heating had to be added, the energy required to heat the house was higher than predicted. Heating load predictions were based on a ground coupled water-to-air heat pump. However, due to the high cost of installing the ground heat exchanger in ledge and rocky soil, an air-to-air heat pump which had a much lower Coefficient of Performance (COP) was substituted; the heating energy required was therefore much more than predicted.

TABLE 11-5

ENERGY FLOW--CARLISLE HOUSE (AVERAGE KWh/DAY)

	Inverter	Load	From Utility	To Utility	Net	PV % of Load
Summer	21*	14	9	16	-7	150
Fall	23	29	26	20	6	79
Winter	18	139	131	10	121	13
Spring (early)	33	97	84	20	64	34
		Best-day inverter output:		47 kWh		
		Worst-day load:		308 kWh (63 DD)		

*Inverter off part time: 28 kWh/day average for inverter-operating days.

The cost of the hardware for the PV system alone was about $100,000 ($90,000 for the modules, $3,000 for the inverter, $4,000 for the array-mounting hardware and installation, and $3,000 for power panels and wiring), or about $13.70/Wp. The system should produce about 9500 kWh per year, having a value of $950/year at 10¢/kWh. From these figures, it can be seen that at least a 5-to-1 cost reduction is required for the system to be cost effective for a 20-year life.

The PV power system operated very well for the first year except for the failure of a contactor in the inverter and high leakage current to the frames of eight of the 126 PV modules. The manufacturer has repaired all of the modules. Electric energy production was as predicted, but the cold weather house loads were higher than expected.

Unfortunately, the house was not occupied from its completion in May 1981 until mid-March 1982. During this time, the house was not energy-managed; that is, no attention was paid to energy-conservation techniques such as closing of drapes, curtains or shades at night in winter to prevent radiation

losses and reduce conductive losses, or judicial use of the woodburning fireplace to augment heating needs. Additional glazing on the north, east and west windows and on the ridge-line clerestory windows was not installed until January 1982. Numerous air leaks were present on defective windows, doors and chimney closings; these have been or will be repaired. Therefore, a fair measure of cold weather heating loads was not possible. It will take at least a year of occupied-house data to evaluate the house's performance properly.

11.4.3 Experimental PV Residences in Hawaii

11.4.3.1 Introduction

The island state of Hawaii presents an unusual situation regarding applications of photovoltaics for residences. For example, its total horizontal insolation of 6 kWh/m^2-day (50-year average) as measured in Honolulu makes it one of the sunniest regions of the U.S. Also, its electric power needs are served almost exclusively by petroleum fuels imported from the mainland states or from other countries. In addition, being composed of a group of islands with scattered population centers, Hawaii cannot utilize gridded systems with large utility plants but rather must use smaller, isolated units, thereby incurring diseconomies of scale. For example, the island of Molokai, where one of the three Hawaiian PV houses is located, is served by a utility of only 5-MW generation capacity. As a result, the electric energy rates in Hawaii are among the highest in the nation, varying in 1982 from a low of about 14¢/kWh in Oahu and Maui to over 18¢/kWh in Molokai. Because of these and other considerations, Lincoln Laboratory contracted with the Hawaii Natural Energy Institute (HNEI) to retrofit three occupied residences with PV systems.

Contributions to this effort were made by the following individuals: Edward C. Kern, Jr., William H. MacLachlan, Miles C. Russell and F. John Solman, III.

11.4.3.2 System Description

The three houses selected for the project encompass a variety of conditions to be expected in such applications. One is a two-story duplex in the Kaliki section of Honolulu which had been part of a redevelopment program several

years ago (Fig. 11-8). Another is a quadruplex in a new public housing area in Pearl City (Fig. 11-9). The third is a forty-year-old ranch house in a Hawaiian Homestead area on the island of Molokai (Fig. 11-10). In addition to choosing houses which represent a range of architectural styles and socio-economic factors, it was also necessary to select those which had a roof area with good exposure and a low tilt angle appropriate for Hawaii's latitude.

CP267-6968

Fig. 11-8. Kalihu PV house.

CP267-6969

Fig. 11-9. Pearl City PV house.

CP267-6970

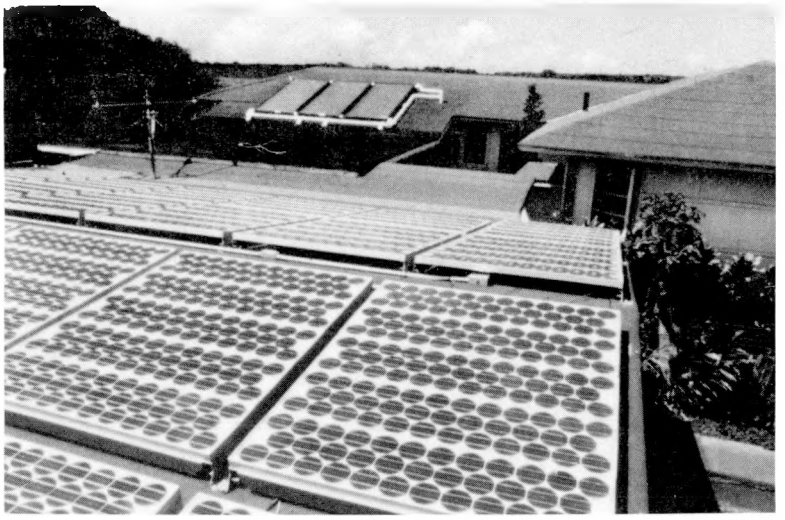

Fig. 11-10. Molokai PV house.

HNEI selected ARCO Solar, Inc. to design, fabricate and install the systems. HNEI designed and installed performance-monitoring units at each residence.

The Pearl City dwelling is part of a newly constructed, two-story, four-unit apartment building owned by the Hawaii Housing Authority, under the U.S. Housing and Urban Development Low Rent Program. It is located in a sub-urban area approximately ten miles southwest of a mountain range. The roof has a 30^{o} tilt facing 235^{o} southwest. The house is occupied by two young children and two adults, one of whom works during the day. The unit is equipped with a solar hot-water heater.

The single-family house in Molokai was selected as typical of homestead areas in Hawaii. The owner-built house is located in a relatively flat rural area of Molokai, close to the airport. The house and attached carport cover about 3,000 $ft.^{2}$ and combine in a one-story frame construction. The carport roof, where the array is located, was rebuilt and structurally strengthened to support the solar equipment. The PV subarrays were symmetrically split between the two roof halves with one grouping facing 223^{o} southwest and the other facing 43^{o} northeast. The tilt is 14^{o}. The residence is owner-occupied by a retired teacher who extensively utilizes a workshop on the

premises. Records show annual electrical energy consumption over the past two years to be about 10,000 kWh/year. A new solar water-heating system provided by ARCO Solar was also installed.

Original designs for the three residences called for one of the rooftop arrays to be of a batten-seam construction and for each of the three structures to have a maximum-power-point tracker (MPPT) to increase inverter efficiency. Both the batten-seam design and the MPPT were later dropped, the latter due to a voltage-stability problem. The ARCO Solar modules used were also modified by the addition of foil backing to act as a moisture barrier. After numerous, mostly minor, site-specific changes, ARCO Solar drawings were accepted by Lincoln Laboratory in January 1981, and PV panels passed reliability testing by Jet Propulsion Laboratory in March 1981.

The PV systems were sized so as to satisfy the approximate annual energy needs of the household. The smallest system, a nominal 2-kW assembly in the urban house in Kalihi, has gas water heating and cooking units. The other two, in larger households in Pearl City and Molokai, are approximately 3.5 kW to 4 kW in size, respectively. The electric-water-heater systems at both sites were supplemented with solar water heaters. The systems were designed so that the utilities involved, through a buyback arrangement, provide credit to the residents for net energy generated by their PV systems. A summary of system characteristics is given in Table 11-6.

The three applications were selected to have differing insolation conditions (close to a usually cloud-shrouded mountain range, further away from the range, and on a relatively flat plain), differing types of residential units (four-plex, duplex, and single-family), differing communities (suburban, central city, and rural), and differing energy-usage profiles.

The PV house in the Kalihi section of Honolulu was selected to exemplify problems involved in retrofitting existing housing in an older central urban area. The house is half of a 10-year-old, two-story frame duplex located about five miles south of a mountain range. The shed-type asphalt shingle roof faces 232^{o} southwest at a tilt of 22^{o}, which is close to the optimum fixed-tilt angle for PV arrays in Honolulu. The roof area available for the array

TABLE 11-6

SITE EQUIPMENT SUMMARY

	Pearl City	Kalihi	Molokai
Tilt	30°	22°	14°
Direction	235°	232°	43° & 223°
Modules* per Subarray	14	14	14
Subarrays per Array	8	4	8
Array Weight (lb.)	5376	2688	5376
Array Area (sq. ft.)	448	224	448
Peak Power	4 kW	2 kW	4 kW
Inverter Size**	4 kW	2 kW	4 kW
Normal Daytime Occupancy	1 adult 2 children	1 adult	2 adults
Date Operational	June 1981	June 1981	June 1981

*ASI 16-2300 Solar Modules

**Windworks, Inc. non-tracking Gemini Synchronous Inverter

measured approximately 400 ft.^{2}. Occupancy consists of four adults, two of whom are usually at home during the day. Records of electrical usage for the past two years show an annual consumption of 3,500 kWh/year.

The need to install the entire system around an existing house produced some interesting problems, ranging from weathersealing a roof penetration to determining compliance with the National Electric Code, occasionally in areas not yet covered. Logistics problems also were present. For example, little engineering guidance was available from the product manufacturer once the equipment had been shipped to the site.

Since the systems were being placed in occupied houses, safety was of paramount importance. The sites were reviewed by an MIT safety officer and by a local Hawaiian safety inspector, and several corrections to the systems resulted from their inspections.

Energy output for the three sites is summarized in Table 11-7. Production from the Molokai site was low during the first few months of operation due to repeated problems with the Gemini inverter, which required frequent resetting of circuit breakers. This unit was ultimately replaced by a new one which has performed well. The data-monitoring systems have performed unreliably since

their initial turn-on, and there have been problems with loss of data due to the required manual changing of data-recording tapes. The particular microloggers in use have experienced several random failures which resulted in considerable loss of data and in repair expense. HNEI's findings and suggestions on the micrologger are periodically conveyed to the manufacturer to aid in product improvement, which is understood to be in progress. The energy flows tabulated below were obtained from the utility-style kilowatt hour meters installed at the three sites, and were not disturbed by problems in the data-logging system.

The reader is referred to Reference 45 for complete information on this project.

TABLE 11-7

HAWAII PV SYSTEMS' ELECTRICAL ENERGY FLOWS
(7/1/81 to 4/30/82)

	Kalihi 2 kW	Pearl City 4 kW	Molokai 4 kW
Total PV Generated	2050.8	4088	3718
Total Exported	835	2976	2078
Total Imported	2947.1	2451	4976.7

A number of lessons have been learned from these three systems. The first is that repairs can and should be done by local people since it is expensive and time-consuming to send a service representative from the mainland to Hawaii. While a service network such as that which exists for TVs and washing machines is not yet warranted for PV systems, the required skills are very similar. Good service documentation and available repair parts are also important.

A second problem encountered with these systems was that of audio and radio noise. In the case of the Kaliki system, noise produced at night was objectionable until a night shutdown was installed. The original inverter at the Molokai house was very noisy and was replaced. Future inverters should be as quiet as other household appliances which operate throughout the day. Radio noise extending into the AM broadcast band was observed at all sites and was primarily conducted via the ac wiring. Due to the use of conduit for the array wires, little noise was radiated. The source of the noise is probably

electrical transients associated with the inverter SCRs. Filters to keep conducted and radiated radio noise confined to the PV system enclosures should be installed on all future units. The FCC specification for filtering of computing devices provides a suitable standard.

For a variety of reasons, the energy produced by the three PV systems averaged about 70% of the amount predicted for the period from 1 July 1981 to 30 April 1982. These reasons include lower than normal insolation as well as downtime for the PV systems. During this period the average insolation was about 8% below normal, so the energy produced was about 22% lower than predicted due to inverter outages and to losses that were not accounted for in the predictions. If periods of significant inverter outages are removed, energy production is about 80% of predicted (8% of the discrepancy is due to lowered insolation and 12% is due to unaccounted losses and some downtime).

11.4.4 Experimental PV Residence at Cape Canaveral, FL

11.4.4.1 Introduction

This unoccupied residence is located at the Florida Solar Energy Center (FSEC), Cape Canaveral, Florida (Fig. 11-11). Federal participation occurred via Lincoln Laboratory's involvement on behalf of DOE. FSEC represented the state of Florida in the experiment. In addition, the local utility, Florida Power and Light, contributed funds to the project. The system became operational in November, 1980. A complete description of the system and a summary of its performance over its first sixteen months of operation is given in Reference 46.

Contributions to this effort were made by Miles C. Russell and F. John Solman,III.

11.4.4.2 System Description

The system contains a 5-kWp standoff-mounted PV array. In effect, there are two completely separate PV systems feeding a common ac distribution point. Two inverters are each tied to a separate 31.25-m^2, 2.5-kWp PV subarray. This unusual arrangement resulted from the evolutionary growth of the system during

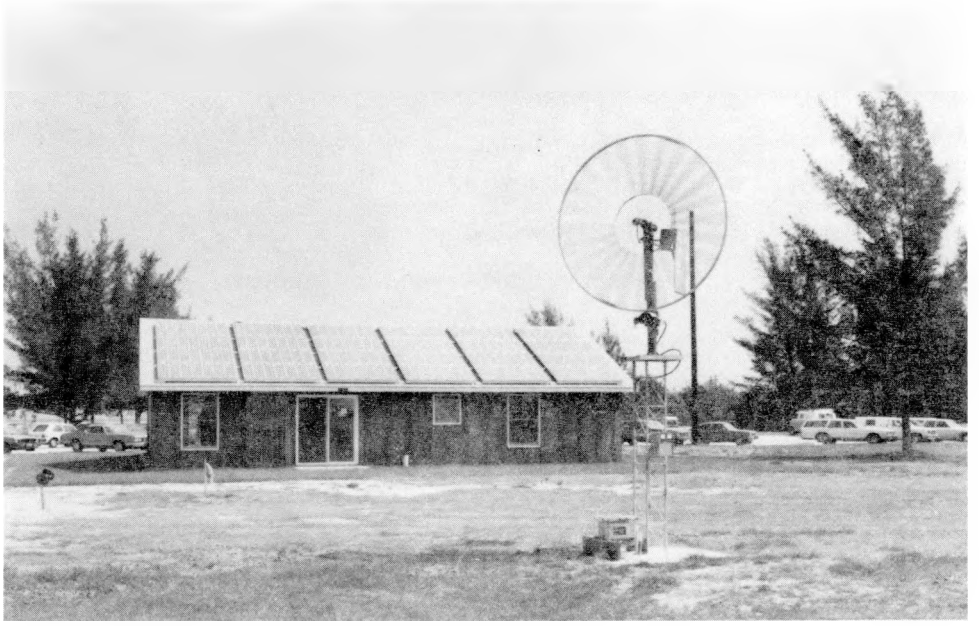

Fig. 11-11. Florida Solar Energy Center PV house.

its design and procurement. It allows convenient, side-by-side comparison of various inverter-current-slope settings, as well as redundant operation in the event of an inverter problem.

Each subarray bank contains six parallel strings of 14 series-wired ARCO 16-2000 PV modules. Each module utilizes a by-pass diode, and each string can be isolated from the active array for current-voltage (I-V) or other diagnostic measurements without disturbing the overall system operation. The array control panel allows either bank to be connected to either inverter. Individual string currents are displayed on an ammeter panel located adjacent to the array control panel. These meters serve as gross indicators of individual string performance and facilitate detection of module electrical degradation or failure.

The power-conditioning subsystem and most of the instrumentation transducers are located in the garage (Fig. 11-12). The inverters, string control and monitoring panels, and kWh meters are wall-mounted for easy service access. The main garage area is not impaired and could be used in a normal

manner if the house were occupied. Except for some intermittent cooling and dehumidification provided by a dedicated heat-pump/water-heater unit, no attempt was made to condition the space surrounding the inverters and instrumentation.

CP267-6714

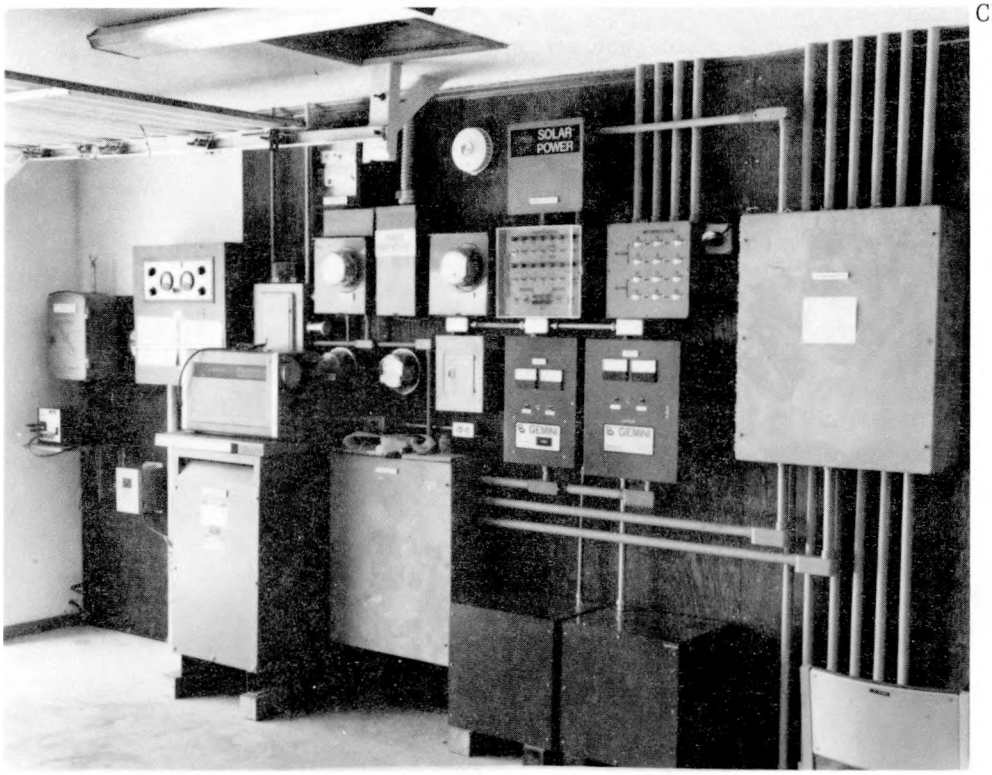

Fig. 11-12. Power-conditioning subsystem at FSEC PV house.

The two Gemini 4-kW inverters in this facility differ somewhat from each other. One inverter, which was purchased by FSEC in 1979, is basically an off-the-shelf model with an air-core inductor in the PV-interface filter unit. The second inverter was modified and supplied by Lincoln Laboratory. This unit has an iron-core inductor in the PV-interface filter and features a dual dc-current-slope-profile setting. This modification was designed by Lincoln Laboratory in an attempt to operate the array more efficiently over a range of input voltages without the use of maximum-power-point tracking (MPPT) circuitry. No MPPT is utilized in either inverter.

Performance measurements for the array are summarized in Table 11-8, which lists the monthly total or irradiance incident on the array, the monthly energy output of the array, and the monthly average array efficiency for the 12-month period.

TABLE 11-8

MONTHLY PERFORMANCE OF FSEC PV HOUSE ARRAY

Month & Year	Irradiance Incident Upon Array (Field Measured, kWh)	Array DC Output (kWh)	Array Efficiency (%)
APR 81	11,989*	914	7.6
MAY 81	12,732*	900	7.1
JUN 81	12,120*	883	7.3
JUL 81	11,594	837	7.2
AUG 81	10,286	759	7.4
SEP 81	10,510	797	7.6
OCT 81	10,258	775	7.6
NOV 81	9,717	776	8.0
DEC 81	8,582	687	8.0
JAN 82	8,452	682	8.1
FEB 82	7,976	634	7.9
MAR 82	10,899	812	7.5

Annual Total Irradiance	125,115 kWh
Annual Total DC Output	9,456 kWh
Annual Average Array Efficiency	7.6%

*Calculated from irradiance measured on a horizontal surface.

The monthly average array efficiency is seen to vary between 7.1 and 8.1%. During the winter months (November to February) the array efficiency is generally high (8.0 $\pm$ 0.1%) because lower ambient tempertures provide a cooling effect on the array (which is passively cooled from both above and below in the stand-off mount used at FSEC). The PV cells in the array run at lower temperatures in these months and hence operate at higher efficiency. The monthly average PV cell temperature at noontime is about 10^{o}C ($\pm$ 3.6) higher than the ambient temperature, but is always lower than the NOCT (normal operating cell temperature) values of 45^{o}C for the modules used. This is also true in the month of July, when the noontime insolation averaged 840 W/m^{2}.

The monthly performance of the complete PV system for sixteen months of system operation is summarized in Table 11-9. The last column in the table, "System Capacity Factor," indicates the fraction of time the system could have

been generating electricity at rated power in order to deliver the same energy as was actually generated and, accordingly, is defined as Capacity Factor = $E/P_{ps}T$, where E is the energy delivered in time interval, T, and P_{ps} is the peak power rating of the system. For the FSEC system, the peak power rating is 4.21 kW, based on peak array power of 5.04 kW (at 1 kW/m^2 irradiance and 45°C NOCT), 4% loss due to module mismatch and dc wiring, and 87% dc-to-ac conversion efficiency at peak array power, which is the average of the two inverters.

TABLE 11-9

MONTHLY PERFORMANCE OF FSEC PV HOUSE SYSTEM

Month & Year	Irradiance Incident Upon Array (Field Measured, kWh)	PV System AC Output (kWh)	System Efficiency %	System Capacity Factor
DEC 80	6,932*	495	7.1	0.16
JAN 81	8,775*	627	7.1	0.20
FEB 81	7,800*	530	6.8	0.19
MAR 81	10,664*	695	6.5	0.22
APR 81	11,989*	788	6.6	0.26
MAY 81	12,732*	776	6.1	0.25
JUN 81	12,120*	746	6.2	0.24
JUL 81	11,594	721	6.2	0.23
AUG 81	10,286	653	6.3	0.21
SEP 81	10,510	654**	6.2**	0.21**
OCT 81	10,258	655	6.4	0.21
NOV 81	9,717	637	6.6	0.21
DEC 81	8,582	530	6.2	0.17
JAN 82	8,452	562	6.6	0.18
FEB 82	7,976	516	6.5	0.18
MAR 82	10,899	676	6.2	0.21

Total Irradiance (for 16 months)	159,286 kWh
Total System AC Output (for 16 months)	10,261 kWh
System Average Efficiency (for 16 months)	6.4%
System Average Capacity Factor (for 16 months)	0.21

*Calculated from irradiance measured on a horizontal surface.
**Approximately 20 kWh "lost" due to shutdown for connection of power to an unrelated, adjacent facility. Because of this loss the system efficiency is reduced by about 0.2% and capacity factor is reduced by approximately 0.01 in September 81.

The monthly system ac-energy generation and house energy usage are compared in Table 11-10. While the FSEC PV house has not yet been subjected to a typical residential load profile, the monthly house energy usage for the last twelve months is close to that for a residence of similar size. The seasonal variations in the energy usage also follow the general trends around this location. Also indicated in Table 11-10 are the net dollar savings due to electricity delivered to the grid, as for the grid-supplied electricity (i.e., buy back ratio = 1), and using electric rates prevalent in Cape Canaveral, Florida.

TABLE 11-10

THE FSEC EXPERIMENTAL PHOTOVOLTAIC RESIDENCE
--OPERATIONAL MONTHLY PERFORMANCE SUMMARY--

Month & Year	House Load (kWh)	PV System AC Supply (kWh)	Rate Per kWh (FPL)	Value of Gen. Electricity*
DEC 80	178	495	$ .056	$27.72
JAN 81	569	627	$ .055	$34.49
FEB 81	233	530	$ .056	$29.68
MAR 81	201	695	$ .065	$45.18
APR 81	476	788	$ .068	$53.58
MAY 81	1,020	776	$ .074	$57.42
JUN 81	1,601	746	$ .073	$54.46
JUL 81	1,884	721	$ .074	$53.35
AUG 81	1,928	653	$ .074	$48.25
SEP 81	808	654	$ .074	$48.36
OCT 81	1,131	655	$ .074	$48.47
NOV 81	960	637	$ .074	$47.14
DEC 81	457	530	$ .076	$40.28
JAN 82	535	562	$ .076	$42.71
FEB 82	464	516	$ .079	$40.76
MAR 82	824	676	$ .080	$54.08

Total Use: 13,269 kWh
Total Supply: 10,261 kWh
Total "Savings" (16 months): $725.93

*Assuming equivalent credit for generation in excess of instantaneous demand.

The FSEC PV residential system has been reliably supplying ac energy to the house loads and/or the utility grid since the start of its operation on 1 December 1980. System operation has been virtually trouble free, and there have been no major malfunctions. Though the harmonic current content and reactive power in the output of the inverters are high, no detrimental effect on the house appliances or the utility line has been detected.

The annual ac energy output of the system has been approximately 8,000 kWh, and the average system efficiency has been 6.4%. From the currently available data, it can be seen that year-to-year monthly ac energy output of the system for each of the four months, December to March, is within 10%. While such comparison in the energy output for only four months is not sufficient, it is indicative of the degree of predictability of the system's generation on a monthly basis.

The only failures that occurred in the PV system during its first sixteen months of operation were open-circuited failures in two out of 168 PV modules. These were replaced with minimal system downtime. While some discoloration of cell connections and interconnections in the modules has been observed, no significant weather-related degradation in power output has yet been detected in this very humid, coastal-zone location. The unscheduled downtime of the PV system was about two hours in sixteen months of operation. The excellent reliability of this system and its low maintenance requirements lead to the conclusion that residential PV systems will probably enjoy a high degree of commercial success if lower cost can be achieved.

11.4.5 Experimental PV Residence in Phoenix, Arizona

11.4.5.1 Introduction

This PV-equipped residence (Fig. 11-13) is one of a group of unoccupied model houses built by John F. Long Properties, Inc., in Phoenix, Arizona. This project represents the first use of a novel batten-and-seam PV module (Fig. 11-14), which was developed by ARCO Solar, Inc., under DOE contract to Jet Propulsion Laboratory. A data-monitoring system was installed in the house, and is operated by Arizona State University. For a complete description of the house and its performance, see Reference 47.

Contributions to this effort were made by the following individuals: Charles H. Cox, III, Edward C. Kern, Jr., Emmanuel E. Landsman, Miles C. Russell and F. John Solman, III.

CP267-6662

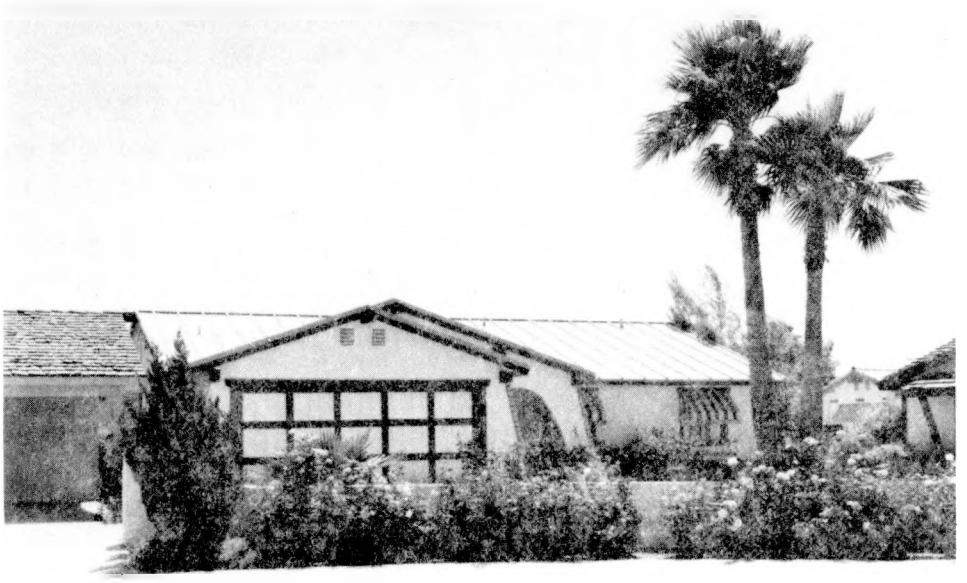

Fig. 11-13. J. F. Long PV house, Phoenix.

CP267-6080

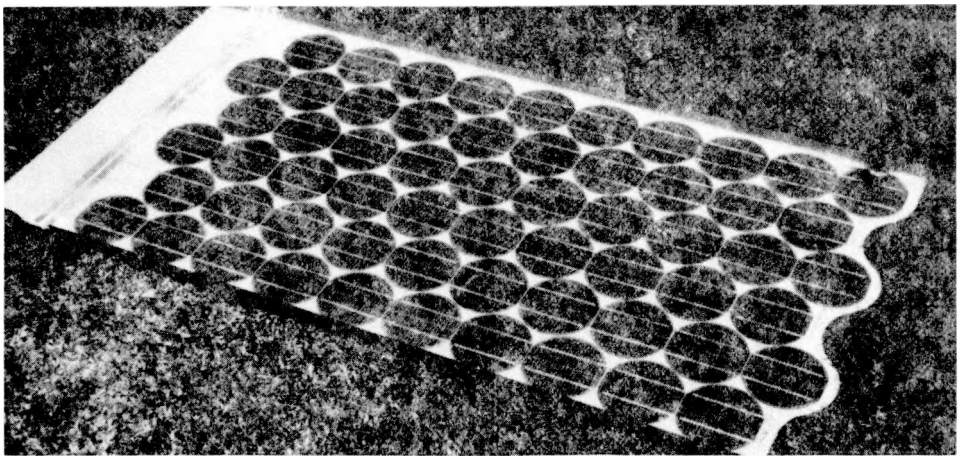

Fig. 11-14. ARCO Solar batten-and-seam PV module.

11.4.5.2 System Description

The interior area of the residence measures 1507 ft.^{2} and the roof comprises in part a south-facing section measuring approximately twenty feet by fifty feet. Prior to installation of the PV system, the asphalt shingles were removed and the roof substructure was recovered with a layer of felt tar paper. Aside from these initial preparations, no other structural modifications were performed on the house, except for the addition of a small room attached to the building to house the power-conditioning equipment (Fig. 11-15).

CP267-6668

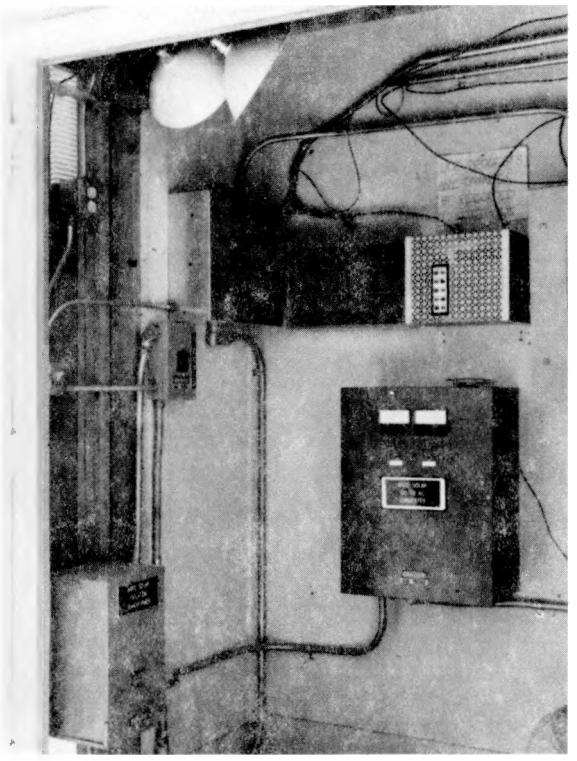

Fig. 11-15. J. F. Long house power-conditioning equipment.

In its final configuration, the PV roof consisted of 120 ARCO Solar Model ASI-9-700 PV modules divided electrically into five subarrays. Each subarray contains 24 series-wired modules. The five subarrays are wired in parallel at a junction box in the power-conditioning room. The PV source is connected to a standard Gemini utility-interactive inverter and filter.

A data-collection system became operational during September 1980. Outputs from 33 transducers were sampled every fifteen minutes by a data logger, and

then stored on a cassette tape for further data reduction and analysis. The tapes were changed every two or three days, and the cassette tapes were sent at the end of each week to Arizona State University, where they were read directly into a computer-disk file. The disk file served as input to an edit-conversion program which edited and checked the data for reasonableness and consistency. The edit program then produced various output records.

During approximately two years of operation, problems were experienced with both the array and the inverter. In the case of the array, the substrate temperature of the modules reached a maximum of 78°C, which was approximately 30°C above the daily maximum ambient temperature. The daily averaged summer substrate temperature ranged between 60° to 62°C, which was approximately 25°C above the daily mean ambient temperature. As a result the array produced less energy than originally projected.

In the original design, the modules were secured to the roof by pressure from the battens, which were attached to clips screwed to the roof. The battens thus pressed down on the modules along the edges. In some cases, the batten pressed on a point very close to the edge of the cell. At high temperatures, the EVA and Korad acrylic cell cover can flow under such pressure and eventually a short between the grounded batten and the cell occurred. The mounting method was changed so that the mounting clips engaged the module at a point sufficiently removed from any internal wiring. The battens are now supported by the clips so they do not press on the face of the module.

It was also observed that those working on the roof tended to step on the battens rather than the module surface, exacerbating the short-circuit failure mode.

Infrared scans of the roof were used successfully to find intermodule shorts by detecting hot spots in the array. It was noted that a hot spot of 6° to 8°C above the average would result from bird droppings shadowing a cell.

Based upon experiences with this first-generation, direct-mount module, recommendations for future designs can be made. Future-generation modules should incorporate revised wire-nut module interconnects, bypass diodes at each module, double-cell interconnects between the tenth and eleventh cell in each series string, replacement of Korad with Tedlar in a module sandwich,

stiffer roof sheathing, improved aesthetic integration of the batten-seam modules to the residence, and a darker background the better to match the solar cell color.

A number of difficulties were experienced with the power-conditioning system, resulting in modifications to the Gemini inverter. The maximum-power-point tracker demonstrated erratic performance and finally was disabled. The inverter unit then was operated in a conventional constant-voltage mode. The inverter also experienced low-frequency instability at low-insolation conditions; this condition also was corrected.

Personnel from Oak Ridge National Laboratories measured the output of the system with a spectrum analyzer in order to determine the level of current harmonics on the utility lines serving this system. The sum of all harmonics, with the PV system disconnected, was 4.9% of the fundamental frequency. With the PV system operating under a light electrical load, the sum of the third, fifth and seventh harmonics was 36%.

REFERENCES

Section 11.2

1. U. S. Department of Energy, "National Photovoltaic Program Multi-Year Program Plan," September 1980.

2. U. S. Department of Energy, Photovoltaic Program, "Residential Application Implementation Plan," (Draft), MIT Energy Laboratory and Lincoln Laboratory, Cambridge, MA, September 1979.

3. Russell, M. C., "Photovoltaic System Evaluation at the Northeast Residential Experiment Station, November 1980-May 1982," MIT Lincoln Laboratory Technical Report, November 1982, DOE/ET/20279-219.

4. New Mexico Solar Energy Institute, "Establishment and Operation of the Southwest Residential Experiment Station," MIT Lincoln Laboratory Technical Report, August 1982, DOE/ET/20279-213.

5. Russell, M. C., et al., "Data Report for the Northeast Residential Experiment Station - June 1981," MIT Lincoln Laboratory Technical Report, August 1981, DOE/ET/20279-154.

6. Russell, M. C., et al., "Data Report for the Northeast Residential Experiment Station - July 1981," MIT Lincoln Laboratory Technical Report, September 1981, DOE/ET/20279-161.

7. Russell, M. C., et al., "Data Report for the Northeast Residential Experiment Station - August 1981," MIT Lincoln Laboratory Technical Report, October 1981, DOE/ET/20279-164.

8. Russell, M. C., et al., "Data Report for the Northeast Residential Experiment Station - September 1981," MIT Lincoln Laboratory Technical Report, October 1981, DOE/ET/20279-165.

9. Russell, M. C., et al., "Data Report for the Northeast Residential Experiment Station - October 1981," MIT Lincoln Laboratory Technical Report, November 1981, DOE/ET/20279-174.

10. Russell, M. C., et al., "Data Report for the Northeast Residential Experiment Station - November 1981," MIT Lincoln Laboratory Technical Report, December 1981, DOE/ET/20279-183.

11. Russell, M. C., et al., "Data Report for the Northeast Residential Experiment Station - December 1981," MIT Lincoln Laboratory Technical Report, April 1982, DOE/ET/20279-192.

12. Russell, M. C., et al., "Data Report for the Northeast Residential Experiment Station - January 1982," MIT Lincoln Laboratory Technical Report, June 1982, DOE/ET/20279-204.

13. Russell, M. C., et al., "Data Report for the Northeast Residential Experiment Station - February 1982," MIT Lincoln Laboratory Technical Report, June 1982, DOE/ET/20279-206.

References (continued)

14. Russell, M. D., et al., "Data Report for the Northeast Residential Experiment Station - March 1982," MIT Lincoln Laboratory Technical Report, June 1982, DOE/ET/20279-208.

15. Russell, M. C. et al., "Data Report for the Northeast Residential Experiment Station - April 1982," MIT Lincoln Laboratory Technical Report, June 1982, DOE/ET/20279-214.

16. Russell, M. C., et al., "Data Report for the Northeast Residential Experiment Station - May 1982," MIT Lincoln Laboratory Technical Report, June 1982, DOE/ET/20279-220.

17. Russell, M. C., "Prototype Residential Photovoltaic Systems Evaluation Plan," MIT Lincoln Laboratory Technical Report, October 1981, DOE/ET/20279-163.

18. Mehalick, E. M., "Design and Fabrication of Prototype Systems for Photovoltaic Residences in the Northeast, Final Report," prepared under contract to Lincoln Laboratory by General Electric Co., November 1981, DOE/ET/20279-175.

19. Solarex Corporation, "Solarex Final Report: Design and Fabrication of a Prototype System for Photovoltaic Residences in the Northeast," prepared under contract to Lincoln Laboratory by Solarex, August 1982, DOE/ET/20279-224.

20. Millner, A. R., "TriSolarCorp Final Report: Design and Fabrication of a Prototype System for Photovoltaic Residences in the Northeast," prepared under contract to Lincoln Laboratory by TriSolarCorp, August 1982, DOE/ET/20279-217.

21. Pittman, P. F., and Dressler, R. T., "Westinghouse Final Report: Design and Fabrication of a Photovoltaic Prototype System for the Northeast," prepared under contract to Lincoln Laboratory by Westinghouse, June 1982, DOE/ET/20279-199.

22. Mehalick, E. M., "General Electric Final Report: Design and Fabrication of a Prototype System for Photovoltaic Residences in the Southwest," prepared under contract to New Mexico Solar Energy Institute for Lincoln Laboratory by General Electric Co., April 1982, DOE/ET/20279-193.

23. TEA, "Total Environmental Action, Inc., Final Report: Design and Fabrication of a Prototype System for Photovoltaic Residences in the Southwest," prepared under contract to New Mexico Solar Energy Institute for Lincoln Laboratory by TEA, June 1982, DOE/ET/20279-209.

24. Millner, A. R., "TriSolarCorp Final Report: Design and Fabrication of a Prototype System for Photovoltaic Residences in the Southwest," prepared under contract to New Mexico Solar Energy Institute for Lincoln Laboratory by TriSolarCorp, August 1982, DOE/ET/20279-218.

References (continued)

25. "BDM Final Report: Design and Fabrication of a Prototype System for Photovoltaic Residences in the Southwest," prepared under contract to New Mexico Solar Energy Institute for Lincoln Laboratory by BDM, August 1982, DOE/ET/20279-225.

26. Sorenson, D. and McNamara, R., "ARTU Final Report: Design and Fabrication of a Prototype System for Photovoltaic Residences in the Southwest," prepared under contract to New Mexico Solar Energy Institute for Lincoln Laboratory by ARTU, October 1982, DOE/ET/20279-234.

27. Gibson, R. and Swanson, T., "Solarex Final Report: Design and Fabrication of a Prototype System for Photovoltaic Residences in the Southwest," prepared under contract to New Mexico Solar Energy Institute for Lincoln Laboratory by Solarex, November 1982, DOE/ET/20279-235.

28. Pittman, P. F. and Dressler, R. T., "Westinghouse Final Report: Design and Fabrication of a Prototype System for Photovoltaic Residences in the Southwest," prepared under contract to New Mexico Solar Energy Institute for Lincoln Laboratory by Westinghouse, November 1982, DOE/ET/20279-236.

29. Yenamandra, R. and Schuetz, P., "ARCO Solar Final Report: Design and Fabrication of a Prototype System for Photovoltaic Residences in the Southwest," prepared under contract to New Mexico Solar Energy Institute for Lincoln Laboratory by ARCO Solar, December 1982, DOE/ET/20279-238.

30. Schaefer, J. F., et al., "Data Report for the Southwest Residential Experiment Station, March-September 1981," prepared for Lincoln Laboratory by the New Mexico Solar Energy Institute, October 1981, DOE/ET/20279-166.

31. Schaefer, J. F., et al., "Data Report for the Southwest Residential Experiment Station - October 1981," prepared for Lincoln Laboratory by the New Mexico Solar Energy Institute, November 1981, DOE/ET/20279-167.

32. Schaefer, J. F., et al., "Data Report for the Southwest Residential Experiment Station - November 1981," prepared for Lincoln Laboratory by the New Mexico Solar Energy Institute, December 1981, DOE/ET/20279-176.

33. Schaefer, J. F. et al., "Data Report for the Southwest Residential Experiment Station - December 1981," prepared for Lincoln Laboratory by the New Mexico Solar Energy Institute, January 1982, DOE/ET/20279-184.

34. Schaefer, J. F., et al., "Data Report for the Southwest Residential Experiment Station - January 1982," prepared for Lincoln Laboratory by the New Mexico Solar Energy Institute, February 1982, DOE/ET/20279-187.

References (continued)

35. Schaefer, J. F., et al., "Data Report for the Southwest Residential Experiment Station - February 1982," prepared for Lincoln Laboratory by the New Mexico Solar Energy Institute, February 1982, DOE/ET/20279-196.

36. Schaefer, J. F., et al., "Data Report for the Southwest Residential Experiment Station - March 1982," prepared for Lincoln Laboratory by the New Mexico Solar Energy Institute, March 1982, DOE/ET/20279-197.

37. Schaefer, J. F., et al., "Data Report for the Southwest Residential Experiment Station - April 1982," prepared for Lincoln Laboratory by the New Mexico Solar Energy Institute, April 1982, DOE/ET/20279-200.

Section 11.3

38. Fenton, H. A. and Much, C. H., "Residential Photovoltaic Experiment Station Data System," presented at the IECI '81 International Conference on Applications of Mini- and Microprocessors, San Francisco, CA, 9-12 November 1981, DOE/ET/20279-155.

39. Hart, G. W., "The Effect of Data Sampling Rate on Utility-Interaction Calculations," Lincoln Laboratory Technical Report, October 1982, DOE/ET/20279-212.

Section 11.4.1

40. Darkazalli, G., "A Description of the University of Texas Arlington Solar Energy Research Facility PV/Thermal Residential System," prepared by UTA under contract to Lincoln Laboratory, March 1979, COO-4577-5.

41. Kern, E. C., "Phase-One Experiment Test Plan, PV/Thermal Residential Experiment," Lincoln Laboratory Technical Report, March 1979, COO-4577-6.

42. Kugle, S., et al., "Phase II Solar Photovoltaic/Thermal Residential Experiment Final Report," prepared by UTA under contract to Lincoln Laboratory, August 1981, COO-4577-10.

Section 11.4.2

43. Nichols, B. E., "The Carlisle House--An All-Solar Electric Residence," Lincoln Laboratory Technical Report, September 1981, DOE/ET/20279-143.

44. Nichols, B. E., "The Carlisle Photovoltaic House: First Eighteen Months," Lincoln Laboratory Technical Report, January 1983, DOE/ET/20279-239.

References (continued)

Section 11.4.3

45. Neill, D. R. and Curtis, G. W., "Hawaii Natural Energy Institute Final Report on Three Innovative Photovoltaic Applications for Residences Experiments," prepared under contract to Lincoln Laboratory by the Hawaii Natural Energy Institute, June 1982, DOE/ET/20279-211.

Section 11.4.4

46. Atmaram, G. H. and Litka, A. H., "The Florida Solar Energy Center Final Report on an Innovative Photovoltaic Applications for Residences Experiment," prepared under contract to Lincoln Laboratory by the Florida Solar Energy Center, June 1982, DOE/ET/20279-210.

Section 11.4.5

47. "Final Report: John F. Long Experimental Photovoltaic House," two volumes, prepared by John F. Long Properties Inc., under contract to Lincoln Laboratory, 1 June 1982, DOE/ET/20279-201.

12.0 SUMMARY OF RESIDENTIAL PV PROJECT

12.1 Conclusions and Lessons Learned

The results of the system studies, technology development and field testing activity discussed in Sections 9 through 11 were the basis for the following conclusions:

Roof-Mounted Systems Produce Adequate Energy: The test results support projections that roof-mounted residential PV systems can easily supply 50 to 70% of the annual electrical energy needs of typical houses.

PV System Performance Models Exist: Existing modeling techniques are sufficiently detailed to permit accurate predictions of PV system performance. This applies to a wide range of system types, including simple utility-interactive systems as well as more complicated systems utilizing on-site storage and/or combined PV/thermal collectors.

Simpler, Utility-Interactive Systems are Preferable: Economic studies indicate that such systems are a better economic choice for the homeowner already connected to or near a utility line than the more complicated variants mentioned above.

PV Systems are Primarily Fuel Savers: Utility-interactive PV systems will, for the most part, afford fuel savings in peaking and intermediate-load-following fossil-fuel plants. Their ability to reduce the need for generation capacity is small.

PV Systems Have Little Impact on Utility Feeders: Computer simulations and supporting measurements in the Northeast and Southwest indicate that the presence of distributed residential PV systems on a utility feeder will have negligible effect on utility feeder operations (power and voltage regulation, power factor, safety, etc.) for PV generation percentages (of the feeder capacity) as high as 25% or more. Also, distributed PV displaces substation power on more than a one-for-one basis because of the reduced line losses. In the case of heavily loaded, older, low-voltage feeders, the "bonus" can be as great as 25-30% at peak load times.

Codes and Standards Exist for Residential PV: Preliminary codes and standards have been generated which make it possible to specify those attributes of PV systems which ensure reasonable quality and a high degree of safety to the homeowner.

PV Arrays Perform Well: In almost every instance, the PV arrays functioned with great reliability. When failures did occur, the resulting effect on system performance was gradual and nondrastic.

High Performance Inverters are Available: There now exist several commercially available inverters with high efficiency and excellent power quality and reliability which appear to be appropriate for widespread use in residential PV systems.

Integration of PV into Residences is Realizable: Integration of PV systems into residences has not proven to be a difficult problem. Array aesthetics appear to be acceptable, and the installation of inverters and associated wiring presented no major problems to electricians and builders.

PV Systems are Relatively Safe: In the course of constructing and operating a total of twenty systems, of which five are inhabited, there was only one accident involving an array installer and none involving the residents of the PV houses. The sole accident involved a construction worker slipping and falling from a roof while installing an array. Although such accidents cannot be totally eliminated, they can be minimized through additional training and simplified array-mounting designs.

Cost and Life are the Determinants of Success: In order for residential PV systems to be economically attractive to a homeowner, their installed cost must be about $2.00 per watt or less, and the useful life of the system must be 30 years or more. Although the Lincoln Laboratory effort was not intended to demonstrate attainment of either of these goals, our experiences indicate that further cost reductions by about a factor of five to ten are required based on costs experienced during the Laboratory's program. Moreover, a relatively "lean" markup in prices from manufacturer through distributor, supplier and installer is required. Regarding life, the results of operating

periods as long as two years makes us optimistic that the 30-year lifetime goal can be attained, but to fracture an old adage, "two swallows don't a summer make....".

12.2 Recommendations for Further Work

Explore More Widespread Use of Retrofit PV Applications: The main thrust of Lincoln Laboratory's effort was to develop systems suitable for installation during residential construction. (The sole exceptions were the Hawaii units.) In view of the extremely large existing stock of houses, DOE should proceed with their plans to develop and evaluate smaller PV systems designed for retrofit installation on existing houses. Particular attention should be given to increasing array efficiency, reducing installation cost, and improving PV array heat-rejection characteristics.

Continue to Explore The Effect of PV on Utility Feeders: The work done in this area by Lincoln Laboratory and its contractors involved case studies of how utility-feeder operation would be affected by PV interconnections in specific locations in the Southwest and Northeast. Since the problem is complex and the feeder installations vary from one utility service area to another, it probably is not possible to perform a generalized analysis of the issues relating to PV/utility-feeder interaction. However, additional case studies are warranted. In particular, more sophisticated treatment should be given to the effects of high PV penetration on a feeder. Also, the analyses performed on radial feeders (fed from one end) should be replicated for other types such as network feeders (fed from two or more places).

Resolve Power Quality Issues: Questions still remain as to the degree to which harmonic currents generated by utility-interactive inverters are harmful to the utility and its customers. Lincoln Laboratory's experience to date indicates that this problem is more imagined than real. Nevertheless, many utilities are very concerned about this issue. Measurements in an authentic environment, as recommended in the previous paragraph, should resolve these issues. Efforts to develop consensus standards, through, for example, the IEEE Standards Coordinating Committee for Photovoltaics, and the Standards Coordinating Committee for Distributed Storage and Generation, should be supported.

Develop Accelerated Life Testing Methods: If residential PV systems are adopted in significant numbers of households, it will only occur after the following major criteria have been satisfied:

- Low first cost (to be affordable)
- High conversion efficiency (to fit on the roof)
- Long life (to justify the cost).

Progress continues to be made on the first criterion, as prices of PV modules and system decrease each year. The second criterion has already been met: 10% overall efficiency is sufficient. The problem lies with demonstrating life. The DOE program should place high priority on developing and validating accelerated testing techniques such that a whole 30-year lifetime of environmental exposure can be crammed into a test program of at most a few years (or less) duration. If this is not accomplished, the PV industry will have to convince prospective buyers to purchase an expensive ($10-$15,000) system on the basis of faith, trust and perhaps warranties extending over only a fraction of the needed life. Without effective accelerated life testing, the rate of diffusion of PV into the residential market will be slowed.

APPENDIX

MIT Lincoln Laboratory Publications Under Photovoltaic Field Tests and Applications Project DOE Contract No. EY-76-C-02-4094

COO No.	
4094-1	Smith, D. V., "Photovoltaic Power in Less Developed Countries," Technical Report, 27 March 1977.
4094-2	Matlin, R. W. and Katzman, M. T., "The Economics of Adopting Solar Photovoltaic Energy Systems in Irrigation," Technical Report, 11 July 1977.
4094-3	Peatfield, C. R. and Jarvinen, P. O., "Photovoltaic Applications in the Southwest for the National Park Service," Technical Report, 28 April 1977.
4094-4	Matlin, R. W., et al., "The 25 Kilowatt Photovoltaic Powered, Agricultural Experiment in Mead, Nebraska," Technical Report, 21 April 1978.
4094-5	Kern, E. C., "Solar Energy Alternatives for the United States Embassy and for Rural Development Projects within the Republic of Upper Volta," Technical Report, 7 March 1978.
4094-6	Forman, S. E., "Visual Defects in Terrestrial Photovoltaic Modules," Technical Report, 21 March 1978.
4094-7	Forman, S. E. and Landsman, E. E., "Safety Procedures for the 25 kW Solar Photovoltaic Array at Mead, Nebraska," Technical Report, 7 April 1978.
4094-8	Forman, S. E., "Summary of Field Experience of PV Modules at Various MIT Lincoln Laboratory Test Sites," Technical Report, 22 March 1978.
4094-9	Much, C. and Stuart, E., "Sun Following Pyrheliometer Mounts for Insolation Data Collection," Technical Report, 2 August 1978.
4094-10	Romaine, W., "Description of the Mead PV Power System," Technical Report, 5 January 1979.
4094-11	Jarvinen, P. O. and Peatfield, C. R., "Photovoltaic Applications for the National Park Service," 12th Intersociety Energy Conversion and Engineering Conference, Washington, DC, 28 August - 2 September 1977.
4094-12	Pope, M. D. and Matlin, R. W., "Field Tests of Photovoltaic Power Systems," 1977 Photovoltaic Solar Energy Conference, Luxembourg, 27-30 September 1977.

COO No.

4094-13 Matlin, R. W., "25 kW PV Powered Irrigation and Grain Drying Experiment," International Solar Energy Congress, New Delhi, India, January 1978.

4094-14 Jarvinen, P. O., "Natural Bridges National Monument, Utah - Solar Photovoltaic Power System Design," Second National Conference on Technology for Energy Conservation, Albuquerque, NM, 24-27 January 1978.

4094-15 Pope, M. D. and Matlin, R. W., "Photovoltaic Power System Field Tests," 1978 IEEE PV Specialists' Conference, Washington, DC, 5-8 June 1978.

4094-16 Landsman, E. E., "Motor Starting with PV Systems," 1978 IEEE PV Specialists' Conference, Washington, DC, 5-8 June 1978.

4094-17 Landsman, E. E., "Maximum Power Trackers for Photovoltaic Arrays," 1978 IEEE PV Specialists' Conference, Washington, DC, 5-8 June 1978.

4094-18 Forman, S. E., "Field Testing and Evaluation of PV Module Performance," 1978 IEEE PV Specialists' Conference, Washington, DC, 5-8 June 1978.

4094-19 Bucciarelli, L. L., et al., "The Mead 25 kW Photovoltaic System," 1978 IEEE PV Specialists' Conference, Washington, DC, 5-8 June 1978.

4094-20 Lyon, E. F., et al., "Design of the Natural Bridges National Monument 100 kW PV Power System," 1978 IEEE PV Specialists' Conference, Washington, DC, 5-8 June 1978.

4094-21 Twersky, M., Fischbach, P. E., "Irrigation Systems for the Solar Photovoltaic Energy Program," Technical Report, 27 November 1978.

4094-22 Sacco, S. B., "Test Plan for Residential Testing at MIT Lincoln Laboratory Systems and Component Test Facilities," Technical Report, 30 October 1978.

4094-23 Forman, S. E., "Endurance and Soil Accumulation Testing of PV Modules at Various MIT Lincoln Laboratory Test Sites," Technical Report, 28 September 1978.

4094-24 Cremin, J. D., "Design, Development and Implementation of Data Acquisition Systems for PV Tests and Applications Project," Technical Report, 28 September 1978.

4094-25 Landsman, E. E., "Classification and Technical Review of DC-AC Inverters for Use in PV Power Systems," Technical Report, 30 April 1979.

COO No.

4094-26 Landsman, E. E., "Static Inverters for PV Applications," 14th Intersociety Energy Conversion Engineering Conference, Boston, MA, 5-10 August 1979.

4094-27 Millner, A. R., "Mead PV System Controller," Technical Report, 31 January 1979.

4094-28 Matlin, R. W., "PV Powered Irrigation Experiments in the U.S.," Atelier Pompage Solaire, Perpignan, France, 3-8 July 1978.

4094-29 Matlin, R. W. and Katzman, M. T., "The Economics of Solar Photovoltaic Energy Systems for Crop Irrigation in the United States," Atelier Pompage Solaire, Perpignan, France, 3-8 July 1978, American Journal of Agriculture Economics, Volume 60, November 1978.

4094-30 Millner, A. R., "National Photovoltaic Information System," Technical Report, 21 March 1978.

4094-31 Millner, A. R., "A Flywheel Energy Storage and Conversion System for Solar Photovoltaic Applications," ASME Gas Turbine Conference, San Diego, CA, 12-15 March 1979.

4094-32 Pope, M. D., "Field Tests of Photovoltaic Power Systems," ASME Gas Turbine Conference, San Diego, CA, 12-15 March 1979.

4094-33 Matlin, R. W., "Design Optimization and Performance Characteristics of a Photovoltaic Microirrigation System for Use in Developing Countries,", Technical Report, 10 July 1979.

4094-34 Much, C. H., et al., "A Microprocessor-Controlled Autonomous Sun-Following Mount for Solar Photovoltaic Energy Planning," Industrial Applications of Microprocessors Conference, Philadelphia, PA, 19-21 March 1979.

4094-35 Millner, A. R., "Solar Module Curve Tracer," Technical Report, 7 February 1979.

4094-36 Millner, A. R., "Solid-State DC Switch," Technical Report, 6 March 1979.

4094-37 Forman, S. E. and Murphy, E. B., "Measuring Dirt on PV Modules," Technical Report, 21 March 1979.

4094-38 Sacco, S. B., "Phase 1 Residential Testing at the MIT Lincoln Laboratory PV Systems Test Facility," Technical Report, 30 March 1979.

COO No.

4094-40 Forman, S. E. and Themelis, M. P., "Quarterly Report for 10/1/78 to 12/31/78 on Photovoltaic Module Performance at Mead, Nebraska, Test Site," Technical Report, 1 April 1979.

4094-41 Sacco, S. B., "Facility Description for the MIT Lincoln Laboratory PV Test Facility," Technical Report, 30 June 1979.

4094-42 Forman, S. E. and Themelis, M. P., "Physical and Electrical Degradation of Photovoltaic Modules after Exposure in Terrestrial Environments," 14th Intersociety Energy Conversion Engineering Conference, Boston, MA, 5-10 August 1979.

4094-43 Bucciarelli, L. L. and Hopkinson, R. F., "Performance of the Mead, Nebraska, 25 kWp Photovoltaic Solar Energy System Comparison with Simulation," 14th Intersociety Energy Conversion Engineering Conference, Boston, MA, 5-10 August 1979.

4094-44 Millner, A. R., and Hay, R. D., "Flywheel Energy Storage Interface Unit for Photovoltaic Applications," 14th Intersociety Energy Conversion Engineering Conference, Boston, MA, 5-10 August 1979.

4094-45 Pope, M. D., Hopkinson, R. F. and Bucciarelli, L. L., "Field Tests of Photovoltaic Power Systems," ISES Silver Jubilee International Solar Exhibition, Atlanta, GA, 28 May - 1 June 1979.

4094-46 Lyon, E. F., "A 100 kW Peak Photovoltaic Power System for the Natural Bridges National Monument," ISES Silver Jubilee International Solar Exhibition, Atlanta, GA, 28 May - 1 June 1979.

4094-47 Forman, S. E., "Photovoltaic Module Performance and Degradation at Various MIT Lincoln Laboratory Test Sites," ISES Silver Jubilee International Solar Exhibition, Atlanta, GA, 28 May - 1 June 1979.

4094-48 Millner, A. R., "A Flywheel Energy Storage and Conversion System for Photovoltaic Applications," International Assembly on Energy Storage, Dubrovnik, 28 May - 1 June 1979.

4094-49 Matlin, R. W., "PV Powered Microirrigation Systems," ISES Silver Jubilee International Solar Exhibition, Atlanta, GA, 28 May - 1 June 1979.

4094-50 Kern, E. C., "Residential Experiments," SERI Photovoltaic Advanced Research and Development Annual Review, Denver, CO, 17 September 1979.

4094-51 Bucciarelli, L. L., "Power Loss in Photovoltaic Arrays Due to Mismatch in Cell Characteristics," Solar Energy, Cambridge, MA, Volume 23, 1979.

COO No.

4094-53 Hopkinson, R. F., "Test Plan for the Mead 25 kW PV Flexible Test Facility, 1979," Technical Report, 15 March 1979.

4094-54 Lyon E. F., "The Design and Construction of a 100 kW Photovoltaic Remote Stand-Alone Power System," 1979 Photovoltaic Solar Energy Conference, Berlin, Germany, 23-26 April 1979.

4094-55 Forman, S. E. and Themelis, M. P., "Quarterly Report Solar Photovoltaic Project Materials, Processes and Testing Activities for the Period 1 January 1979 - 31 March 1979," Technical Report, 30 June 1979.

4094-56 Landsman, E. E., "A Unifying Derivation of Switching DC-DC Converter Topologies," 1979 Power Electronics Specialists' Conference, San Diego, CA, 19-21 June 1979.

4094-57 Millner, A. R., "A Flywheel Energy Storage and Conversion System for Photovoltaic Applications," Progress Report for the Mechanical and Magnetic Energy Storage Annual Review, U.S. Department of Energy, Washington, DC, 19-22 August 1979.

4094-58 Katzman, M. T., "Regional Differences in Energy Costs: Their Persistence and Implications for Solar Photovoltaics," Technical Report, September 1979.

4094-59 Raghuraman, P., "On Influencing the Operating Temperatures of Motorola and ARCO Solar Photovoltaic Modules," Technical Report, October 1979.

4094-60 Forman, S. E. and Themelis, M. P., "Quarterly Report Solar Photovoltaic Project Materials, Processes and Testing Activities for the Period 1 April - 30 June 1979," Technical Report, October 1979.

4094-61 Brench, B. L., "Snow Covering Effects on the Power Output of Solar Photovoltaic Arrays," Technical Report, December 1979.

4094-62 Cadieux, R. N. "Battery Charge/Solar Array Controller for a Residential Size Photovoltaic Power System," Technical Report, October 1979.

4094-63 Millner, A. R., "Scaling Laws for Flywheel System Components," Technical Report, October 1979.

4094-64 Hornig, C. F., et al., "Solar Photovoltaic Module Degradation from Electro-Corrosion," Technical Report, 15 May 1980.

4094-65 Sheldon, D. B., "Phase Two Experiment Test Plan Solar Photovoltaic/Thermal Residential Experiment," Technical Report, 23 January 1980.

COO No.

4094-66 Raghuraman, P., "Analytical Prediction of Liquid Photovoltaic/ Thermal Flat-Plate Collector Performance," Technical Report, 29 November 1979.

4094-68 Hopkinson, R. F. "Performance of a PV-Powered 20-hp DC-AC Irrigation System and a 3 kW Nitrogen Generator," 14th IEEE Photovoltaic Specialists' Conference, San Diego, CA, 7-10 January 1980.

4094-69 Forman, S. E. and Themelis, M. P., "Performance Reliability of Photovoltaic Modules at Various MIT Lincoln Laboratory Test Sites," 14th IEEE Photovoltaic Specialists' Conference, San Diego, CA, 7-10 January 1980.

4094-70 Millner, A. R. and Dinwoodie, T., "System Design, Test Results, and Economic Analysis of Flywheel Energy Storage and Conversion System for Photovoltaic Applications," 14th IEEE Photovoltaic Specialists' Conference, San Diego, CA, 7-10 January 1980.

4094-71 Brench, B. L., et al., "Simulation of the Performance of a 100 kW Peak Photovoltaic System," 14th IEEE Photovoltaic Specialists' Conference, San Diego, CA, 7-10 January 1980.

4094-72 Bucciarelli, L. L., et al., "The Energy Balance Associated with the Use of a Maximum Power Point Tracker in a 100 kW Peak Power System," 14th IEEE Photovoltaic Specialists' Conference, San Diego, CA, 7-10 January 1980.

4094-73 Kern, E. C. and Millner, A. R., "Performance of a Photovoltaically Powered Air-Conditioning System," 14th IEEE Photovoltaic Specialists' Conference, San Diego, CA, 7-10 January 1980.

4094-74 Hendrie, S. D. and Raghuraman, P., "A Comparison of Theory and Experiment for Photovoltaic/Thermal Collector Performance," 14th IEEE Photovoltaic Specialists' Conference, San Diego, CA, 7-10 January 1980.

4094-75 Russell, M. C., "Residential System Designs for the Northeast and Southwest," 14th IEEE Photovoltaic Specialists' Conference, San Diego, CA, 7-10 January 1980.

4094-78 Much, C. H. and Rothenheber, P. J., "Microprocessor Based Control of the Photovoltaic Solar Power System for AM Radio Station," IECI 80 Applications of Mini- and Micro-Computers, Philadelphia, PA, 17-19 March 1980.

4094-79 Bucciarelli, L. L. and Grossman, B. L., "A Comparison of Two Techniques for the Simulation of PV Systems," Second Annual Systems Simulation and Economics Analysis Conference, San Diego, CA, 23-25 January 1980.

COO No.

4094-80 Sheldon, D. B. and Russell, M. C., "A Review of Combined Photovoltaic/Thermal Collector - Solar Assisted Heat Pump Options," presented at the Heat Pump Technology Conference, Oklahoma State University, Stillwater, OK, 14-15 April 1980.

4094-81 Nichols, B. E., "A Lightening Strike at Bryan, Ohio," Technical Report, February 1980.

4094-82 Cadieux, R. N., "Description of Battery State-of-Charge Controller," Energy Systems Engineering Technical Note, May, 1981.

4094-83 Forman, S. E. and Themelis, M. P., "Materials, Processes and Testing Laboratory, Technical Progress Report: July, August, September, October 1979," Technical Report, 15 March 1980.

4094-85 Nichols, B. E., "A Solar Photovoltaic Power System for a Radio Station," Technical Report, December 1980.

4094-86 Murphy, E. B., "Measuring Dirt on Photovoltaic Modules, Part II," Technical Report, November 1980.

4094-87 Solman, F. J. and Nichols, B. E., "Design, Construction and Evaluation of Two Large Photovoltaic Power Systems," 1980 Annual Meeting of American Section of ISES, Phoenix, AZ, 1-5 June 1980.

4094-88 Hendrie, S. D. and Raghuraman, P., "An Advanced Combined Photovoltaic/Thermal Air Collector: Design and Testing," 1980 Annual Meeting of American Section of ISES, Phoenix, AZ, 1-5 June 1980.

4094-89 Raghuraman, P. and Hendrie, S. D., "Analytical Predictions of Liquid and Air Photovoltaic/Thermal Flat-Plate Collector Performance," ASME Winter Annual Meeting, Chicago, IL, 16-21 November 1980.

4094-90 Klein, D. N., "Interim Performance Criteria Document Development Implementation Plan and Procedures for Photovoltaic Energy Systems," Technical Report, 1 August 1980.

4094-91 Hay, R. D., et al., "Performance Testing and Economic Analysis of a Photovoltaic Energy Storage and Conversion System," 1980 Flywheel Technology Symposium, Tamarron, CO, 19-24 October 1980.

4094-92 Hay, R. D., et al., "Residential Photovoltaic Flywheel Storage System Performance and Cost," Intersociety Energy Conversion Engineering Conference, Seattle, WA, 18-22 August 1980.

MIT Lincoln Laboratory Publications Under DOE Contract No. DE-AC02-76ET-20279

No.

20279-93 P. Raghuraman, "Analytical Prediction of the Performance of an Air Photovoltaic/Thermal Flat-Plate Collector," Technical Report, 30 April 1980.

20279-94 Benoit, A. E., "Construction of a PV Power System at Natural Bridges National Monument," Technical Report, December 1980.

20279-95 Murphy, E. B., "Measuring PV Module Delamination," Technical Report, January 1981.

20279-96 Cox, C. H., III, "Residential Photovoltaic Systems Costs," 15th Intersociety Energy Conversion Engineering Conference, Seattle, WA, 18-22 August 1980.

20279-97 Cox, C. H., III, "Design of Solar Cells for Use in Photovoltaic/Thermal Collectors," ASME Winter Annual Meeting, Chicago, IL, 16-21 November 1980.

20279-98 Solman, F. J., et al., "The 100-kWp Photovoltaic Power System at Natural Bridges National Monument," 15th Intersociety Energy Conversion Engineering Conference, Seattle, WA, 18-22 August 1980.

20279-99 Kern, E. C., "Residential Photovoltaics Systems," 15th Intersociety Energy Conversion Conference, Seattle, WA, 18-22 August 1980.

20279-100 Russell, M. C., "Solar Photovoltaic Systems for Residences in the Northeast," 5th National Passive Solar Conference, University of Massachusetts at Amherst, Amherst, MA, 19-26 October 1980.

20279-101 Forman, S. E. and Caunt, J. W., "A Portable, X-Y Translating, Infrared Microscope for Remote Inspection of Photovoltaic Solar Arrays," presented at the International Symposium for Testing and Failure Analysis, Los Angeles, CA, 27 October 1980.

20279-102 Bucciarelli, L. L. and Rangarajan, A., "Dynamic Analysis of a Magnetically Suspended Energy Storage Wheel," presented at the Flywheel Technology Symposium, Tamarron, CO, 19-24 October 1980.

20279-103 Darkazalli, G., "Phase I Solar Photovoltaic/Thermal Residential Experiment," Final Report, 1 July 1980.

20279-104 Kern, E. C., "Residential Tests and Applications," National Conference on Renewable Energy Technologies, Honolulu, HI, 7-13 December 1980, extended abstract.

No.

20279-105 Solman, F. J., "The Photovoltaic Power System at Natural Bridges National Monument," National Conference on Renewable Energy Technologies, Honolulu, HI, 7-13 December 1980, extended abstract.

20279-106 Jarvinen, P. O., "Solar Related Flywheel Systems," National Conference on Renewable Energy Technologies, Honolulu, HI, 7-13 December 1980, extended abstract.

20279-107 Hay, R. D. and Jarvinen, P. O., "Inertial Energy Storage for Peak Power Demand Reduction," Symposium of Peaking Power, AMSE Winter Meeting, Chicago, IL, 16-21 November 1980.

20279-108 Hopkinson, R. F., "Safety Procedures for the 100 kW Solar Photovoltaic System at Natural Bridges National Monument," Technical Report, September 1981.

20279-109 Kern, E. C., "The Residential Use of Photovoltaics," 1980 Photovoltaic Solar Energy Conference, Cannes, France, 27-31 October 1980.

20279-110 Klein, D. N., "Photovoltaic Operations Manual - Radio Station WBNO," Technical Report, September 1980.

20279-111 Aiello, W. A. and Raghuraman, P., "Performance of a Combined Photovoltaic/Thermal Flat-Plate Liquid Collector," ASME Solar Energy Division's Solar Heating and Cooling Operational Results Conference, Reno, NV, 28 April - 1 May 1981.

20279-112 Forman, S. E., "Detection of Electrically Failed Photovoltaic Modules at MIT Lincoln Laboratory Test Sites," Technical Report, February 1981.

20279-113 Forman, S. E. and Themelis, M. P., "Materials, Processes and Testing Laboratory, Technical Progress Report: November, December 1979, January, February 1980," Technical Report, 30 November 1980.

20279-114 Forman, S. E. and Themelis, M. P., "Materials, Processes and Testing Laboratory, Technical Progress Report: March, April, May, June 1980," Technical Report, January 1981.

20279-115 Landsman, E. E., "Analysis and Test of Line-Commutated Inverters for Use in Photovoltaic Power Systems," Technical Report, February 1981.

20279-116 Klein, D. N., "Safety Analysis Report, Natural Bridges National Monument 100 kW PV Power System," Technical Report, September 1981.

No.

20279-117 Forman, S. E. and Themelis, M. P., "Materials, Process and Testing Laboratory, Technical Progress Report: July, August, September, October 1980," Technical Report, January 1981.

20279-118 Brench, B. L., "Operational Experiences in Lead-Acid Batteries for Photovoltaic Systems," presented at the 15th IEEE Photovoltaic Specialists' Conference, Orlando, FL, 11-15 May 1981.

20279-119 Forman, S. E., "Detection of Electrically Failed Photovoltaic Modules at Selected MIT Lincoln Laboratory Test Sites," presented at the American Section of the International Solar Energy Society Annual Meeting, Philadelphia, PA, 27-30 May 1981.

20279-120 Sheldon, D. B., "Heat Pumps and Utility Interactive Photovoltaic Power Systems," presented at the American Section of International Solar Energy Society Annual Meeting, Philadelphia, PA, 27-30 May 1981.

20279-122 Bullwinkel, H. J. and Hopkinson, R. F., "Three-Year Performance Study of the Mead, Nebraska, 25-kWp Photovoltaic Power System," presented at the American Section of International Solar Energy Society Annual Meeting, Philadelphia, PA, 27-30 May 1981.

20279-123 Russell, M. C., "Residential Photovoltaic System Design and Testing," presented at the 16th Intersociety Energy Conversion Engineering Conference, Atlanta, GA, 9-14 August 1981.

20279-124 Zwibel, H. S. and Schaefer, J. F., "The Southwest Residential Experiment Station: The First Year," presented at the American Section of the International Solar Energy Society Annual Meeting, Philadelphia, PA, 27-30 May 1981.

20279-125 Grossman, B. L., "Simulated Performance of the Stand-Alone Photovoltaic System at Natural Bridges National Monument," Technical Report, March, 1981.

20279-126 Forman, S. E. and Themelis, M. P., "Reliability of Terrestrial Photovoltaic Modules at Various DOE/MIT Lincoln Laboratory Test Sites," presented at the 15th IEEE Photovoltaic Specialists' Conference, Orlando, FL, 11-15 May 1981.

20279-127 Landsman, E. E., "Analysis of Test of Line-Commutated Inverters for Use in Residential Photovoltaic Power Systems," presented at the IEEE Photovoltaic Specialists' Conference, Orlando, FL, 11-15 May 1981.

20279-128 Landsman, E. E., "Loss of Line Shutdown for A Line-Commutated Utility-Interactive Inverter," MIT Lincoln Laboratory Energy Systems Engineering Technical Note, March 1981.

No.

20279-129 Strong, S. J. and Nichols, B. E., "Solar Photovoltaic Residence in Carlisle, Massachusetts," presented at the American Section of International Solar Energy Society Annual Meeting, Philadelphia, PA, 27-30 May 1981.

20279-130 Jarvinen, P. O., Brench, B. L., Hay, R. D., and Rasmussen, N. E., "Testing and Evaluation of a Solar Photovoltaic Flywheel Energy Storage System," presented at the 16th Intersociety Energy Conversion Engineering Conference, Atlanta, GA, 9-14 August 1981.

20279-131 Sheldon, D. B. and Frank, S. M., "Retrofitting Residences with Photovoltaic/Thermal Collector Systems," presented at the 16th Intersociety Energy Conversion Engineering Conference, Atlanta, GA, 9-14 August 1981.

20279-132 Russell, M. C., "Residential Photovoltaic Power Systems for The Northeast," presented at the 15th IEEE Photovoltaic Specialists' Conference, Orlando, FL, 11-15 May 1981.

20279-133 Nichols, B. E. and Strong, S. J., "The Carlisle House: An All Solar Electric Lived-In Residence," presented at the IEEE Photovoltaic Specialists' Conference, Orlando, FL, 11-15 May 1981.

20279-134 Jarvinen, P. O., Brench, B. L., and Rasmussen, N. E., "Performance Characteristics of Solar Photovoltaic Flywheel Storage Systems," presented at the 15th IEEE Photovoltaic Specialists' Conference, Orlando, FL, 11-15 May 1981.

20279-135 Solman, F. J. and Grossman, B. L., "Operating Experience with the Natural Bridges National Monument Photovoltaic Power System," presented at the 15th IEEE Photovoltaic Specialists' Conference, Orlando, FL, 11-15 May 1981.

20279-136 Rasmussen, N. E. and Branz, H. M., "The Dependence of Delivered Energy on Power Conditioner Electrical Characteristics for Utility-Interactive PV Systems," presented at the 15th IEEE Photovoltaic Specialists' Conference, Orlando, FL, 11-15 May 1981.

20279-137 Hendrie, S. D., Raghuraman, P., and Cox, C. H. III, "Liquid Photovoltaic/Thermal Collectors for Residential Applications," presented at the 15th IEEE Photovoltaic Specialists' Conference, Orlando, FL, 11-15 May 1981.

20279-138 Rasmussen, N. E., "Effect of Harmonic Voltages on Induction Motors," MIT Lincoln Laboratory Energy Systems Engineering Technical Note, March 1981.

No.

20279-139 Forman, S. E. and Themelis, M. P., "Materials, Processes and Testing Residential Technical Progress Report October and December 1980, January and February 1981," Technical Report, 15 April 1981.

20279-140 Forman, S. E., "Performance of Terrestrial Photovoltaic Modules at MIT Lincoln Laboratory Experimental Photovoltaic Systems," Technical Report, 30 April 1981.

20279-141 Raghuraman, P. and Kern, E. C., "Information Gathering, Data Reduction and Information Dissemination for Residential Experiment Station Operations," Technical Report, July 1981.

20279-142 Coleman, S. D., "Operations Manual for Photovoltaic Power Systems--Natural Bridges National Monument," Technical Report, February 1982.

20279-143 Nichols, B. E., "The Carlisle House--An All Solar Electric Residence," Technical Report, September 1981.

20279-145 Landsman, E. E., "Evaluation Tests of Abacus 6-kVA Utility-Interactive Inverter," Energy Systems Engineering Technical Note, August 1981.

20279-146 Raghuraman, P. and Kon, D., "On Reducing Convective Losses from Cover Glazings of Solar Thermal Collectors," ASME Winter Annual Meeting, Washington, DC, 15-20 November 1981.

20279-147 Solman, F. J., "Photovoltaic Systems Performance Experience," presented at the 15th IEEE Photovoltaic Specialists' Conference, Orlando, FL, 11-15 May 1981.

20279-149 Forman, S. E., "Using Measurements to Detect Electrical Problems in Operational Photovoltaic Arrays," presented at SERI Commerical Photovoltaic Measurements Workshop, Vail, CO, 27-29 July 1981.

20279-150 "Solar Photovoltaic Residential Project, Project Integration Meeting, Agenda and Abstracts," 27-29 July 1981, Cambridge, MA.

20279-151 Forman, S. E., Themelis, M. P., "Materials, Processes and Testing Laboratory Residential Technical Progress Report, March-June 1981," Technical Report, 15 August 1981.

20279-152 Forman, S. E., Themelis, M. P., "Materials, Processes and Testing Laboratory Technical Progress Report, March-June 1981," Technical Report, 15 August 1981.

No.

20279-153 Brench, B. L., "Application, Sizing, Testing and Performance of the Photovoltaic Battery Subsystem at Natural Bridges National Monument, Utah," Technical Report, November 1981.

20279-154 Russell, M. C., et al, "Data Report for the Northeast Residential Experiment Station - June 1981," Technical Report, August 1981.

20279-155 Fenton, H. A., Much, C. H., "Residential Photovoltaic Experiment Station Data System," presented at the IECI '81 International Conference on Applications of Mini and Microprocessors, San Francisco, CA, 9-12 November 1981.

20279-156 Warner, T. H., Cox, C. H., III, "A High Power I-V Curve Tracer Employing a Capacitive Load," presented at the Commercial Photovoltaic Measurements Workshop, Vail, CO, 27-29 June 1981, December 1982, Solar Cells, The Netherlands.

20279-157 Jarvinen, P. O., "Advanced Flywheel Storage System," Progress Report for the Mechanical Magnetic and Underground Energy Storage 1981 Annual Contractors Review, Washington, DC, 24-26 August 1981.

20279-158 McNeill, B. W., Solman, F. J., "Performance of an Experimental Photovoltaic Powered House," presented at the American Section of the International Solar Energy Society Annual Meeting, Philadelphia, PA, 27-30 May 1981.

20279-159 Jarvinen, P. O., "A Flywheel Energy Storage and Conversion System for Photovoltaic Applications - Final Report," Technical Report, March, 1982.

20279-160 Forman, S. E., Themelis, M. P., "Materials, Processes and Testing Technical Progress Report, November, December 1980, January, February 1981," Technical Report, 30 January 1982.

20279-161 Russell, M. C., et al, "Data Report for the Northeast Residential Experiment Station - July 1981," Technical Report, September, 1981.

20279-162 Nowlan, M. J., "Design and Fabrication of Air and Liquid Cooled Photovoltaic/Thermal Collectors," prepared for MIT Lincoln Laboratory by Spire Corporation as subcontractor, March 1981.

20279-163 Russell, M. C., "Prototype Residential Photovoltaic Systems Evaluation Plan," Technical Report, September 1981.

No.

20279-164 Russell, M. C., Raghuraman, P., Mahoney, P. C., "Data Report for the Northeast Residential Experiment Station - August 1981," Technical Report, October 1981.

20279-165 Russell, M. C., Raghuraman, P., Mahoney, P. C., "Data Report for the Northeast Residential Experiment Station - September 1981," Technical Report, October 1981.

20279-166 Schaefer, J. F., et al, "Data Report for the Southwest Residential Experiment Station, March-September 1981," prepared for MIT Lincoln Laboratory by the New Mexico Solar Energy Institute, 30 October 1981.

20279-167 Schaefer, J. F., et al, "Data Report for the Southwest Residential Experiment Station, October 1981," prepared for MIT Lincoln Laboratory by the New Mexico Solar Energy Institute, 16 November 1981.

20279-168 Hendrie, Susan D., "Photovoltaic/Thermal Collector Development Program - Final Report," Technical Report, March 1982.

20279-169 Kern, E. C. and Solman, F. J., "Shared Inverter Residential Photovoltaic System Concept," MIT Lincoln Laboratory Energy Systems Engineering Technical Note, December 1981.

20279-170 Branz, H. M., Hart, G. W., Cox, C. H., III, "The Photovoltaic Array/Power Conditioner Interface," Technical Report, September 1982.

20279-171 Solman, F. J., Bullwinkel, H. J., Doucet, J. D., and Brench, B. L., "A Photovoltaic System with Energy Storage - Natural Bridges National Monument 100-kW System," presented at the AIAA 20th Aerospace Sciences Conference, Orlando, FL, 11-14 January 1982.

20279-172 Forman, S. E. and Themelis, M. P., "Materials, Processes and Testing Residential Technology Progress Report, July August, September, October 1981," Technical Report, December 1981.

20279-173 Forman, S. E. and Themelis, M. P., "Materials, Processes and Testing Report, July, August, September, October 1981," Technical Report, February 1982.

20279-174 Russell, M. C., Raghuraman, P. and Mahoney, P. C., "Data Report for the Northeast Residential Experiment Station - October 1981," Technical Report, November 1981.

No.

20279-175 Mehalick, E. M., "Design and Fabrication of Prototype Systems for Photovoltaic Residences in the Northeast," prepared for MIT Lincoln Laboratory by Advanced Energy Programs Department, General Electric, King of Prussia, PA, November 1981.

20279-176 Schaefer, J. F., et al "Data Report for the Southwest Residential Experiment Station, November 1981," prepared for MIT Lincoln Laboratory by the New Mexico Solar Energy Institute, December, 1981.

20279-177 Solman, F. J., et al, "Maintenance Manual for the PV Power System at Natural Bridges National Monument," Technical Report, July 1982.

20279-178 Baird, R. H., et al, "System Design Drawings for the PV Power System at Natural Bridges National Monument," Technical Report, 30 May 1982.

20279-180 Coleman, S. D., Ed, "Power Processing Subsystems for the 100-kWp Solar Photovoltaic Power System at the Natural Bridges National Monument in Utah," Technical Report, July 1982.

20279-182 Russell, M. C., et al, "Data Report for the Northeast Residential Experiment Station - November 1981," Technical Report, December 1981.

20279-183 Hart, G. W., Raghuraman, P., "Residential Photovoltaic System Simulation: Thermal Aspects," presented at the ASME Solar Energy Division Fourth Annual Technical Conference, Albuquerque, NM, 26-30 April 1982.

20279-184 Schaefer, J. F., et al., "Data Report for the Southwest Residential Experiment Station, December, 1981," prepared for MIT Lincoln Laboratory by the New Mexico Solar Energy Institute, 29 January 1982.

20279-185 Katzman, M. T., and Katzman, A. C., "Economic and Financial Analysis of Residential Photovoltaic Systems: The Impact of Solar Photovoltaics on Utilities - Final Report," Technical Report, February 1982.

20279-186 Cox, C. H., III, "Residential Photovoltaic Power Conditioner Subsystem Test Procedures," Technical Report, February, 1982.

20279-187 Schaefer, J. F., et al., "Data Report for the Southwest Residential Experiment Station, January, 1982," prepared for MIT Lincoln Laboratory by the New Mexico Solar Energy Institute, 23 February 1982.

No.

20279-188 Forman, S. E. and Themelis, M. P., "Materials, Processes and Testing Laboratory Final Report Summarizing Module Performance at MIT Lincoln Laboratory Experimental Photovoltaic Test Sites, 1977-1982," Technical Report, June 1982.

20279-189 Themelis, M. P., "Final PV Module Degradation Analysis Report," Technical Report, June 1982.

20279-190 Forman, S. E. and Themelis M. P., "Final Materials, Processes and Testing Progress Report for Residential and Nonresidential Applications - November, December, January, February, March 1981-1982," Technical Report, June 1982.

20279-191 Landsman, E. E., Rasmussen, N. E., Cox, C. H., III, "Development of A DC-to-AC Inverter based on Waveshaping," Technical Report, June 1982.

20279-192 Russell, M. C., et al., "Data Report for the Northeast Residential Experiment Station - December 1981," Technical Report, April 1982.

20279-193 Mehalick, E. M., "General Electric Final Report: Design and Fabrication of a Prototype System for Photovoltaic Residences in the Southwest," prepared by Advanced Energy Programs Department, General Electric for MIT Lincoln Laboratory, under contract to New Mexico Solar Energy Institute, April 1982.

20279-195 Forman, S. E. and Klein, D. N., "Safety Inspection Guidelines for Photovoltaic Residences," Technical Report, January 1982.

20279-196 Schaefer, J. F., et al., "Data Report for the Southwest Residential Experiment Station - February 1982," prepared for Lincoln Laboratory by the New Mexico Solar Energy Institute, February 1982.

20279-197 Schaefer, J. F., et al., "Data Report for the Southwest Residential Experiment Station - March 1982," prepared for MIT Lincoln Laboratory by the New Mexico Solar Energy Institute, March 1982.

20279-198 Russell, M. C., Raghuraman, P., and Hart, G. W., "On Insolation Measurements Using Pyranometers and Solar Cell Devices," presented at the IECEC Conference, Los Angeles, CA, 8-13 August 1982.

20279-199 Pittman, P. F. and Dressler, R. T., "Westinghouse Final Report: Design and Fabrication of a Photovoltaic Prototype System for the Northeast," prepared by Westinghouse Advanced Energy Systems Division under contract to MIT Lincoln Laboratory, June 1982.

No.

20279-200 Schaefer, J. F., et al., "Data Report for the Southwest Residential Experiment Station - April 1982," prepared for MIT Lincoln Laboratory by the New Mexico Solar Energy Institute, April 1982.

20279-201 "Final Report: John F. Long Experimental Photovoltaic House," two volumes, prepared by John F. Long Properties, Inc., under contract to MIT Lincoln Laboratory, 1 June 1982.

20279-202 Hart, G. W. and Raghuraman, P., "Simulation of Thermal Aspects of Residential Photovoltaic Systems," Technical Report, June 1982.

20279-204 Russell, M. C., et al, "Data Report for the Northeast Residential Experiment Station - January 1982," Technical Report, June 1982.

20279-205 Nichols, B. E., "Evaluation of Recent Residential Inverters," Technical Report, August 1982.

20279-206 Russell, M. C., et al., "Data Report for the Northeast Residential Experiment Station - February 1982," Technical Report, June 1982.

20279-207 Hart, G. W and Raghuraman, P., "Electrical Aspects of Photovoltaic System Simulation," Technical Report, June 1982.

20279-208 Russell, M. C., et al., "Data Report for the Northeast Residential Experiment Station - March 1982," Technical Report, June 1982.

20279-209 "Total Environmental Action, Inc., Final Report: Design and Fabrication of a Prototype System for Photovoltaic Residences in the Southwest," prepared for MIT Lincoln Laboratory under TEA contract with New Mexico Solar Energy Institute, June 1982.

20279-210 Atmaram, G. H. and Litka, A. H., "The Florida Solar Energy Center Final Report on an Innovative Photovoltaic Applications for Residences Experiment," prepared under contract to MIT Lincoln Laboratory by the Florida Solar Energy Center, June 1982.

20279-211 Neill, D. R. and Curtis, G. W., "Hawaii Natural Energy Institute Final Report on Three Innovative Photovoltaic Applications for Residences Experiments," prepared under contract to MIT Lincoln Laboratory by the Hawaii Natural Energy Institute, June 1982.

No.

20279-212 Hart, G. W., "The Effect of Data Sampling Rate on Utility Interaction Calculations," Technical Report, October 1982.

20279-213 "Establishment and Operation of the Southwest Residential Experiment Station, May 1980-April 1982, Final Report," prepared by the New Mexico Solar Energy Institute under contract to MIT Lincoln Laboratory, June 1982.

20279-214 Russell, M. C., et al., "Data Report for the Northeast Residential Experiment Station - April 1982," Technical Report, June 1982.

20279-215 Cox, C. H., III and Warner, T. H., "Photovoltaic I-V Curve Measurement Techniques," Technical Report, August 1982.

20279-216 Tabors, R. D., "Market and Economic Analysis of Residential Photovoltaic Systems: Final Report," prepared by MIT Energy Laboratory under contract to MIT Lincoln Laboratory, July 1982.

20279-217 Millner, A. R., "TriSolarCorp Final Report: Design and Fabrication of a Prototype System for Photovoltaic Residences in the Northeast," prepared by TriSolarCorp under contract to MIT Lincoln Laboratory, August 1982.

20279-218 Millner, A. R., "TriSolarCorp Final Report: Design and Fabrication of a Prototype System for Photovoltaic Residences in the Southwest," prepared for MIT Lincoln Laboratory under TriSolarCorp contract with New Mexico Solar Energy Institute, August 1982.

20279-219 Russell, M. C., "First-Year Evaluation of Prototype Residential Photovoltaic Systems at the Northeast Residential Experiment Station," Technical Report, November 1982.

20279-220 Russell, M. C., et al., "Data Report for the Northeast Residential Experiment Station - May 1982," Technical Report, June 1982.

20279-221 Sheldon, P., Solman, F. J. and Nichols, B. E., "Effects on the Utility Feeder of Utility-Interactive Inverters at the Northeast Residential Experiment Station," Technical Report, November 1982.

20279-222 Fitzer, J., et al., "Impact of Residential Utility-Interactive PV Power Systems on the Utility," prepared by University of Texas-Arlington under contract to MIT Lincoln Laboratory, September 1982.

No.

20279-223 Nichols, B. E. and Katzman, M. T., "Solar Photovoltaic Power for Broadcasting Stations: An Engineering and Economic Analysis," Technical Report, August 1982.

20279-224 "Solarex Final Report: Design and Fabrication of a Prototype System for Photovoltaic Residences in the Northeast," prepared by Solarex Corporation under contract to MIT Lincoln Laboratory, August 1982.

20279-225 "BDM Final Report: Design and Fabrication of a Prototype System for Photovoltaic Residences in the Southwest," prepared by BDM for MIT Lincoln Laboratory under contract to New Mexico Solar Energy Institute, August 1982.

20279-226 Branz, H. M., "The Effect of Operating-Point-Control Strategy on the Annual Energy Production of Degraded Photovoltaic Arrays," presented at the 16th IEEE PV Specialists' Conference, San Diego, CA, 27-30 September 1982.

20279-227 Forman, S. E. and Themelis, M. P., "Review of PV Module Performance at DOE/MIT Lincoln Laboratory Test Sites During the Period 1977-1982," presented at the 16th IEEE PV Specialists' Conference, San Diego, CA, 27-30 September 1982.

20279-228 Cox, C. H., III, et al., "Reduction of Photovoltaic Cell Reverse Breakdown by a Peripheral Bypass Diode," presented at the 16th IEEE PV Specialists' Conference, San Diego, CA, 27 September-1 October 1982.

20279-229 Cox, C. H., III and Warner, T. H., "Swept Measurement of High Power I-V Curves," presented at the 16th IEEE PV Specialists' Conference, San Diego, CA, 27 September-1 October 1982.

20279-230 Nichols, B. E. and Russell, M. C., "Prototype Residential Photovoltaic Systems: Evaluation Results," presented at the 16th IEEE PV Specialists' Conference, San Diego, CA, 27 September-1 October 1982.

20279-231 Mahoney, P. C. and Hart, G. W., "Data Report for the Northeast Residential Experiment Station - June 1982," Technical Report, October 1982.

20279-232 Kern, E. C., "Photovoltaic Energy Systems: A Project Prospective," MIT Energy Laboratory, presented at the 16th IEEE PV Specialists' Conference, San Diego, CA, 27 September-1 October 1982.

No.

20279-233 Hart, G. W., "A Residential Photovoltaic System Simulation: Electrical Aspects," MIT Energy Laboratory, presented at the 16th IEEE PV Specialists' Conference, San Diego, CA, 27 September-1 October 1982.

20279-234 Sorenson, D and McNamara, R., "ARTU Final Report: Design and Fabrication of a Prototype System for Photovoltaic Residences in the Southwest," prepared for MIT Lincoln Laboratory under contract to New Mexico Solar Energy Institute October 1982.

20279-235 Gibson, R., and Swanson, T., "Solarex Final Report: Design and Fabrication of a Prototype System for Photovoltaic Residences in the Southwest," prepared for MIT Lincoln Laboratory under contract to New Mexico Solar Energy Institute, November 1982.

20279-236 Pittman, P. F. and Dressler, R. T., "Westinghouse Final Report: Design and Fabrication of a Prototype System for Photovoltaic Residences in the Southwest," prepared for MIT Lincoln Laboratory under contract to New Mexico Solar Energy Institute, November 1982.

20279-237 Kern, E. C., "Isolation Transformers for Utility-Interactive Photovoltaic Systems," Technical Report, November 1982.

20279-238 Yenamandra, R. and Schuetz, P., "ARCO Solar Final Report: Design and Fabrication of a Prototype System for Photovoltaic Residences in the Southwest," prepared for MIT Lincoln Laboratory under contract to New Mexico Solar Energy Institute, December 1982.

20279-239 Nichols, B. E., "The Carlisle Photovoltaic House: First Seventeen Months of Operation," Technical Report, February 1983.